

**Project 7-3940
Axial Capacity of Augercast Piles for Bearing**

Report No. 7-3940-2

**AXIAL PERFORMANCE OF
CONTINUOUS-FLIGHT-AUGER PILES FOR BEARING**

Final Report to the Texas Department of Transportation

by

**M. W. O'Neill
C. Vipulanandan
A. Ata
F. Tan**

Center for Innovative Grouting Materials and Technology (CIGMAT)

University of Houston

Houston, Texas

August, 1999

1. Report No. 7-3940-2	2. Government Accession No.	3. Recipient's Catalog No.	
4. Title and Subtitle Axial Performance of Continuous-Flight-Auger Piles for Bearing		5. Report Date August, 1999	
		6. Performing Organization Code	
7. Author(s) O'Neill, M. W., Vipulanandan, C., Ata, A., and Tan, F.		8. Performing Organization Report No. UHCE 7-3940-2	
9. Performing Organization Name and Address University of Houston Center for Innovative Grouting Materials and Technology 4800 Calhoun Road Houston, Texas 77204-4791		10. Work Unit No. (TRAIS)	
		11. Contract or Grant No.	
12. Sponsoring Agency Name and Address Texas Department of Transportation Research and Technology Transfer Office P. O. Box 5080 Austin, Texas 78763-5080		13. Type of Report and Period Covered Final Report Sep. 1997 - Aug. 1999	
		14. Sponsoring Agency Code	
15. Supplementary Notes Study conducted in cooperation with the U.S. Department of Transportation, Federal Highway Administration. Research project title Axial Capacity of Augercast Piles for Bearing			
16. Abstract Technology for the construction of continuous-flight-auger (CFA) piles has advanced to the point where these types of piles potentially can be considered as reliable as other types of piling (driven piles, drilled shafts) for supporting bearing loads produced by highway structures. To provide a basis for the axial design and construction of CFA soils in the coastal soils of the Houston District of the Texas Department of Transportation, a thorough comparison was made of several axial capacity prediction methods and capacities of CFA piles measured in numerous load tests performed for the private sector. The current TxDOT design method for drilled shafts was found to provide the most accurate prediction of pile capacity in predominantly clay soil profiles, while the FHWA design method for drilled shafts was the most accurate in predominantly sand and mixed sand-clay profiles. Data on grout pressures, grout volumes, grout mix designs and grout placement procedures were also collected from experts and assembled into a preliminary construction specification. A special effort was made to construct (and carefully monitor the construction of) three instrumented test piles at three geologically diverse sites in the Houston District: (1) a stiff clay site, (2) a site with a profile consisting of stiff clay and loose, waterbearing sand, and (3) a site consisting of dry, medium dense sand. Analysis of the axial load test results confirmed the preliminary findings given above and also confirmed that with appropriate construction controls CFA piles can be installed with high axial capacity and a high degree of structural integrity.			
17. Key Words Piles, grout, clay, sand, Houston, auger, axial capacity, settlement, load tests, database		18. Distribution Statement No restrictions. This document is available to the public through the National Technical Information Service, Springfield, Virginia 22161.	
19. Security Classif. (of this report) Unclassified	20. Security Classif. (of this page) Unclassified	21. No. of Pages 254	22. Price

This page is intentionally blank.

ENGINEERING DISCLAIMER

The contents of this report reflect the views of the authors, who are responsible for the facts and the accuracy of the data presented herein. The contents do not necessarily reflect the official view or policies of the Texas Department of Transportation. This report does not constitute a standard or a regulation.

There was no invention or discovery conceived or first actually reduced to practice in the course of or under this contract, including any art, method, process, machine, manufacture, design or composition of matter, or any new and useful improvement thereof, or any variety of plant which is or may be patentable under the patent laws of the United States of America or any foreign country.

This page is intentionally blank.

PREFACE

The research reported herein was motivated by a desire on the part of the Texas Department of Transportation to transfer the technology of continuous-flight-auger (CFA) piles; which have been used successfully as foundations for sound walls, industrial facilities, and buildings; to the design and quality assurance of CFA piles to sustain axial bearing loads from bridges and similar structures.

CFA piles are constructed by continuously augering a borehole, usually of relatively small diameter, into the earth and injecting cementitious grout through the hollow stem of the auger as it is withdrawn, after which reinforcing steel is inserted into the grout. The process is rapid and therefore cost-effective. The potential for the production of defects during the rapid construction process can be minimized by monitoring grout take and pressure supplied to the grout column. Measurements of these parameters were performed during the course of this project.

The principal focus of the research project was to construct CFA piles, full-sized, at three geotechnically diverse sites around the Houston area to verify the robustness of the construction process and the validity of construction monitoring procedures, both of which are required for bridge construction. The three instrumented test piles were also subjected to axial load tests to failure and the resulting data included with numerous other recent local load tests in a database, against which several potential geotechnical design methods were tested. Recommendations for design procedures were thereby developed. Careful observation of the construction of the test piles and conversations with practitioners led to the updating of an earlier preliminary construction specification for CFA piles with a view toward their use as load-bearing piles for bridges and similar structures.

ABSTRACT

This study addresses preliminary construction specifications and design methods for axially loaded CFA piles in different soil conditions typical of those found in the Houston District of the Texas Department of Transportation. A database for load tests on CFA piles in the Houston-Gulf coast area and Florida was established. Three detailed axial load tests on instrumented CFA piles in varying soil conditions typical of those found in the Houston area were performed and added to the database. The predictive results from seven simple potential design methods for axially loaded CFA piles and the results of the pile load tests in the database were compared and evaluated, from which optimum design methods were identified.

The preliminary construction specification recommended for CFA piles in the final report for Project 7-3921 was modified slightly based on the observations of the installation of the three test piles, grouting data from a large production project consisting of several hundred CFA piles and conversations with practicing engineers.

Based on the results of this study, it appears that if proper monitoring is carried out, CFA piles can be effective and reliable foundation load-bearing elements.

SUMMARY

Files of consulting engineers and contractors, as well as the literature, were reviewed for results of load tests on continuous-flight-auger (CFA) piles in the Houston area or in areas geologically similar to the Houston area. A database, consisting of a quantitative description of soil property profiles and load test results, was compiled for recent load tests to failure conducted on CFA piles in sand, clay and mixed sand-clay soil profiles. Seven methods for predicting the capacity of driven piles, drilled shafts and CFA piles were applied to the prediction of the capacities of the piles in the database. Two methods, the TxDOT (Houston District) method and the FHWA method, were found to be the most appropriate methods of those studied in clay (TxDOT) and in sand / mixed clay-sand profiles (FHWA), respectively. Based upon the bias and scatter in the database, factors of safety and resistance factors corresponding to reliability indices of 3.0 and 3.5 were deduced mathematically.

During installation of the test piles constructed specifically for this project, automated and visual monitoring was performed. The differences in the automated and visual monitoring were significant enough to suggest that automated monitoring should be performed on CFA piles that will be used to support bearing loads from bridges and similar structures. Monitoring procedures are reflected in the proposed preliminary construction specification, which was modified from the specification developed in Project 7-3921.

IMPLEMENTATION STATEMENT

The design method presented in this report is intended to be used directly by the Texas Department of Transportation (TxDOT) in the design of CFA piles for bearing loads. The updated preliminary construction specification given in Chapter 6 is offered for consideration by TxDOT to be included in its standard specifications after internal review by appropriate persons and committees. It is appropriate that both the design procedures and preliminary construction specification be used next in a formal implementation project, in which CFA piles are designed, installed and monitored on a bridge or bridges in the Houston District designated by TxDOT.

ACKNOWLEDGMENTS

The authors are grateful to the personnel from the TxDOT Houston District laboratory, under the direction of Mr. Stanley Yin, who assisted in selecting test sites, performing soil tests, and installing ground instruments. The authors also acknowledge Mr. Joe Thomas of the University of Houston for his assistance in conducting field and laboratory tests; to Ms. Yinan Weng for performing most of the laboratory tests described in Appendix D; to Berkel and Company, Inc., for installing the test piles and the reaction systems; to Fugro-McClelland Southwest, Inc., for acting as visual inspectors during test pile construction and for making cross-hole ultrasonic readings; to Mr. Norman Peterson, for constructing and calibrating the pile and ground instrumentation; to Pile Dynamics, Inc., for providing equipment and personnel for automated construction monitoring; and to Dr. Mauricio Ochoa of Emcon, Inc., for providing the CFA pile installation data for the Ingleside Cogeneration Project contained in Appendix C.

TABLE OF CONTENTS

	Page
LIST OF FIGURES	xii
LIST OF TABLES	xviii
1. INTRODUCTION	1
1.1. BACKGROUND.....	1
1.2. CFA PILES.....	2
2. LITERATURE SEARCH.....	7
3. DATABASE FOR CFA PILES.....	15
3.1. GENERAL INFORMATION.....	15
3.2. POTENTIAL DESIGN METHODS TESTED AGAINST THE DATABASE.....	16
3.2.1. Wright and Reese (1979).....	17
3.2.2. Neely (1991).....	18
3.2.3. Laboratoire Des Ponts et Chaussées (LPC) (1981).....	20
3.2.4. FHWA (Reese and O'Neill) (1988).....	23
3.2.5. Coyle and Castello (1981).....	25
3.2.6. API [2A-LRFD] (1993).....	30
3.2.7. TxDOT – Houston District (1972).....	32
3.3. DATABASE.....	38
3.3.1. Sources of the database.....	38
3.3.2. Format.....	38

3.3.3. Failure criterion.....	40
3.3.4. Calculations from the database.....	40
3.4. COMMENTARY.....	59
4. FIELD TESTS.....	63
4.1. GENERAL INFORMATION.....	63
4.2. SITE CONDITIONS.....	65
4.2.1. NGES-UH site.....	65
4.2.2. Baytown site.....	66
4.2.3. Rosenberg site.....	66
4.3. CONSTRUCTION OF TEST PILES.....	73
4.3.1. Soil pressure gauge.....	91
4.3.2. Integrity testing program.....	96
4.4. LOAD TESTING.....	98
5. ANALYSIS OF DATABASE.....	125
5.1. RE-APPLICATION OF DESIGN METHODS INCLUDING NEW TEST DATA.....	125
5.2. RESISTANCE FACTORS AND FACTORS OF SAFETY.....	140
5.2.1. LRFD method.....	140
5.2.2. ASD method.....	147
6. CONSTRUCTION SPECIFICATION.....	155
6.1. INTRODUCTION.....	155
6.2. REVISED PRELIMINARY SPECIFICATION.....	156
7. CONCLUSIONS AND RECOMMENDATIONS.....	181

7.1. CONCLUSIONS.....	181
7.2. RECOMMENDATIONS FOR FURTHER RESEARCH	183
REFERENCES.....	185
APPENDIX A. Examples of Calculations of CFA Pile Capacities from Database	191
APPENDIX B. Cross-hole Ultrasonic Logs of Test Piles at Variable Power Settings and Measured Grout Take Ratios for Test Piles.....	211
APPENDIX C. Ingleside Cogeneration Project, Ingleside, Texas, CFA Pile Data..	219
APPENDIX D. Chemical Resistance of Auger Grouts.....	229

LIST OF FIGURES

Figure	Page
3.1. Skin friction factor versus pile length (Neely 1991).....	19
3.2. Maximum skin friction versus cone tip resistance (LPC 1981).....	21
3.3. Coyle and Castello's pile capacity versus friction angle and embedment (1981).	26
3.4. Correlation between angle of internal friction, ϕ , and standard penetration test, N	27
3.5. α -factor versus undrained shear strength of clay (Coyle and Castello - Tomlinson 1981).....	29
3.6. Coyle and Castello - Tomlinson method in clay.....	50
3.7. API method in clay.....	51
3.8. LPC method in clay.....	51
3.9. FHWA method in clay.....	52
3.10. TxDOT method in clay.....	52
3.11. Wright and Reese method in sand.....	53
3.12. Neely method in sand.....	53
3.13. Coyle and Castello method in sand.....	54
3.14. API method in sand.....	54
3.15. LPC method in sand.....	55
3.16. FHWA method in sand.....	55
3.17. Coyle and Castello - Tomlinson method in mixed soil profiles.....	56
3.18. API method in mixed soil profiles.....	56

3.19.	LPC method in mixed soil profiles.....	57
3.20.	FHWA method in mixed soil profiles.....	57
4.1.	Sketch map of UH test site.....	67
4.2.	Layout of test pile and reaction piles (UH).....	67
4.3.	Boring log for UH test site.....	68
4.4.	Sketch map of Baytown test site.....	69
4.5.	Layout of test pile and reaction piles (Baytown).....	69
4.6.	Boring log for Baytown test site.....	70
4.7.	Sketch map of Rosenberg test site.....	71
4.8.	Layout of test pile and reaction piles (Rosenberg).....	71
4.9.	Boring log for Rosenberg test site.....	72
4.10.	Schematic of steel cage and sister bars at three sites.....	74
4.11.	Velocity of penetration (augering) and extraction (grouting).....	78
4.12.	Record of grout volume ratio versus depth for UH test pile (by flowmeter).....	81
4.13.	Records of maximum and minimum pump grout pressure versus depth for UH test pile.....	82
4.14.	Record of grout volume ratio versus depth for Baytown test pile (by flowmeter)	83
4.15.	Records of maximum and minimum pump grout pressure versus depth for Baytown test pile.....	84
4.16.	Record of grout volume ratio versus depth for Rosenberg test pile (by flowmeter)	85

4.17. Records of maximum and minimum pump grout pressure versus depth for Rosenberg test pile.....	86
4.18. Grout volume versus depth for the UH test pile.....	88
4.19. Grout volume versus depth for the Baytown test pile.....	88
4.20. Grout volume versus depth for the Rosenberg test pile.....	89
4.21. Layout of pressure gauge and test pile.....	92
4.22. Lateral effective soil pressure for installation of CFA test pile at the NGES - UH site.....	93
4.23. Lateral effective soil pressure for installation of CFA test pile at the Baytown site.....	94
4.24. Lateral effective soil pressure for installation of CFA test pile at the Rosenberg site.....	95
4.25. Applied load versus settlement (1 minute).....	100
4.26. Applied load versus settlement (3 minutes).....	101
4.27. Applied load versus depth (UH site, Method 1).....	102
4.28. Applied load versus depth (UH site, Method 2).....	103
4.29. Applied load versus depth (Baytown site, Method 1).....	104
4.30. Applied load versus depth (Baytown site, Method 2).....	105
4.31. Applied load versus depth (Rosenberg site, Method 1).....	106
4.32. Applied load versus depth (Rosenberg site, Method 2).....	107
4.33. Applied load versus depth (Rosenberg site, second cycle, Method 1.....	108
4.34. Applied load versus depth (Rosenberg site, second cycle, Method 2.....	109
4.35. Unit side resistance versus settlement (UH site).....	112

4.36.	Unit toe resistance versus settlement (UH site).....	113
4.37.	Unit side resistance versus settlement (Baytown site).....	114
4.38.	Unit toe resistance versus settlement (Baytown site).....	115
4.39.	Unit side resistance versus settlement (Rosenberg site).....	116
4.40.	Unit toe resistance versus settlement (Rosenberg site).....	117
4.41.	Unit side resistance versus settlement (Rosenberg site, second cycle).....	118
4.42.	Unit toe resistance versus settlement (Rosenberg site, second cycle).....	119
4.43.	Horizontal effective pressure versus applied load.....	123
5.1.	Coyle and Castello - Tomlinson method in clay.....	129
5.2.	API method in clay.....	129
5.3.	LPC method in clay.....	130
5.4.	FHWA method in clay.....	130
5.5.	TxDOT method in clay.....	131
5.6.	Wright and Reese method in sand.....	131
5.7.	Neely method in sand.....	132
5.8.	Coyle and Castello method in sand.....	132
5.9.	API method in sand.....	133
5.10.	LPC method in sand.....	133
5.11.	FHWA method in sand.....	134
5.12.	Coyle and Castello - Tomlinson method in mixed soil profiles.....	134
5.13.	API method in mixed soil profiles.....	135
5.14.	LPC method in mixed soil profiles.....	135
5.15.	FHWA method in mixed soil profiles.....	136

5.16.	TxDOT method in mixed soil profiles.....	136
5.17.	Correlation between SPT and TxDOT cone penetrometer in sand.....	139
5.18.	Resistance factor versus ratio of dead to live load (TxDOT method – clay)....	146
5.19.	Resistance factor versus ratio of dead to live load (FHWA method – sand).....	146
5.20.	Resistance factor versus ratio of dead to live load (FHWA method – mixed soil profile).....	147
5.21.	Safety factor versus ratio of dead to live load (TxDOT – clay).....	149
5.22.	Safety factor versus ratio of dead to live load (FHWA – sand).....	150
5.23.	Safety factor versus ratio of dead to live load (FHWA – mixed soil profile)....	151
5.24.	Design relationship for settlement prediction from field tests.....	153
B.1.	Cross-hole ultrasonic log of UH test pile.....	212
B.1.	Cross-hole ultrasonic log of UH test pile (Continued).....	213
B.2.	Cross-hole ultrasonic log of Baytown test pile.....	214
B.3.	Cross-hole ultrasonic log of Rosenberg test pile.....	215
B.4.	Grout ratio for UH test pile.....	216
B.5.	Grout ratio for Baytown test pile.....	216
B.6.	Grout ratio for Rosenberg test pile.....	217
D.1.	pH versus concentration percentage of sulfuric and hydrochloric acid.....	229
D.2.	Experimental setup.....	233
D.3.	Map of failed auger grout specimen in 2 % Na ₂ SO ₄	235
D.4.	Variation of pH at the end of one cycle of immersion time for auger grout specimens.....	236

D.5.	Change in pH at the end of one cycle for concrete specimens (a) Wet group	
	(b) Dry group.....	237
D.6.	Change in weight versus immersion time for auger grout specimens.....	238
D.7.	Change in weight versus immersion time for the dry group concrete	
	specimens.....	239
D.8.	Change in weight versus immersion time for the wet group concrete	
	specimens.....	239
D.9.	Calcium leachate versus number of cycles of leaching for auger grout	
	specimens.....	244
D.10.	Calcium leachate versus number of cycles of leaching for dry concrete.....	246
D.11.	Calcium leachate versus number of cycles of leaching for wet concrete.....	247
D.12.	Variation of pulse velocity of the auger grout specimens.....	248
D.13.	Variation of pulse velocity of cement concrete specimens.....	249

LIST OF TABLES

Table	Page
3.1. Design parameters for cohesionless siliceous soils (API, 1993).....	33
3.2. Database collection list.....	38
3.3. General information for test pile (example).....	39
3.4. Load-settlement data (example).....	40
3.5. Soil data (example).....	41
3.6. Summary of measured and predicted capacities for CFA piles in clay.....	42
3.7. Summary of measured and predicted capacities for CFA piles in sand.....	44
3.8. Summary of measured and predicted capacities for CFA piles in mixed soil profiles.....	46
3.9. Ratios of measured to predicted capacities of CFA piles in clay.....	49
3.10. Ratios of measured to predicted capacities of CFA piles in sand.....	49
3.11. Ratios of measured to predicted capacities of CFA piles in mixed soil profiles....	50
4.1. Grout mix proportions for the test piles.....	75
4.2. Material properties of the grout for the test piles.....	75
4.3. Installation of test piles.....	76
4.4. Properties of the CFA pile rig.....	76
4.5. Calculated and observed rates of penetration of the auger for three test piles	79
5.1. Ratios of measured to predicted capacities of CFA piles in clay.....	126
5.2. Ratios of measured to predicted capacities of CFA piles in sand.....	127
5.3. Ratios of measured to predicted capacities of CFA piles in mixed soil profiles..	128
5.4. Calculation of resistance factor for TxDOT method in clay.....	143

5.5. Calculation of resistance factor for FHWA method in sand.....	144
5.6. Calculation of resistance factor for FHWA method in mixed soil profiles.....	145
5.7. Calculation of factor of safety for TxDOT method in clay.....	149
5.8. Calculation of factor of safety for FHWA method in sand.....	150
5.9. Calculation of factor of safety for FHWA method in mixed soil profiles.....	151
D.1. Number of Auger Grout and Cement Concrete Specimens Tested.....	230
D.2. Composition and Properties of Auger Grout and Concrete.....	232
D.3. Typical Appearance of Auger Grouts and Solutions at the End of First Test Cycle.....	234
D.4. Typical Appearance of Concrete and Solutions at the End of First Test Cycle...	235
D.5. Effect of Chemical Solutions for Auger Grout Specimens after Two Years of Immersion.....	240
D.6. Effect of Different Chemical Solutions for Dry Concrete (500 Days of Immersion).....	242
D.7. Effect of Different Chemical Solutions for Wet Concrete (500 Days of Immersion).....	242
D.8. Amount of Calcium Leached for Auger Grouts (Two Years of Immersion).....	244
D.9. Effect of Different Chemical Solutions for Concrete (500 Days of Immersion)..	245
D.10.Effect of Different Chemical Solutions in the Pulse Velocity for Auger Grouts (Two Years of Immersion).....	247
D.11.Effect of Different Chemical Solutions on Pulse Velocity for Dry Cement Concrete (1.5 Years of Immersion).....	249
D.12.Effect of Different Chemical Solutions on Pulse Velocity for Wet Cement	

Concrete (1.5 Years of Immersion).....	250
D.13.Compression Strength of Selected Auger Grouts.....	251

CHAPTER 1 INTRODUCTION

1.1. BACKGROUND

Continuous-flight-auger (CFA) piles, also known as augered-cast-in-place (ACIP) piles or "augercast" piles, have been used in the private sector in the United States and in both the private and public sectors in Europe for many years. However, their use on public-sector transportation projects in Texas and in the United States has been limited to small secondary structures that exert very small bearing loads. Examples include foundations for sound walls and overhead signs. In Europe, however, CFA piles have been used extensively in transportation structures to support large bearing loads. Under some circumstances CFA piles can be both efficient carriers of bearing loads and more economical to install than competing foundations systems and should be considered as an alternative foundation system for transportation structures in Texas, especially in the relatively soft soils in the Texas coastal plain near Houston.

The TxDOT report "Specification and Design Criteria for the Construction of Continuous Flight Auger Piles in the Houston Area" by Hassan, O'Neill and Vipulanandan was produced previously to describe the behavior of CFA piles in the overconsolidated clays in Houston under lateral loading. A design procedure was recommended and tested against the results of full-scale load tests, and a provisional construction specification was given in that report. The current document describes a parallel study for CFA piles under compressive loading, but it expands the soil types considered to moist and saturated sands and mixed sand-clay stratigraphy in addition to

overconsolidated clay. Design procedures for axial resistance are recommended, and some revisions in the provisional construction specification are given.

1.2. CFA PILES

CFA piles are formed by rotating a continuous-flight, hollow-shaft auger into the ground to a predetermined tip elevation. Grout is then injected continuously through the auger shaft as the auger is being withdrawn. A reinforcing steel cage can then be inserted into the grout after the auger is fully withdrawn. CFA piles have some unique advantages over many types of driven, displacement-type piles.

- Based on anecdotal information, CFA piles may be an economic alternative compared to other pile types, mainly because material costs are relatively low and installation is fast.
- Vibrations and noise levels are low.
- CFA piles can be constructed in limited access conditions where conventional driving equipment cannot be operated and premanufactured piles cannot fit geometrically.
- CFA pile length can be easily adjusted in the field where a termination refusal criteria can be specified rather than a tip elevation criterion.

Despite those advantages, potential construction problems have been identified in the past that may adversely influence the integrity of the CFA piles and produce a relatively large settlement of adjacent structures. The integrity of CFA piles is highly dependent on the construction control and the skill of the contractor's field personnel. For those reasons, the use of CFA piles is not widespread in transportation structures in the USA.

In the past 25 years in the Houston-Galveston-Beaumont area, one notable problem has been a high failure rate of CFA piles subjected to axial load tests. The reasons lie in the structural defects associated with rapid extraction of the auger, in which suction pressures are exerted on the grout being charged at the outlet orifice at the bottom of the auger, which then forms a neck. Those structural defects are due to improper construction controls.

The use of CFA piles has been limited within TxDOT because there have been no accepted construction specifications and design methods. The objective of the document is to determine what quality controls are needed if CFA piles are to be used as bearing piles for structures and to develop the best simple design method to predict reliably the ultimate resistance and load-settlement behavior of CFA piles in soils in the Houston-Gulf Coast area.

Recommended design methods and construction specifications for axially loaded CFA piles in different typical soil conditions will be provided herein. They were developed through the following systematic process.

1. A database for load tests on CFA piles in the Houston-Gulf coast area was established. Tests on CFA piles installed and load tested in Florida were added to this database in order to arrive at an adequate number of tests in coarse-grained soils. The database includes soil conditions and axial load test data for those test piles.
2. Seven simple design methods for CFA piles were identified, and the results of the pile load tests in the database were compared with results predicted by these design methods for three different stratigraphic conditions: stiff clay, sand and mixed clay-

sand profiles. These conditions are typical of the conditions encountered within the geographic area of the Houston District of TxDOT. Each of these design methods was tested against the database.

3. A full-scale CFA pile was installed at three sites (NGES-UH, Baytown and Rosenberg). During the installation of these piles, a Pile Installation Recorder (PIR) was used to monitor the construction of the test piles in addition to conventional manual monitoring. The PIR measurements automatically document the augering and grouting processes and produce a graphical record of total grout volume pumped and grout pump pressure versus auger tip depth. The test piles were subjected to axial loading tests, which were analyzed to develop load-settlement and load distribution curves and thus to relate pile performance to soil conditions, pile installation parameters and installation procedures.
4. The results of the loading tests on the three test piles that were tested exclusively for this study were merged into the database, and the database was reanalyzed to determine the method that produced the most accurate prediction of capacity in each of the three typical soil profiles considered. Based on measures of scatter in the predictions, resistance factors and factors of safety were suggested.
5. The preliminary construction specification provided in the previous study documented earlier in this chapter was modified slightly. The modification was made using experience gained from the observations of:
 - the installation of the three test piles and the twelve reaction piles that were installed to load the test piles,

- grouting data from a large production project consisting of several hundred CFA piles, and
- the installation in the previous study of four laterally loaded CFA test piles and one reaction pile.

This page is intentionally blank.

CHAPTER 2 LITERATURE SEARCH

Augered piles are commonly used for building and transportation construction in Europe and other parts of the world (O'Neill, 1994). The continuous-flight-auger (CFA) pile system, more recently termed the augered, cast-in-place (ACIP) pile system, is used extensively. A CFA pile is constructed using the following process. Soil is excavated from a cylindrical column in the ground by using a single-helix, continuous, rotary auger. Once the plan elevation of the toe is reached, the auger is lifted slightly (150 - 300 mm) and the space between the auger toe and the base of the excavation is grouted with high-pressure grout or concrete with very fine coarse aggregate. This process continues as the auger is slowly withdrawn. Immediately after the excavation is grouted, the fluid grout is screened by hand from the surface to remove any floating clumps of soil, and a reinforcing cage is then inserted into the fresh grout by pushing or vibrating it into place.

CFA piles installed in clean sand can sometimes cause disturbance of the surrounding soil if the auger rotates without vertical penetration. An experimental test program was described by Kenny and Andrawes (1997). The laboratory test procedure using small augers simulated the field condition of the auger boring through sand from the ground surface, hitting an obstruction at depth and continuing to rotate with no penetration of the auger. During the test, the volume of the sand transported by the auger, the surface settlement, the extent of the zone of the disturbed sand and the change in density of the sand were monitored. The results from the test show: (a) the volume of

transported sand was highest during the first few rotations after which it rapidly reduced and reached a steady state, (b) during overrotation, the sand transportation was only significant when the auger was shallow and in loose sand, (c) the greatest amount of transported sand also resulted in the greatest surface settlement, and (d) the greatest settlement is close to the auger periphery and reduces away from the auger. The surface settlement can be negligible at a distance of 50% of the auger length from the auger. Densification of the sand near the auger periphery was observed during the penetration stage, followed by loosening during the overrotation stage.

A case describing the installation of about 200 CFA piles was presented by Leznicki, Esrig and Gaibrois (1991). After installation of the first 19 CFA piles, a large settlement of the ground surface occurred due to overrotation during the augering operation. In order to minimize the settlement, the following revised technical procedures were adopted: (a) reduce the number of rotations per minute (the average penetration speed of the auger was 1.8-2.3 m/min), (b) withdraw the auger without rotation while continuing to grout when the auger bit was 9.3-12.2 m from the surface, (c) keep the systolic grouting pressures above 1725 kPa (250 psi), (d) control the properties of the grout, and (e) begin CFA pile installation only after the grout has arrived at the site and has been inspected. Those technical procedures enabled the contractor to install the CFA piles successfully.

The previous case history illustrates potential problems that can occur when using CFA piles following conventional practice. The conventional CFA pile rig was developed in the United States in the late 1940s. In the early days of the CFA system, the norm was to make the piles out of grout. However, work in Belgium, France, and

Holland in the 1960s and 1970s showed that it was possible to use conventional pumpable concrete mixes with small coarse aggregate economically. Some problems occurred, however, with both grout and concrete piles. Pile load test results sometimes indicated poor base load-settlement characteristics, and necking within the pile was relatively common.

In 1980 a modern CFA pile rig, termed the "Starsol" system by its developer, the Soletenche Corporation of France, was introduced into European practice to minimize these problems (Whitworth, 1994). The essential features of the Starsol system were the provision of a larger internal concrete tremie (conduit) within the auger, high torque capabilities and the routine use of an automated monitoring system for quality control termed the "Enbesol" system. Enbesol, whose readout device is located in the cab of the drill rig, monitors and displays in real time the applied torque, rate of rotation, and rate of penetration for the auger. Once the auger has penetrated to the intended depth of the pile, grout or concrete is introduced through the tremie under pressure, and the auger is slowly withdrawn. During withdrawal, the Enbesol system monitors and displays in real time the grout/concrete pressure and the volume of grout/concrete placed. The operator of the Starsol rig is trained to identify anomalies in the Enbesol output, and if an anomaly occurs to take immediate action to remedy the situation. The Starsol piling technique has proven successful in France, where, between 1985 and 1994, about 100,000 piles were constructed. Two to three percent of this number were for highway and railway bridges (Whitworth, 1994).

Practice in the United States, however, continued after 1980 with the conventional system, which involved manual monitoring of grout volumes, grout

pressures, rate of penetration of the auger, and rate of withdrawal of the auger by someone other than the rig operator. The Deep Foundations Institute, based on results such as the case history described earlier, developed a construction guideline that proved helpful in reducing the incidence of necked piles and excessive ground settlement with the conventional system of construction and monitoring (DFI, 1994). Only recently have automated monitoring devices, generally resembling Enbesol, been introduced into practice in the United States.

CFA piles are considered by some to be the pile of choice when the subsurface conditions consist of saturated granular soils. Cutter and Warder (1998) presented a paper on the disturbance to the soil due to the installation of full-sized CFA piles. The extent and significance of the disturbance depended on the soil and ground water conditions, the method of pile installation and the sensitivity of the surroundings. Papers by Van Weele (1988) and Van Impe (1988) clearly indicate that CFA pile installation through loose to medium dense sandy soils below the ground water level can lead to significant overexcavation and subsidence of the ground surface. During the pile installation, the reasons leading to overexcavation and subsidence of the ground surface are as follows:

- **Drilling with rigs whose torque is too low.** "Underpowered" rigs lead to partial filling of the auger from the soil excavated by the bit at the tip of the auger and allow the partially filled auger flights to accept loosened soil from the sidewalls, which results in decompression of the soil surrounding the pile and consequent loss in pile capacity. Hassan et al. (1997), provide a simple formula that describes whether the torque is adequate by relating the rate of penetration to rate of rotation for an auger

of a given design. *[Note: Rigs that would be classified by Van Impe as underpowered are commonly used in the United States. European rigs such as the Starsol rig have much higher torque capabilities than do U. S. rigs and so tend not to produce this problem. However, U. S. contractors argue that the economic advantage of CFA piles can be lost by requiring the use of heavier, more highly-powered rigs than those currently in service. The solution to this problem, if current U. S. construction practice continues, appears to be avoidance of sites that contain loose, waterbearing sands with no cohesion. The current research project addresses the problem of such sites and also sites with moist sand.]*

- **Inappropriate installation procedures.** Extracting the auger before pumping grout to the bottom of the borehole with adequate pressure and/or failure to retain adequate grout pressure while the auger is being withdrawn (for example, as a result of extracting the auger too quickly) can lead to soil decompression, overexcavation, ground subsidence, or movement of adjacent structures. *[Note: These effects can be minimized by continuously monitoring the grout volume and grout pressure.]*
- **Penetration of a hard refusal layer.** As the bit at the bottom of the auger penetrates rock or other hard material, the rate of penetration slows, resulting in overrotation. This can result in the same problems that occur when the torque on the rig is too low.
- **Lateral stress relaxation.** If CFA piles are installed where the soil at the toe of a slope or in front of an earth retaining system is in a state of high lateral stress, the possibility of soil decompression and overexcavation is significantly increased.

Lacy presented a paper at the Sixth Annual Great Lakes Geotechnical and Geoenvironmental Conference on CFA piles, in which he suggested some performance criteria for CFA pile construction (Lacy, 1998). The continuous integrity of CFA piles should be controlled by monitoring the volume of grout pumped for each 1.5 m of auger withdrawal. A grout volume of 1.10 to 1.15 times the neat volume of the auger hole needs to be pumped for each increment of auger withdrawal. It is more successful for pile installation if the auger is withdrawn slowly instead of removed more quickly in interrupted increments. In order to avoid significant soil decompression due to the large amount of soil being raised to the ground surface on the auger flights, high-torque, low-speed augers need to be used. Using these methods, the number of auger rotations per unit of penetration equal to the auger pitch has at some sites been reduced from 20 to 2, largely reducing the volume of soil removed from the borehole.

With the wide use of the CFA piles in buildings and to some extent in transportation structures, a number of different methods have been developed to estimate the bearing capacities of CFA piles. Wright and Reese (1979) presented a method for bored piles and CFA piles in sand. Neely (1991) established a design method for CFA piles in sand. Bustamante and Gianselli (1981) developed a design procedure for H-piles, driven piles and bored piles termed the LPC method. Reese and O'Neill (1988) developed a method for drilled shafts termed the FHWA method. Coyle and Castello (1981) presented a design method to estimate the capacities of driven piles. The American Petroleum Institute (API, 1993) presented a design method, also for driven piles. TxDOT, in 1972, developed a method to estimate pile capacities in clay and sand.

This method has been modified through local experience in the Houston District of TxDOT. Detailed information on those design methods will be given in Chapter 3.

McVay et al. (1994) evaluated the performance of 21 CFA piles constructed and load tested in Florida (primarily in sand) and used five different design methods to predict the pile capacities to compare with measured pile bearing capacities. After the comparison, they concluded that the methods proposed by Reese and O'Neill (FHWA method) and by Wright and Reese are the best methods to predict the ultimate capacity. For the pile installation, they concluded that the construction parameters that had the greatest influence on axial capacity were the rate of penetration, grout fluidity, grout pumping pressures and rates, and the rate of extraction of the auger. McVay et al. recommended that (a) the pitch of the auger be reduced to one-half of the auger's outer diameter, (b) the grout pressure be monitored and maintained as the auger is being withdrawn, and (c) the grout "take" be monitored to show that it is 1.2 to 1.5 times the neat volume of the borehole. *[Note: It is observed that the recommendations of McVay and Lacy are quite different concerning the grout take ratios. This undoubtedly reflects differences in the geological environments in which the two investigators worked. An objective of the present study will be to determine appropriate grout ratios for typical subsurface conditions in the Houston/Texas Gulf Coast area.]*

This page is intentionally blank.

CHAPTER 3 DATABASE FOR CFA PILES

3.1. GENERAL INFORMATION

In the Houston District of the Texas Department of Transportation (TxDOT), near-surface soils are generally both relatively soft and metastable, which requires the use of deep foundations to support bridges and other structures. Historically, the Houston District has used either driven piles (usually prestressed concrete) or drilled shafts for this purpose. While these foundation types have had a long history of success, CFA piles, also referred to locally as "augercast" piles or "augered, cast-in-place" (ACIP) piles, may prove more economical and environmentally effective than drilled shafts or driven piles for application as load-bearing piles on certain types of highway structures in appropriate subsurface conditions.

CFA piles are used frequently in the private sector in the Houston area, mostly in industrial plants and commercial development projects. Geotechnical consultants use various design methods to predict the resistance of such piles. The methods vary; some consider CFA piles as driven piles [API (1993) and Coyle and Castello (1981)], while others view them as drilled shafts [Wright and Reese (1979) and Reese and O'Neill (1988), and TxDOT (1972)]. Lately, a number of design methods specific to CFA piles have been proposed [Neely (1991) and LPC (1981)].

The following is a review of seven design methods that can potentially be used to predict the ultimate compressive capacity of CFA piles. The results from 43 CFA test piles (database collected for this review) are compared to the predictions from these

seven design methods to evaluate the accuracy of those methods. A brief discussion of each design method is given first, followed by a summary of the database.

3.2. POTENTIAL DESIGN METHODS TESTED AGAINST THE DATABASE

Seven potential design methods were selected for the database:

- Method (1): Wright and Reese (1979),
- Method (2): Neely (1991),
- Method (3): Laboratoire Des Ponts et Chaussées (LPC) (1981),
- Method (4): FHWA (Reese and O'Neill) (1988),
- Method (5): Coyle and Castello - Tomlinson (1981),
- Method (6): API [2A-LRFD] (1993), and
- Method (7): TxDOT-Houston District, (1972).

As with all piles, all of the above design methods assume CFA piles resist applied load through side resistance (skin friction) and toe resistance (end bearing).

The total ultimate load is evaluated using the equation,

$$Q_t = Q_s + Q_p , \quad (3.1)$$

where

Q_t = ultimate capacity of the pile,

Q_s = capacity in side resistance, and

Q_p = capacity in toe resistance or end bearing.

The general equation for side resistance can be written as

$$Q_s = \pi D \int_{z=0}^{z=L} f_s(z) dz , \quad (3.2a)$$

or as

$$Q_s = f_{sa} \pi DL, \quad (3.2b)$$

where

D = nominal pile diameter (= diameter of the auger),

z = depth

L = penetration of the pile,

$f_s(z)$ = unit side resistance at depth z, and

f_{sa} = average unit side resistance over the length L of the pile.

The area of the side of the pile, $A_s = \pi DL$.

The general equation for toe (tip, base) resistance can be written as

$$Q_p = q_p A_p, \quad (3.3)$$

where

q_p = the ultimate unit toe resistance (end bearing), and

A_p = the end bearing area of the pile.

3.2.1. Wright and Reese (1979)

Wright and Reese (1979) presented a design method for predicting the ultimate capacity of drilled shafts and CFA piles in sand. The average unit side resistance is given by

$$f_{sa} = P_0' K_s \tan \phi \leq 0.15 \text{ MPa (1.6 tsf)}, \quad (3.4)$$

where

P_0' = average vertical effective stress along the pile (the effective stress at the center of the pile),

K_s = lateral earth pressure coefficient (taken by Wright and Reese as 1.1), and

ϕ = angle of internal friction of the sand (using a weighted average angle of internal friction of each layer in a layered sand).

The ultimate unit toe resistance for the pile is given by

$$q_p (tsf) = 2/3 N \leq 40 \text{ tsf, or} \quad (3.5a)$$

$$q_p (MPa) = 0.064 N \leq 3.8 \text{ MPa,} \quad (3.5b)$$

where N is the value from the standard penetration test (SPT) in blows/0.3m (blows/ft) near the toe of the pile.

3.2.2. Neely (1991)

Neely (1991) summarized the results from a database of 66 CFA pile tests in sand and established that the average unit side resistance can be computed by

$$f_{sa} = \beta P_0' \leq 0.135 \text{ MPa (1.4 tsf),} \quad (3.6)$$

where

β = $K_s \tan \delta$,

K_s = coefficient of lateral earth pressure (not necessarily equal to 1.1), and

δ = angle of friction at the pile-soil interface.

β was found to be dependent on the length of the pile, as shown in Figure 3.1. It is evident from Figure 3.1 that the β -factor decreases with increasing pile length and approaches a minimum constant value of 0.2 for pile lengths in excess of about 24 m (80 ft). Neely (1991) suggested limiting the maximum value of the average side resistance in

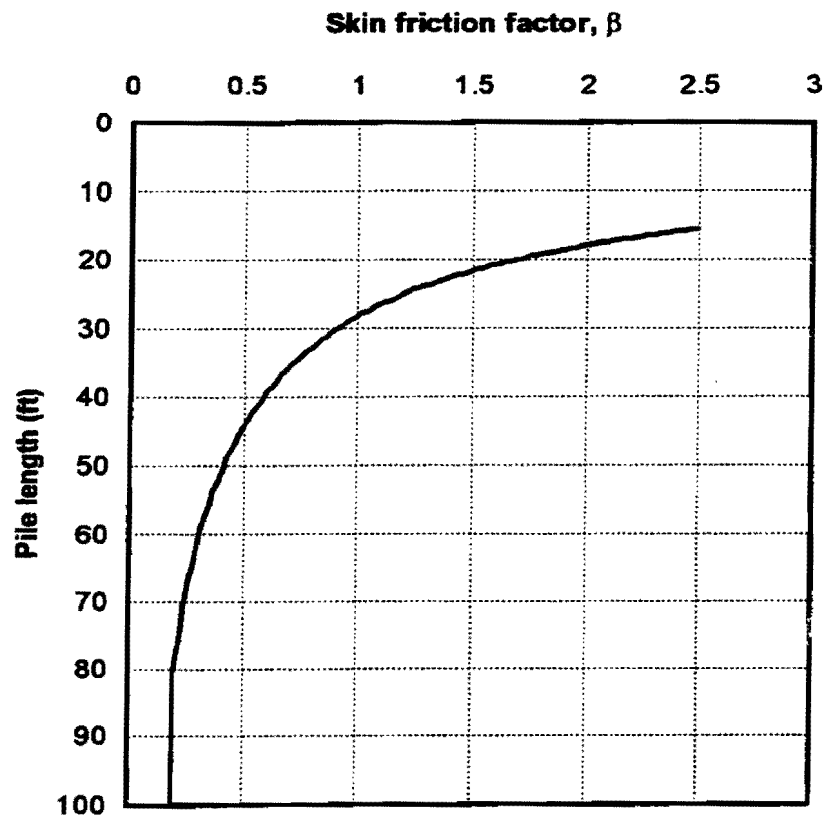


Figure 3.1. Skin friction factor versus pile length (Neely, 1991)

Equation (3.6) to 135 kPa (1.4 tsf), which corresponds to the maximum value evaluated from the pile load tests considered in his study.

Using data from both compression and tension testing, Neely (1991) estimated the ultimate unit toe resistance from

$$q_p (tsf) = 1.9 N \leq 7.2 \text{ MPa (75 tsf)}, \quad (3.7)$$

where N (SPT) is the number of blows per 0.3 m (blows/ft) near the toe of the pile. The unit toe resistance is limited to 7.2 MPa (75 tsf), which corresponds to the largest value derived from the load tests in the database.

3.2.3. Laboratoire Des Ponts et Chaussées (LPC) (1981)

Bustamante and Gianselli (1981) developed a design procedure for both driven and bored piles in cohesive and cohesionless soils. The procedure uses the results from the in situ cone-point resistance, q_c , to calculate the side resistance and the toe resistance capacities.

For CFA piles Figure 3.2 (a) is used to evaluate the unit side resistance for piles in cohesive layers, while Figure 3.2 (b) is used to evaluate the unit side resistance for piles in cohesionless layers. The value of $f_s(z)$ is determined by interpolation between the two limiting curves in Figures 3.2 (a) and (b) based on the average q_c along the pile. The total ultimate side resistance capacity in layered soils can be calculated as

$$Q_s = \sum \Delta Q_{si} = \sum A_{si} f_{si}, \quad (3.8)$$

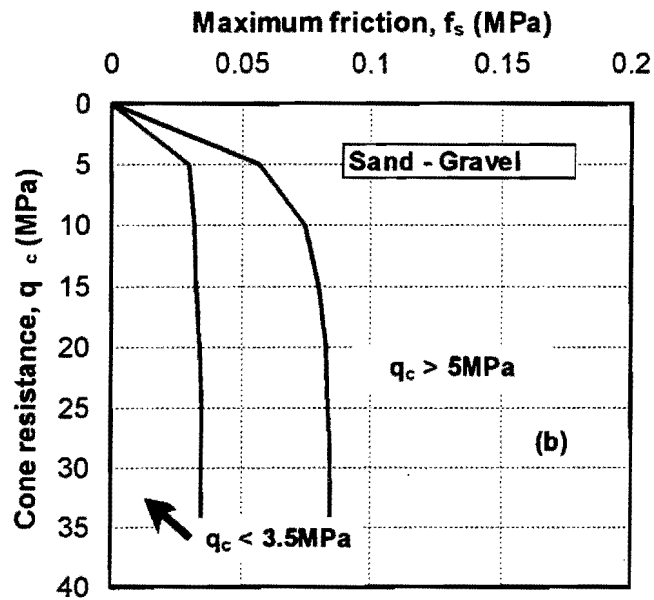
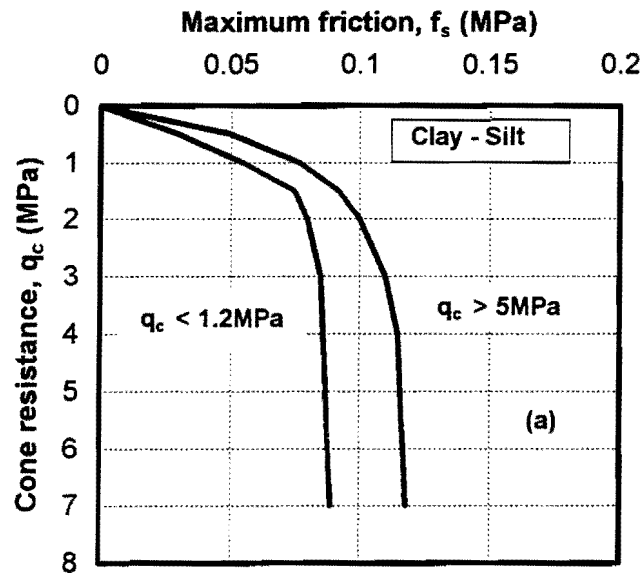


Figure 3.2. Maximum skin friction versus cone - tip resistance (LPC, 1981)
(a) cohesive soil (b) cohesionless soil

where

ΔQ_{si} = side resistance for each layer i of the pile,

A_{si} = $\pi D \Delta L_i$, and

ΔL_i = length of the pile in layer i .

The ultimate unit toe resistance, q_p , of a CFA pile by the LPC approach is given by the following expressions.

$$\text{For cohesionless soils:} \quad q_p = 0.15 q_c, \quad (3.9)$$

$$\text{For cohesive soils:} \quad q_p = 0.375 q_c. \quad (3.10)$$

In the database assembled herein, CPT data were available for only one case. For all other pile test sites, SPT data or laboratory test data for undrained shear strength were the only available soil strength test results. Schmertmann (1967) provided a correlation between q_c and N (SPT) from pile tests in Florida sands. According to Schmertmann (1967), the q_c value may be estimated by the following expressions.

$$\text{For sand:} \quad q_c \text{ (tsf)} = 3.5 N, \text{ and} \quad (3.11)$$

$$\text{For clay:} \quad q_c = s_u N_c + P_0, \quad (3.12)$$

where

s_u = undrained shear strength of the soil,

N_c = bearing capacity factor, usually taken as 17, and

P_0 = total overburden pressure at the center of the soil layer.

Commentary

Equations (3.11) and (3.12) were used to estimate the q_c values at the sites considered in this study. These correlations may provide (in some cases) good estimates of the q_c values, but the LPC method is not recommended for calculation of CFA pile capacities within TxDOT because these correlations have not been verified for Texas coastal soils and because TxDOT does not routinely use the cone penetrometer test.

3.2.4. FHWA (Reese and O'Neill) (1988)

Reese and O'Neill (1988) developed a design procedure for drilled shafts using an extensive database of drilled shaft load tests in both cohesive and cohesionless soils. At a given depth z along the pile (midpoint of a soil layer), the unit side resistance for a pile in sand is given by

$$f_s(z) = K P_0' \tan \phi, \quad (3.13)$$

where

P_0' = vertical effective stress at depth z (center of layer),

K = earth pressure coefficient, and

ϕ = angle of internal friction of the soil in the layer.

For design purposes the term $K \tan \phi$ is replaced by β , given as

$$\beta = K \tan \phi = 1.5 - 0.135 (z)^{0.5}, \quad 0.25 \leq \beta \leq 1.2, \quad (3.14)$$

where z is the depth in feet.

The unit toe resistance, q_p , is based on the N value from the in situ SPT at the toe of the pile, according to the following equations:

$$q_p \text{ (tsf)} = 0.6 N, \quad 0 \leq N \leq 75, \quad (3.15a)$$

$$q_p \text{ (MPa)} = 0.057 N, \quad 0 \leq N \leq 75, \text{ or} \quad (3.15b)$$

$$q_p = 4.3 \text{ MPa (45 tsf)}, \quad N > 75. \quad (3.16)$$

In the case of cohesive soils, the unit side resistance, $f_s(z)$, is determined by

$$f_s(z) = 0.55 s_u(z) \leq 0.26 \text{ MPa (2.75 tsf)}, \quad (3.17)$$

where $s_u(z)$ is the undrained shear strength of the soil in the center of a layer (depth z).

In the original method proposed by Reese and O'Neill, the uppermost 1.5 m (5 ft) in clay is assumed to carry zero side resistance for design purposes, since clay can shrink away from the pile near the surface. The lower 1.0 diameter along the pile (if in clay) is also eliminated because of base-side interaction. As applied to the analysis of the assembled database of CFA pile load tests, however, neither zone was considered as non-contributing. Near the surface the soil generally is protected by a thin grout layer after construction of test piles, which prevents the clay from drying out before a load test, so the noncontribution of the surficial soil to side resistance is probably not applicable to the load test conditions. In a CFA pile the bottom 1.0 diameter is a small distance and was not eliminated for convenience in making the computations. In design

practice, however, it is expected that designers would employ the non-contributing zones documented above.

Furthermore, the Reese and O'Neill method was applied on an average basis for side resistance computations. That is, f_{sa} was taken as $0.55 s_u$ (average along the pile) in cohesive soil profiles because for most load tests not enough undrained shear strength data were available to characterize the soil layer by layer, and Equation (3.2b) was used to make the calculations.

The unit end bearing resistance for piles in cohesive soils is determined as

$$q_p = N_c s_u \leq 3.8 \text{ MPa (40 tsf)} , \quad (3.18)$$

where N_c is a bearing capacity factor taken as 9, and s_u is the undrained shear strength of the soil in the vicinity of the pile toe.

3.2.5. Coyle and Castello (1981)

Coyle and Castello (1981) estimate the side resistance of piles driven in sand from Figure 3.3 using the angle of internal friction of the sand, ϕ , and the ratio of the pile's embedded depth, L , to its width, D . Coyle and Castello (1981) recommend that the angle of internal friction, ϕ , be obtained from Figure 3.4, the correlation given by Peck et al. (1974) for the number of blows N (from the SPT) vs. ϕ . In the case of silty sands below the water table, Coyle and Castello recommend that N -values from the SPT in excess of 15 be corrected to a value termed N' with the following expression and that N' be used in place of N in Figure 3.4.

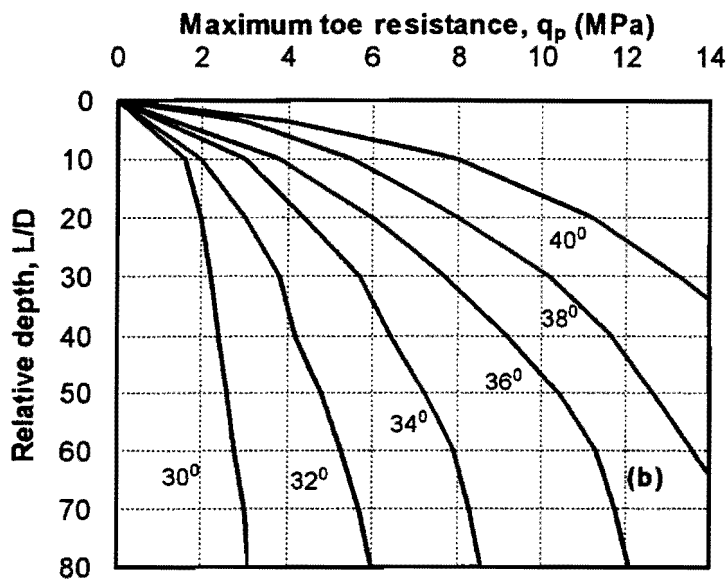
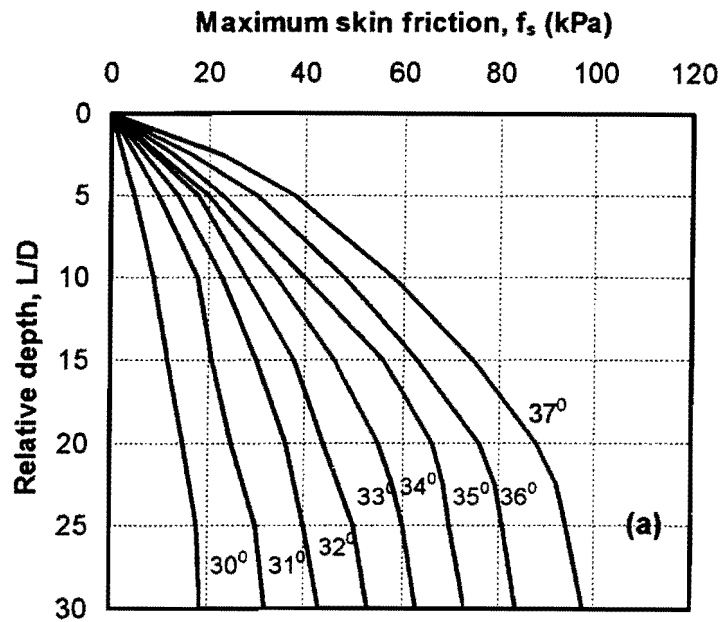


Figure 3.3. Coyle and Castello's pile capacity versus friction angle and embedment
(a) Maximum unit skin friction versus embedment
(b) Maximum unit end bearing versus embedment
Coyle and Castello (1981)

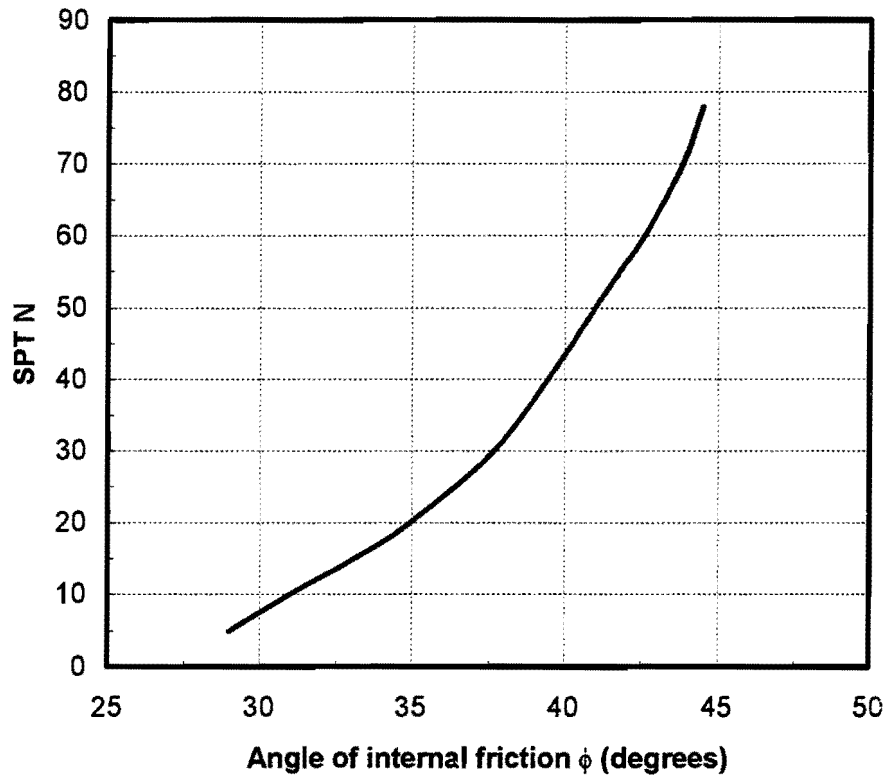


Figure 3.4. Correlation between angle of internal friction, ϕ , and standard penetration test N value (after Peck et al., 1974)

$$N' = 15 + 0.5 (N - 15) \quad (3.19)$$

From Figure 3.3 (a) unit skin friction can be obtained from ϕ and L/D . The unit end bearing, q_p , at the pile is estimated from Figure 3.3 (b) as a function of L/D and ϕ of the soil at the toe, where the maximum toe resistance should not exceed 9.58 MPa (100 tsf) for driven piles founded in sand.

In the case of clays Coyle and Castello (1981) recommended the use of Tomlinson's method (1957) where the average unit side resistance, f_{sa} , is given by

$$f_{sa} = \alpha s_{ua} \quad (3.20)$$

The α -factor, which varies between 0.2 and 1.0, is given in Figure 3.5 as a function of the average undrained shear strength, s_{ua} , of the clay layer along the pile.

The end bearing capacity, q_p , is given by

$$q_p = 9 s_u \quad (3.21)$$

where s_u is the undrained shear strength of the clay layer at the toe.

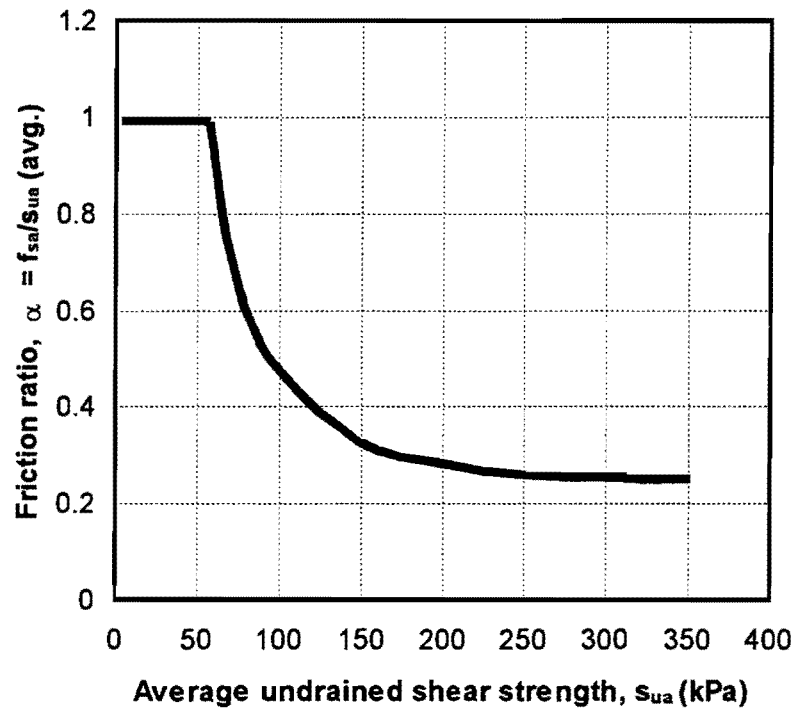


Figure 3.5. α - factor versus undrained shear strength of clay, per Tomlinson [Coyle and Castello (1981)]

3.2.6. API [2A-LRFD] (1993)

The API general equation for evaluating the ultimate bearing capacity of piles, Q_t , including belled piles, is applied using Equations (3.1), (3.2), and (3.3). Although the API method was developed to calculate the capacity of driven steel pipe piles, it is of interest to compare the predictions with other potential CFA pile design methods, where the CFA pile is viewed as analogous to a plugged, driven pipe pile.

Cohesive soils.

For piles in cohesive soils, the unit side resistance, $f_s(z)$, at any point along the pile is calculated by

$$f_s(z) = \alpha s_u(z) , \quad (3.22)$$

where

α = dimensionless correlation factor, and

$s_u(z)$ = undrained shear strength at depth z (center of a layer).

The α -factor is computed by

$$\alpha = 0.5 \psi^{-0.5} \quad \psi \leq 1.0, \text{ and} \quad (3.23)$$

$$\alpha = 0.5 \psi^{-0.25} \quad \psi > 1.0, \quad (3.24)$$

with the constraint that $\alpha \leq 1.0$,

where

$\psi = s_u(z)/\sigma'_0(z)$ for the depth of interest, and

$\sigma_0'(z)$ = vertical effective soil pressure at depth z (center of a layer).

For underconsolidated clays, the value α can usually be taken as 1.0.

In cohesive soils, the unit toe resistance, q_p , is computed by

$$q_p = 9 s_u , \quad (3.25)$$

where s_u is the value of undrained shear strength at the toe.

For piles considered to be plugged (as in the case of CFA piles), the end bearing pressure can be assumed to act over the entire cross section of the pile.

Cohesionless soils.

For pipe piles in cohesionless soils, the unit side resistance at depth z is

$$f_s(z) = K \sigma_0'(z) \tan \delta , \quad (3.26)$$

where

K = dimensionless coefficient of lateral earth pressure (ratio of horizontal to vertical normal effective stress), and

δ = friction angle between the soil and pile wall at depth z .

For open-ended pipe piles driven unplugged, it is usually appropriate to assume K as 0.8 for both tension and compression loading. Values of K for full displacement piles (plugged or closed-ended) may be assumed to be 1.0, which was the value used in analyzing the database. Table 3.1 is used for the selection of δ if other data are not available. The value of $f_s(z)$ does not indefinitely increase linearly with the overburden pressure. In such cases $f_s(z)$ is limited to the values given in Table 3.1.

For piles in cohesionless soils, the unit end bearing, q_p is computed by

$$q_p = \sigma_{ot}' N_q, \quad (3.27)$$

where

σ_{ot}' = vertical effective overburden pressure at the pile toe, and

N_q = dimensionless bearing capacity factor (Table 3.1).

3.2.7. TxDOT (1972)–Houston District

Cohesive soils.

1. Side resistance.

The TxDOT–Houston District design method for drilled shafts was used as a candidate design method. The side resistance (friction capacity) is based on the shear strength of the soils penetrated and the perimeter and the length of the pile or drilled shaft. The pile or drilled shaft length is therefore selected to be a function of its diameter, the design load and the shear strength of the various soil strata penetrated. The shear strength is determined by laboratory unconfined or undrained triaxial compression tests.

Table 3.1 Design parameters for cohesionless siliceous soils* (API, 1993)

Density	Soil Description	Soil-Pile Friction Angle(δ), degrees	Limiting Skin Friction Values, kPa (kips/ft ²)	N _q	Limiting Unit End Bearing Values, MPa (kips/ft ²)
Very loose Loose Medium	Sand Sand-Silt** Silt	15	47.8 (1.0)	8	1.9 (40)
Loose Medium Dense	Sand Sand-Silt** Silt	20	67.0 (1.4)	12	2.9 (60)
Medium Dense	Sand Sand-Silt**	25	81.3 (1.7)	20	4.8 (100)
Dense Very dense	Sand Sand-Silt**	30	95.7 (2.0)	40	9.6 (200)
Dense Very dense	Gravel Sand	35	114.8 (2.4)	50	12.0 (250)

* The parameters listed in this table are intended as guidelines only. Where detailed information such as *in situ* cone tests, strength tests on high quality samples, model tests, or pile driving performance is available, other values may be justified.

** Sand-Silt includes those soils with significant fractions of both sand and silt. Strength values generally increase with increasing sand fraction and decrease with increasing silt fraction.

The TxDOT–Houston District design method for drilled shafts implies an ultimate unit side resistance at depth z (center of a layer), $f_s(z)$, according to

$$f_s(z) = 0.7 s_u(z) , s_u \leq 120 \text{ kPa (1.25 tsf)}. \quad (3.28)$$

$s_u(z)$ is half of the compression strength of the soil at depth z (representing a layer of thickness Δz). When $s_u > 120$ kPa (1.25 tsf), s_u is taken equal to a limiting value of 120 kPa (1.25 tsf). TxDOT–Houston District ordinarily applies a factor of safety of 2 to obtain an allowable value from this equation. Therefore,

$$Q_s = \pi D \sum f_s(z) \Delta z, \quad (3.29)$$

where the summation is carried out over all layers (i) in the soil profile and

Q_s = ultimate side resistance (units of force),

$f_s(z)$ = ultimate unit side resistance at depth z (representing Layer i), and

Δz = thickness of Layer i .

As with the FHWA method, when the surficial soil layer is clay, $f_s(z)$ is taken as zero to a depth of 1.5 m (5 ft). This was not done when analyzing the CFA pile load tests in the database, however, for the reasons given Section 3.2.4. [It is expected that side resistance would be excluded in the top 1.5 m (5 ft) in normal design practice. A factor of safety of 2 is normally used for side resistance with this method].

2. Toe resistance.

The TxDOT–Houston District design method uses the blow count from a TxDOT dynamic cone penetrometer (N_{TxDOT}) and a net allowable end bearing resistance of $N_{\text{TxDOT}}/16.5$ (tsf) in stiff clays and sand-clay mixtures and uses a presumptive upper limit for allowable toe resistance in such clay soils [q_p (all.)] of 2.0 tsf. The equation for the limiting value that is used is:

$$q_p \text{ (all.)} = 2 \text{ tsf (0.19 MPa)}, \text{ or} \quad (3.30)$$

$$Q_p \text{ (all.)} = q_p \text{ (all.)} A_p. \quad (3.31)$$

While N_{TxDOT} values were not available for the load tests in the database, the clay soils at the pile toes were stiff enough, according to measured values of s_u , that the limit in Equations (3.30) and (3.31) were always applicable and were therefore used in the database calculations. End bearing was always included, regardless of the pile diameter.

Houston District design practice is to exclude end bearing in drilled shafts if the toe diameter is less than 0.61 m (24 in.). Because of the way CFA piles are constructed, which assures that end bearing is present, end bearing was included in the calculations. In design practice TxDOT engineers who use this method may still choose to eliminate end bearing, which would be conservative.

Assuming that the allowable value of end bearing is based on a factor of safety of 2, which is the usual practice in the Houston District,

$$Q_p (\text{ultimate}) = 2 Q_p (\text{all.}) . \quad (3.32)$$

Cohesionless soils.

Generally, the TxDOT design method is based upon visual soil classification and the TxDOT dynamic cone penetrometer test. If the TxDOT penetrometer test gives N_{TxDOT} values less than 45 blows per foot (0.3 m) without increase in the number of blows for the last 6 inches (0.15 m), the sand is in a loose state and would be a poor material in end bearing but would serve well in skin friction. If the penetrometer shows a marked increase in the number of blows for the second 6 inches (0.15 m) and N_{TxDOT} is above 45 blows per foot (blows / 0.3 m), the sand is reasonably dense, and the higher the value of N_{TxDOT} the better the material is in end bearing.

1. Side resistance

The value for the allowable unit side resistance, $f_s(z)$ (all.), for each sand layer in the profile is determined for the average value of N_{TxDOT} for the layer using Equation (3.33).

$$f_s(z)(all.) (tsf) = 0.7 [N_{TxDOT} / 80] , \quad N_{TxDOT}/80 \leq 120 \text{ kPa (1.25 tsf)} \quad (3.33)$$

The ultimate side resistance $f_s(z)$ is then given by

$$f_s(z) = 2 f_s(z) (all.) \quad (3.34)$$

The TxDOT cone penetrometer test was not used to characterize the soil for any of the historical load tests whose data were acquired for the database, although TxDOT cone penetrometer test data were acquired for the specific test sites at which new load tests were performed specifically for this project.

In the analysis of the load tests in the database, correlations could have been made between N_{SPT} and N_{TxDOT} , and pile capacities could then have been computed using the estimated values of N_{TxDOT} , since N_{SPT} values were always available at CFA pile test sites where sand layers existed. For example, a correlation is suggested by Touma (1972), and other correlations have been made by the Houston District. However, these correlations are extremely scattered and did not agree with the correlations made between SPT and TxDOT cone tests for this project at sites where new CFA piles were constructed.

This lack of correlation was undoubtedly caused by fundamental differences in the two types of dynamic penetration tests. The TxDOT cone test uses a solid steel cone penetrometer that is 76 mm (3 inches) in diameter, with a 60° apex, while the standard penetration test uses a blunt-ended split spoon penetrometer that is 51 mm (2 inches) in outer diameter and is hollow. While the energy per blow applied in both tests is similar, the TxDOT cone test uses a heavier hammer with a lower theoretical strike velocity than the standard penetration test. Methods for lifting and dropping the hammer may also be different. For example, commercial soil exploration companies often use the standard cathead and rope method, while TxDOT uses a semi-automatic trip hammer.

For this reason no comparisons were made between the ultimate capacities of CFA piles in the database computed by the TxDOT method and measured ultimate capacities if there was sand in the soil profile. The TxDOT method was used at two sites on which new CFA piles were installed and load tested, covered in Chapter 5.

2. Toe resistance

The allowable toe resistance of drilled shafts with bases in sand is computed from Equation (3.35).

$$q_p (all.) (tsf) = N_{TxDOT} / 11 \leq 2 \text{ tsf (0.19 MPa)} . \quad (3.35)$$

As with toes in clay, a 2 tsf (0.19 MPa) limit is applied. For the only CFA pile considered in this report whose toe was in sand (Rosenberg Test Pile, Chapter 4), N_{TxDOT} (at the toe) was 52. The limiting allowable value was applied in the calculations for the

ultimate resistance for that pile, using the TxDOT method, with a factor of safety of 2, resulting in a computed ultimate value of 4 tsf (0.38 MPa).

3.3. DATABASE

3.3.1. Sources of the database

A total of 43 CFA test piles were recorded in the database. Twenty-three of these CFA test piles are within the Texas coastal area and 20 CFA test piles are in the state of Florida. Among the 43 piles, there are 12 test piles in clay, 18 test piles in sand, and 13 test piles in mixed soil (clay - sand) profiles. Table 3.2 presents a list of the data source and location of each test pile.

Table 3.2 Database collection list

SOURCE	LOCATION	NUMBER OF TESTS
Berkel & Company	Kemah, TX	2
Berkel & Company	Brownsville, TX	1
Berkel & Company	Freeport, TX	1
L.G. Barcus and Sons	Port Arthur, TX	1
L.G. Barcus and Sons	Silsbee, TX	1
L.G. Barcus and Sons	Sugar Land, TX	2
L.G. Barcus and Sons	Port Lavaca, TX	1
L.G. Barcus and Sons	Mission, TX	1
L.G. Barcus and Sons	Nederland, TX	1
L.G. Barcus and Sons	Pasadena, TX	1
Eustis Engineering Company	Baytown, TX	2
L.G. Barcus and Sons	Athens, TX	1
Buchanan/Soil Mechanics	Galveston, TX	2
PSI, Inc., Houston	Freeport, TX	3
Mc Vay et al., (1994)	Florida	20
Berkel & Company	Bryan, TX	1

3.3.2. Format

Three tables were produced for each test in the database:

- *General information table.* This table includes the project ID, soil type(s), grout take and drilling time data, where available. An example is shown in Table 3.3.

Table 3.3 General information for test pile (example)

Project ID:	1KE/BE
Soil type:	Soft to stiff clay over medium dense sand
Date constructed:	8/6/97
Date tested:	8/13/97
Diameter (mm):	406.4
Depth (m):	21.34
Grout strength (7days)	
1. Cube (kPa):	
2. Cylinder (kPa):	
Grout strength (28days)	
1. Cube (kPa):	
2. Cylinder (kPa):	
Grout take (m ³)	3.65
Time of drilling	
1. Start:	
2. Finish:	
Time of grouting	
1. Start:	
2. Finish:	

- *Load-settlement data table.* This table gives values of load vs. settlement for the pile load test. An example is shown in Table 3.4.
- *Soil properties data table.* This table documents, as available, water table depth, SPT data, CPT data, dry unit weight (γ_d), water content (w), liquid and plastic limits (LL, PL), plasticity index (PI), undrained shear strength (s_u), and drained angle of internal friction and cohesion (ϕ' , c') An example is shown in Table 3.5.

Data regarding the distribution of resistance in side shear and toe bearing are not given in the database, since these data were not acquired in the load tests. One of the benefits of the load tests performed especially for this project is that the test piles were instrumented to permit discrimination of side shear and toe resistance. The database itself is in the "Excel" format and is maintained at the University of Houston.

Table 3.4 Load-settlement data (example)

Load (kN)	Settlement (mm)
0	0
222.5	0.46
445	1.14
667.5	1.98
890	3.0
1112.5	4.11
1335	5.66
1557.5	9.53
1780	25.91
1335	25.78
890	23.65
445	22.02
0	20.27

3.3.3. Failure criterion

Pile failure is defined as the applied load corresponding to a settlement of 5 % of the nominal diameter of the pile. Pile "capacity" is always based on this criterion.

3.3.4. Calculations from the database

Example of the calculation of pile capacity from soil conditions documented in the database are shown in Appendix A. Presented in Tables 3.6, 3.7, and 3.8 are the predicted capacities for 43 CFA piles for each of the design methods described earlier in this chapter

Table 3.5 Soil data (example)

SPT		CPT			TxDOT		Depth (m)	SOIL	γ_d (kN/m ³)	w (%)	LL (%)	PL (%)	PI	s_u (kPa)	ϕ' (deg)	c' (kPa)
Depth (m)	N_{SPT}	Depth (m)	q_c (kPa)	f_s (kPa)	Depth (m)	N_{TxDOT}										
Boring No. 1																
Location: 6.0 m from test pile																
Water table: 3.66 m during drilling, 1.7 m after 72 hours																
Comments: Dry Auger from 0 to 3.66m																
6.71		0.61	1254	51.7			0.61	C*								
7.92	2	1.52	1343.1	39.3			1.52	C								
19.51		2.13	1558.7	22			2.13	C	16.7	20				62.24		
21.95	17	2.9	1440.8	21.1			2.9	C								
23.16	53	3.66	699.3	8.6			3.66	C	15.7	25				31.12		
24.38	60	5.49	492.4	2.9			5.49	C		24	23		3			
		6.71	1277	1.9			6.71	C	14.3	32				10.05		
		7.92	2266.6	51.7			7.92	S**								
		9.45	1314.4	35.5			9.45	C	14.9	29				55.54		
		10.97	2307.8	49.8			10.97	C								
		12.8	2624.9	30.7			12.8	C	14.4	32				79.00		
		14.3	2894.1	90.1			14.3	C								
		15.8	3057	80.5			15.8	C	13.7	35				104.38		
		17.4	1925.6	37.4			17.4	C								
		19.5	3212.2	114			19.5	C	16.5	21				116.35		
		21.7	15567.5	27.8			21.7	S		18						
							23.16	S		22						

* : clay

** : sand

Table 3.6 Summary of measured and predicted capacities for CFA piles in clay

Predicted Capacities (kN)							Measured Capacities (kN) 5% Dia.
Project	Capacity	Coyle	API	LPC	FHWA	TxDOT	
2KE/BE	Q _s	964	914	1253	715	1036	
	Q _p	136	136	113	136	50	
	Q _t	1100	1050	1366	851	1086	1424
5FP/BE	Q _s	588	414	695	423	634	
	Q _p	109	135	86	109	50	
	Q _t	697	549	781	532	684	800
7PA/BS	Q _s	1811	2092	2558	1926	2673	
	Q _p	192	192	162	193	63	
	Q _t	2003	2284	2720	2119	2736	1770
13NL/BS	Q _s	898	508	894	453	694	
	Q _p	111	111	89	111	63	
	Q _t	1009	619	983	564	757	1400
14PA/BS	Q _s	843	738	1122	788	1454	
	Q _p	97	97	79	97	63	
	Q _t	940	835	1201	885	1517	2140
22BA/EU	Q _s	412	373	545	435	637	
	Q _p	77	77	60	77	28	
	Q _t	489	450	605	512	665	350
23BA/EU	Q _s	382	271	455	281	435	
	Q _p	70	70	54	70	28	
	Q _t	452	341	509	351	463	640
24AT/BS	Q _s	509	397	642	393	578	
	Q _p	176	176	134	176	50	
	Q _t	685	573	776	569	628	655
44TA/MCM	Q _s	1343	1269	1824	1414	1599	
	Q _p	169	119	116	196	38	
	Q _t	1512	1388	1939	1610	1637	1690
45TA/MCM	Q _s	1637	1721	2002	1984	2065	
	Q _p	196	119	133	222	38	
	Q _t	1833	1840	2135	2206	2103	2135

**Table 3.6 Summary of measured and predicted capacities for CFA piles in clay
(continued)**

Predicted Capacities (kN)							Measured Capacities (kN) 5% Dia.
Project	Capacity	Coyle	API	LPC	FHWA	TxDOT	
55PA/BS	Q _s	1020	933	1322	667	-	
	Q _p	113	113	94	113	-	
	Q _t	1133	1046	1416	780	-	1334
56PA/BS	Q _s	684	655	817	370	-	
	Q _p	81	81	68	81	-	
	Q _t	765	736	885	451	-	907

Note: Appropriate data were not available for computing pile capacities by the TxDOT method for the last two load tests in Table 3.6.

Table 3.7 Summary of measured and predicted capacities for CFA piles in sand

Predicted Capacities (kN)								Measured Capacities (kN) 5% Dia.
Project	Capacity	Wright	Neely	Coyle	API	LPC	FHWA	
25PB/MCM	Q _s	306	364	515	202	543	384	
	Q _p	208	593	478	329	164	187	
	Q _t	514	957	993	531	707	570	294
26TV/MCM	Q _s	418	390	666	245	809	496	
	Q _p	130	370	370	187	102	117	
	Q _t	548	760	1036	432	911	613	560
27VB/MCM	Q _s	765	553	731	419	653	858	
	Q _p	123	352	352	262	97	111	
	Q _t	888	905	1083	681	750	969	979
29ST/MCM	Q _s	494	555	700	274	679	539	
	Q _p	201	574	560	391	159	181	
	Q _t	695	1129	1260	665	838	720	667
30WH/MCM	Q _s	315	582	387	177	515	416	
	Q _p	188	537	387	342	148	169	
	Q _t	503	1119	774	519	663	585	783
31RU/MCM	Q _s	383	435	600	250	609	447	
	Q _p	131	373	410	273	103	118	
	Q _t	514	808	1010	523	712	565	694
32ST/MCM	Q _s	795	496	722	630	1018	920	
	Q _p	195	556	305	577	154	175	
	Q _t	990	1052	1027	1207	1172	1095	445
33ST/MCM	Q _s	347	397	669	262	743	418	
	Q _p	208	593	560	346	164	187	
	Q _t	555	990	1229	608	907	605	818
34TI/MCM	Q _s	761	532	651	342	920	724	
	Q _p	71	204	560	144	56	64	
	Q _t	832	736	1211	486	976	788	890

**Table 3.7 Summary of measured and predicted capacities for CFA piles in sand
(continued)**

Predicted Capacities (kN)								Measured Capacities (kN) 5% Dia.
Project	Capacity	Wright	Neely	Coyle	API	LPC	FHWA	
35ST/MCM	Q _s	1350	986	855	560	875	1217	
	Q _p	149	426	550	377	118	135	
	Q _t	1499	1412	1405	937	993	1352	1201
36TA/MCM	Q _s	764	637	455	459	530	923	
	Q _p	325	926	387	685	256	292	
	Q _t	1089	1563	842	1144	786	1215	1156
37JA/MCM	Q _s	383	697	335	222	362	486	
	Q _p	169	482	346	394	133	152	
	Q _t	552	1179	681	616	495	638	712
38SA/MCM	Q _s	914	631	918	564	955	993	
	Q _p	135	384	660	341	106	121	
	Q _t	1049	1015	1578	905	1061	1114	979
39ST/MCM	Q _s	679	594	928	379	742	789	
	Q _p	223	635	665	344	175	201	
	Q _t	902	1229	1593	723	917	990	890
40PA/MCM	Q _s	1006	598	1289	647	1020	979	
	Q _p	573	1633	1584	865	451	516	
	Q _t	1579	2231	2873	1512	1471	1495	1975
41CO/MCM	Q _s	469	555	607	305	529	571	
	Q _p	253	722	428	525	200	228	
	Q _t	722	1277	1035	830	729	799	979
42PO/MCM	Q _s	514	511	363	268	515	674	
	Q _p	266	259	377	515	210	82	
	Q _t	780	770	740	823	725	756	560
43PA/MCM	Q _s	614	511	847	366	804	674	
	Q _p	266	759	611	555	210	240	
	Q _t	880	1270	1458	921	1014	914	667

Table 3.8 Summary of measured and predicted capacities for CFA piles in mixed soil profiles

Predicted Capacities (kN)						Measured Capacities (kN) 5% Dia.
Project	Capacity	Coyle	API	LPC	FHWA	
1KE/BE	Q _s	1224	1199	1852	1030	
	Q _p	650	510	268	127	
	Q _t	1874	1709	2120	1157	1780
4BS/BE	Q _s	965	1172	1654	1213	
	Q _p	155	155	117	119	
	Q _t	1120	1327	1771	1333	1446
8SI/TE	Q _s	1112	1051	1243	1045	
	Q _p	1142	1091	265	302	
	Q _t	2254	2141	1508	1347	2090
9SL/MA	Q _s	1232	772	1048	765	
	Q _p	1642	1092	619	707	
	Q _t	2874	1869	1667	1472	1485
10SL/MA	Q _s	1675	1335	1494	1250	
	Q _p	1642	1392	619	707	
	Q _t	3316	2727	2113	1957	2135
11PL/BS	Q _s	509	529	823	622	
	Q _p	454	275	124	142	
	Q _t	963	804	947	764	925
12MI/BS	Q _s	545	481	652	710	
	Q _p	397	294	80	91	
	Q _t	942	775	732	801	1475
46GA/B/SMI	Q _s	508	377	462	395	
	Q _p	407	364	174	200	
	Q _t	915	741	636	595	680
47GA/B/SMI	Q _s	1035	700	1064	1230	
	Q _p	50	50	53	50	
	Q _t	1085	750	1117	1280	1470
48FP/BT	Q _s	926	702	986	749	
	Q _p	596	333	105	120	
	Q _t	1522	1035	1091	869	1245

Table 3.8 Summary of measured and predicted capacities for CFA piles in mixed soil profiles (continued)

Predicted Capacities (kN)						Measured Capacities (kN) 5% Dia.
Project	Capacity	Coyle	API	LPC	FHWA	
49FP/BT	Q_s	1516	1537	2009	1610	
	Q_p	103	103	82	103	
	Q_t	1619	1641	2091	1714	2135
50FP/BT	Q_s	1014	844	1145	1416	
	Q_p	103	103	80	103	
	Q_t	1117	947	1225	1519	1815
51BR/BE	Q_s	1193.4	1945.4	1648.3	2074.2	
	Q_p	283	283	208	283	
	Q_t	1476.4	2228.4	1856.3	2357.2	2556

using the soil information provided in the database, where Q_s is the predicted side resistance, Q_p is the predicted toe resistance, and Q_t is their sum. The "Project" notation is: pile number, followed by an abbreviation of the location (e. g., "PA" for Port Arthur)/ information source (e. g., BS for L. G. Barcus). Also given in Tables 3.6, 3.7, and 3.8 is the maximum measured capacity as determined from the load-settlement data (corresponding to a pile-head movement of 5 % of the pile diameter). The ratio of the measured to the predicted capacity (M/P) for each test pile is then presented in Tables 3.9, 3.10 and 3.11 along with the mean, the standard deviation (St. Dev.) and the coefficient of variation (COV) of the M/P ratio. The values of the mean, St. Dev., and COV were determined by the following equations.

$$\text{Mean} = \frac{\sum_{i=1}^n (M/P)_i}{n}, \quad (3.36)$$

$$\text{St. Dev.} = \sqrt{\frac{\sum_{i=1}^n [(M/P)_i - \text{Mean}]^2}{(n-1)}}, \quad (3.37)$$

$$\text{COV} = \frac{\text{St.Dev.}}{\text{Mean}}, \quad (3.38)$$

where

$(M/P)_i$ = the ratio of measured to predicted capacity for the test pile, and

n = the number of test piles.

Values of predicted vs. measured capacities are plotted in Figure 3.7 to Figure 3.23. Figure 3.6 to Figure 3.10 show CFA piles in clay; Figure 3.11 to

Table 3.9 Ratios of measured to predicted capacities of CFA piles in clay

Project	Coyle	API	LPC	FHWA	TxDOT
2KE	1.29	1.36	0.89	1.67	1.31
5FP	1.15	1.46	1.02	1.49	1.17
7PA	0.88	0.77	0.65	0.84	0.65
13NL	1.39	2.26	1.42	2.48	1.85
14PA	2.28	2.56	1.78	2.42	1.41
22BA	0.72	0.78	0.58	0.68	0.76
23BA	1.42	1.88	1.26	1.82	1.38
24AT	0.96	1.14	0.84	1.15	1.04
44TA	1.12	1.22	0.87	1.05	1.03
45TA	1.16	1.16	1.00	0.97	1.02
55PA	1.18	1.28	0.94	1.71	-
56PA	1.19	1.23	1.02	2.00	-
Mean	1.23	1.42	1.02	1.52	1.16
St. Dev.	0.39	0.55	0.33	0.60	0.35
COV	0.32	0.38	0.32	0.39	0.30

Table 3.10 Ratios of measured to predicted capacities of CFA piles in sand

Project	Wright	Neely	Coyle	API	LPC	FHWA
25PB	0.57	0.31	0.30	0.55	0.42	0.52
26TV	1.02	0.74	0.54	1.30	0.61	0.92
27VB	1.10	1.09	0.90	1.43	1.30	1.01
29ST	0.96	0.59	0.53	1.00	0.79	0.93
30WH	1.56	0.70	1.01	1.52	1.18	1.33
31RU	1.35	0.86	0.68	1.33	0.97	1.23
32ST	0.45	0.42	0.43	0.37	0.38	0.41
33ST	1.47	0.83	0.67	1.35	0.90	1.35
34TI	1.08	1.20	0.74	1.82	0.91	1.12
35ST	0.80	0.85	0.85	1.28	1.20	0.88
36TA	1.06	0.74	1.37	1.01	1.47	0.95
37JA	1.28	0.60	1.04	1.15	1.43	1.11
38SA	0.93	0.96	0.62	1.09	0.93	0.88
39ST	0.99	0.72	0.56	1.23	0.97	0.90
40PA	1.25	0.88	0.69	1.30	1.35	1.32
41CO	1.35	0.77	0.94	1.18	1.35	1.22
42PO	0.72	0.72	0.76	0.68	0.78	0.74
43PA	0.76	0.53	0.46	0.72	0.66	0.73
Mean	1.04	0.75	0.73	1.13	0.98	0.98
St. Dev.	0.31	0.22	0.26	0.36	0.34	0.27
COV	0.29	0.29	0.36	0.32	0.34	0.28

Table 3.11 Ratios of measured to predicted capacities of CFA piles in mixed soil profiles

Project	Coyle	API	LPC	FHWA
1KE	0.95	1.04	0.84	1.54
4BS	1.30	1.09	0.82	1.09
8SI	0.93	0.98	1.39	1.56
9SL	0.52	0.79	0.89	1.01
10SL	0.65	0.78	1.01	1.09
11PL	0.96	1.15	0.98	1.20
12MI	1.56	1.92	2.00	1.85
46GA	0.74	0.92	1.06	1.14
47GA	1.35	1.96	1.32	1.15
48FP	0.82	1.20	1.14	1.43
49FP	1.32	1.30	1.02	1.25
50FP	1.61	1.92	1.49	1.19
51BR	1.72	1.15	1.37	1.09
Mean	1.11	1.25	1.18	1.28
St. Dev.	0.39	0.42	0.33	0.25
COV	0.35	0.34	0.28	0.19

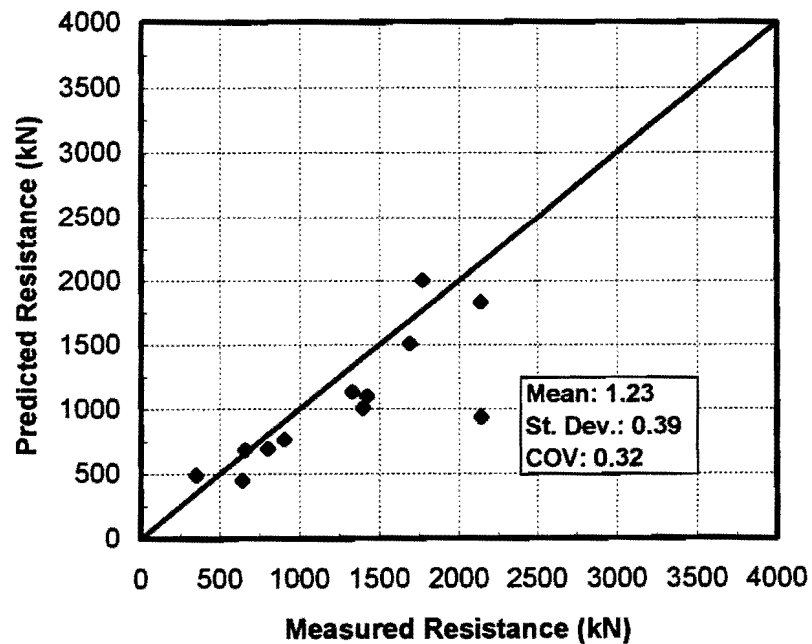


Figure 3.6. Coyle and Castello - Tomlinson method in clay

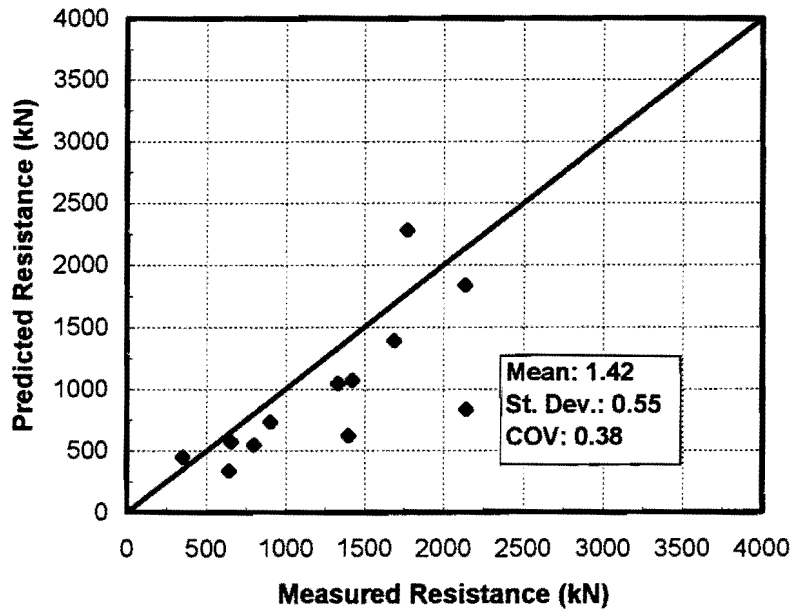


Figure 3.7. API method in clay

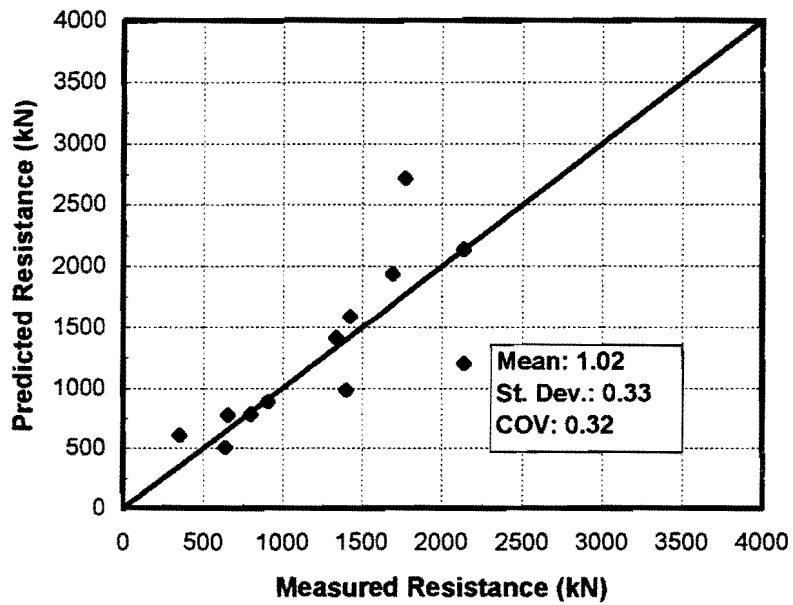


Figure 3.8. LPC method in clay

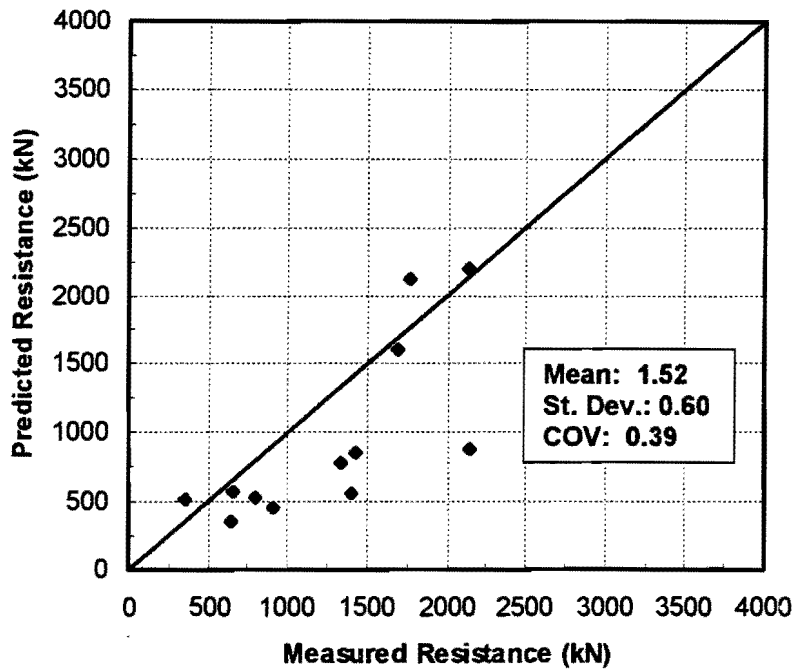


Figure 3.9. FHWA method in clay

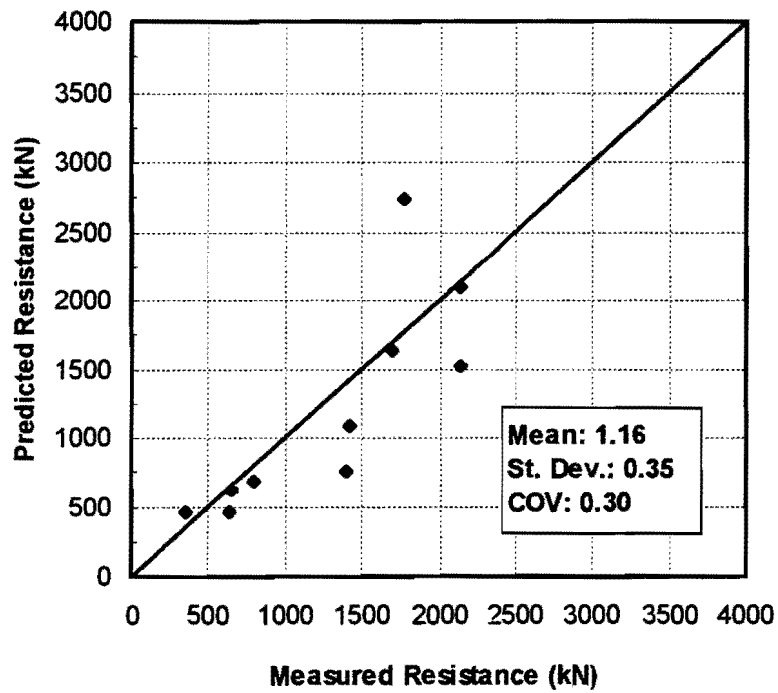


Figure 3.10. TxDOT method in clay

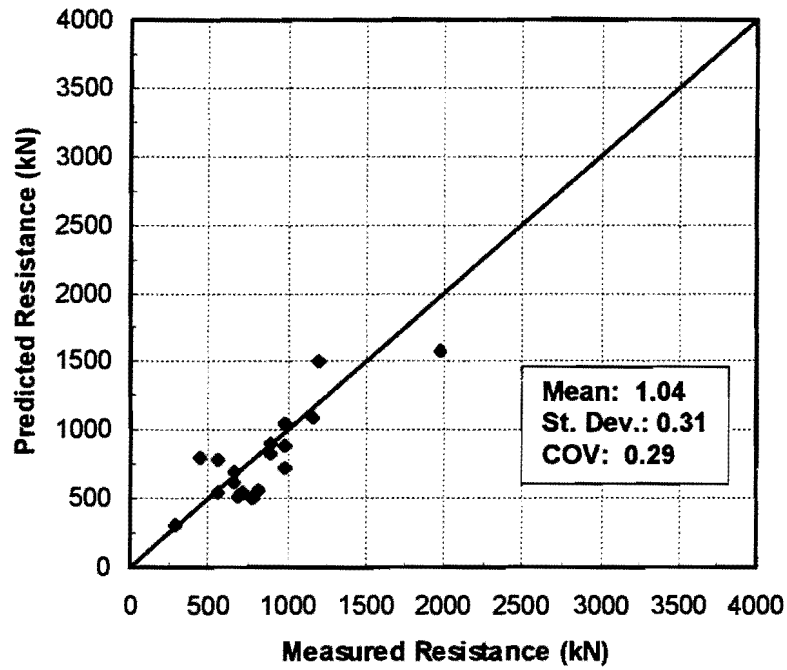


Figure 3.11. Wright and Reese method in sand

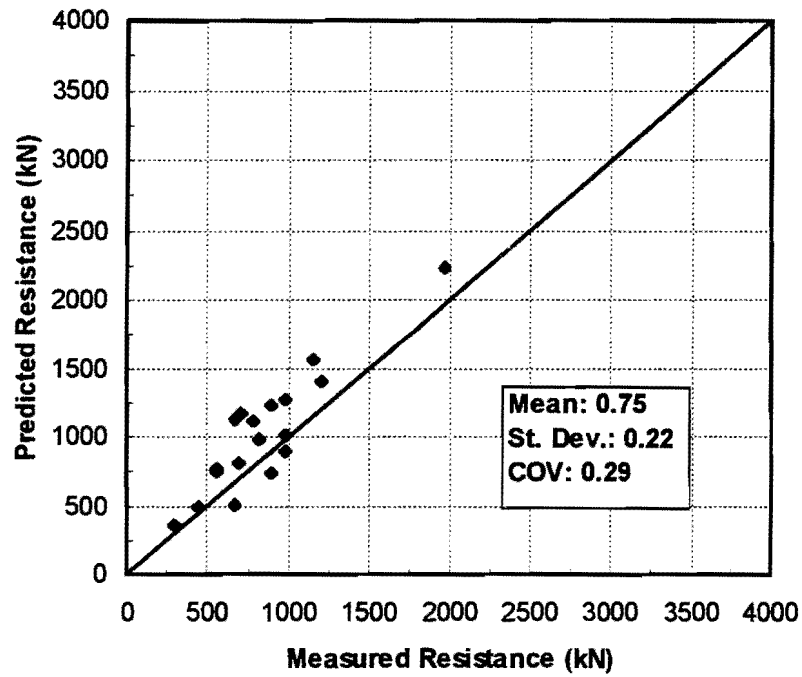


Figure 3.12. Neely method in sand

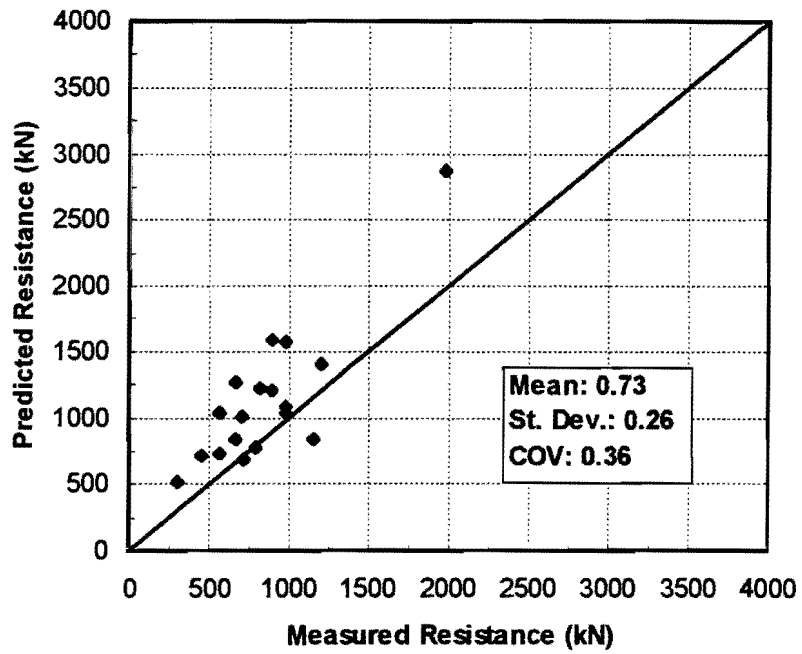


Figure 3.13. Coyle and Castello method in sand

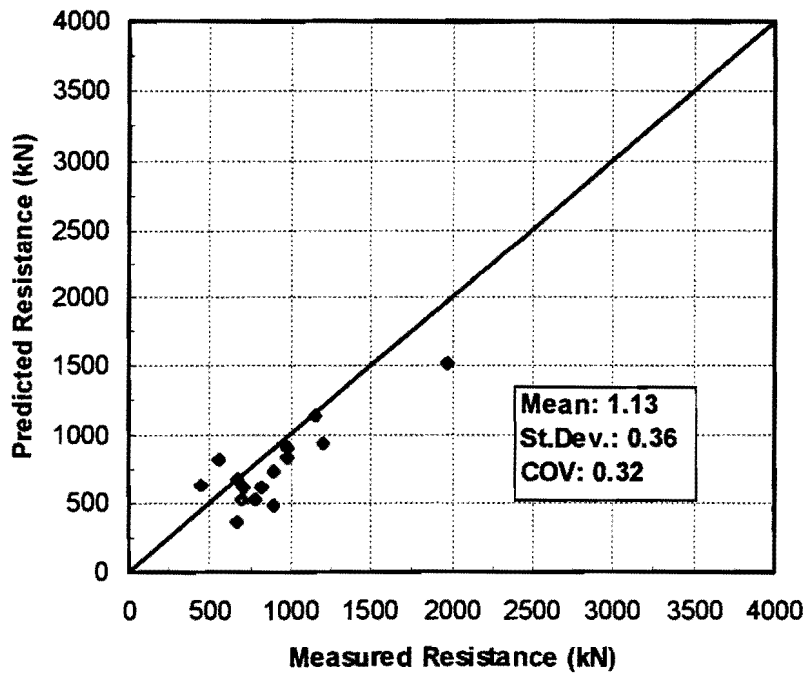


Figure 3.14. API method in sand

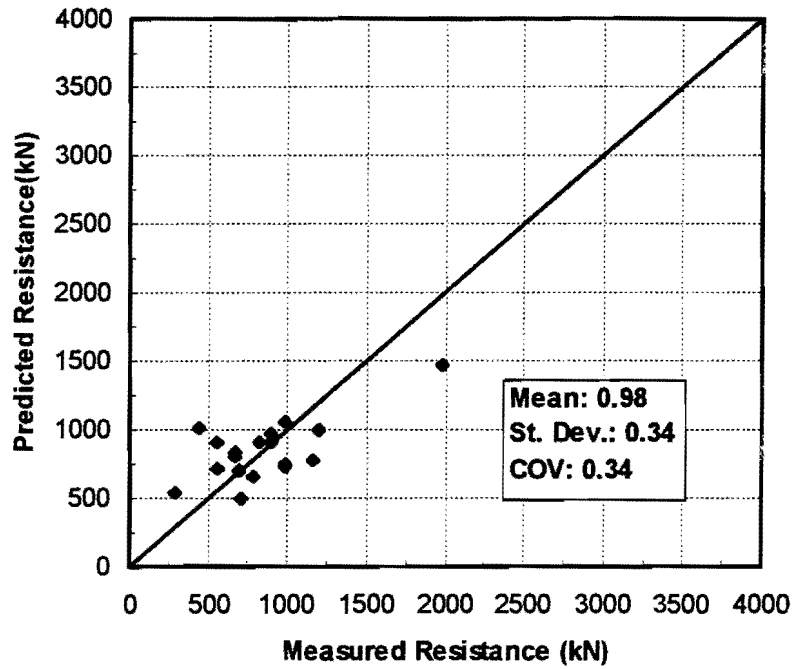


Figure 3.15. LPC method in sand

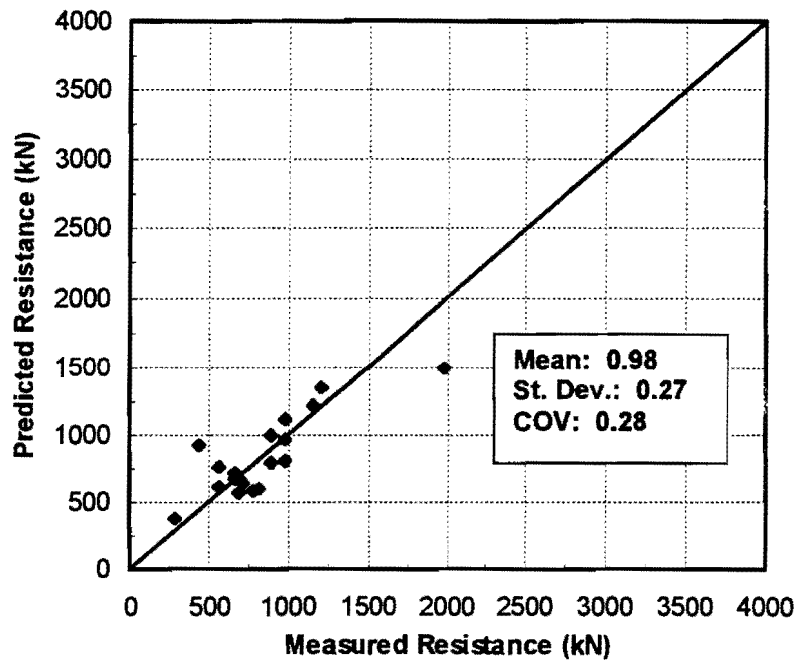


Figure 3.16. FHWA method in sand

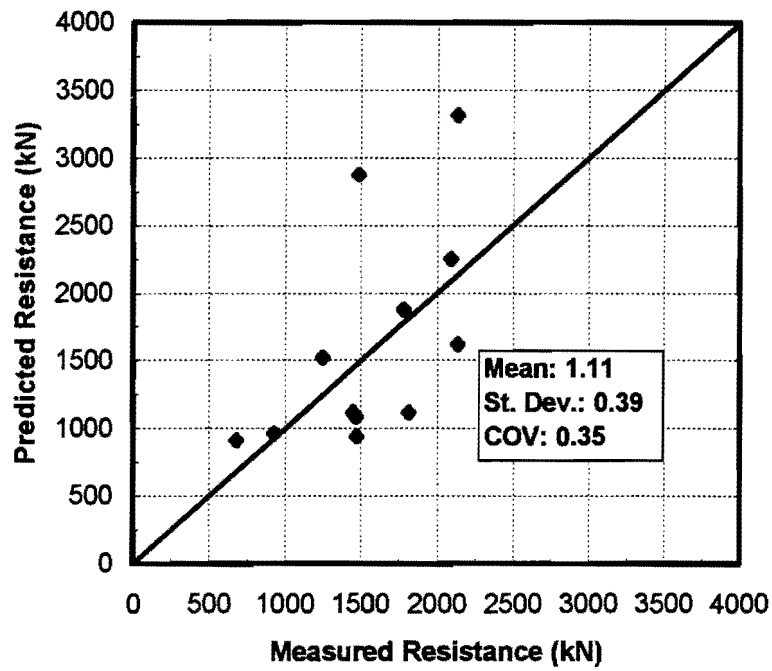


Figure 3.17. Coyle and Castello - Tomlinson method in mixed soil profiles

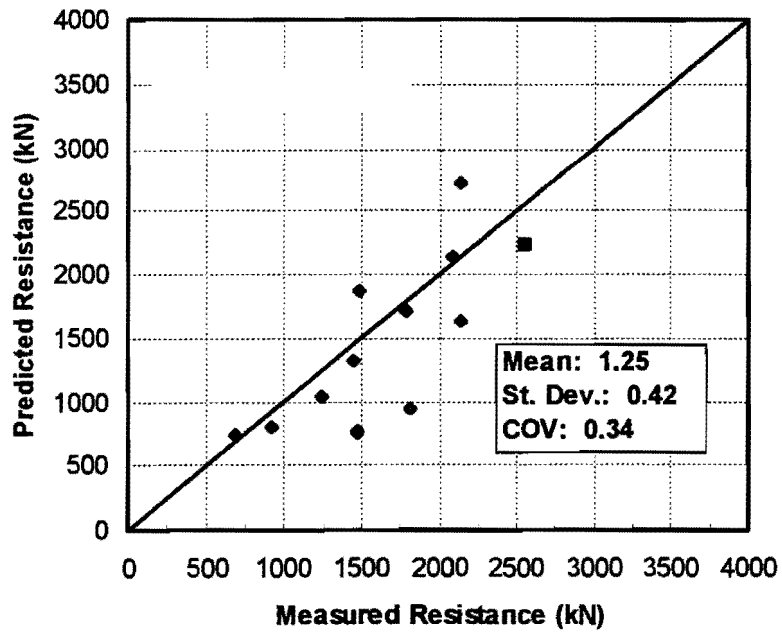


Figure 3.18. API method in mixed soil profiles

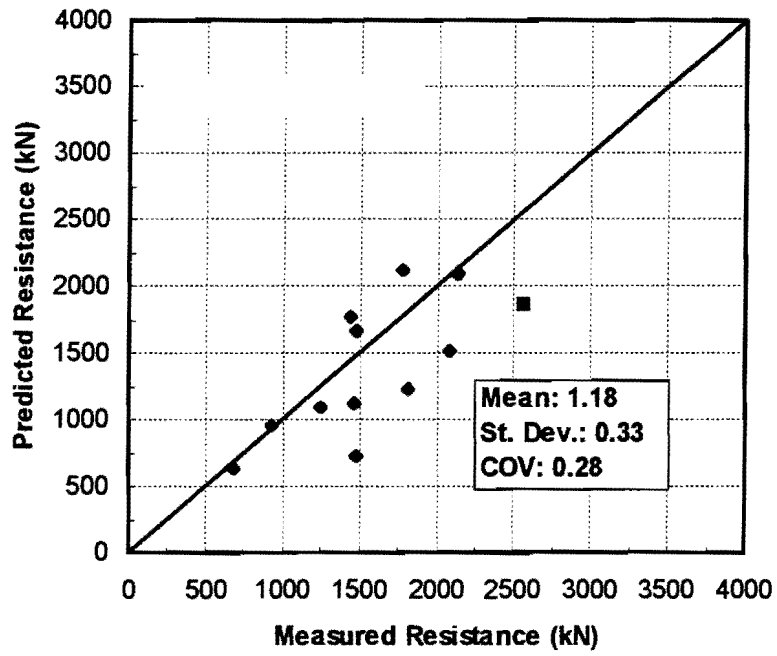


Figure 3.19. LPC method in mixed soil profiles

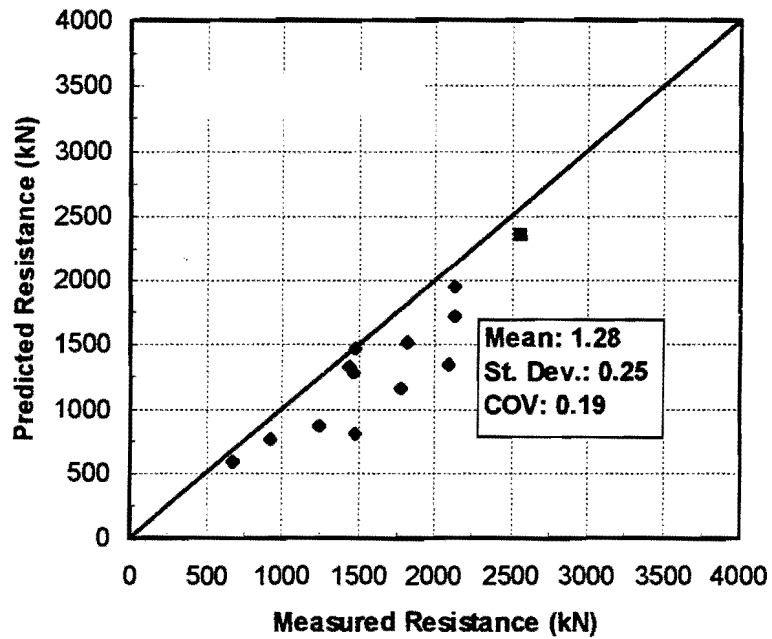


Figure 3.20. FHWA method in mixed soil profiles

Figure 3.16 show CFA piles in sand; Figure 3.17 to Figure 3.20 show CFA piles in mixed soil profiles.

3.4. COMMENTARY

Compilation of the database has permitted comparisons to be made between seven design methods and measurements of compressive resistances for 43 CFA piles (18 in sand, 12 in clay and 13 in mixed sand-clay soil profiles). Of the design methods examined, the LPC method (method based on the cone penetrometer test) consistently gave the most accurate predictions (method with the mean value of M/P nearest 1). Scatter (precision) in the LPC method, as measured by the coefficient of variation (COV), was generally equivalent to or slightly better than that of the other methods. It is conceivable that the inferred accuracy was fortuitous, because the CPT data that were input into the calculations were synthesized from SPT data (for sands) and laboratory compression test data (for clays), as described earlier in this chapter. For this reason, and because TxDOT does not routinely conduct CPT tests for bridge foundation design, this method will not be recommended; however, it is recommended that TxDOT consider performing CPT tests in the future at sites of CFA pile construction and load tests. If the method proves to be accurate and economical to perform, consider using the static cone as a foundation design tool in the Houston District.

At clay sites, the next most accurate method was the TxDOT method (Houston District) for drilled shafts. It tended to predict CFA pile capacity that was on the average about 16 % conservative, with a COV comparable to that of the LPC method. Since the load tests in the database did not include any instrumented piles, it is not

possible to state whether the conservatism was vested in side resistance or in base resistance. However, O'Neill (1998) reported, after analyzing numerous loading tests on drilled shafts with diameters of 0.76 m (30 in.) to 0.91 m (36 in.) in the Houston area, that ultimate toe resistance in drilled shafts has always been at least 0.96 MPa (10 tsf). This condition was observed even when the drilled shafts were constructed under poorly controlled bentonitic slurries and showed evidence of trapped sediments under the base when the shafts were exhumed. Considering the relatively minor differences in construction methods between drilled shafts and CFA piles, it seems unreasonably conservative to limit arbitrarily the unit toe resistance to 0.38 MPa (4 tsf) in Houston area soils.

The remaining five methods all seem to have merit in one or more types of soil profiles. In clay soil profiles (Table 3.9) which are common profiles in the Houston District, the driven pile method of Coyle-Castello-Tomlinson gave slightly more conservative, average predictions (mean value of measured to predicted capacity in Table 3.9) than the TxDOT method, with a similar COV. The API and FHWA methods were much more conservative than the LPC, TxDOT and Coyle methods in clay profiles in the Houston District. The FHWA and API methods also had much higher coefficients of variation than the other three methods — exceeding 0.35 in clay profiles. The coefficient of variation is significant because it reflects, along with the mean M/P ratio, at least qualitatively, the value of the factor of safety or geotechnical ultimate limit state resistance factor that should be used in design. This issue will be covered later in this report. Overall, the TxDOT (Houston District) drilled shaft method appears to be

appropriate for estimating the ultimate capacity of CFA piles for axial load in clay soil profiles.

Purely sand profiles are relatively uncommon in the Houston District, although occasional sites have such profiles. Much of the sand site data came from load tests conducted in Florida. For sand profiles the TxDOT method was not tested against the database for reasons described earlier. Of the remaining methods, excluding the LPC method based on the static cone penetrometer test, the FHWA and Wright/Reese methods were the most accurate (had means of M/P closest to 1). See Table 3.10. Both methods also had similar coefficients of variation. The FHWA method was slightly more accurate and is easier to apply; therefore, the FHWA method is recommended for use in the design of CFA piles in purely sand profiles pending the establishment of a reliable database of CFA pile tests that are performed at sand (and mixed sand-clay) sites where TxDOT cone tests are also performed. Two such tests (in mixed sand-clay profiles that were mostly sand) are described later in this report.

In mixed soil (clay-sand) profiles, the most accurate method was the Coyle-Castello-Tomlinson method (Table 3.11). In fact, that method was slightly more accurate in terms of the mean value of M/P than even the LPC method. The FHWA method had a mean value of M/P of 1.28, which made it the most conservative of the four methods examined in mixed clay-sand profiles. However, in mixed soil profiles, the lowest coefficient of variation was clearly achieved with the FHWA method, which, because of its relative reliability may make this method more consistent with the factors of safety that are commonly used by TxDOT for piles and drilled shafts (a value of 2). The issue of appropriate values of factors of safety and resistance factors that should be

considered for CFA piles in the Houston District, considering the performance of the piles in the database and new piles tested for this project (Chapter 4), are addressed in Chapter 5 for selected design methods.

This page is intentionally blank.

CHAPTER 4 FIELD TESTS

4.1. GENERAL INFORMATION

In order to resolve issues regarding the ability of the design methods to predict both side resistance and toe resistance accurately in various soil profiles found in The Houston District of TxDOT, three instrumented test piles were constructed and subjected to loading tests.

- The first of these piles was installed at the National Geotechnical Experimentation Site at the University of Houston (NGES-UH), which consists of a clay soil profile. The clay has been preconsolidated.
- The second was installed just west of the north approach to the Fred Hartmann Bridge (SH 146) in Baytown, Texas, in a mixed soil profile containing a significant thickness of very loose, waterbearing fine sand.
- The third was installed along US 90A west of Rosenberg, Texas, at a site that consisted of a surficial layer of clay overlying loose to dense moist sand entirely above the water table (mixed soil profile).

These three soil profiles are considered to represent typical (NGES-UH) and extreme (Baytown and Rosenberg) sites in The Houston District regarding both impediments to construction and prediction of capacity of CFA piles. Installation details for both the test piles and reaction piles (four per test pile) were observed and recorded, and the three test piles were loaded axially in compression to plunging failure. Loading tests were of the "Texas Quick Method" type, in which small increments of load are

added to the head of the pile by means of a calibrated hydraulic jack every three to four minutes until the pile plunges.

Pile installation was monitored both manually and by use of a Pile Installation Recorder™ (PIR) (proprietary product of Pile Dynamics Incorporated). Manual observations included times of drilling and grouting, rate of penetration and rotation of the auger, grout volume placed versus depth of the auger tip (by counting pump strokes, performed by Fugro-McClelland Southwest, Inc.) and lateral effective pressure in the soil at a depth of 3.0 m and approximately one diameter away from the pile versus auger tip elevation (on test piles only). PIR monitoring included continuous measurement of the volume of grout placed versus auger tip elevation, using a magnetic flowmeter and a rotational potentiometer, and continuous measurement of the pressure in the grout line at either the pump outlet on the ground surface or at the tip of the auger. The PIR was used on all three test piles, all four reaction piles at the NGES-UH and two reaction piles at Rosenberg. Cross-hole sonic logging was used to investigate the integrity of the grouting process for all three test piles. Single-hole sonic logging was also attempted in three of the reaction piles at the NGES-UH; however, those tests were unsuccessful.

The test piles were instrumented by tying calibrated sister bars to the reinforcing steel cages that were thrust into the grout immediately after the test piles were grouted. The sister bars were constructed from #4 deformed steel reinforcing bars, 0.914 m (3 ft) long, and turned on a lathe in the middle to accept bonded foil strain gauges wired to form full Wheatstone bridges and protected by several layers of waterproofing. The sister bars were calibrated in a testing machine in the laboratory before they were

installed in the field. Two sister bars were placed at each load-measurement elevation on the cage to cancel the effects of bending.

Lateral effective pressures were measured in the soil by means of thin circular steel diaphragms that were instrumented with bonded foil strain gauges. The diaphragms had diameters of 102 mm (4 in.) and were fixed to thick steel rings around their edges. One side of the diaphragm cell was placed directly against the soil, while a protective filter was placed on the other side to allow only water pressure to act on the instrumented diaphragm. Therefore, the differential pressure that was registered was always an effective pressure. The cells were placed facing horizontally at the bottoms of 3-m-deep (10-ft-deep) boreholes, 152 mm (6 in.) in diameter. The zone around the cell was backfilled with tamped ASTM C-33 sand to a depth of 0.3 m (1 ft), and the remaining portion of the borehole was backfilled with excavated material. The lateral pressure cells were calibrated in the laboratory with known water pressures acting on one side of the cell before and after they were used in the field.

4.2. SITE CONDITIONS

4.2.1. NGES-UH site

The NGES-UH is a well-known test site for foundations. It is a microdelta depositional site of Pleistocene age within the Beaumont formation. A sketch map of the NGES-UH test site is shown in Figure 4.1. The test pile layout is shown in Figure 4.2. A soil boring log is shown in Figure 4.3. N_{TxDOT} , N_{SPT} , undrained shear strength s_u , and soil classification are listed on the log. The ground water was encountered at a depth of 2.1 m (7 ft) below the existing ground surface after completion of the boring.

4.2.2. Baytown site

The Baytown test site is located near the Fred Hartmann Bridge on State Highway 46 in Baytown, Texas. Figure 4.4 shows the location of the test site, and Figure 4.5 shows the pile layout. Four boring logs were available, located on Figure 4.4. Boring 6 was used to define the soil conditions for the test pile because it is closest to the test pile. The boring is shown in Figure 4.6. The boring initially encountered a stratum of brown silty clay to a depth 0.9 m (3 ft) below the existing ground surface. This was compacted fill for an old road. The underlying sand is natural alluvium from the San Jacinto river. The ground water level was about 3.0 m (10 ft) below the ground surface upon the completion of the boring. This coincided with the water level in the adjacent estuary.

4.2.3. Rosenberg site

The Rosenberg test site is located just south of the intersection of the new alignment of State Highway 36 and US Highway 90A, approximately four miles west of Rosenberg, Texas (Figure 4.7). Three boring logs in the immediate area were available. These logs were denoted Boring logs 901, 902 and 903. Boring log 902 was used to represent the soil conditions at the site of the test pile, since it was closest to the test pile. The layout of the test pile and reaction piles is shown in Figure 4.8, and the log of boring 902 is reproduced in Figure 4.9. The sand in the split spoon test at a depth of 10.7 m (35-ft), which was 1.5 m (ft) below the toe of the test pile, appeared to be cemented. No free water was encountered. The sand was moist and generally free of fines.

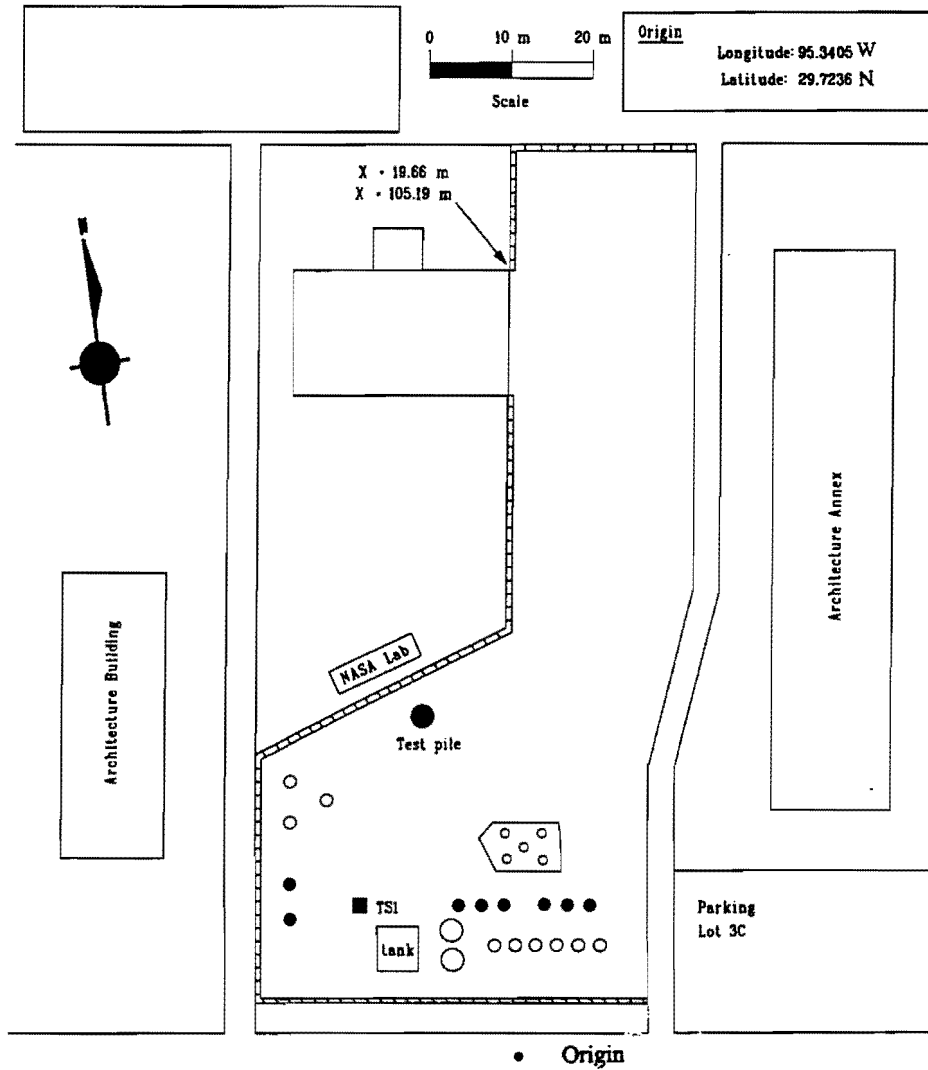


Figure 4.1. Sketch map of UH test site

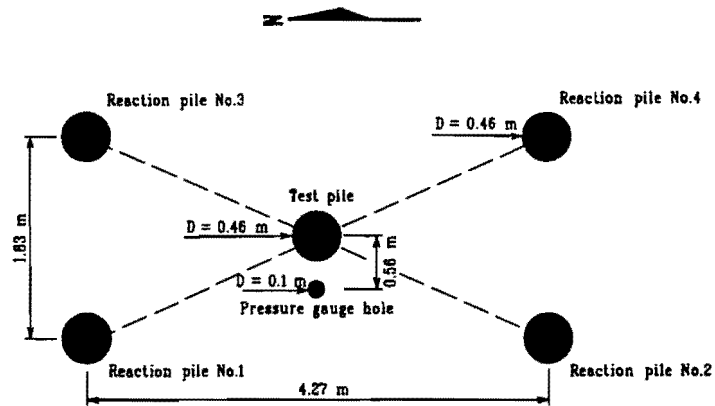



Figure 4.2. Layout of test pile and reaction piles (UH)

Depth (m)	Log	N_{TxDOT} (Blows/0.30 m)	N_{SPT} (Blows/0.30 m)	s_u (kPa)	Soil classification
1.5			5	65.1	SANDY CLAY, RED WITH SILTY SAND LAYERS
3.0		20	11		
4.6		16	12		
6.1		18	18		
7.6		18	18	103.5	SANDY CLAY, TAN, BECOMING VERY SANDY BELOW 10.7 M
9.1		36	7		
10.7		28/0.13 m	18		
12.2		56	34		
13.7		37	23	136	CLAY, SANDY, RED
15.2		52	18		SANDY CLAY
16.8	32				
18.3	100/0.24 m				
19.8	61/0.10 m				

Toe of test pile

Figure 4.3. Boring log for UH test site

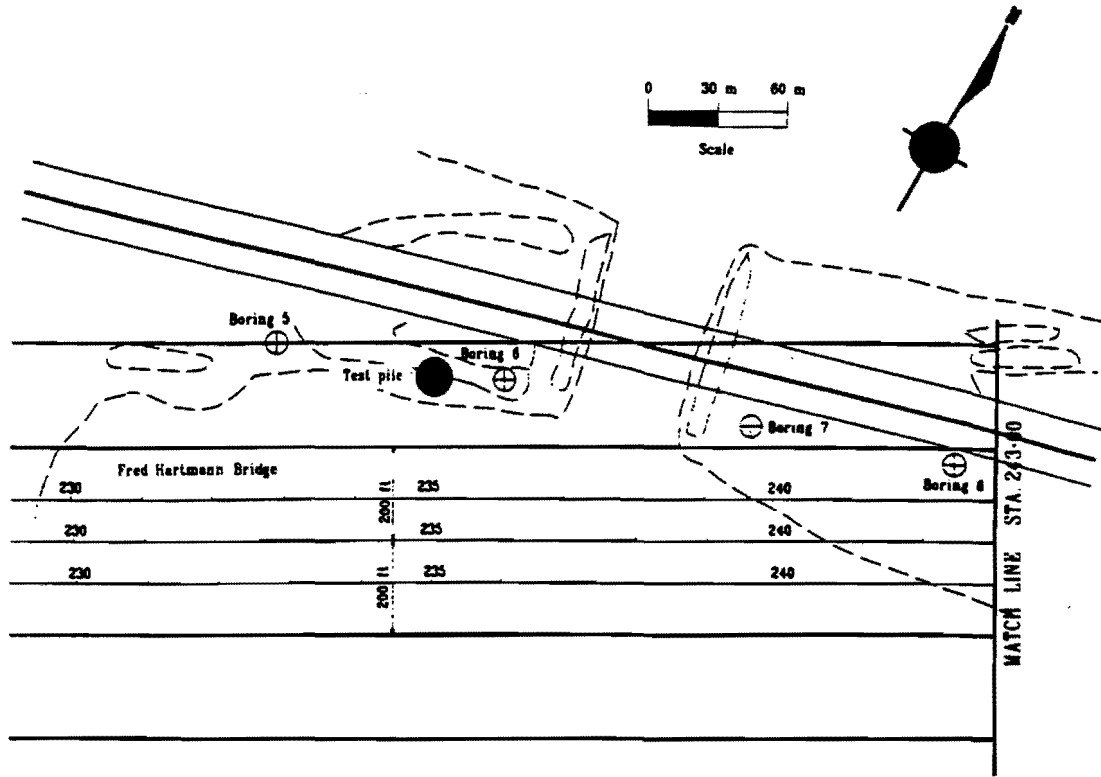


Figure 4.4. Sketch map of Baytown test site

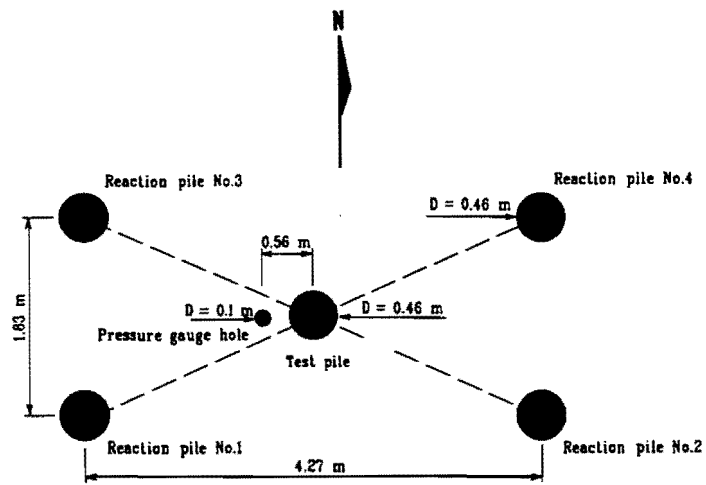

















Figure 4.5. Layout of test pile and reaction piles (Baytown)

Depth (m)	Log	N_{TxDOT} (Blows/0.30 m)	N_{SPT} (Blows/0.30 m)	s_u (kPa)	Soil classification	
1.5			50/0.27 m	104.7	BROWN SILTY CLAY	
3.0		29	71		SAND, TAN, FINE	
4.6		24	27			
6.1		1	10			
7.6		6	2			
9.1		3	2			
10.7		5	10			
12.2		39	17			
13.7		39	5			
15.2		30	50/0.25 m	104.7		CLAY, TAN, BROWN
16.8		34				SANDY CLAY, TAN, BROWN
18.3		35				
19.8		52		104.7		
21.3		72				
22.9		64				

Toe of test pile

Figure 4.6. Boring log for Baytown test site

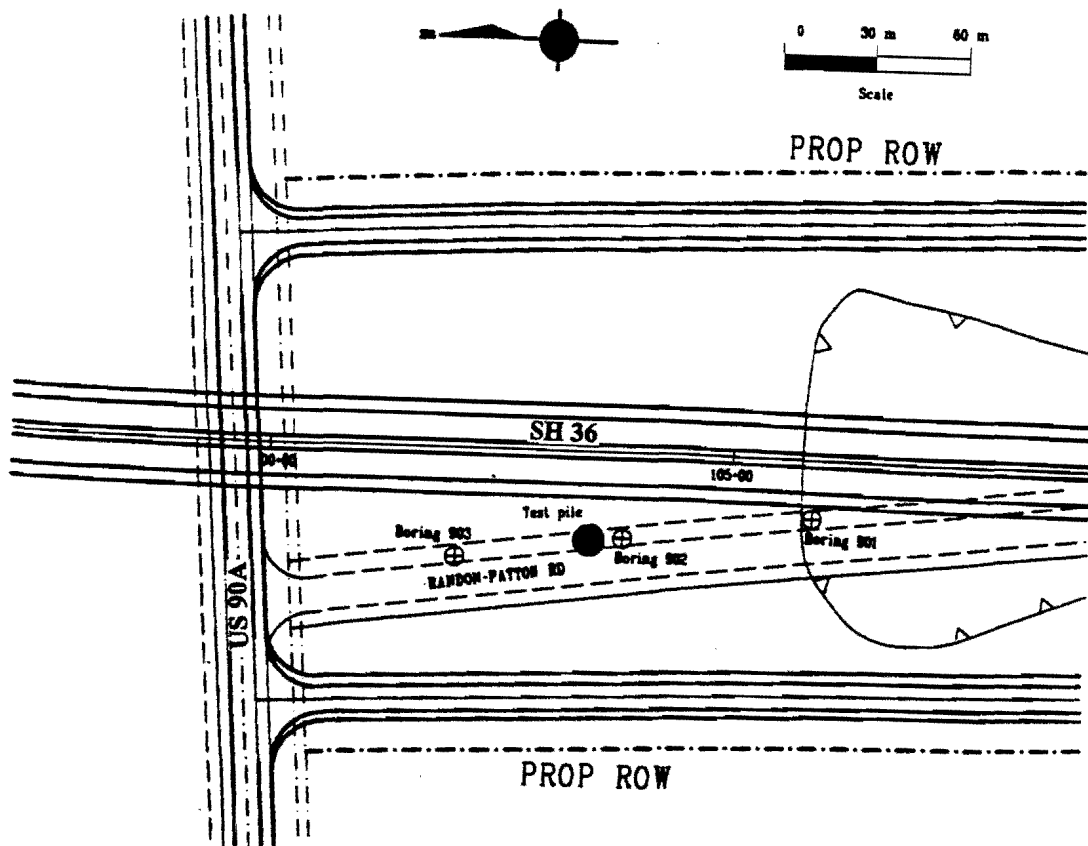


Figure 4.7. Sketch map of Rosenberg test site

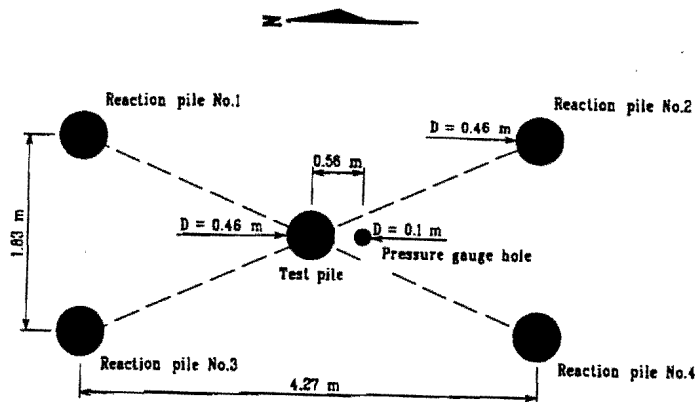






Figure 4.8. Layout of test pile and reaction piles (Rosenberg)

Depth (m)	Log	N_{TxDOT} (Blows/0.30 m)	N_{SPT} (Blows/0.30 m)	s_u (kPa)	Soil classification
1.5		14	25	95.7	CLAY, GRAY AND TAN, SANDY
3.0		21	41	95.7	CLAY, SANDY, BROWN AND GRAY
4.6		14	21		SAND, BROWN, SL COMPACT
			23		
			25		
6.1		9	26		
7.6		35	45		SAND, BROWN
9.1		52	50/0.25 m		SAND
10.7		100/0.13 m	50/0.17 m		
12.2		43			
13.7		65			
15.2		73			
16.8		70			
18.3		100/0.24 m			
19.8		100/0.12 m			
21.3		66			
22.9		27			

Toe of test pile

No water encountered

Figure 4.9. Boring log for Rosenberg test site

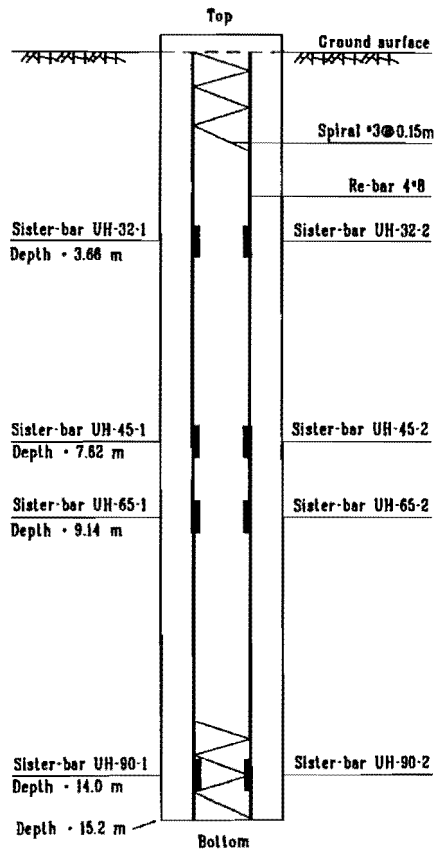
4.3. CONSTRUCTION OF TEST PILES

The test piles and the reaction piles were installed by Berkel and Company Contractors, Inc., of Bonner Springs, Kansas. The three test piles were surrounded by the reaction piles, as shown in Figures 4.2, 4.5 and 4.8. At the UH and Baytown test sites, the diameter of the test pile was 0.46 m (18 in.) and the length was 15.2 m (50 ft). The diameter and length of reaction piles were 0.46 m (18 in.) and 12.2 m (40 ft). At the Rosenberg test site, the test pile diameter was 0.46 m and the length was 9.1 m (30 ft); the diameter and length of the reaction piles were 0.46 m (18 in.) and 9.1 m (30 ft). The long distance between reaction piles was 4.27 m (14 ft), the short distance is 1.83 m (6 ft).

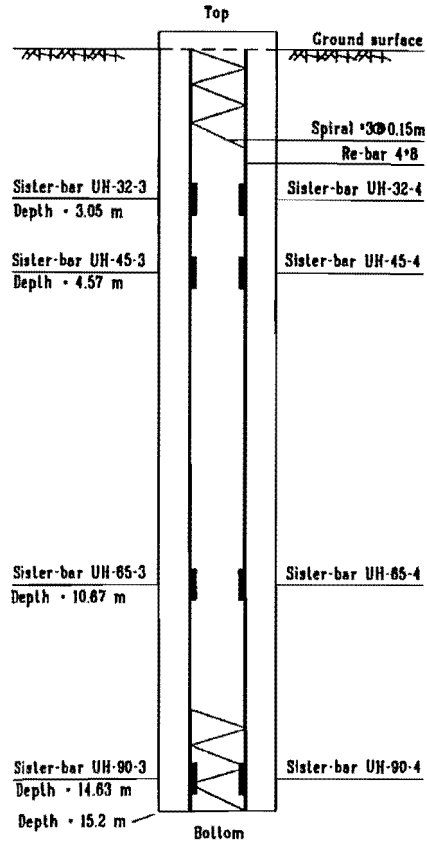
The longitudinal reinforcing steel used was four, # 8 grade 60 steel deformed bars for each test pile, which represents about one percent steel for all test piles, and which is the standard TxDOT minimum.

In order to determine the load distribution along a test pile during an axial load test, eight sister bars were arranged for each test pile. The locations of those sister bars are shown in Figure 4.10.

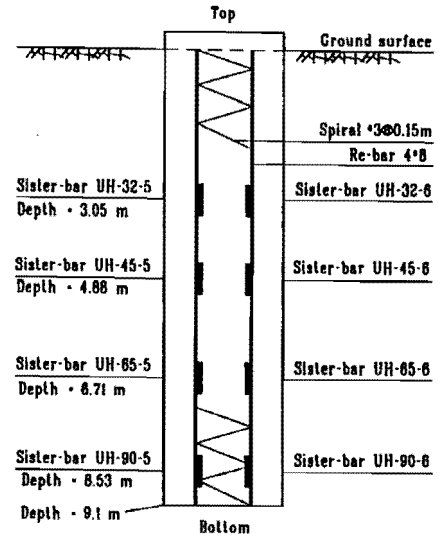
The test piles were installed by rotating a continuous hollow-stem flight auger into the ground until a specified depth was achieved and pumping sand-cement grout through the auger stem under pressure as the auger was slowly withdrawn to fill the drilled hole. The proportions of the grout materials used in all test piles are presented in Table 4.1. The mechanical and material properties of grout are given in Table 4.2, and



(A) UH



(B) BAYTOWN



(C) ROSENBERG

Figure 4.10. Schematic of steel cage and sister bars at three sites

construction data relative to pile installation and testing are listed in Table 4.3. Further information on the long-term behavior of this grout is given in Appendix D.

Table 4.1 Grout mix proportions for the test piles

Constituent	Amount (kN/m³)
Cement (Type I portland)	4.38
Sand (ASTM C-33)	12.92
Fly ash	1.31
Water	2.43
Additive (Fluidizer)*	0.022
Non-shrink additive	None

* Proprietary product of Berkel and Company

Table 4.2 Material properties of the grout for the test piles

Material property	Test results		
	UH	Baytown	Rosenberg
Setting time (hours)	5.3	5.8	6.0
Shrinkage (ASTM C 1090)	0.015%	0.015%	0.015%
Efflux time (ASTM C 939)	24 sec.	12 sec.	28 sec.
Compressive strength (after 28 days) -Standard 3" x 6" plastic mold	23.2 MPa	30.8 MPa	33.1 MPa
Modulus of grout (GPa)	19.3	21.4	24.8

Table 4.3 Installation of test piles

UH test pile	Baytown test pile	Rosenberg test pile
DC 17 March 98	DC 24 March 98	DC 8 April 98
SD 0243	SD 1119	SD 1055
FD 0250	FD 1126	FD 1058
SG 0250	SG 1126	SG 1109
FG 0255	FG 1134	FG 1113
DT 5 May 98	DT 7 May 98	DT 9 May 98

Notes: DC Date pile constructed
SD Time drilling started
FD Time drilling completed
SG Time grouting started
FG Time grouting completed
DT Time pile tested

The properties of the CFA pile rig used in constructing test and reaction piles are listed in Table 4.4.

Table 4.4. Properties of the CFA pile rig

Property	Value	
Maximum torque (kN-m)	51.5	
Horsepower	325	
Gear box (weight, kN)	22.3	
Pitch of the auger (m)	0.261 (10.5 in.)	
Diameter of the stem of the auger	Outside (m)	0.099 (3.9 in.)
	Inside (m)	0.074 (2.9 in.)

Figure 4.11 shows the penetration velocity of the auger during augering and grouting for the three test piles. The average downward rate of penetration of the auger for the UH, Baytown and Rosenberg test piles was 2358.6 mm/min, 2824.8 mm/min and 2373.0 mm/min, respectively. While installing the Rosenberg test pile, some difficulty was encountered with one of the PIR instrument leads between auger tip depths of 2.5 and 4.0 m, and augering was temporarily stopped to fix the problem. Penetration velocity data were lost in that depth interval.

Van Impe et al. (1991) recommended that the speed of penetration of the auger, v , be at least as high as the value given by the following equation to prevent mining of soil surrounding the pile being installed.

$$v \geq np (1 - d_0^2 / d^2), \quad (4.1)$$

where v is expressed of units of length per minute and

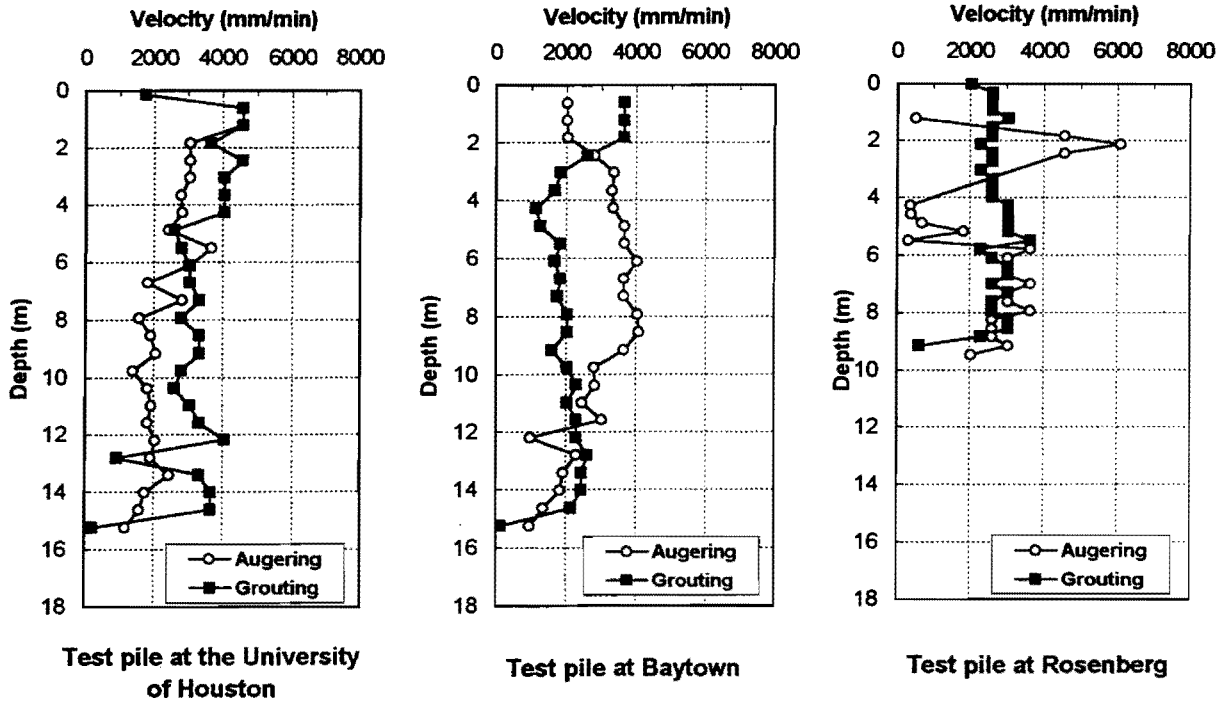
n = average rate of revolution of the auger (rpm),

p = pitch of the auger (length per turn),

d_0 = the outer diameter of the stem of the auger, and

d = the outside diameter of the auger from tip to tip of the auger flights.

The calculated and observed rates of penetration of the auger are listed with other components of Eq. (4.1) in Table 4.5.



Note: Velocities were obtained by videotaping the operations. Markers were placed on both the auger and the stationary leads, and relative displacements were read from the videotape approximately every 15 seconds, as indicated by the timer on the videotape machine.

Figure 4.11. Velocity of penetration (augering) and extraction (grouting)

Table 4.5. Calculated and observed rates of penetration of the auger for three test piles

CFA test pile	d (mm)	d ₀ (mm)	Auger Pitch (mm)	N (rpm)	v Eq. (4.1) mm/min	v ₀ Observed mm/min	Ratio of v ₀ /v
UH	457.2	99.1	260.4	47	11664	2358.6	0.20
Baytown	457.2	99.1	260.4	49	12160	2824.8	0.23
Rosenberg	457.2	99.1	260.4	52	12904	2373	0.18

Equation (4.1) is based on the assumption that the volume of the auger stem that penetrates the soil for each revolution of the auger must exceed the volume of the soil that can be held between the flights of the auger over a length equal to one turn of the auger. This ensures that the volume of soil invaded by the auger shaft is greater than amount of soil that can be removed, thus ensuring that the soil is compressed rather than decompressed. That is, the auger should be "screwed" into the soil. From Table 4.5, it is clear that the rig used to install the test piles for this project did not achieve the condition required by Equation (4.1). To have done so would have required a rig with a much higher torque, similar to the rigs that operate in Europe. The inability of the rig to satisfy Equation (4.1), however, did not seem to impair the capacities of either the UH or Rosenberg test piles, based on the measured incremental grout take ratios and loading test data presented later in this chapter. At the Baytown site, however, the loose, fine, waterbearing sand between depths of 4.6 m (15 ft) and 10.7 m (35 ft) required about 2.9 times as much grout to fill the excavation as the theoretical volume of the excavation, and the load transfer in that depth range was low, so that it is possible that the low rate

of penetration / high rate of rotation may have produced some depressuring and mining of that soil.

A PIR was used to monitor the installation of the CFA piles. The PIR included a magnetic flow meter in the grout line to measure precisely the delivered grout volume, a pressure transducer in the grout line at the pump outlet to measure line pressure, a position sensor on the leads to measure auger depth, and a pressure transducer placed at the auger tip to measure the grout pressure at the auger tip. These PIR measurements automatically document the augering and grouting processes and result in a profile of grout volume pumped versus auger tip depth. The operator of the control unit can tell immediately if insufficient grout has been placed at any position along the pile or if the grout pressure has been reduced below the overburden pressure. The PIR records of the minimum and maximum grout pressure at the pump vs. elevation of the auger tip, and the grout ratio (grout placed/theoretical volume) vs. elevation of the auger tip are shown in Figure 4.12 through Figure 4.17 for the three test piles. For three test piles, the grout volume ratio exceeds 1.0 except for the UH test pile, from depths of 0.6 m to 4.2 m, where the grout volume ratio is slightly less than 1.0. The average grout volume ratio for the UH, Baytown and Rosenberg test piles were 1.18, 1.52 and 1.77, respectively. The low grout take ratios near the top of the UH test pile were probably caused by the fact that grout was observed returning to the surface through the auger flights when the auger tip was at a depth of about 4.6 m (15 ft). At this point the operator of the pump reduced the rate of pumping, apparently to avoid wasting grout. That is, the hole was essentially completely full of grout once the auger tip reached a depth of 4.6 m (15 ft), and it was no longer necessary to continue pumping grout to achieve a grout take ratio of greater

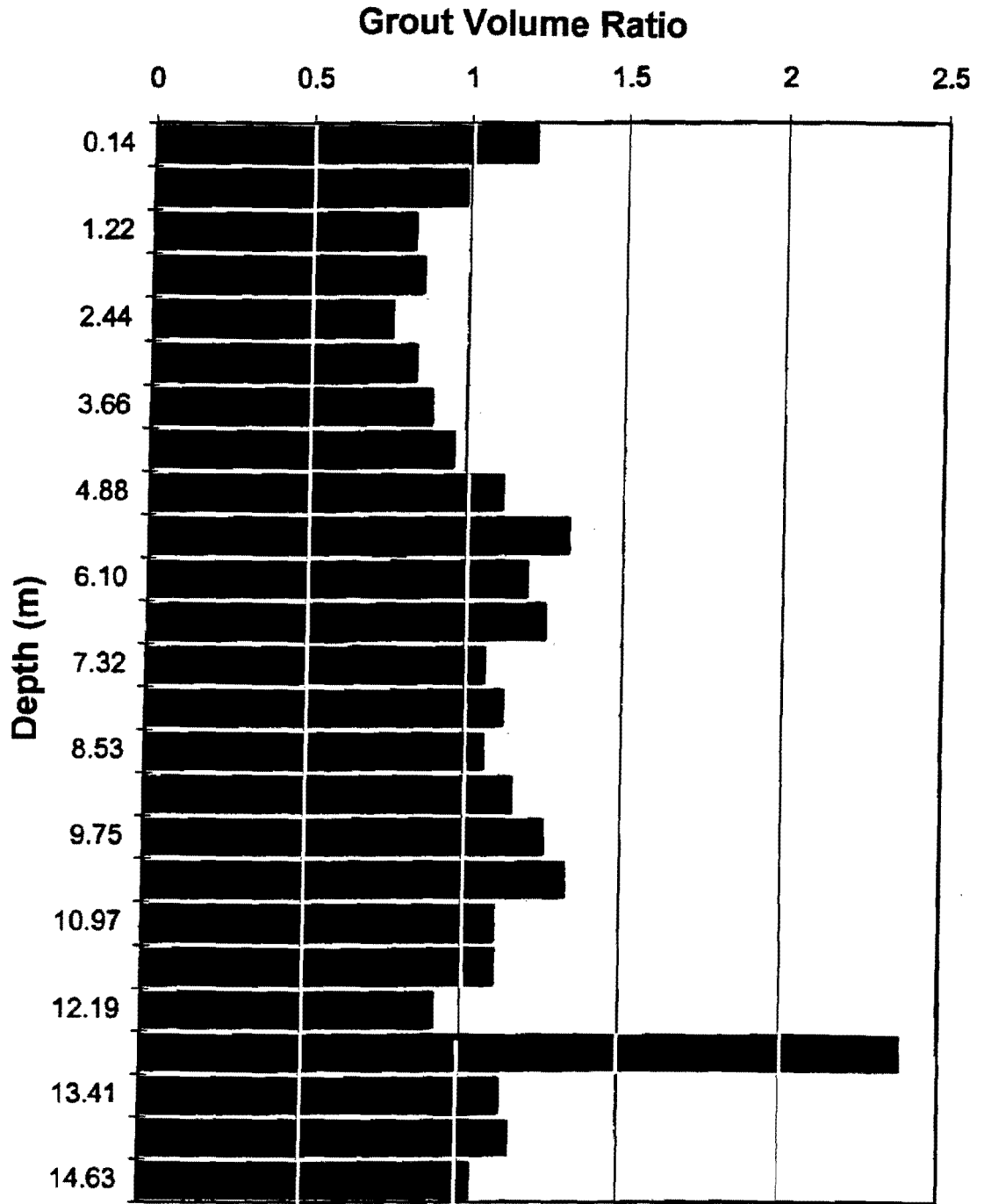


Figure 4.12. Record of grout volume ratio versus depth for UH test pile (by flowmeter)

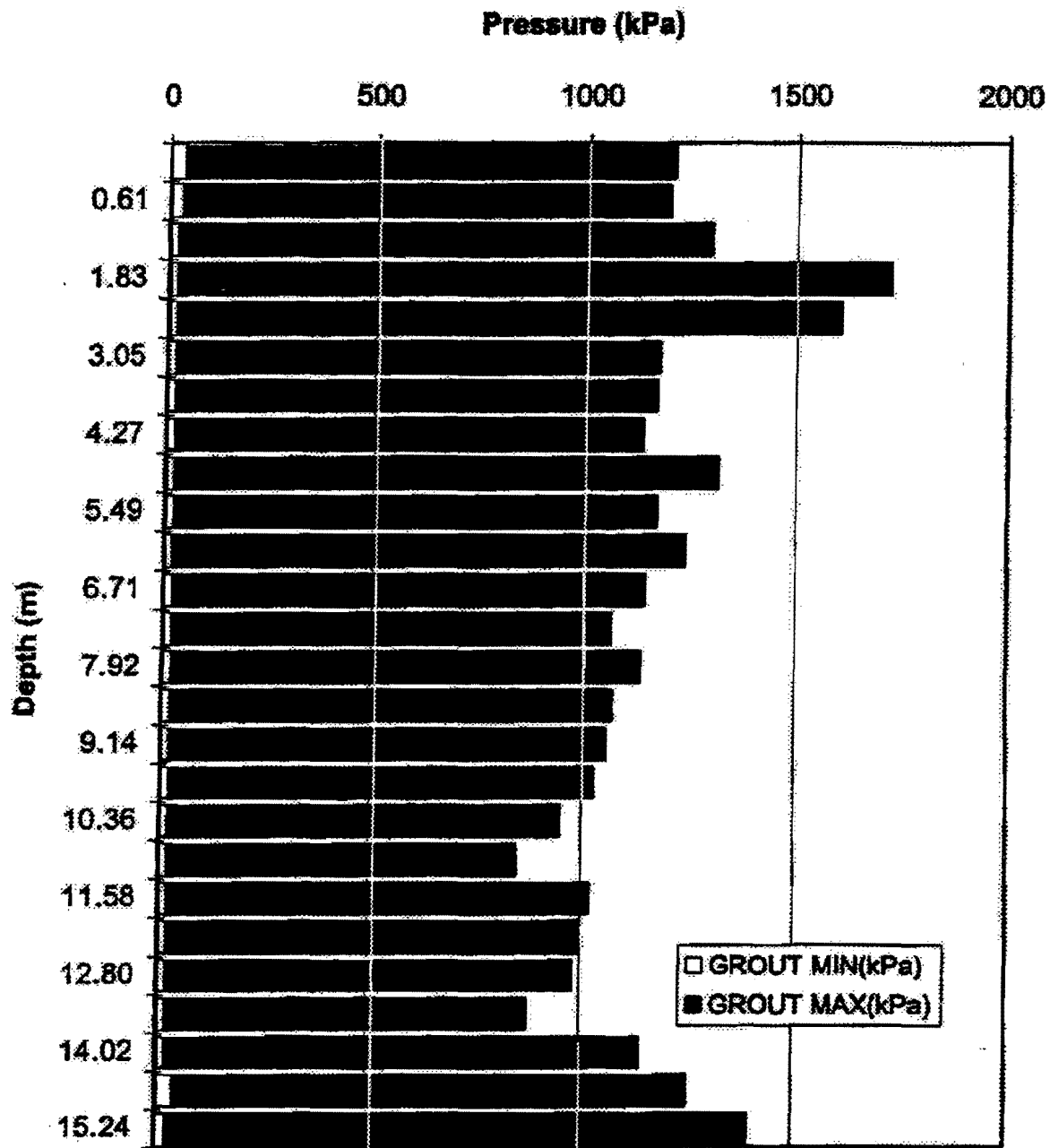


Figure 4.13. Records of maximum and minimum pump grout pressure versus depth for UH test pile

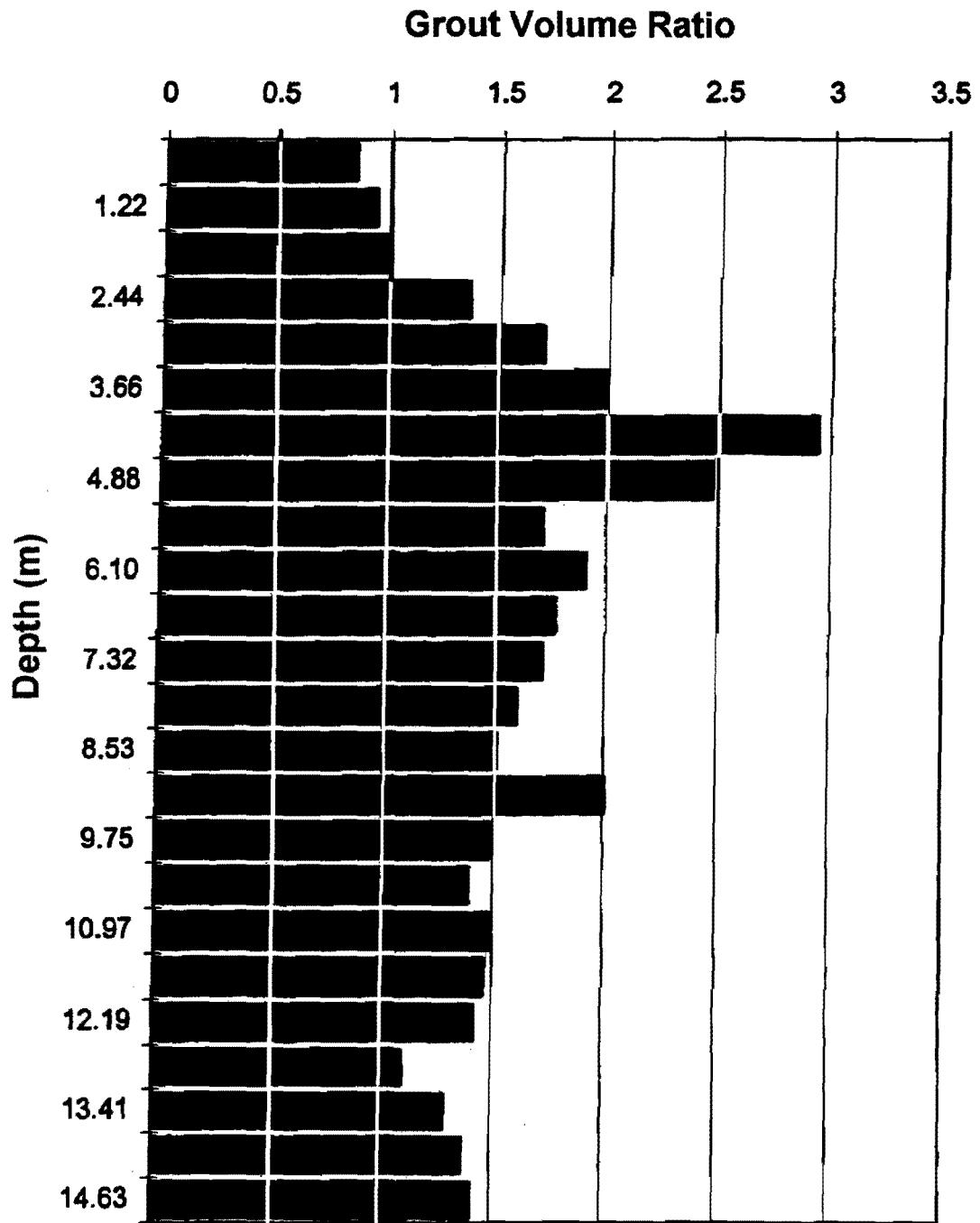


Figure 4.14. Record of grout volume ratio versus depth for Baytown test pile (by flowmeter)

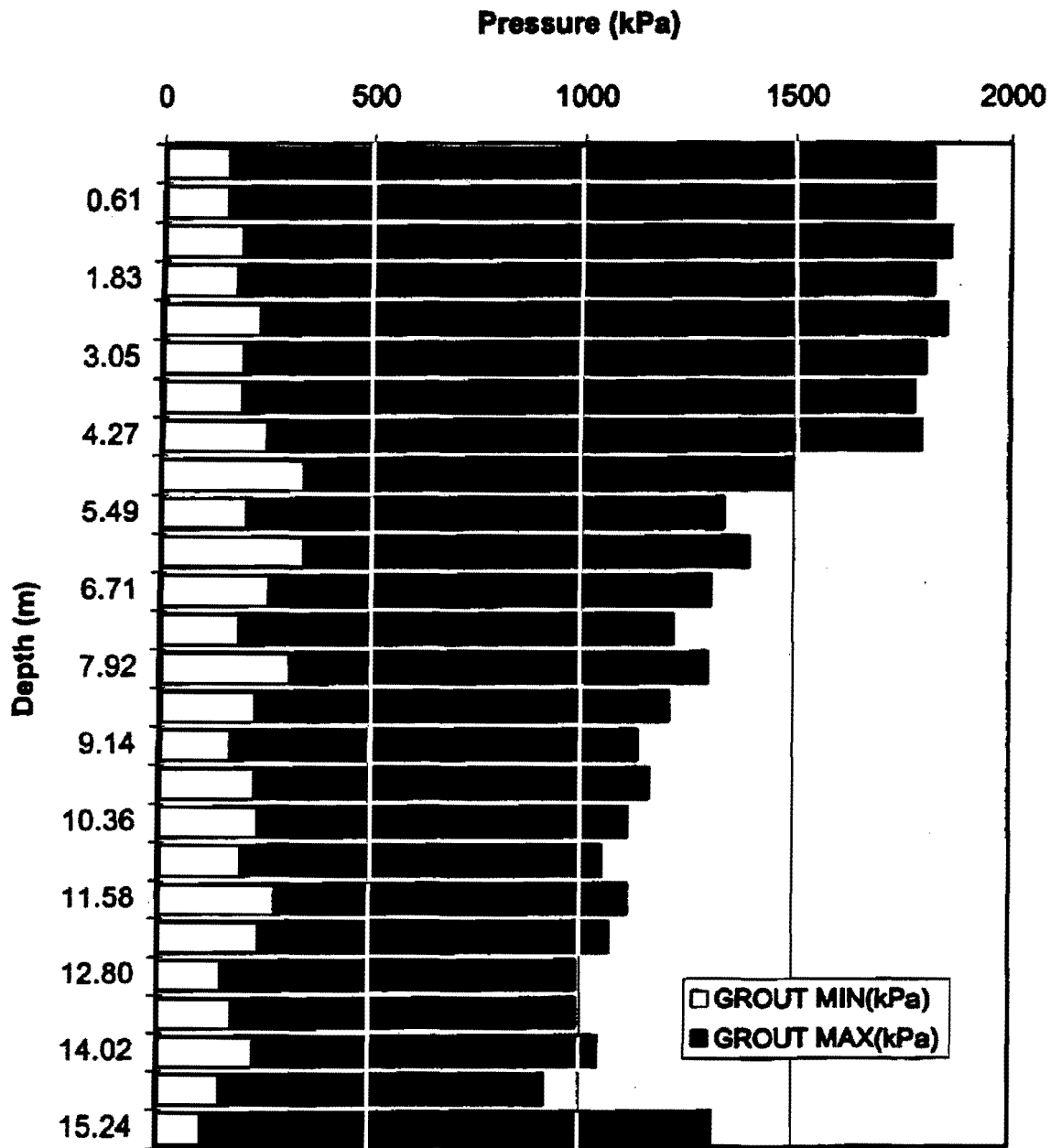


Figure 4.15. Records of maximum and minimum pump grout pressure versus depth for Baytown test pile

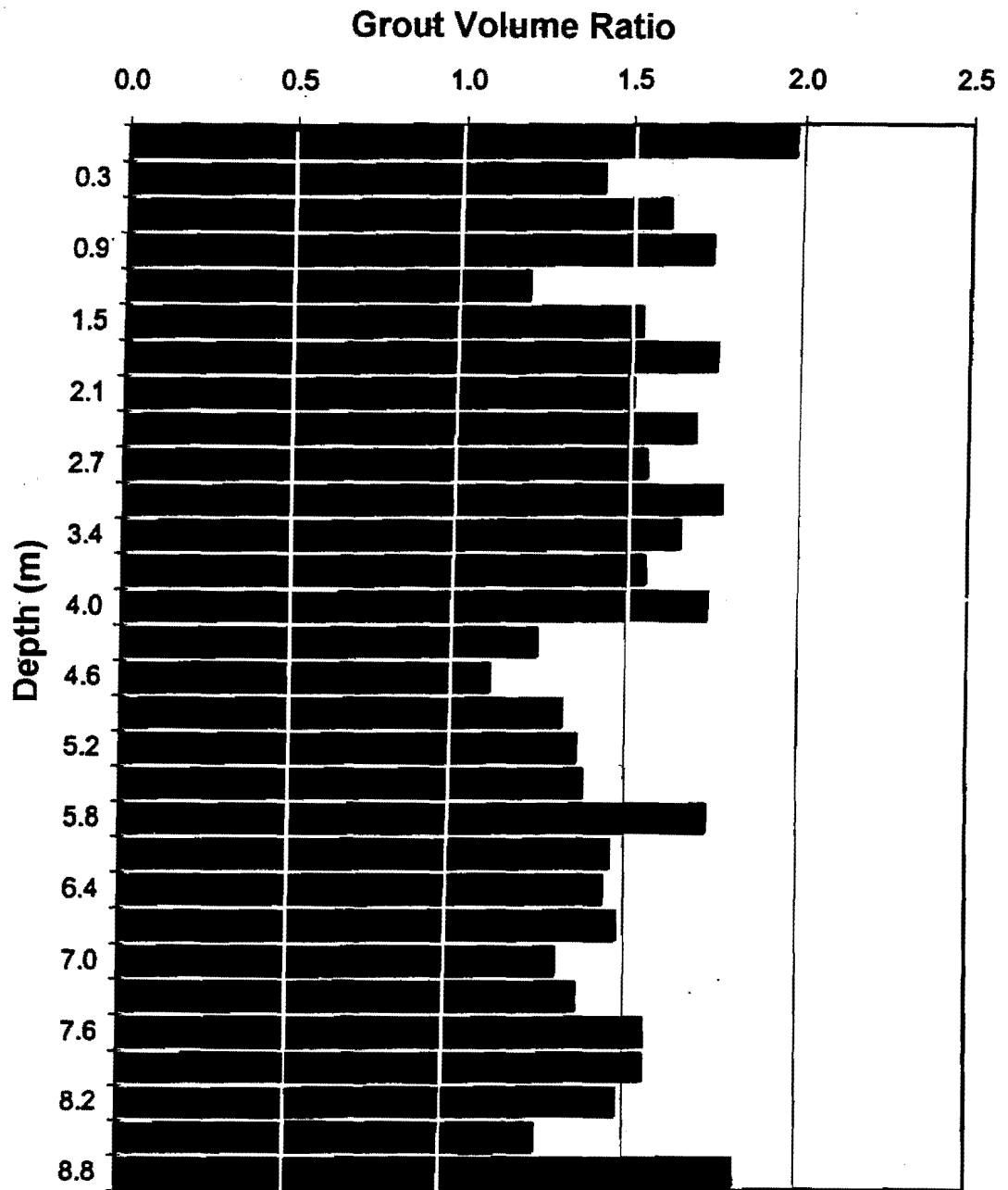


Figure 4.16. Record of grout volume ratio versus depth for Rosenberg test pile (by flowmeter)

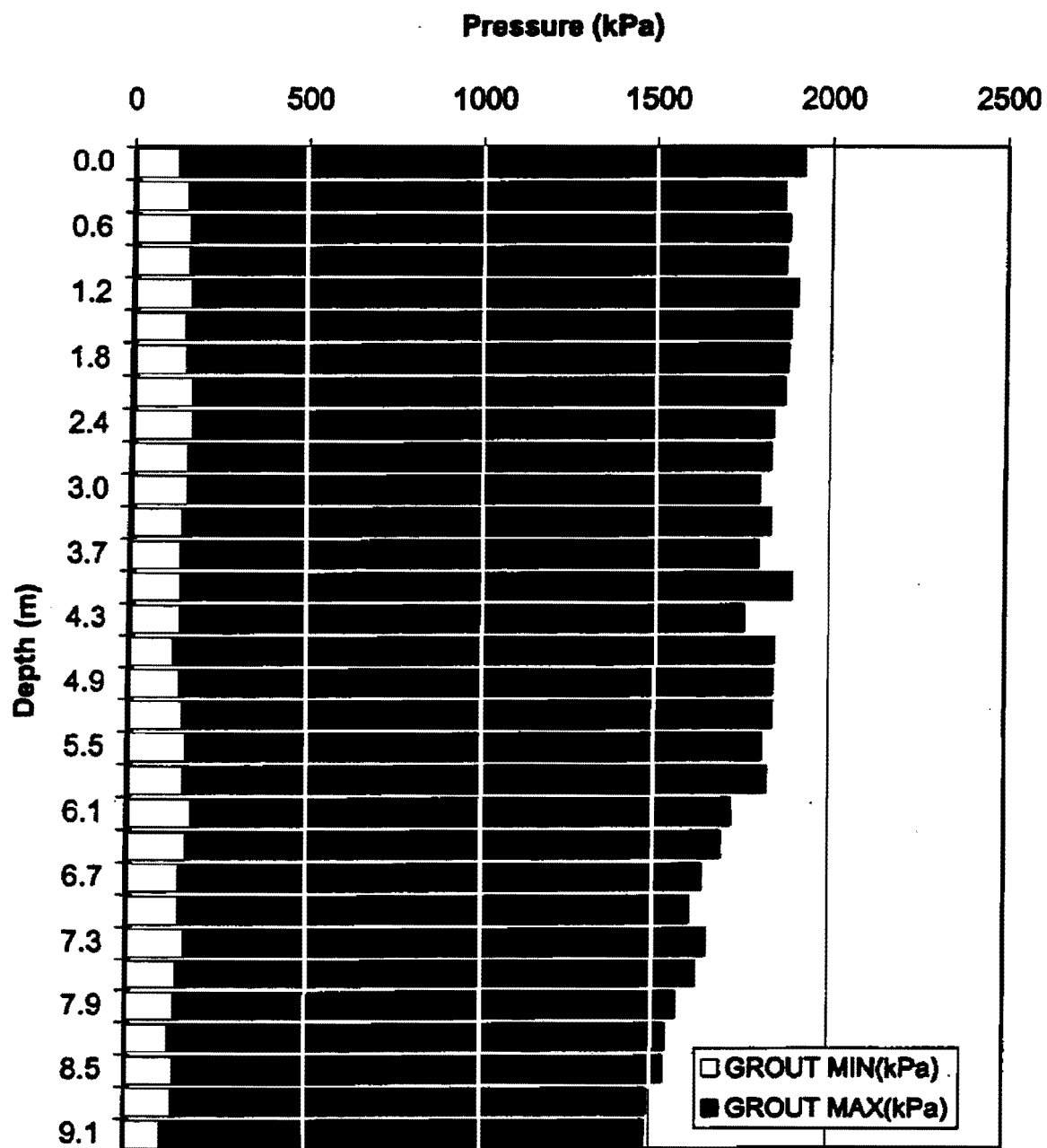


Figure 4.17. Records of maximum and minimum pump grout pressure versus depth for Rosenberg test pile

than 1.0 to ensure that the pile was constructed to the correct diameter. Since the soil above a depth of 4.2 m (14 ft) was a stiff clay, maintenance of a grout take ratio greater than 1.0 was also not necessary to prevent collapse of soil back into the hole.

During the installation of the test piles, the grout volume was also determined manually by counting pump strokes while simultaneously reading the depth of the auger tip from markings on the side of the auger. Prior to beginning grouting, the volume of the piston-type pump was calibrated by pumping several strokes of grout into a "55-gallon" drum. This calibration process is not especially accurate because the drum is not usually filled with an even number of pump strokes, so that number of pump strokes to fill the drum is an estimate and thus the volume of grout pumped per stroke is also an estimate.

The grout volumes measured by the magnetic flowmeter in the PIR system are compared with the volumes of grout determined by counting pump strokes in Figure 4.18 through Figure 4.20 and in Appendix B. In those figures, the theoretical volume is the neat volume, assuming a hole diameter of 0.46 m (18 in.). It is clear that the counting of pump strokes (manual method) overestimated the volume measured with the PIR in all cases, perhaps due to inadequate calibrations and perhaps due to changes in the stroke volume as the grouting operation progressed. Close observation of Figures 4.18 through 4.20 also indicates that grout take ratios, which are proportional to the slopes of the curves, can be either greater or smaller with the pump stroke method than with the PIR method. This may be due to the counter having to decide to which depth increment to assign a particular stroke when the stroke falls in between depth increments.

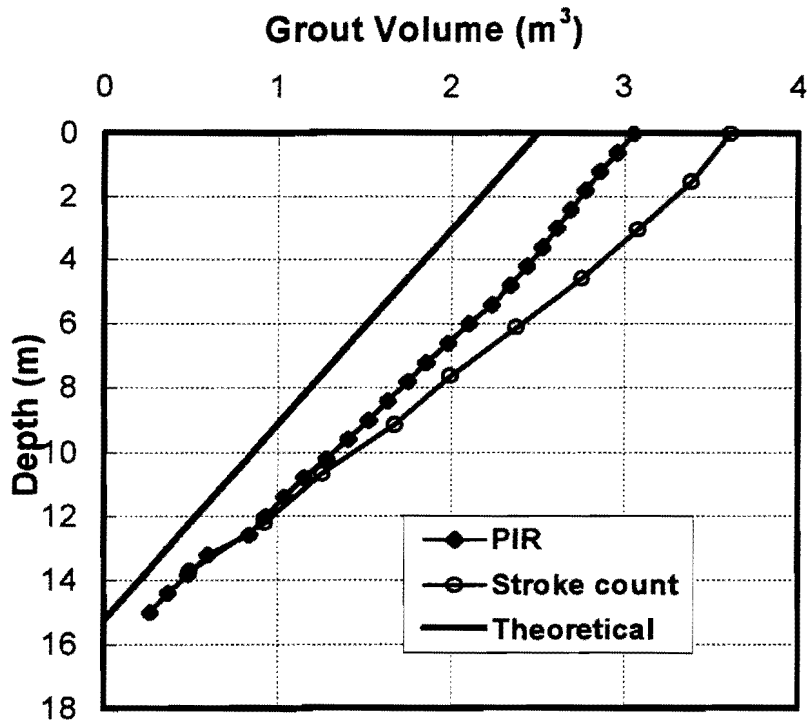


Figure 4.18. Grout volume versus depth for the UH test pile

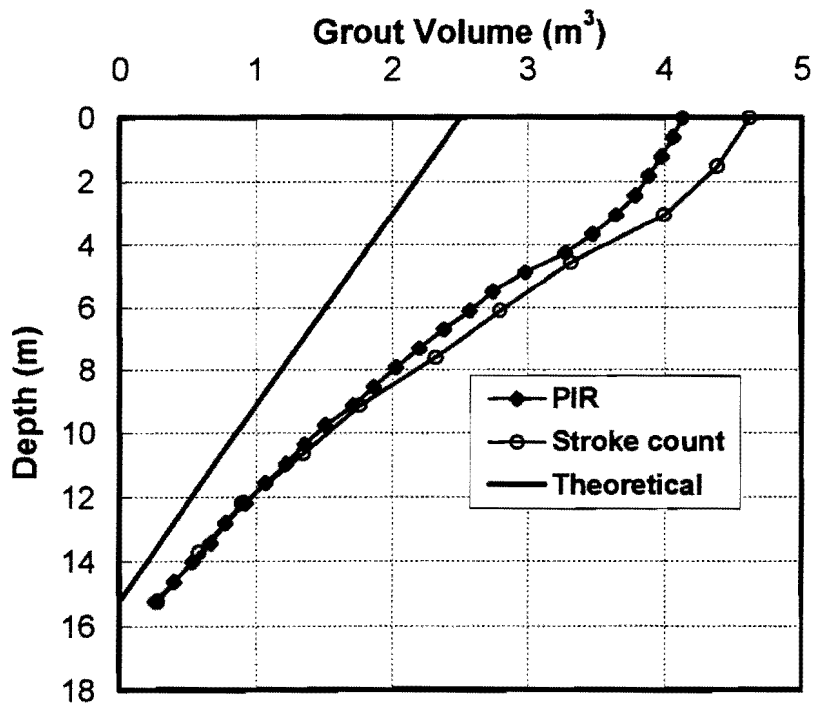


Figure 4.19. Grout volume versus depth for the Baytown test pile

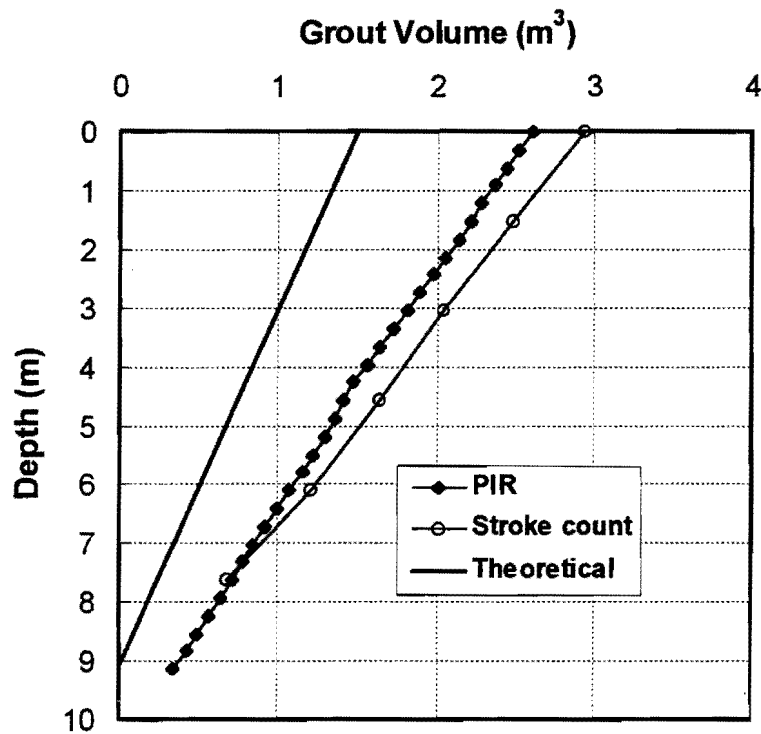


Figure 4.20. Grout volume versus depth for the Rosenberg test pile

Based on this research, it appears that monitoring of grout take by means of a calibrated magnetic flowmeter, such as the device used in the PIR system, is much preferred to manual monitoring of pump strokes.

Maximum (systolic) grout pressures were maintained around 1000 kPa (145 psi) at the pump for the UH test pile (stiff clay site), 1000 kPa to 1750 kPa (145 to 250 psi) (increasing as the auger was withdrawn) at the pump for the Baytown test pile (loose, waterbearing sand site) and 1500 kPa to 1900 kPa (200 to 275 psi) at the pump for the Rosenberg test pile (moist sand site). These pressures appear to have produced adequate capacities in the respective test piles.

The minimum (diastolic) pump pressures were in the order of 30 to 50 kPa (4.4 to 7.3 psi) at UH, 150 - 300 kPa (22 to 44 psi) at Baytown and 75 to 125 kPa (11 to 18 psi) at Rosenberg. It is desirable to maintain grout pressures at the tip of the auger that are higher than the ambient total pressures in the ground at the elevation of the auger tip. Maintaining such pressures at the pump should be adequate to ensure that this criterion is met. At UH and Baytown, these total ground pressures would have been around 290 kPa (42 psi) at the maximum depth of the pile (15.3 m or 50 ft). The measured diastolic pressures at the pump were much lower than this at UH and, on the average, somewhat lower at Baytown. At Rosenberg, where the maximum depth of the pile was only 9.1 m (30 ft), a diastolic grout pressure of only about 175 kPa (25 psi) is necessary. However, that value was not achieved at the pump.

These diastolic pressure shortfalls do not necessarily mean that the diastolic pressures in the grout at the discharge orifice on the auger were lower than the total ambient overburden stress in the soil, because there is potentially significant grout head in the stem of the auger. Unfortunately, it was found to be very difficult to measure the grout pressure at the outlet orifice of the auger, due to space limitations for the pressure transducers and their lead wires, and such data could not be reliably obtained for the test piles in this project.

Note is made of the fact that the reinforcing cages, consisting of about 1 % longitudinal steel, were thrust into the unset grout at UH and Baytown very easily to a depth of 15.3 m (50 ft) within five to six minutes of completion of grouting. At both of these sites, the water table was high. At the Rosenberg site, where the sand was not saturated, some difficulty was encountered in pushing the cage to its full penetration of

9.1 m (30 ft) when it was installed within 5 to 6 minutes of completion of grouting. This was most likely produced by the fact that the unsaturated sand took water from the grout and decreased its fluidity very quickly, which suggests that it may not be possible to push cages into fluid grout at sites with sand and low water tables if the cages are longer than about 9.1 m (30 ft). This does not necessarily mean that CFA piles should not be installed at such sites, as a complete reinforcing cage may not be necessary to resist tension or flexural loads to depths of greater than 9.1 m (30 ft).

4.3.1. Soil pressure gauge

Because the rig that was used to install the test piles did not conform to the requirements of Equation (4.1), it was considered advisable to measure the lateral effective stress in the soil near the test piles as they were constructed in order to determine if depressuring of the soil was occurring during construction. The horizontal diaphragm-type pressure gauges described earlier were installed at each test site two days before installing each test pile. The layout of the pressure gauge and test pile is shown in Figure 4.21. The layout was identical at each test site.

The change in measured lateral effective earth pressure for each site is shown in Figures 4.22, 4.23 and 4.24. These figures are plotted to give change in measured lateral effective earth pressure (σ'_h) vs. depth of the tip of the auger during both drilling (penetration) and grouting (extraction). At the NGES-UH the results are anomalous. First, the horizontal soil pressure decreases up to the depth of the pressure gauge, following which there is essentially no change during the remainder of drilling and grouting. It is likely that this behavior was caused by densification of the backfill sand

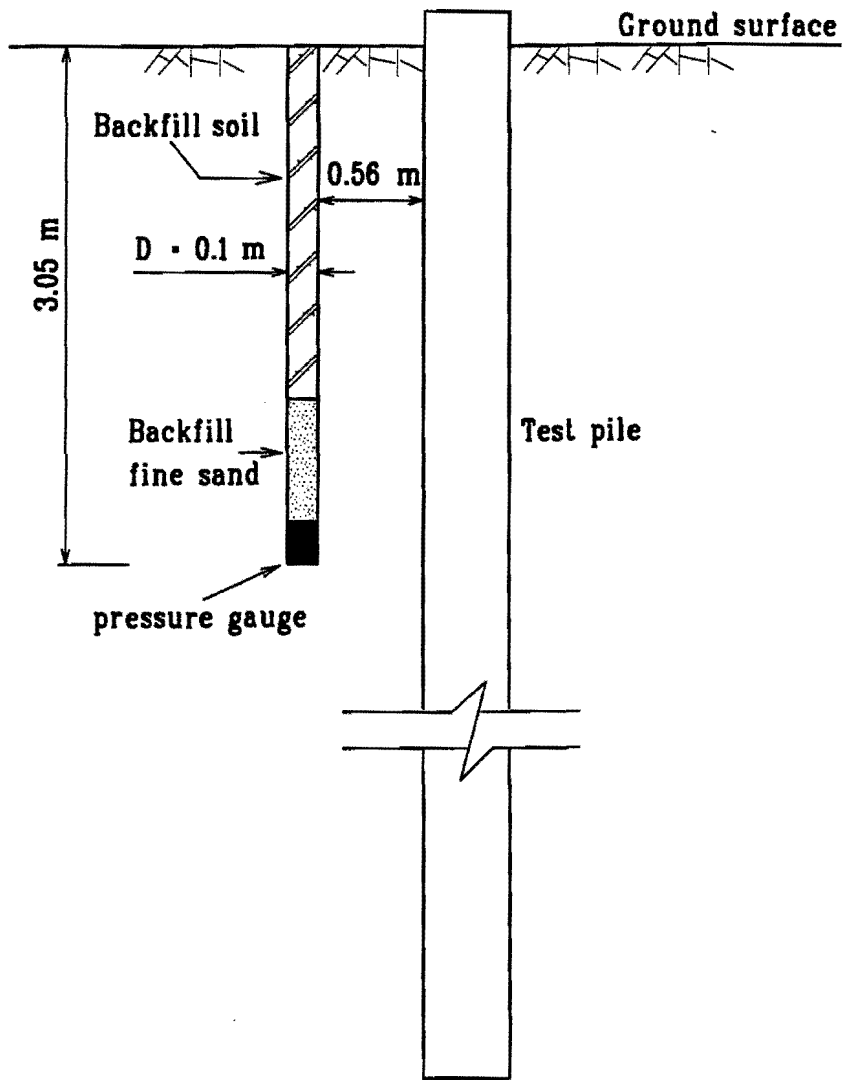


Figure 4.21. Layout of pressure gauge and test pile

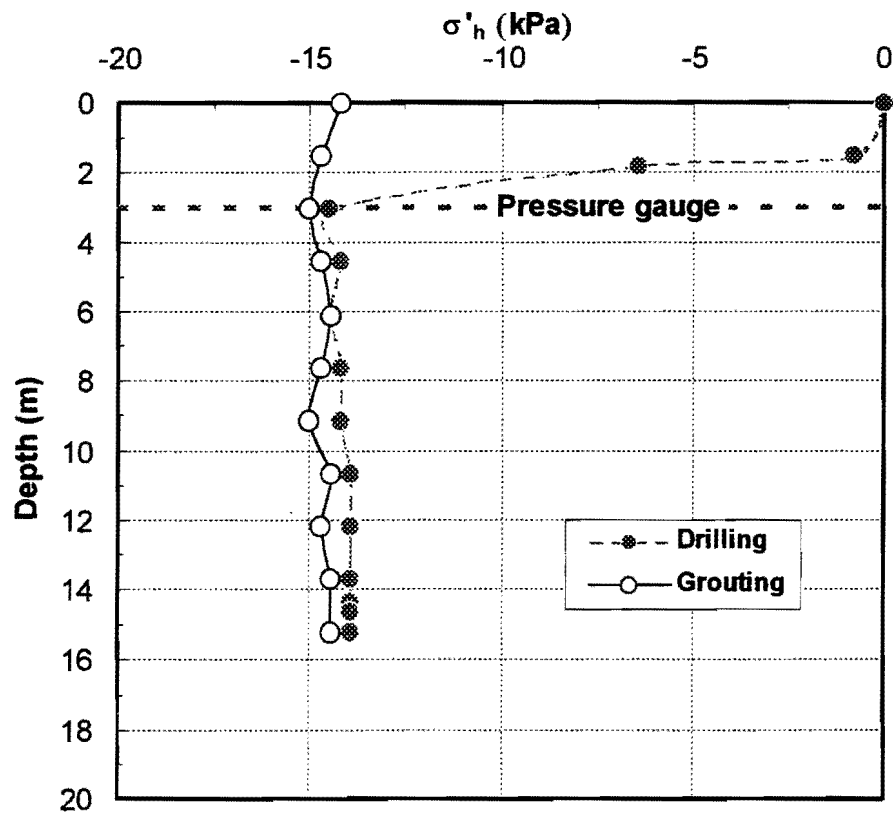


Figure 4.22. Lateral effective soil pressure for installation of CFA test pile at the NGES-UH site

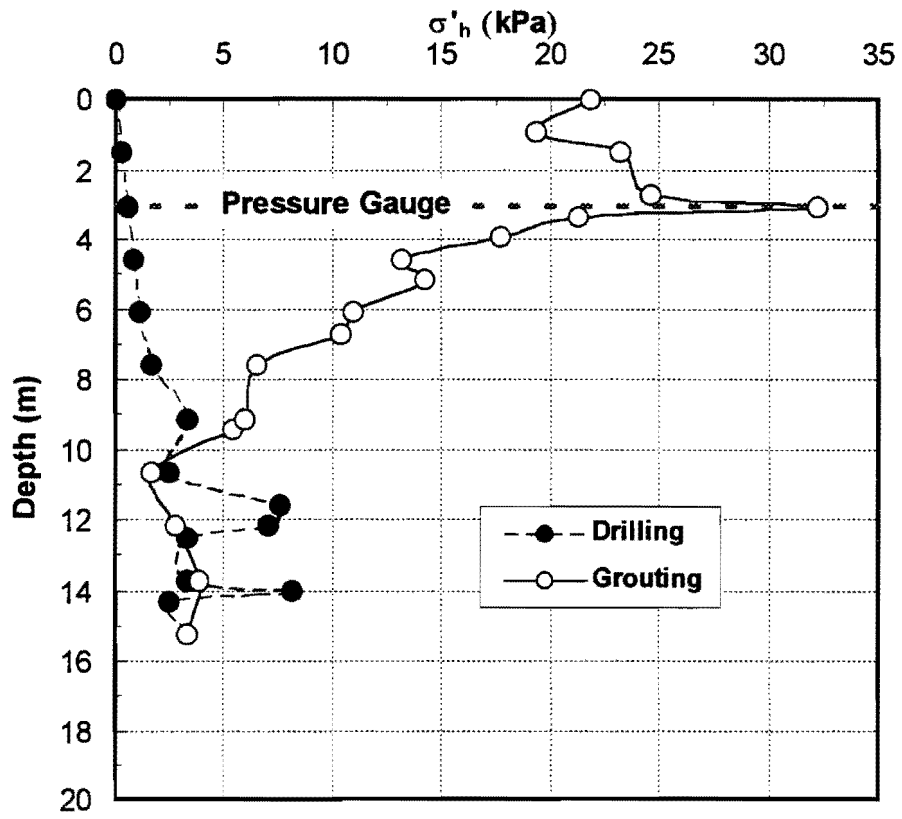


Figure 4.23. Lateral effective soil pressure for installation of CFA test pile at the Baytown site

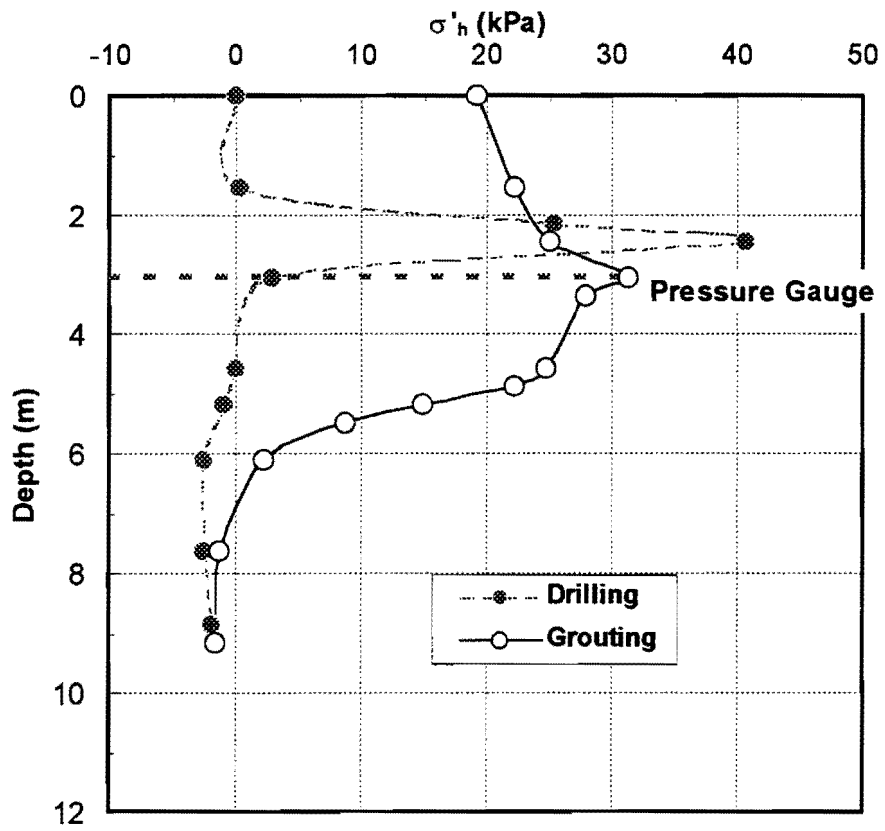


Figure 4.24. Lateral effective soil pressure for installation of CFA test pile at the Rosenberg site

and arching of the sand within the cylindrical clay "container" (borehole for the cell) as the auger tip approached the cell, but because the stiff clay was stiffer than the backfill material, the backfill material did not deform further after the auger tip passed its elevation and thus the cell did not register pressure changes.

At Baytown and Rosenberg, where the natural soil closely matched the backfill (i. e., sand), the readings were much more plausible. At Baytown, σ'_h increased very slightly as the borehole was excavated and then increased markedly as the hole was grouted, especially as the auger tip reached a depth of within about 5 m below the pressure gauge. After completion of the pile installation, σ'_h had increased by 22 kPa (3.2 psi), indicating that the construction operation had a positive effect on soil strength. A similar result was observed at Rosenberg, where a large increase in σ'_h occurred when the auger tip passed the cell during excavation, and the net increase in σ'_h upon completion of construction was 19.5 kPa (2.8 psi). It can be concluded from these data that the CFA pile rig used in the study did not have a negative effect at the sand sites (Baytown and Rosenberg), but it must be emphasized that neither cell was placed in a "running sand" (waterbearing, loose, clean sand).

4.3.2. Integrity testing program

Crosshole sonic logging (CSL) integrity tests were performed on the test piles. The ultrasonic logging was conducted under set grout conditions one to two days after pile installation.

In the CSL test the transmitter and receiver probes are lowered to the bottoms of two Schedule 40 steel access tubes capped on the bottom and filled with water (to

provide good acoustic coupling with the set grout). In this study the access tubes were tied securely onto the cages at opposite ends of a diagonal (280 mm apart from center to center) before the piles were constructed and thrust into the unset grout along with the cage and sister bars immediately after grouting the piles. Data were then collected after the grout set as both probes were slowly raised within the access tubes. Two displays of data were used:

1. Travel time of acoustic pulses from one probe (signal probe) to the other (receiver probe).
2. Relative energy of the acoustic pulses versus elapsed time at the receiver probe.

The arrival times and signal energies should be relatively constant with depth in a well-constructed CFA pile. Increases in arrival time and decreases in signal energy represent anomalies that may indicate nonhomogeneous grout, soil inclusions, or reduced cross-sections. The CSL test record will show a complete break in the signal if the pile is completely separated.

In the tests for this research project, Fugro-McClelland Southwest, Inc., who performed the CSL tests, also used software with the control and recording system that allowed manual adjustment of the power level in the transmitter and gain at the receiver. This was done because anomalies that are not detectable at one power/gain setting may be detectable at another. Using different settings, each of the test piles was logged five to six times. Typical results are given in Appendix B. The CSL data indicated that the UH test pile was without anomalies except for one small break in the data at a depth of 9.2 m (30.2 ft) that was traced to the presence of a piece of duct tape on a joint of an

access tube. For both the Baytown and Rosenberg test piles, the CSL results showed that the pile installation did not produce any significant nonuniformities.

4.4. LOAD TESTING

Axial load tests were performed by jacking a test pile against reaction beams anchored by four piles using a pneumatically powered jacking system. The jacking system consisted of a hydraulic jack and an electronic load cell. Both the load cell and the hydraulic jack were placed inside a reaction strut and supported by the reference beam. Both jack pressure and the load cell were read during the loading tests. The load readings never varied by more than one percent. Two dial gauges attached on the top of the test pile and suspended from reference beams and were used to monitor the axial settlement of the test pile.

The loading tests were designed to produce compressive axial forces in the piles by applying axial loads to the tops of the pile. The Texas Quick Test method was used. This method included the following procedures:

1. Load the pile in 178-kN (20.0-ton) increments to failure. Hold each load until 3 minutes has elapsed. Take readings 1 minute and 3 minutes after each new load is applied.
2. Hold the failure load until the settlement reaches 50 mm (2.0 inches).
3. Unload the test pile in 534-kN (60-ton) decrements until the load is zero. Hold each new load for 3 minutes. Take readings 1 minute and 3 minutes after each new load is applied.

For the UH and Baytown test piles, only one cycle of loading was applied. For the Rosenberg test pile, two cycles loading to failure were applied. Figures 4.25 and 4.26 show the load-settlement results for the three test piles at 1 minute and 3 minutes. Figure 4.27 through Figure 4.34 show the applied load distribution along the length of the pile measured with the sister bars. Sister bars are short segments of #4 rebar that are machined and arrayed with bonded electrical strain gauge bridges, calibrated in the laboratory, and affixed to the reinforcing cage. During loading, strain was measured in the hardened grout at various depths along the piles by reading the sister bars.

The gauge outputs were converted automatically to strain with the data acquisition system and then converted off line to load in the pile by multiplying the average strain in the two sister bars at one level by the composite Young's modulus of the pile and pile's cross-sectional area. It was assumed when calculating the loads from the sister bar readings that the pile diameter was the theoretical diameter of 0.46 m. This is an important consideration for any designer using the results of these tests, because the resulting calculations for unit side resistance and unit base resistance, rather than being true values based on the actual pile diameter are apparent values based on the theoretical size of the pile. The designer should therefore apply the results of this study to nominal pile sizes and not sizes that are estimated based on grout ratios and similar evidence that the true diameter may be greater than the nominal diameter. [The grout ratio is not an accurate measure of the diameter of a CFA pile at a given depth, as some of the excess grout is always pumped up the auger flights rather than out into the soil.]

It was not physically possible to place sister bars or a load cell at the exact bottom of the pile; therefore, toe resistance had to be estimated by extrapolating the

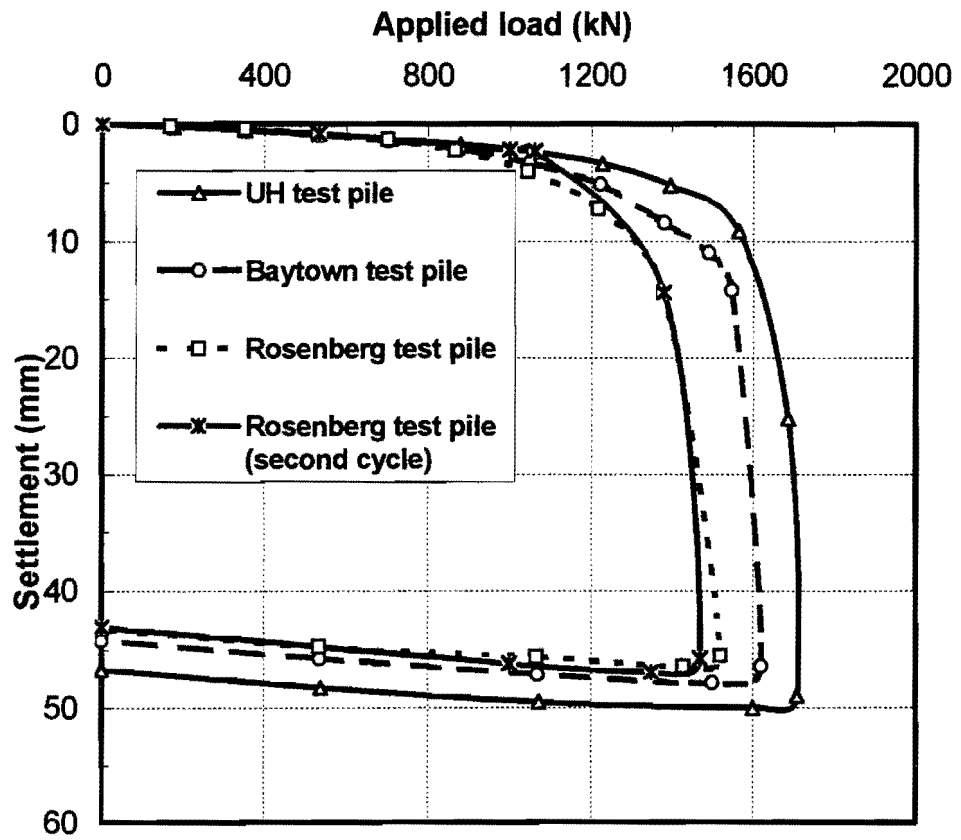


Figure. 4.25. Applied load versus settlement (1 minute)

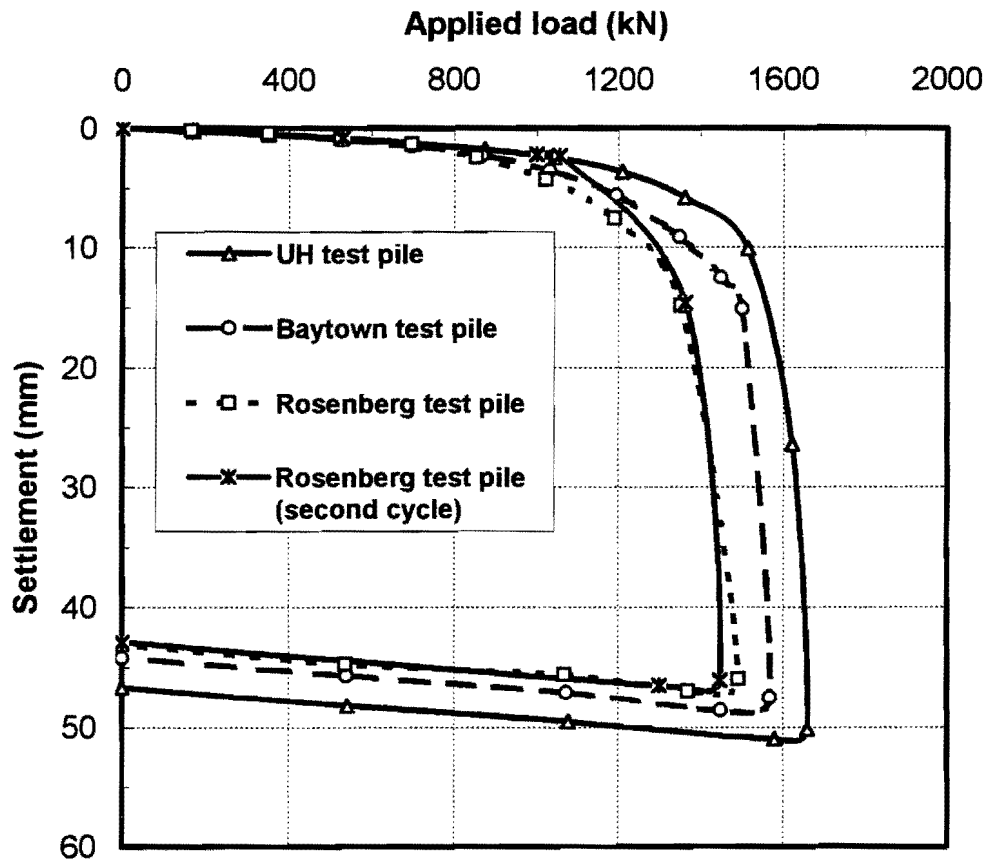


Figure. 4.26. Applied load versus settlement (3 minutes)

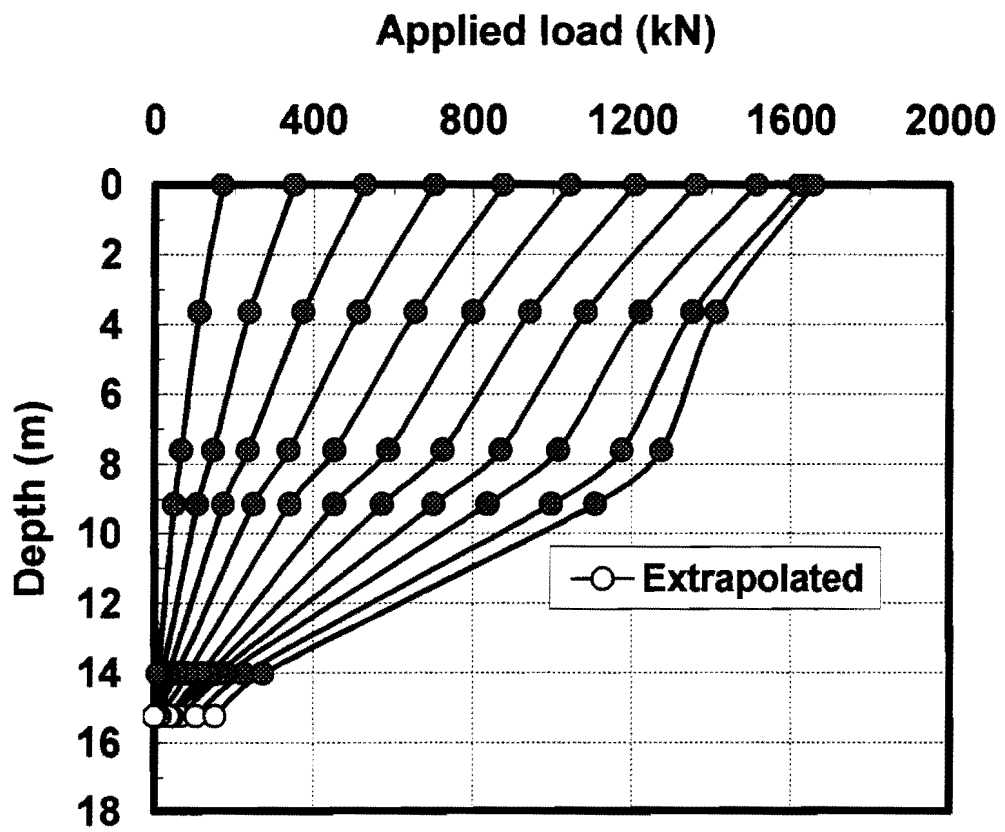


Figure 4.27. Applied load versus depth (UH site) (Method 1)

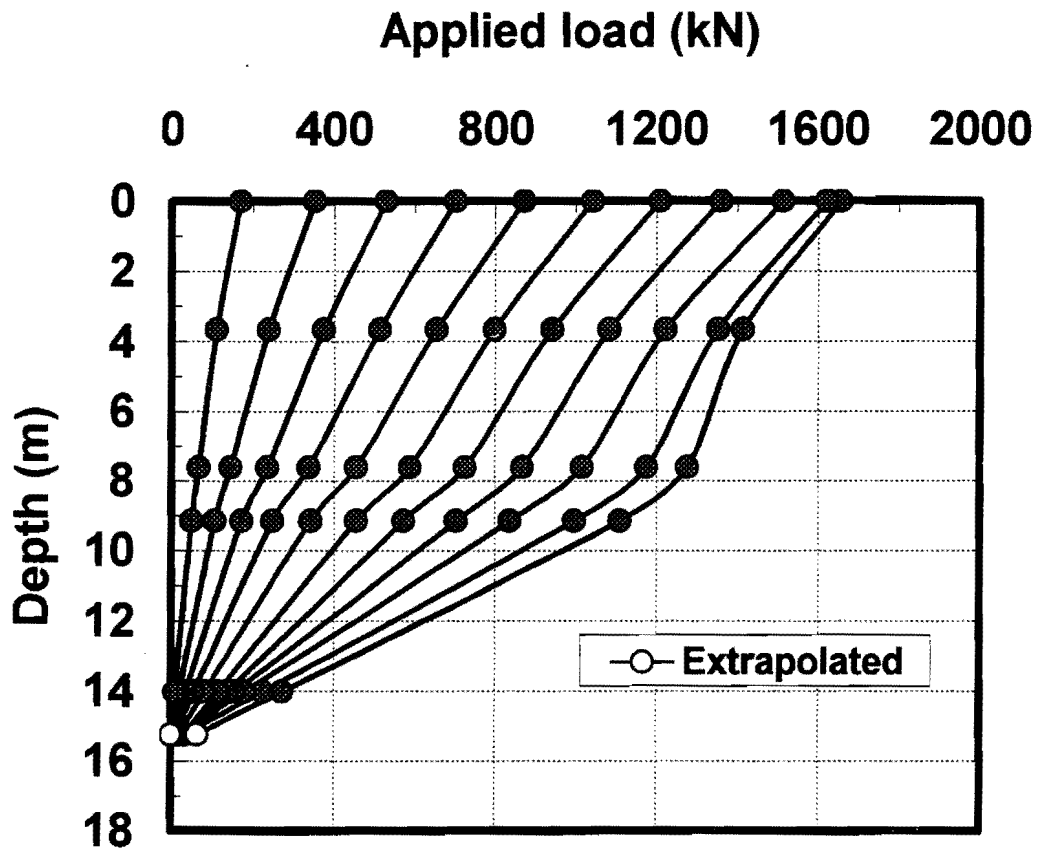


Figure 4.28. Applied load versus depth (UH site) (Method 2)

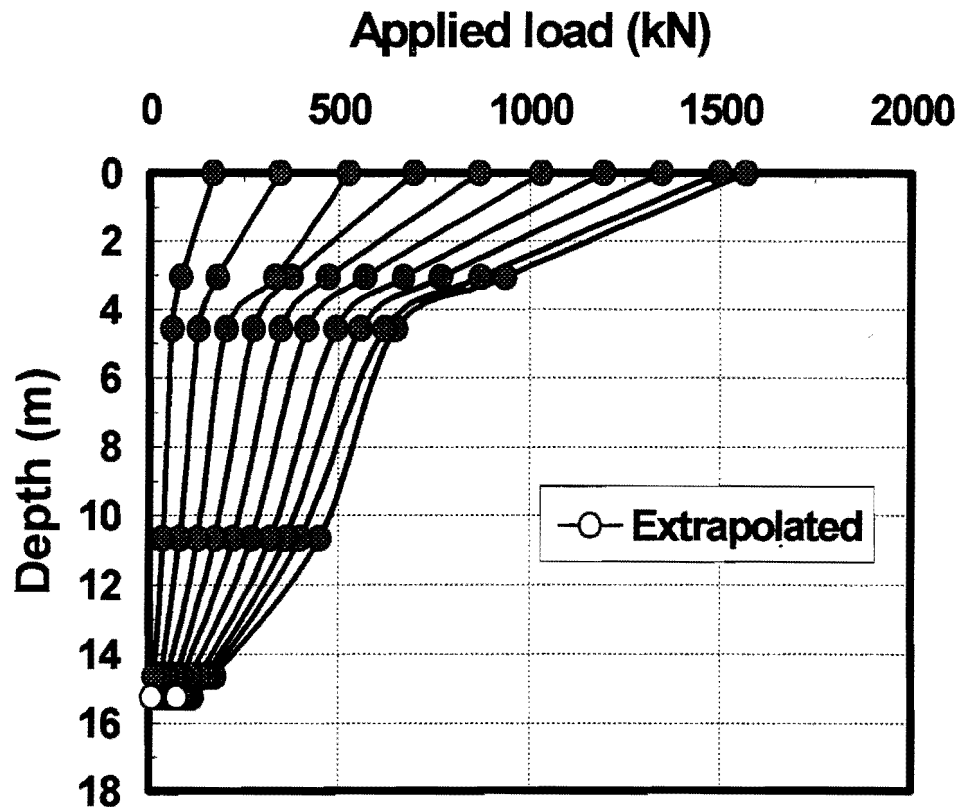


Figure 4.29. Applied load versus depth (Baytown site) (Method 1)

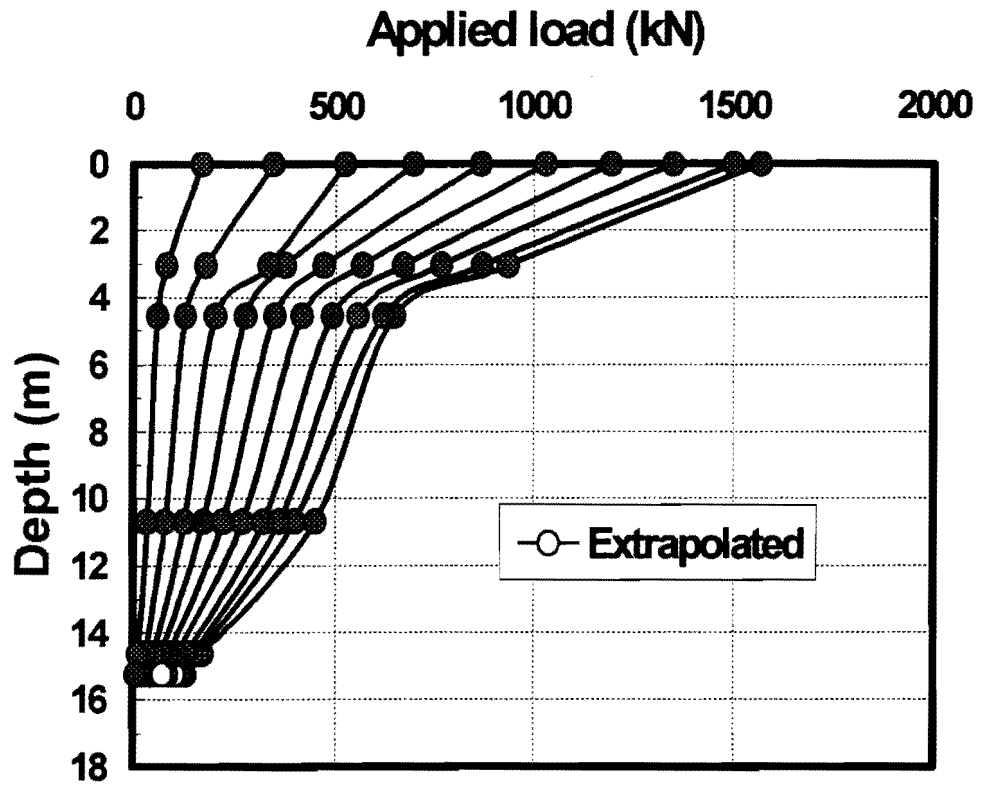


Figure. 4.30. Applied load versus depth (Baytown site) (Method 2)

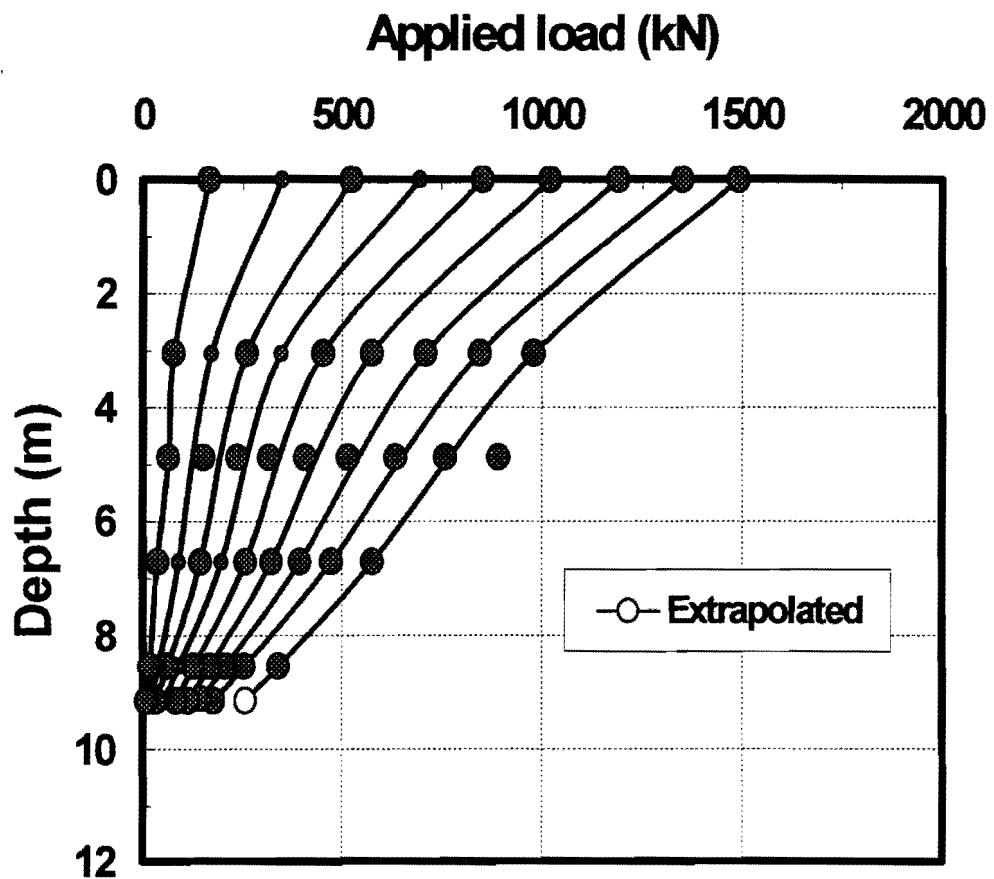


Figure 4.31. Applied load versus depth (Rosenberg site) (Method 1)

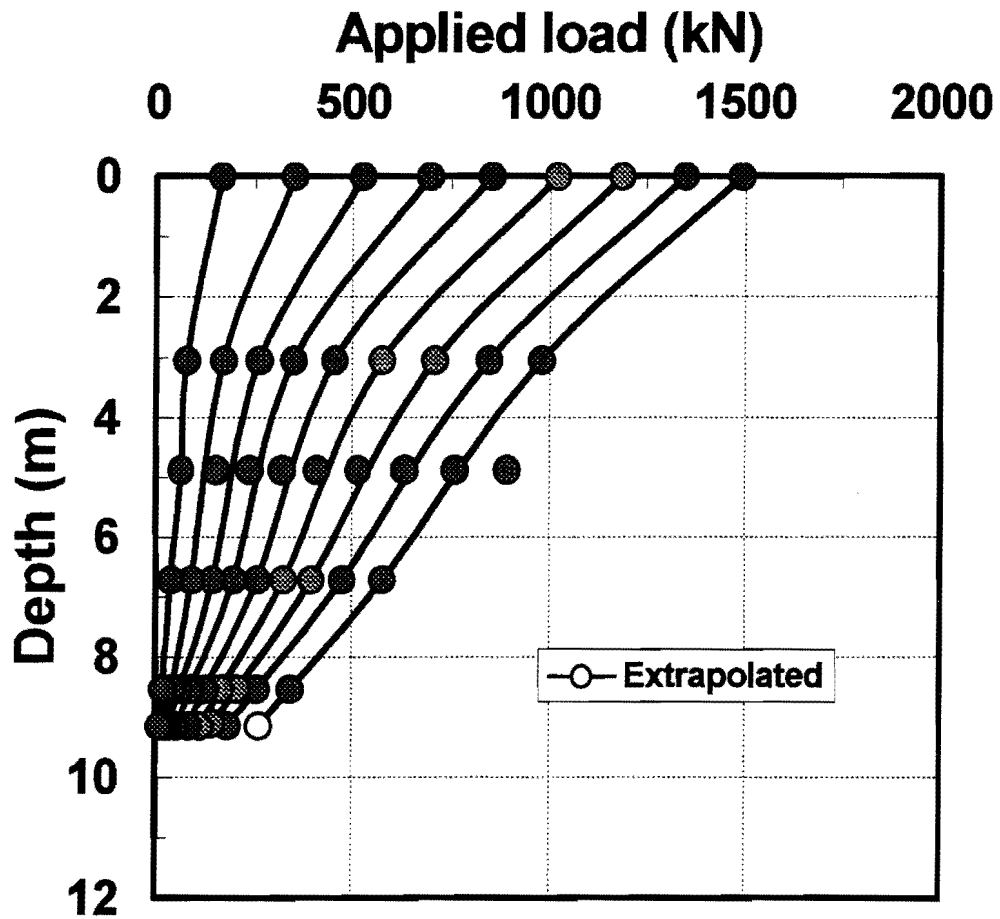


Figure 4.32. Applied load versus depth (Rosenberg site) (Method 2)

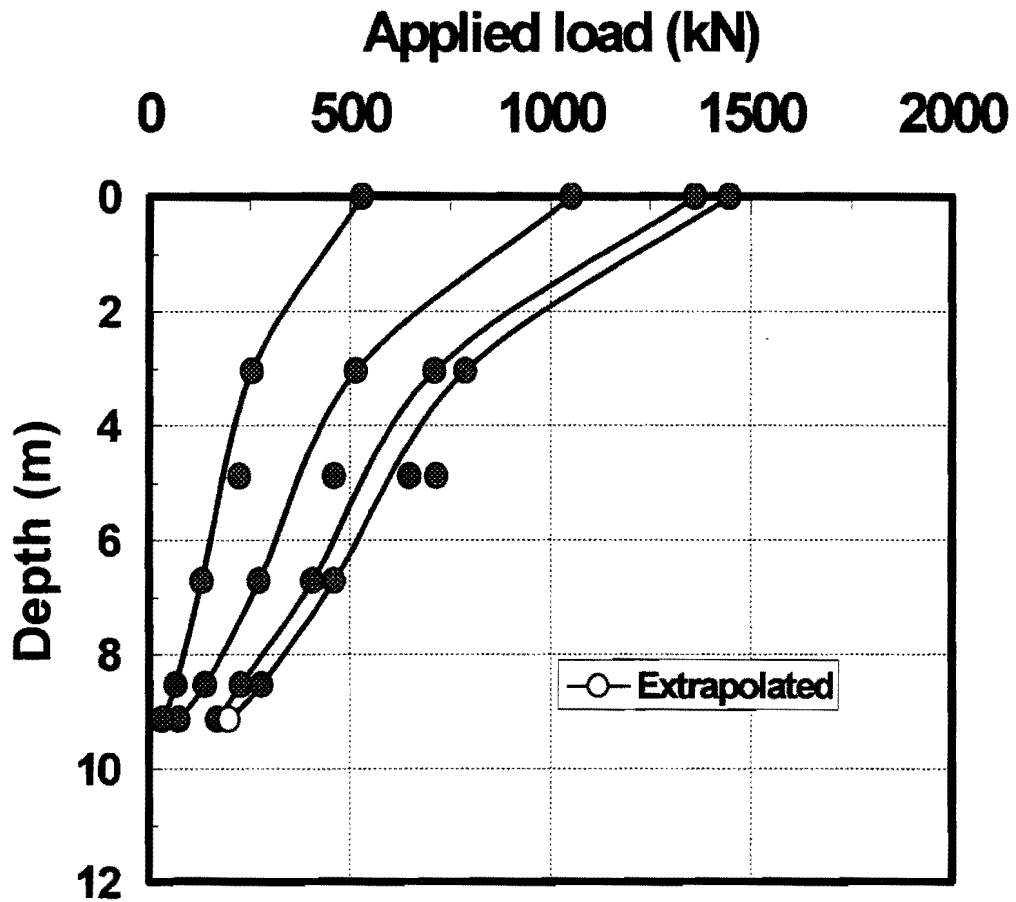
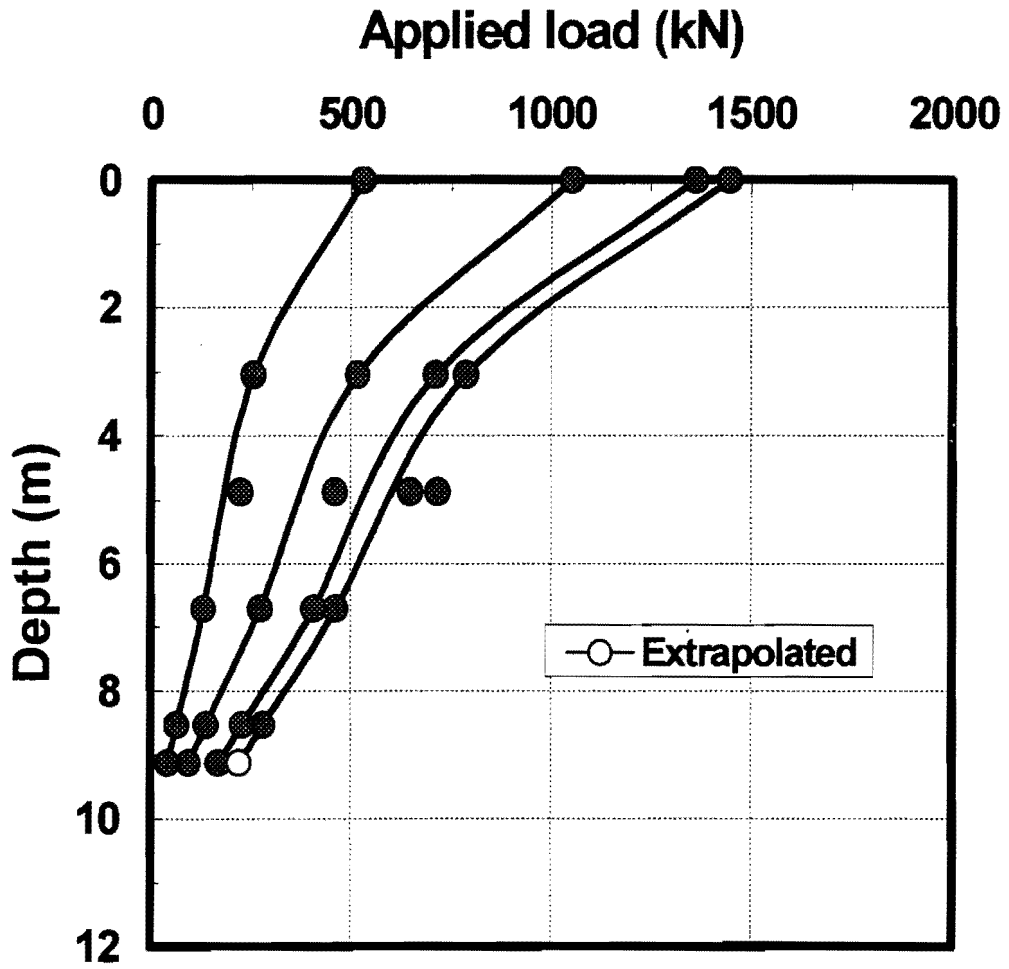


Figure 4.33. Applied load versus depth
(Rosenberg site) (Second cycle)
(Method 1)



**Figure 4.34. Applied load versus depth
(Rosenberg site) (Second cycle)
(Method 2)**

sister bar readings from elevations higher up the pile. Two methods were used for doing this extrapolation. In Method 1 a straight-line fit was made of the loads determined from the sister bars at the four depths at which the bars were placed, and that line was extrapolated to the toe of the pile to give the load in the pile there. In Method 2 a straight line was drawn on the plot of load versus depth in the pile between the lowest two sister bar readings, and that line was extrapolated to the toe of the pile to give the load there. For this reason, Figures 4.27 through 4.34 show two families of load vs. depth relations for each loading test — one based on Method 1 for estimating toe resistance and one based on Method 2.

Once a family of load vs. depth relationships were generated, unit load transfer curves, sometimes called "t-z" curves, were derived using a simple procedure.

- At selected depths along the pile, but not at the toe, the slope of the load vs. depth relation was determined from each of the load-depth curves. Each of the resulting values was divided by the nominal circumference of the pile to give unit side (shearing) resistance.
- At the same depths the settlements at that depth (local settlements) corresponding to the shearing resistances computed in the above step were determined by subtracting from the settlement measured at the pile head the area under the load vs. depth relationship from the pile head to the depth of interest divided by the composite Young's modulus of the pile material times the nominal cross-sectional area of the pile.
- The resulting number pairs (unit side resistance, f_s , and local settlement, w) were then plotted for the loading portion of the test.

- At the pile toe the procedure was similar except that the extrapolated toe load was used directly. This load was then divided by the nominal cross-sectional area of the pile to give the net unit soil reaction stress at the toe of the pile, q , and the relation between q and w (local settlement at the pile toe) was plotted.

The results of these calculations are given in Figures 4.35 through 4.42, in which z is the depth below the ground surface. Figures 4.25 through 4.42 provide considerable insight into the mechanisms for soil resistance along CFA piles in Houston-area soils.

- First, the values of q_{\max} given by Methods 1 and 2 are similar for the Baytown and Rosenberg test piles. At Baytown, complete failure was observed at the pile toe, which is expected since the soil at that depth was a stiff, saturated clay. At Rosenberg the soil was strain hardening, and toe resistance was still increasing at a settlement of 46 mm (1.81 in.). This is also expected, since the toe was located in a dense sand. q_{\max} at Rosenberg at a settlement of 46 mm (1.81 in., or 10 % of the nominal pile diameter) was about twice that at Baytown, which is also expected, considering the types of soil in which the toes were embedded.
- At UH, the toe behavior was very different depending upon whether Method 1 or Method 2 was used to determine toe resistance. For both cases the toe resistance builds up very slowly and the soil appears to be strain hardening, which is more typical of drained behavior (sand or silt) than of undrained behavior (saturated clay). The soil at the toe level in Figure 4.3 is described as a sandy clay. Apparently, the sand seams allowed for some drainage during the loading test. The soil at that level had an undrained shear strength of 136 kPa (1.4 tsf), so that one would expect based on theoretical considerations ($q_{\max} = 9 s_u$) that q_{\max} would be at least 1.2 MPa at toe

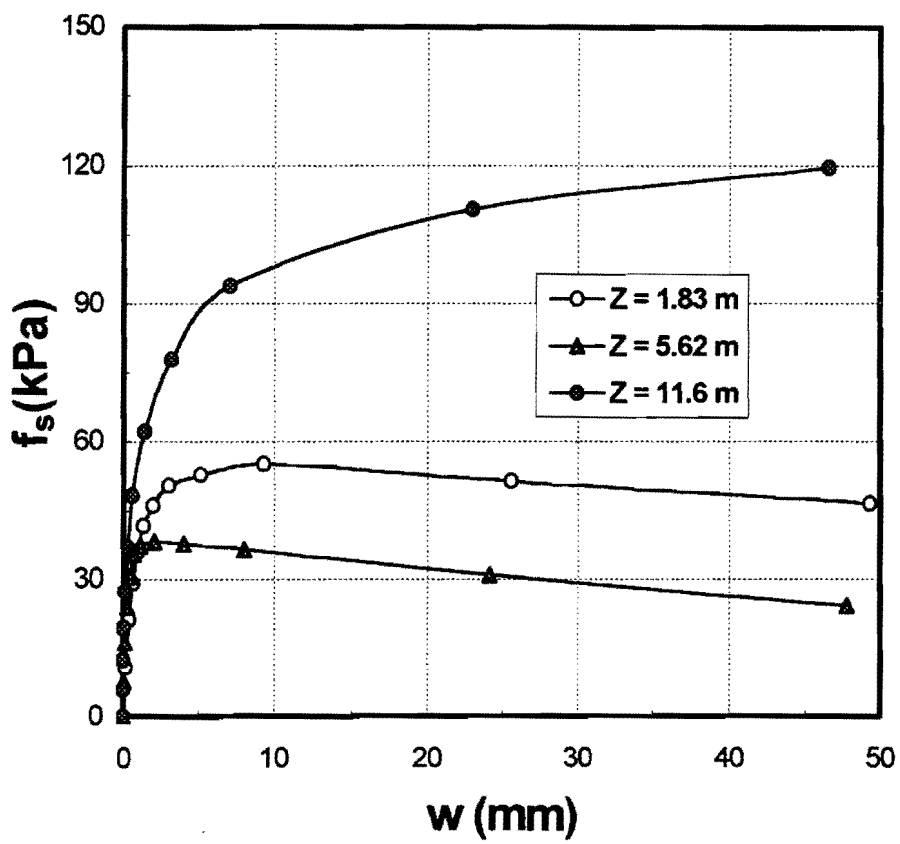


Figure 4.35. Unit side resistance versus settlement (UH site)

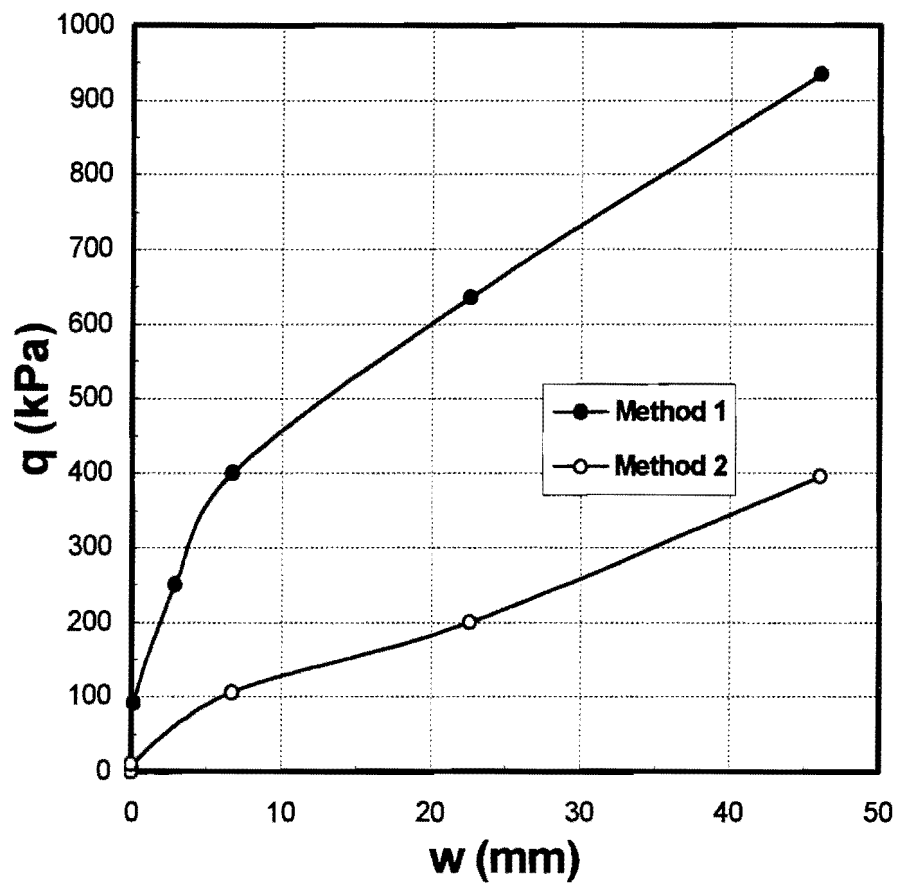


Figure 4.36. Unit toe resistance versus settlement (UH site)

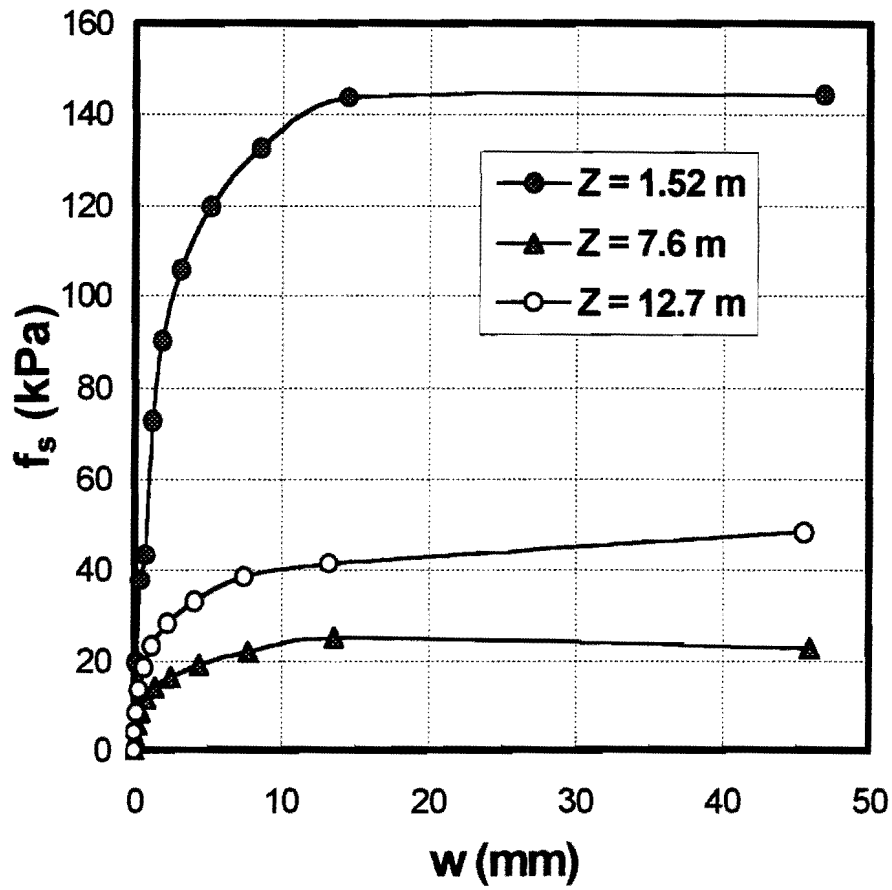


Figure 4.37. Unit side resistance versus settlement (Baytown site)

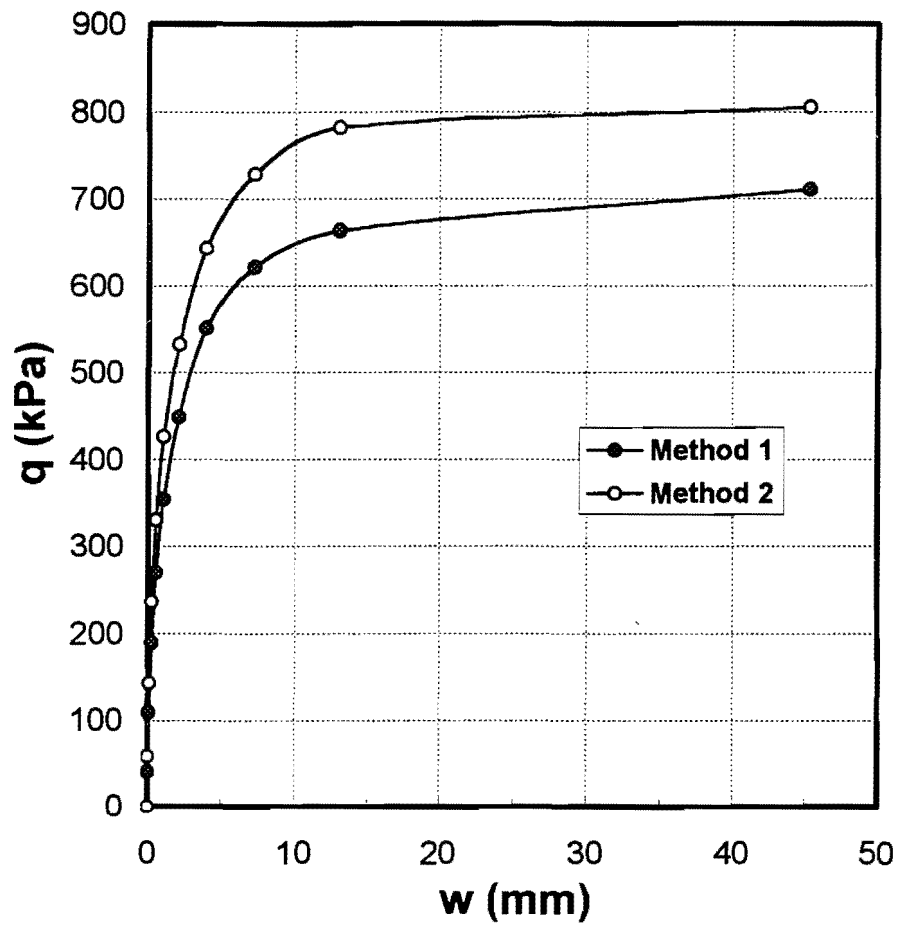


Figure 4.38. Unit toe resistance versus settlement (Baytown site)

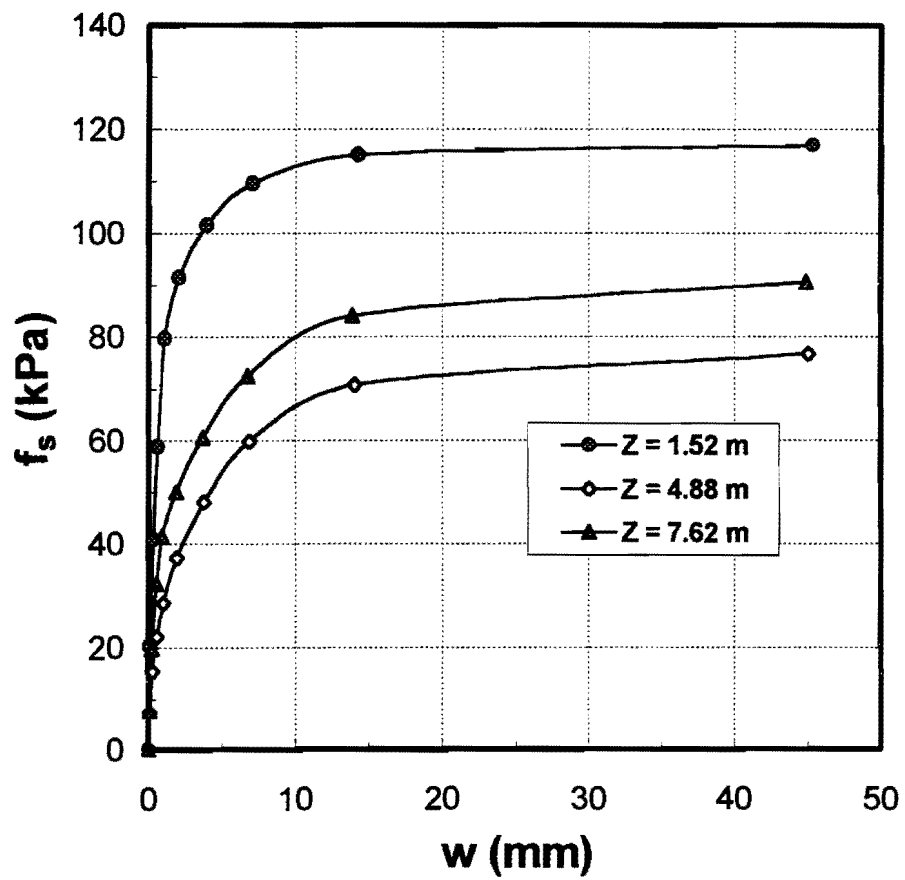


Figure 4.39. Unit side resistance versus settlement (Rosenberg site)

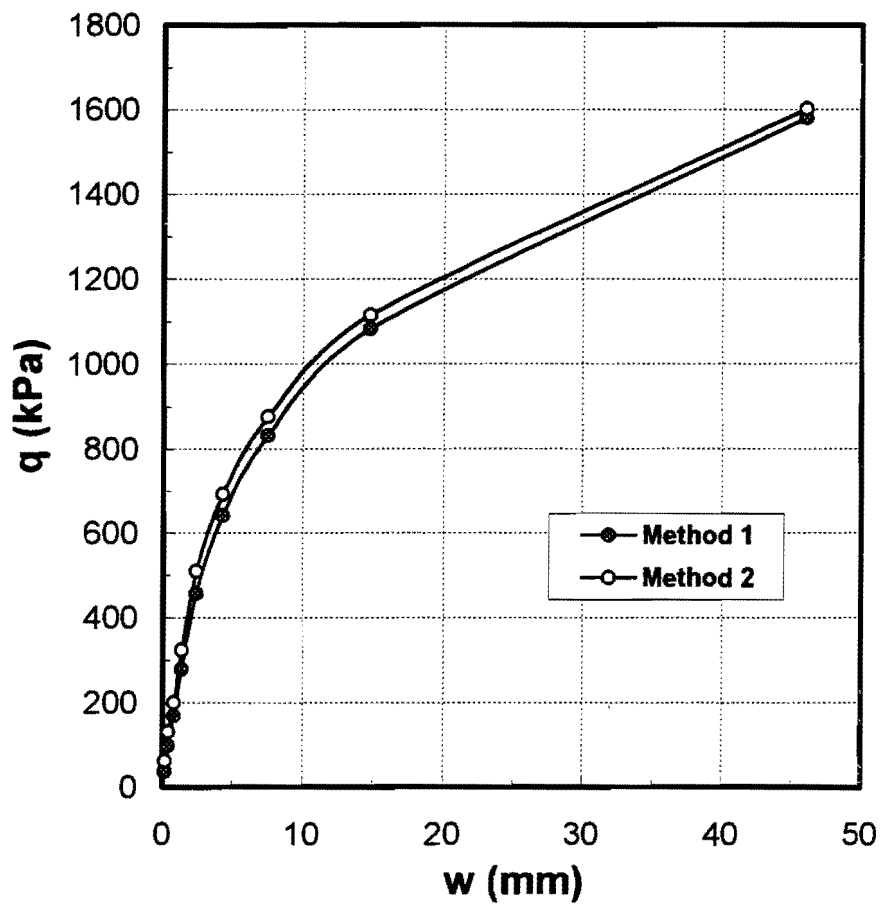


Figure 4.40. Unit toe resistance versus settlement (Rosenberg site)

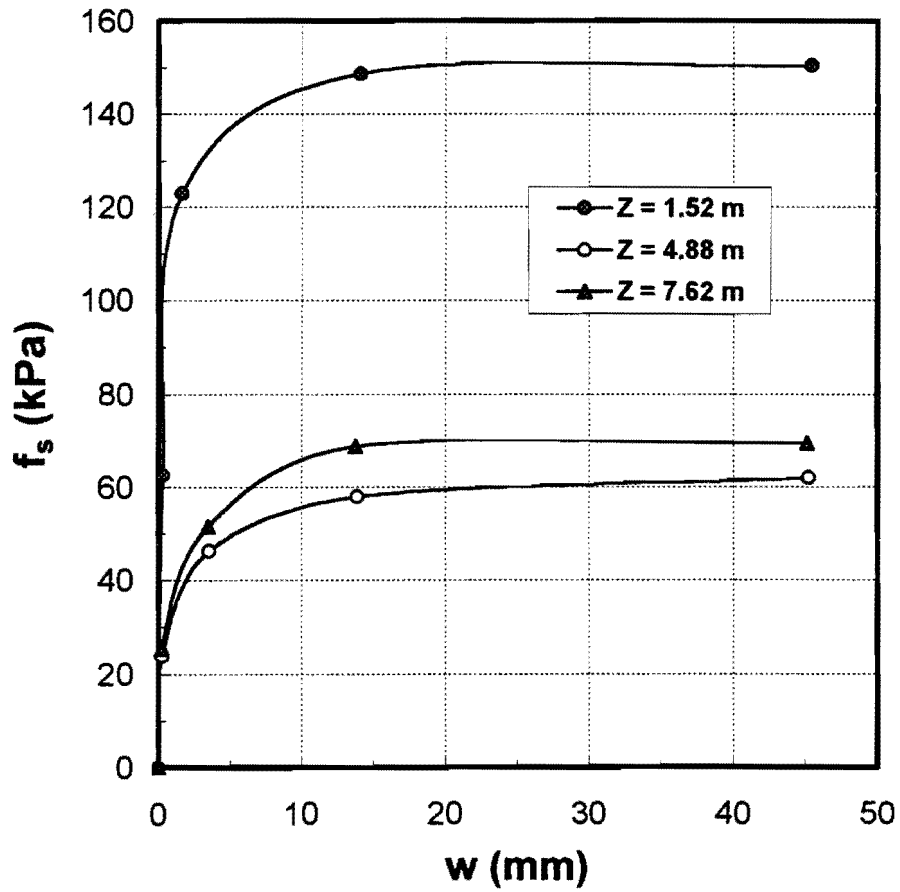


Figure 4.41. Unit side resistance versus settlement (Rosenberg site) (Second cycle)

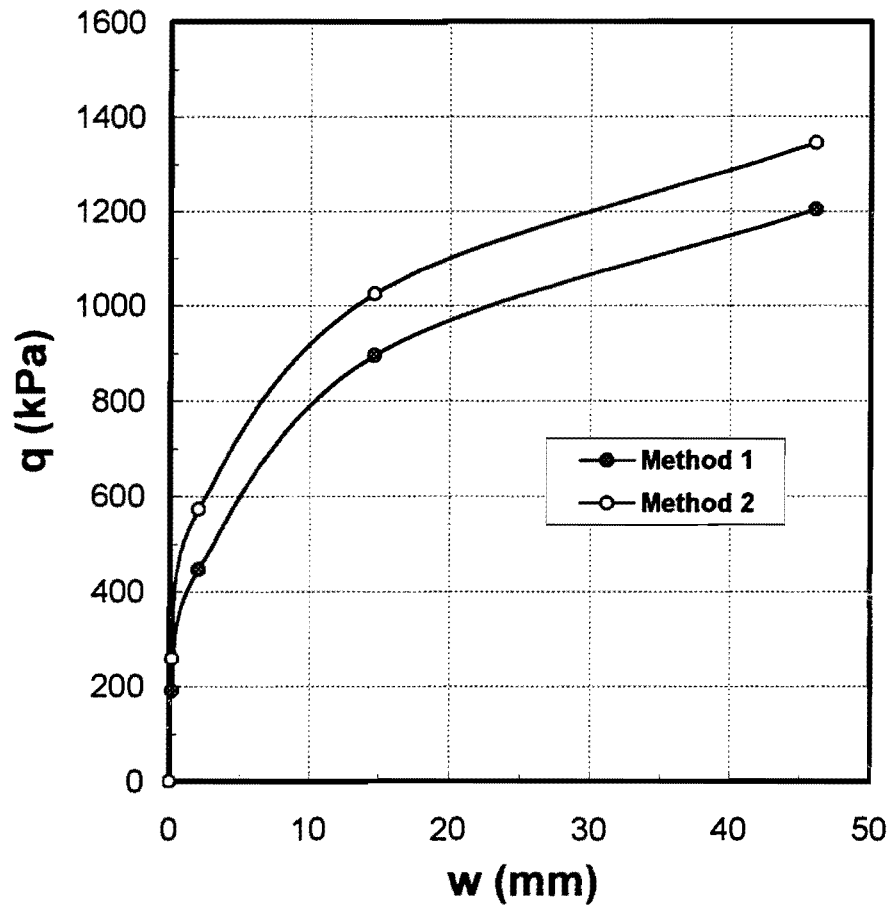


Figure 4.42. Unit toe resistance versus settlement (Rosenberg site) (Second cycle)

failure. Method 1 gave a value of $q_{\max} = 0.93$ MPa at a settlement of 46 mm (1.81 in., or 10 % of the nominal pile diameter); however, Method 2 gave only 0.40 MPa at the same settlement. It must be concluded that Method 1 is the more accurate method for assessing toe resistance at the UH site. Having reached this conclusion, it appears that among the three loading tests, the maximum toe resistance (at a settlement of 10 % of the pile diameter) was always at least 800 kPa (8.35 tsf), which is more than twice the presumptive value used by TxDOT for drilled shafts (Chapter 3).

- The side load transfer profiles are qualitatively similar to the natural soil strength profiles. For example, at Baytown little shear load was transferred to the soil between depths of 4.4 and 10.7 m. It is observed from Figure 4.6 that the N_{TxDOT} values in this depth range were between 1 and 6, indicating a very loose soil. Above and below this depth range, where higher load transfer occurred (e. g., Figure 4.29), N_{TxDOT} values were between 24 and 39. At the UH site, the highest side load transfer occurred below a depth of about 10 m (e. g., Figure 4.27), which coincides with a layer of very sandy clay having a higher undrained shear strength than the clay above it (Figure 4.3). At the Rosenberg site, the side load transfer was relatively uniform with depth, although a slight decrease occurred between depths of about 3 and 7 m (e. g., Figure 4.31), which coincided with the lowest penetrometer blow counts (Figure 4.9).
- At the UH site, Figure 4.35 indicates that the maximum unit side resistance in the clay at a depth of 5.62 m (18.4 ft) was approximately 38 kPa (0.4 tsf). The undrained shear strength of the soil at this depth is 65.1 kPa (0.68 tsf), so that

$38/65.1 = 0.58$ times the undrained shear strength was converted to maximum unit side resistance. At a depth of 11.6 m (38 ft), the maximum unit side resistance was 120 kPa (1.25 tsf), compared with the undrained shear strength of 136 kPa (1.42 tsf), for a strength conversion ratio (α) of 0.88. At the Baytown site, at a depth of 12.7 m (41.7 ft), the maximum side resistance (Figure 4.37) was 48 kPa (0.61 tsf). At that depth (corresponding to the top of the lower clay), the undrained shear strength was 104.7 kPa, for a strength conversion ratio of 0.46. It therefore appears that the full shear undrained shear strength of clay soil should not be used in computing ultimate side shear resistance in CFA piles, as is recommended in the TxDOT design method for drilled shafts (Chapter 3).

These observations suggest that the properties of the natural soil can be used to estimate the capacity of CFA piles.

- The three test piles all developed capacities of between 1300 kN (146 tons) (Rosenberg) and 1600 kN (180 tons) (UH) at a settlement of 5 % of the pile diameter (i. e., 23 mm or 0.91 in.). The pile at Rosenberg, despite being only 60 percent as long as the others, developed a resistance that was almost as high. This is attributable to the type of soil (medium dense to dense moist sand) in which it was founded. The Baytown and UH test piles were the same nominal size, and the Baytown test pile developed about 90 % of the capacity of the UH test pile, despite the more unfavorable soil conditions at the Baytown site. A much greater volume of grout was required to construct the Baytown test pile, however.
- Finally, the settlements of all three test piles were less than 2 mm (0.1 in.) at a load corresponding to one-half of the plunging (failure) load. This is certainly within the

tolerable settlement limit for any bridge that TxDOT would construct and is typical of the settlement that could be expected for a driven pile of similar cross-sectional area and length. The settlement was controlled mainly by side resistance (skin friction), which was essentially fully developed in all test piles at a settlement of 8 to 12 mm (0.3 to 0.5 in.). At the ultimate condition (settlement of 5 % of the pile diameter in these tests), the proportion of applied load carried by the pile toes was 10 % (UH), 8 % (Baytown), and 17 % (Rosenberg). Therefore, at a load equal to one-half of the failure load, side shear resistance had not been fully mobilized, and the settlement was understandably small. Settlement could conceivably increase, perhaps considerably, if CFA piles are installed in closely spaced groups, due to cumulative soil disturbance and to overlapping stress fields in the soil during loading. The same statement could be made for driven piles or drilled shafts. Investigation of group action in CFA piles was beyond the scope of this project.

The pressure gauges were monitored to observe the change of effective horizontal soil pressure during load testing at the three test sites. Figure 4.43 shows the relation between the horizontal soil pressure and the load applied to the head of the pile. The test results trends were the same as that in the pile installation, pressures are anomalous at the UH site and as expected at the Baytown and Rosenberg sites. Relatively large increases in lateral effective pressure were observed at the Baytown and Rosenberg sites during loading.

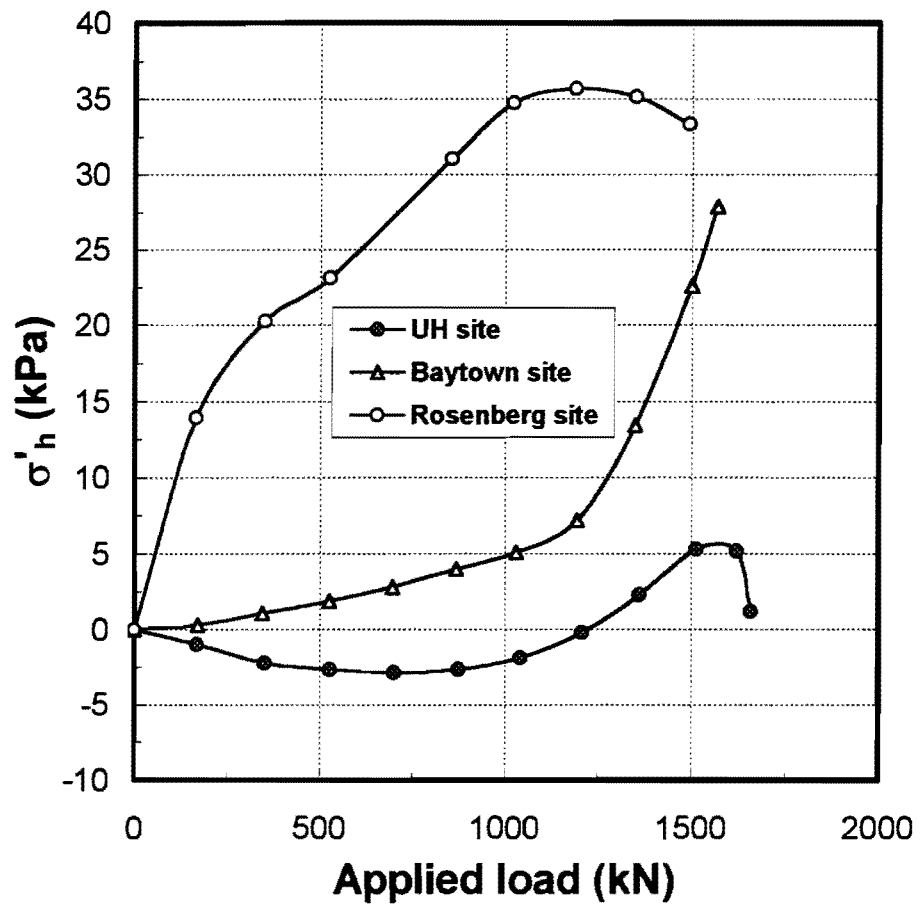


Figure 4.43. Horizontal effective pressure versus applied load

This page is intentionally blank.

CHAPTER 5 ANALYSIS OF DATABASE

5.1. REAPPLICATION OF DESIGN METHODS INCLUDING NEW TEST DATA

Once the loading tests described in Chapter 4 were conducted and analyzed, they were then merged into the database described in Chapter 3, increasing the size of the database from 43 to 46 CFA pile load tests. The capacities of the new test piles were computed according to the various design methods described in Chapter 3, and the ratios of measured to computed total capacities were added to the database. Finally, the mean values, standard deviations, and coefficients of variation were recomputed for each class of soil (clay, sand, mixed profile). The results are tabulated in Tables 5.1 through 5.3 and shown graphically in Figures 5.1 through 5.16.

The addition of the new tests did not change the conclusions drawn in Chapter 3 regarding which design methods are the most appropriate for CFA piles in Texas coastal soils. However, CPT data were available at the UH site, and, using those data, the LPC method yielded the most accurate prediction of pile capacity at UH. The recommended method for clay, the TxDOT Method, produced a slightly conservative prediction of pile capacity at UH (Table 5.1). No changes were made in the data for sand sites, Table 5.2, because none of the new tests was conducted in a purely sand profile. The FHWA method, which is the recommended method for sands and mixed soil profiles, yielded quite accurate predictions for the Baytown and Rosenberg mixed

Table 5.1 Ratios of measured to predicted capacities of CFA piles in clay

Project	Coyle	API	LPC	FHWA	TxDOT
2KE/BE	1.29	1.36	0.89	1.67	1.31
5FP/BE	1.15	1.46	1.02	1.49	1.17
7PA/BS	0.88	0.77	0.65	0.84	0.65
13NL/BS	1.39	2.26	1.42	2.48	1.85
14PA/BS	2.28	2.56	1.78	2.42	1.41
22BA/EU	0.72	0.78	0.58	0.68	0.76
23BA/EU	1.42	1.88	1.26	1.82	1.38
24AT/BS	0.96	1.14	0.84	1.15	1.04
44TA/MCM	1.12	1.22	0.87	1.05	1.03
45TA/MCM	1.16	1.16	1.00	0.97	1.02
<i>UH site</i>	<i>1.33</i>	<i>1.34</i>	<i>1.09</i>	<i>1.40</i>	<i>1.12</i>
55PA/BS	1.18	1.28	0.94	1.71	-
56PA/BS	1.19	1.23	1.02	2.00	-
Mean	1.24	1.42	1.03	1.51	1.16
St. Dev.	0.37	0.52	0.32	0.57	0.32
COV	0.30	0.37	0.31	0.38	0.35

Table 5.2 Ratios of measured to predicted capacities of CFA piles in sand

Project	Wright	Neely	Coyle	API	LPC	FHWA
25PB/MCM	0.57	0.31	0.30	0.55	0.42	0.52
26TV/MCM	1.02	0.74	0.54	1.30	0.61	0.92
27VB/MCM	1.10	1.09	0.90	1.43	1.30	1.01
29ST/MCM	0.96	0.59	0.53	1.00	0.79	0.93
30WH/MCM	1.56	0.70	1.01	1.52	1.18	1.33
31RU/MCM	1.35	0.86	0.68	1.33	0.97	1.23
32ST/MCM	0.45	0.42	0.43	0.37	0.38	0.41
33ST/MCM	1.47	0.83	0.67	1.35	0.90	1.35
34TI/MCM	1.08	1.20	0.74	1.82	0.91	1.12
35ST/MCM	0.80	0.85	0.85	1.28	1.20	0.88
36TA/MCM	1.06	0.74	1.37	1.01	1.47	0.95
37JA/MCM	1.28	0.60	1.04	1.15	1.43	1.11
38SA/MCM	0.93	0.96	0.62	1.09	0.93	0.88
39ST/MCM	0.99	0.72	0.56	1.23	0.97	0.90
40PA/MCM	1.25	0.88	0.69	1.30	1.35	1.32
41CO/MCM	1.35	0.77	0.94	1.18	1.35	1.22
42PO/MCM	0.72	0.72	0.76	0.68	0.78	0.74
43PA/MCM	0.76	0.53	0.46	0.72	0.66	0.73
Mean	1.04	0.75	0.73	1.13	0.98	0.98
St. Dev.	0.31	0.22	0.26	0.36	0.34	0.27
COV	0.29	0.29	0.36	0.32	0.34	0.28

Table 5.3 Ratios of measured to predicted capacities of CFA piles in mixed soil profiles

Project	Coyle	API	LPC	FHWA	TXDOT
1KE/BE	0.95	1.04	0.84	1.54	-
4BS/BE	1.30	1.09	0.82	1.09	-
8SI/TE	0.93	0.98	1.39	1.56	-
9SL/MA	0.52	0.79	0.89	1.01	-
10SL/MA	0.65	0.78	1.01	1.09	-
11PL/BS	0.96	1.15	0.98	1.20	-
12MI/BS	1.56	1.92	2.00	1.85	-
46GA/B/SMI	0.74	0.92	1.06	1.14	-
47GA/B/SMI	1.35	1.96	1.32	1.15	-
48FP/BT	0.82	1.20	1.14	1.43	-
49FP/BT	1.32	1.30	1.02	1.25	-
50FP/BT	1.61	1.92	1.49	1.19	-
<i>Baytown</i>	<i>1.33</i>	<i>1.39</i>	<i>1.33</i>	<i>0.96</i>	<i>1.75</i>
<i>Rosenberg</i>	<i>0.87</i>	<i>0.68</i>	<i>0.77</i>	<i>0.98</i>	<i>2.05</i>
51BR/BE	1.72	1.15	1.37	1.09	-
Mean	1.11	1.22	1.16	1.24	1.90
St. Dev.	0.37	0.42	0.33	0.25	(0.18)
COV	0.34	0.34	0.28	0.20	(0.10)

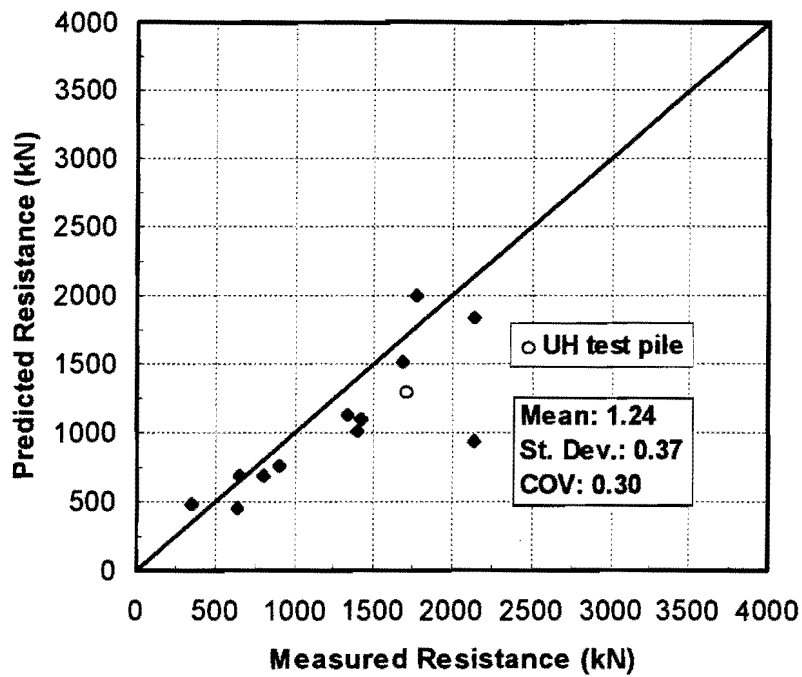


Figure 5.1. Coyle and Castello - Tomlinson method in clay

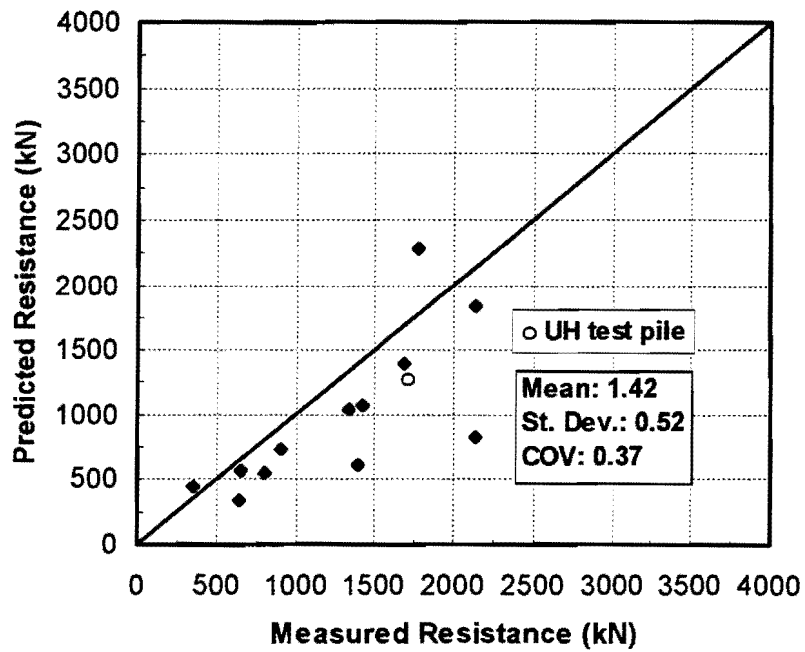


Figure 5.2. API method in clay

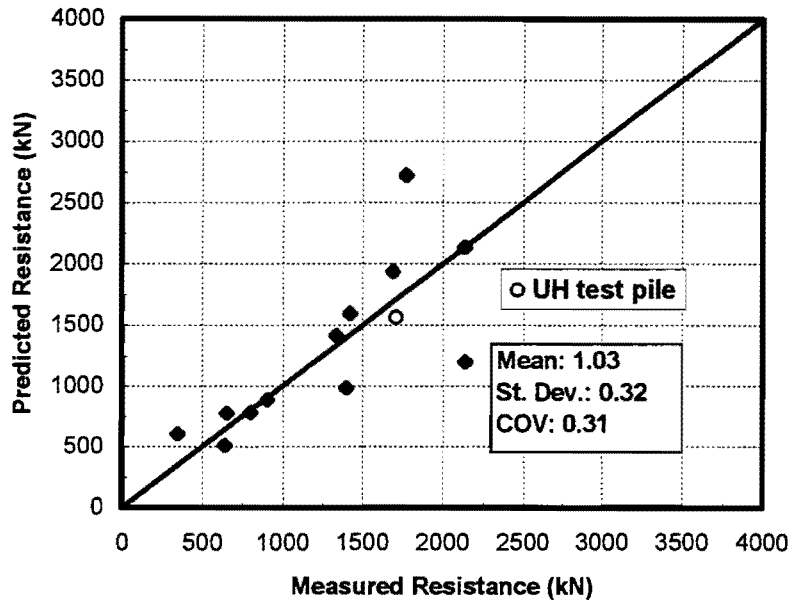


Figure 5.3. LPC method in clay

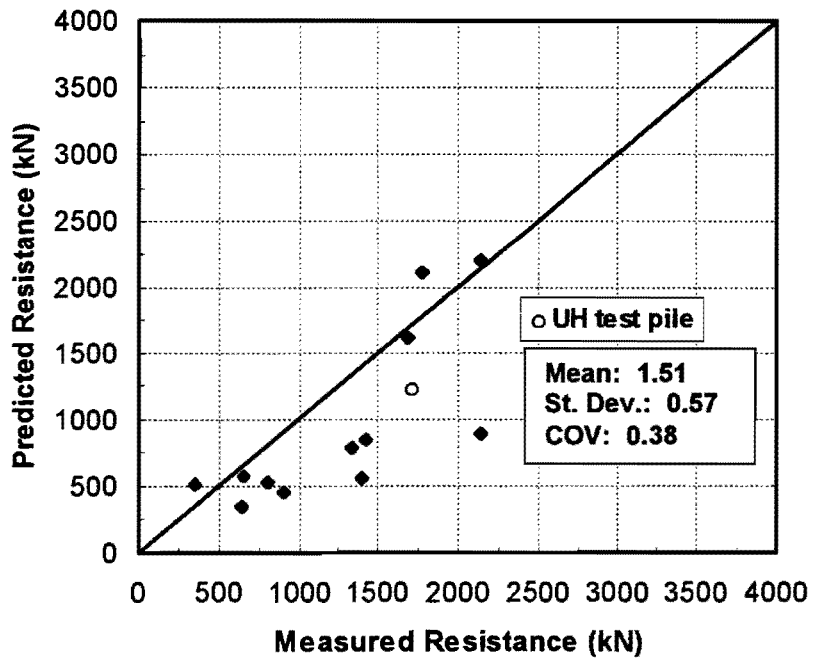


Figure 5.4. FHWA method in clay

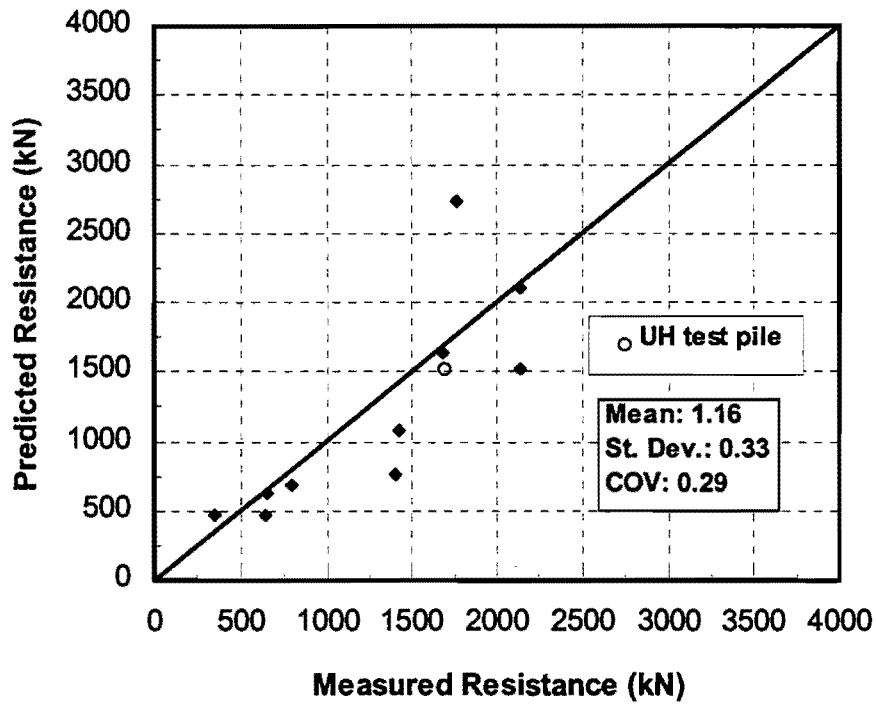


Figure 5.5. TxDOT method in clay

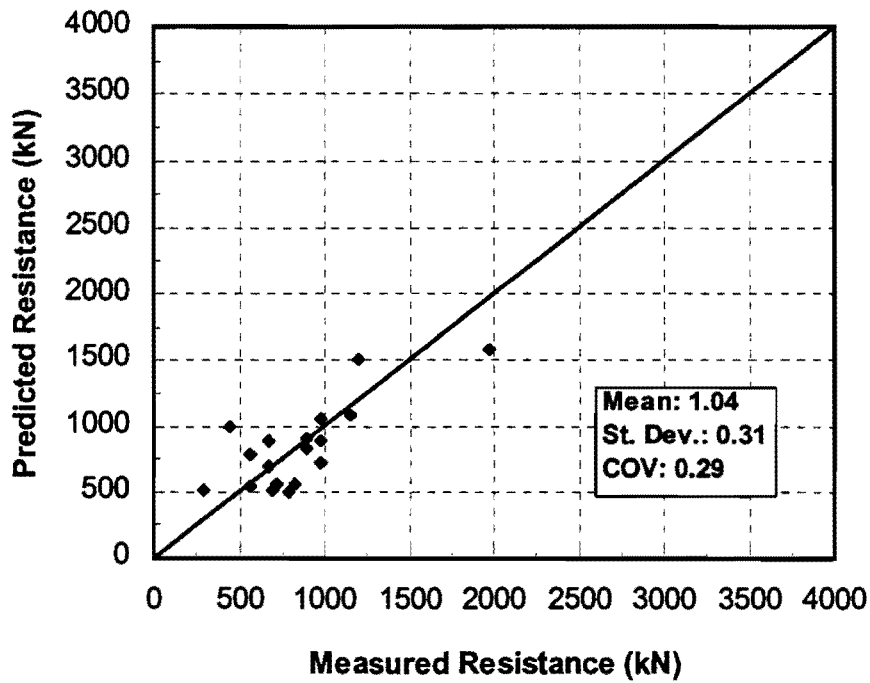


Figure 5.6. Wright and Reese method in sand

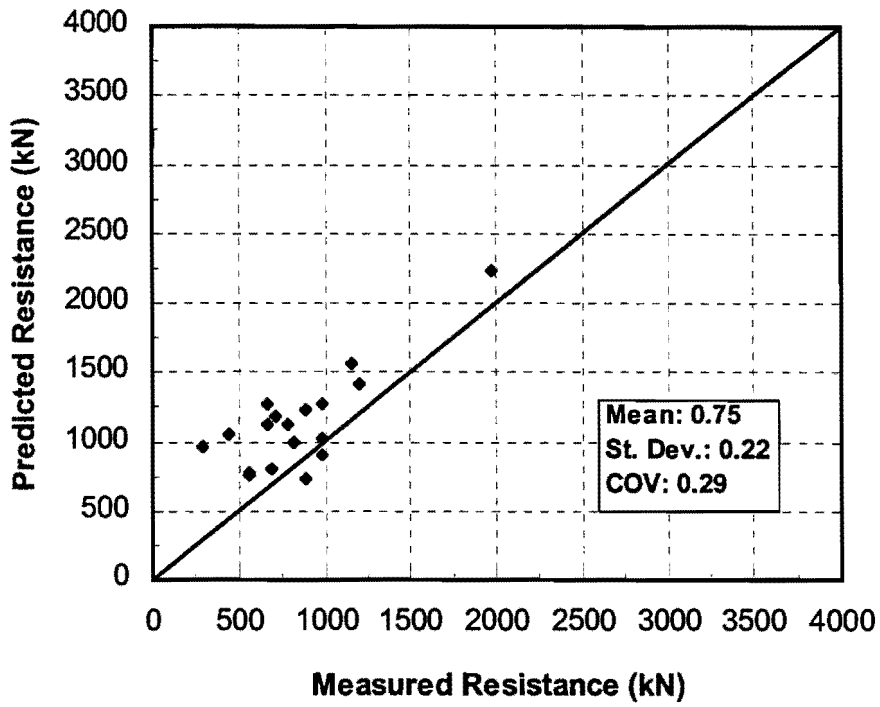


Figure 5.7. Neely method in sand

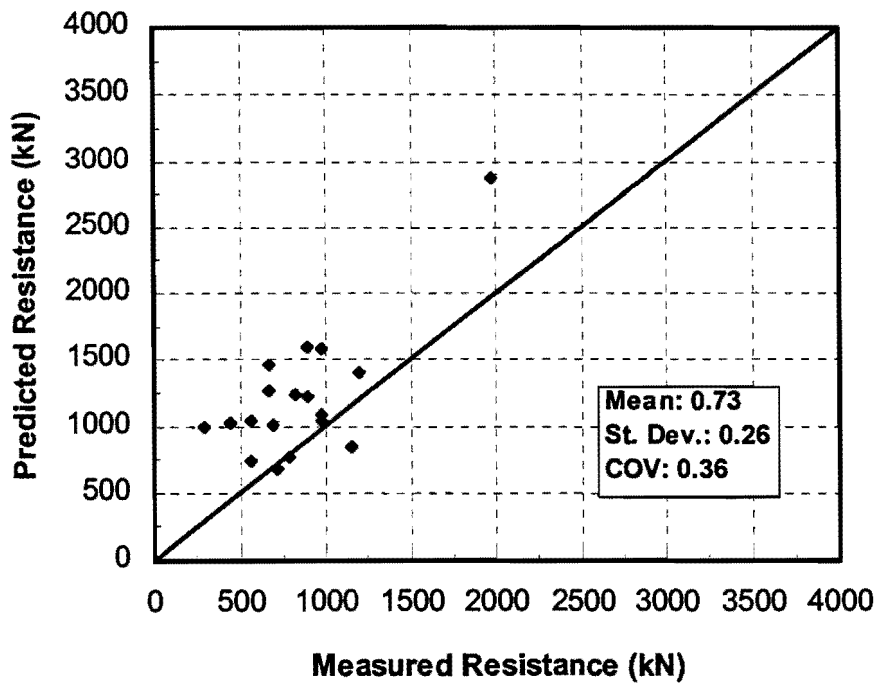


Figure 5.8. Coyle and Castello method in sand

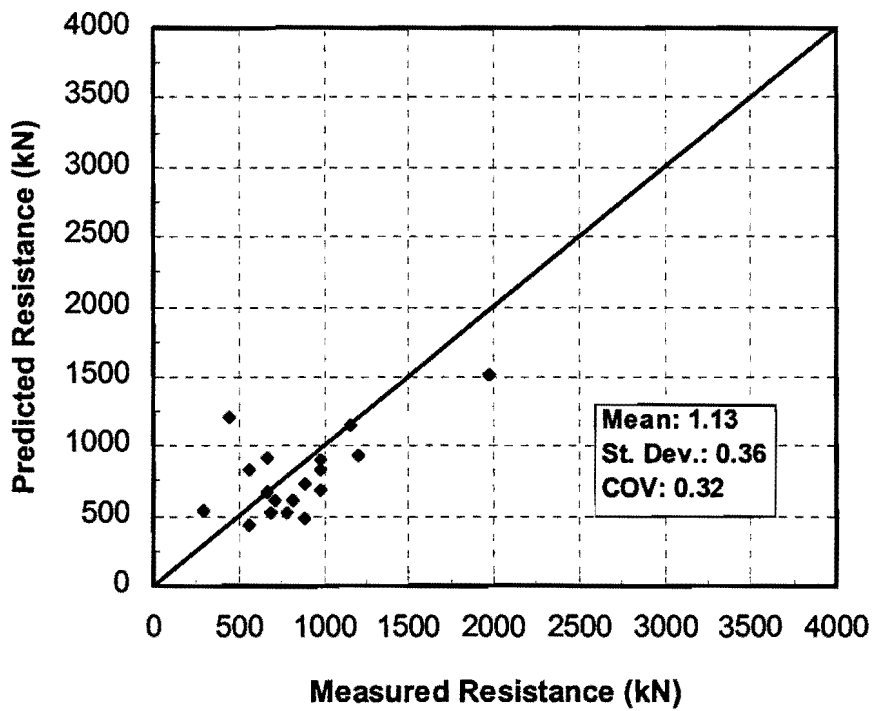


Figure 5.9. API method in sand

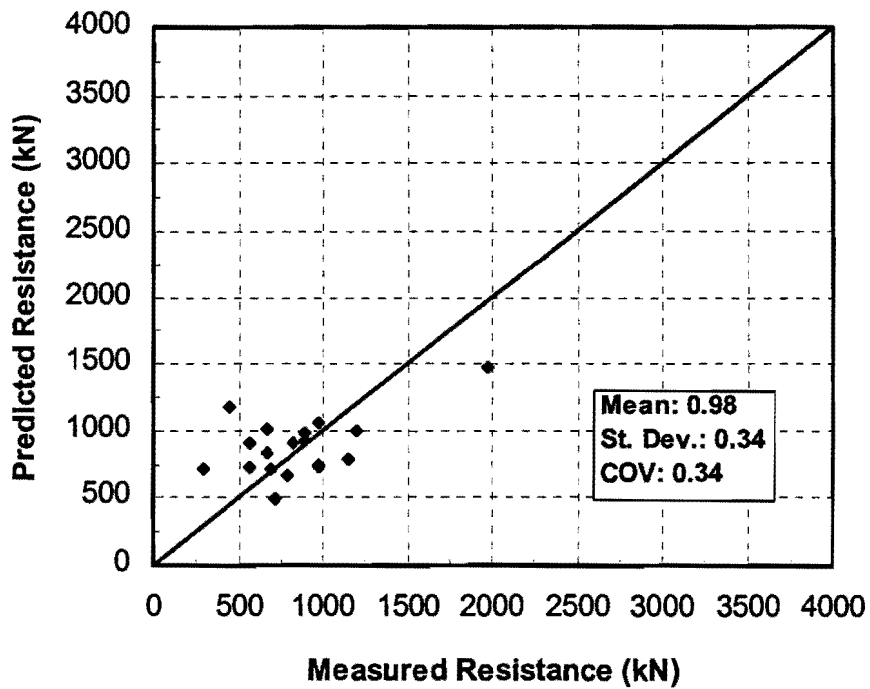


Figure 5.10. LPC method in sand

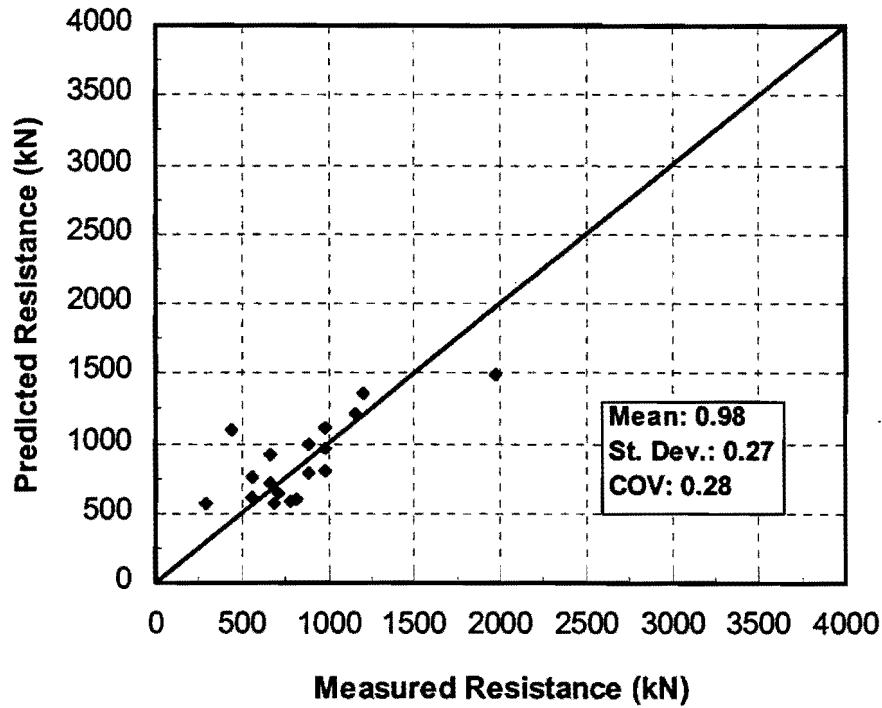


Figure 5.11. FHWA method in sand

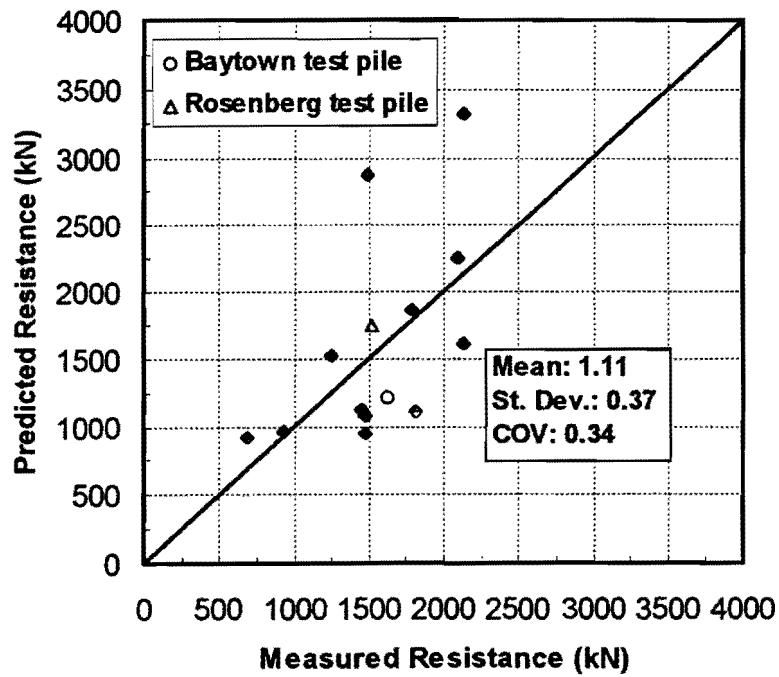


Figure 5.12. Coyle and Castello - Tomlinson method in mixed soil profiles

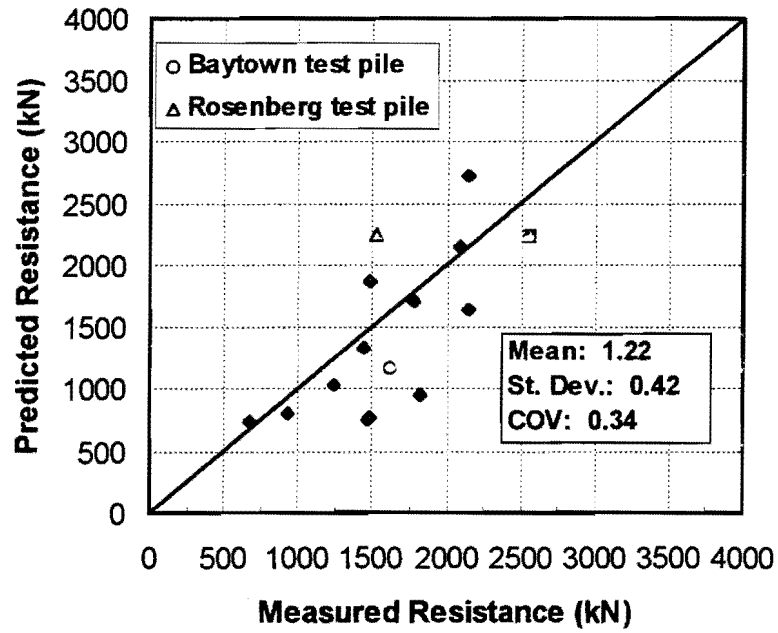


Figure 5.13. API method in mixed soil profiles

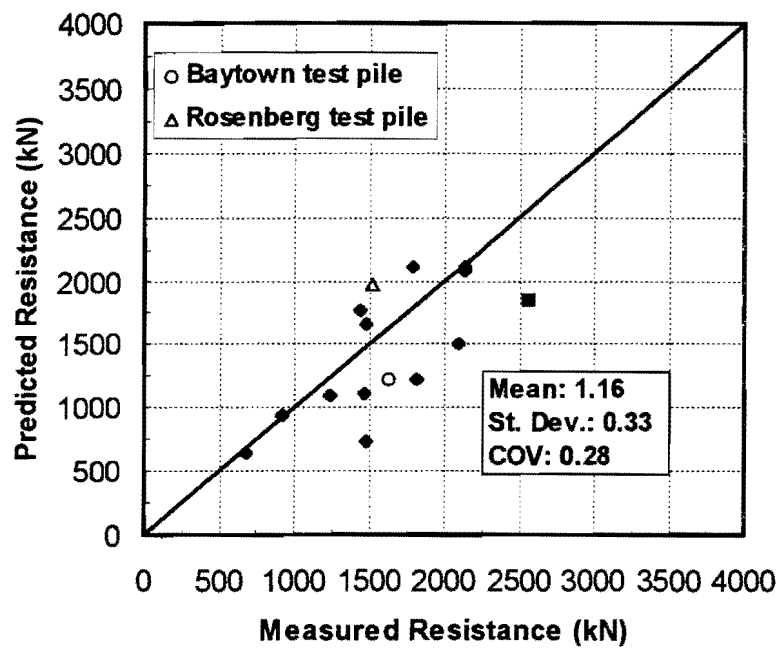


Figure 5.14. LPC method in mixed soil profiles

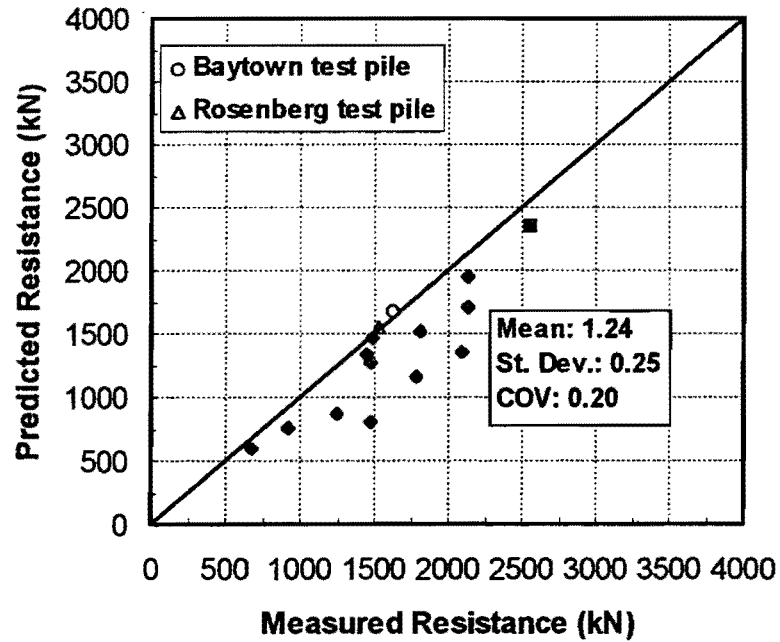


Figure 5.15. FHWA method in mixed soil profiles

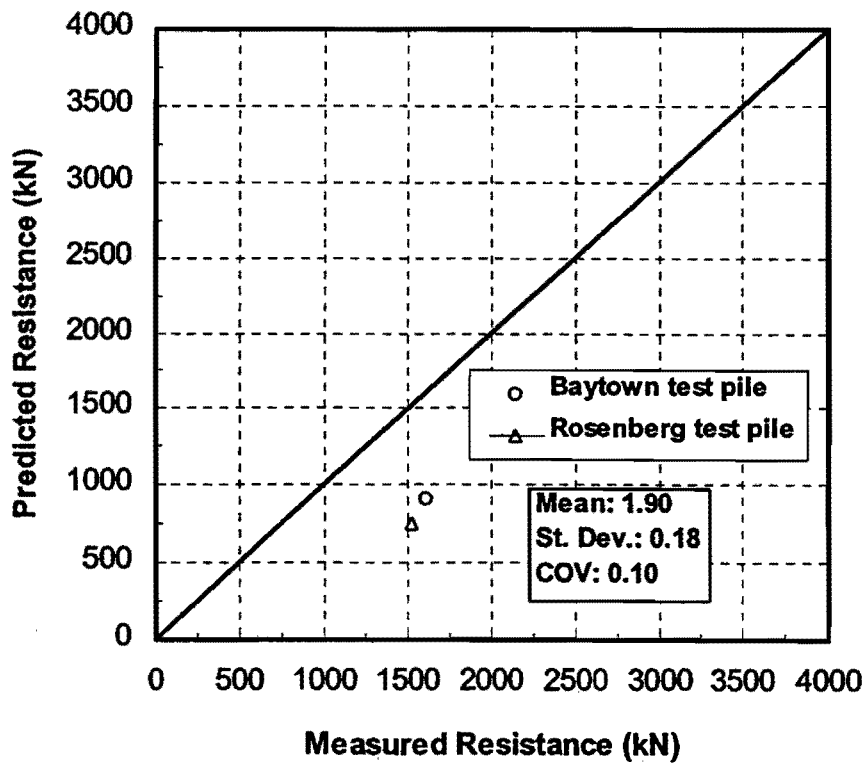


Figure 5.16. TxDOT method in mixed soil profiles

soil profile sites (Table 5.3). The TxDOT method yielded compressive capacities that averaged almost twice those that were measured at the two mixed profile sites (Baytown and Rosenberg).

Commentary on the TxDOT design method

While the TxDOT (Houston District) method performed well for clay sites, it was very conservative for the two mixed profile sites (Baytown and Rosenberg) at which new load tests were conducted. The capacities of these test piles were developed substantially in sand, either in side resistance, end bearing, or both. As stated in Chapter 3, the TxDOT design method for drilled shafts in sand is generally based upon visual soil classification and TxDOT cone penetrometer test data (N values). Some insight into the apparent discrepancy can be gained by considering earlier studies for TxDOT that related the N value from the standard penetration test (SPT) to the N value from the TxDOT cone in sands within the Houston District and similar Texas coastal soils (Touma, 1972). In particular, the following average correlations were obtained.

$$N_{\text{TxDOT}} = 1.43 N_{\text{SPT}} \text{ (clay)} \quad (5.1)$$

$$N_{\text{TxDOT}} = 2.0 N_{\text{SPT}} \text{ (sand)} \quad (5.2)$$

For the current tests at Baytown and Rosenberg, TxDOT cone and SPT tests were performed in parallel. The capacity calculations for these two piles proceeded using the in situ data directly from the TxDOT cone tests at the test sites, and the ratios of the measured to predicted capacities for these two piles were about 2.0. It seems that use

of the actual in situ data from the TxDOT cone in the prediction of the ultimate capacities of CFA piles severely underestimated the pile capacities.

Examining the situation further, the data for N_{SPT} versus N_{TxDOT} , from Touma, 1972, are replotted in Figure 5.17 after excluding the data points for which $N_{SPT} > 60$ in sand. Values greater than 60 are assumed to represent cemented sands or very dense sands that will be excluded from consideration here. The side-by-side results from the SPT and TxDOT cone tests from the two current test sites (Baytown and Rosenberg) were then added to the data from Touma (1972) and are also shown in Figure 5.17. The resulting linear correlations between the SPT and the TxDOT test results are as follows:

$$N_{TxDOT} = 1.48 N_{SPT} \text{ (sand)} \quad (5.3)$$

However, as can be seen on Figure 5.17, the results are very scattered and to some extent appear to be site specific. Both sets of TxDOT cone tests performed for the current project tended to produce ratios of N_{TxDOT}/N_{SPT} that were lower than those reported by Touma. At the Rosenberg site (moist, medium dense sand) the average value for N_{TxDOT}/N_{SPT} appears to be less than 1.0. At Baytown (submerged, loose sand), it appears to be greater than 1.0 but slightly less than 1.48. At this point it cannot be determined whether the variable correlation is due to differences in the way either the TxDOT cone penetration tests or the standard penetration tests were performed in the study of Touma and in the current study, to some unknown difference in soil response in the two studies that may reflect site specific differences in correlations, or to some other effect. Figure 5.17 confirms, however, the correctness of the decision not to estimate pile capacities

with the TxDOT method in sand profiles or mixed sand-clay profiles by using correlations between SPT data and the TxDOT cone N value.

The low ratios of N_{TxDOT} to N_{SPT} at the two new test sites, relative to archival data (i. e., Touma, 1972), appear to be associated with the fact that the TxDOT method for drilled shafts (Houston District) underpredicted CFA pile capacities at those sites. Until this issue is resolved, no conclusions can be drawn from the lack of correlation in Figure 5.16. Further inquiry into this phenomenon is beyond the scope of this project but clearly merits further consideration.

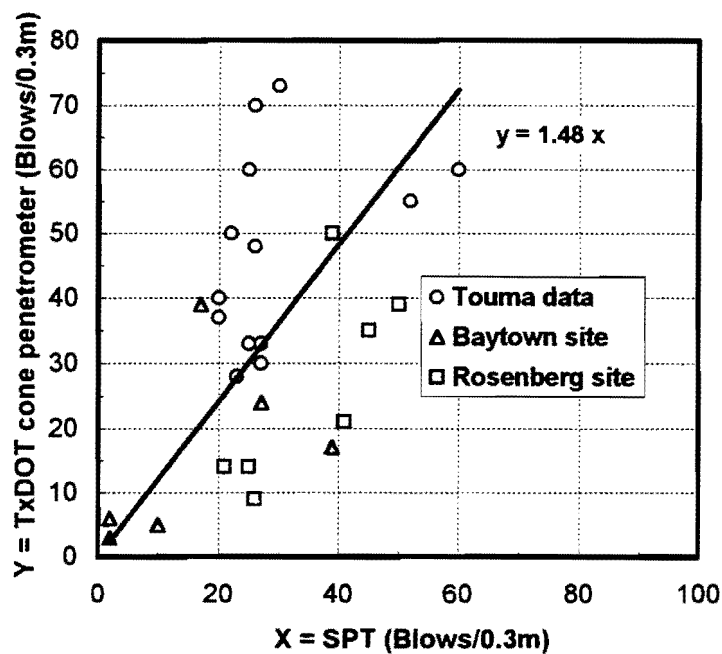


Figure 5.17. Correlation between SPT and TxDOT cone penetrometer in sand

5.2. RESISTANCE FACTORS AND FACTORS OF SAFETY

The calculation of nominal capacity from one of the recommended design methods is only one step in the design process. An equally important step is the estimation of an appropriate strength-state resistance factor [if design is being done in a load and resistance factor design (LRFD) format] or factor of safety [if design is being done in an allowable stress design (ASD) format]. Resistance factors and factors of safety are often chosen based on experience. In the private sector factors of safety of 2 to 3 are usually used with CFA piles; however, the existence of the database described earlier allows for the computation of appropriate factors of safety and resistance factors based on a target level of reliability. This topic is the subject of this section.

5.2.1. LRFD method

The general LRFD design equation can be expressed as

$$\eta \sum_i \gamma_i Q_i = \sum_i \phi_i R_i \quad (5.4)$$

where

Q_i = i th nominal load component,

γ_i = load factor for i th load component,

R_i = i th computed resistance component,

ϕ_i = resistance factor for i th resistance component, and

η = structural performance factor, which can range from 0.95 to 1.05.

Equation 5.4 can also be applied in the following simple form.

$$\eta \sum_i \gamma_i Q_i = \phi R, \quad (5.5)$$

where the resistance factor ϕ is used for the sum of all components of resistance, R .

The following equation is used to calculate the resistance factor for Equation (5.5).

$$\phi = \frac{\lambda_R (\gamma_D \frac{Q_{DN}}{Q_{LN}} + \gamma_L)}{(\lambda_D \frac{Q_{DN}}{Q_{LN}} + \lambda_L) (\sqrt{(1+V_R^2)/(1+V_D^2+V_L^2)}) \exp \left[\beta_T \sqrt{\ln((1+V_R^2)(1+V_D^2+V_L^2))} \right]} \quad (5.6)$$

where

ϕ = resistance factor,

Q_{DN} = nominal dead load,

Q_{LN} = nominal live load,

γ_D = load factor for dead load = 1.25 (AASHTO value),

γ_L = load factor for live load = 1.75 (AASHTO value),

λ_D = bias factor for dead load, = 1.04,

λ_L = bias factor for live load, = 1.60,

λ_R = bias factor for resistance,

V_D = COV of dead load, = 0.09,

V_L = COV of live load, = 0.18,

V_R = COV of resistance, and

β_T = target reliability index.

In evaluating Equation (5.6), it is assumed that the data are distributed lognormally, that the ratio of dead load to live load ranges from 1.0 to 2.0, and values of γ_D , γ_L , λ_L , V_L , λ_D , V_D obtained from Yoon and O'Neill (1997) are appropriate. Values of λ_R and V_R are obtained from the database (Tables 5.1 through 5.3), in which λ_R is the bias factor for the method, which can be taken to be the mean ratio of measured to computed capacity for a given method. V_R is the coefficient of variation of that ratio for a given method. It is also necessary to choose a target reliability index, β_T , which denotes the probability that a particular pile will develop its plunging load due to errors in evaluating the load components and estimating the pile capacity. Values of β_T of 3.0 to 3.5 were selected for analysis. The former value represents a theoretical reliability of 0.9987, and the latter represents a theoretical reliability of 0.9998. Actual reliabilities should be somewhat higher, as the design methods do not account for factors such as bearing capacity of the footing to which the piles are fixed.

Calculations of ϕ by Equation (5.6) are shown for the TxDOT method in clay and the FHWA method in sand and mixed soil profiles in Tables 5.4 through 5.6 and Figures 5.18 through 5.20. It is clear that the resistance factor depends on both the method used to design the pile and the type of soil in which the pile is placed. For a reliability of CFA piles of 0.9998 ($\beta_T = 3.5$) in mixed soil profiles, $\phi = 0.51$ appears appropriate if the FHWA method is used.

Table 5.4 Calculation of resistance factor for TxDOT method in clay

TxDOT method ($\beta_T = 3.0$)

1	2	3	4	5	6	7	8	9	10	11	12	13	14	15	16	17	18	19
Q_{Dn}/Q_{Ln}	γ_D	γ_L	λ_D	λ_L	λ_R	$6*(2*1+3)$	$4*1+5$	V_R	$1.0+9^2$	V_D	V_L	a^*	$10*13$	$14^{0.5}$	β_T	b^*	c^*	ϕ
1.00	1.25	1.75	1.04	1.60	1.16	3.48	2.64	0.35	1.12	0.09	0.18	1.04	1.17	1.08	3.00	0.16	3.26	0.37
1.20	1.25	1.75	1.04	1.60	1.16	3.77	2.85	0.35	1.12	0.09	0.18	1.04	1.17	1.08	3.00	0.16	3.26	0.38
1.40	1.25	1.75	1.04	1.60	1.16	4.06	3.06	0.35	1.12	0.09	0.18	1.04	1.17	1.08	3.00	0.16	3.26	0.38
1.60	1.25	1.75	1.04	1.60	1.16	4.35	3.26	0.35	1.12	0.09	0.18	1.04	1.17	1.08	3.00	0.16	3.26	0.38
1.80	1.25	1.75	1.04	1.60	1.16	4.64	3.47	0.35	1.12	0.09	0.18	1.04	1.17	1.08	3.00	0.16	3.26	0.38
2.00	1.25	1.75	1.04	1.60	1.16	4.93	3.68	0.35	1.12	0.09	0.18	1.04	1.17	1.08	3.00	0.16	3.26	0.38

TxDOT method ($\beta_T = 3.5$)

1	2	3	4	5	6	7	8	9	10	11	12	13	14	15	16	17	18	19
Q_{Dn}/Q_{Ln}	γ_D	γ_L	λ_D	λ_L	λ_R	$6*(2*1+3)$	$4*1+5$	V_R	$1.0+9^2$	V_D	V_L	a^*	$10*13$	$14^{0.5}$	β_T	b^*	c^*	ϕ
1.00	1.25	1.75	1.04	1.60	1.16	3.48	2.64	0.35	1.12	0.09	0.18	1.04	1.17	1.08	3.50	0.16	3.97	0.31
1.20	1.25	1.75	1.04	1.60	1.16	3.77	2.85	0.35	1.12	0.09	0.18	1.04	1.17	1.08	3.50	0.16	3.97	0.31
1.40	1.25	1.75	1.04	1.60	1.16	4.06	3.06	0.35	1.12	0.09	0.18	1.04	1.17	1.08	3.50	0.16	3.97	0.31
1.60	1.25	1.75	1.04	1.60	1.16	4.35	3.26	0.35	1.12	0.09	0.18	1.04	1.17	1.08	3.50	0.16	3.97	0.31
1.80	1.25	1.75	1.04	1.60	1.16	4.64	3.47	0.35	1.12	0.09	0.18	1.04	1.17	1.08	3.50	0.16	3.97	0.31
2.00	1.25	1.75	1.04	1.60	1.16	4.93	3.68	0.35	1.12	0.09	0.18	1.04	1.17	1.08	3.50	0.16	3.97	0.31

Note: $a^* = 1.0+11^2+12^2$
 $b^* = \ln(10*13)$
 $c^* = \exp(16*17^{0.5})$
 $\phi = 7/(8*15*18)$
 The numbers (#1,2,3...) represent the column number.

Table 5.5 Calculation of resistance factor for FHWA method in sand

FHWA method ($\beta_T = 3.0$)

1	2	3	4	5	6	7	8	9	10	11	12	13	14	15	16	17	18	19
Q_{Dn}/Q_{Ln}	γ_D	γ_L	λ_D	λ_L	λ_R	$6*(2*1+3)$	$4*1+5$	V_R	$1.0+9^2$	V_D	V_L	a^*	$10*13$	$14^{0.5}$	β_T	b^*	c^*	ϕ
1.00	1.25	1.75	1.04	1.60	0.98	2.94	2.64	0.28	1.08	0.09	0.18	1.04	1.12	1.06	3.00	0.12	2.77	0.38
1.20	1.25	1.75	1.04	1.60	0.98	3.19	2.85	0.28	1.08	0.09	0.18	1.04	1.12	1.06	3.00	0.12	2.77	0.38
1.40	1.25	1.75	1.04	1.60	0.98	3.43	3.06	0.28	1.08	0.09	0.18	1.04	1.12	1.06	3.00	0.12	2.77	0.38
1.60	1.25	1.75	1.04	1.60	0.98	3.68	3.26	0.28	1.08	0.09	0.18	1.04	1.12	1.06	3.00	0.12	2.77	0.38
1.80	1.25	1.75	1.04	1.60	0.98	3.92	3.47	0.28	1.08	0.09	0.18	1.04	1.12	1.06	3.00	0.12	2.77	0.39
2.00	1.25	1.75	1.04	1.60	0.98	4.17	3.68	0.28	1.08	0.09	0.18	1.04	1.12	1.06	3.00	0.12	2.77	0.39

FHWA method ($\beta_T = 3.5$)

1	2	3	4	5	6	7	8	9	10	11	12	13	14	15	16	17	18	19
Q_{Dn}/Q_{Ln}	γ_D	γ_L	λ_D	λ_L	λ_R	$6*(2*1+3)$	$4*1+5$	V_R	$1.0+9^2$	V_D	V_L	a^*	$10*13$	$14^{0.5}$	β_T	b^*	c^*	ϕ
1.00	1.25	1.75	1.04	1.60	0.98	2.94	2.64	0.28	1.08	0.09	0.18	1.04	1.12	1.06	3.50	0.12	3.28	0.32
1.20	1.25	1.75	1.04	1.60	0.98	3.19	2.85	0.28	1.08	0.09	0.18	1.04	1.12	1.06	3.50	0.12	3.28	0.32
1.40	1.25	1.75	1.04	1.60	0.98	3.43	3.06	0.28	1.08	0.09	0.18	1.04	1.12	1.06	3.50	0.12	3.28	0.32
1.60	1.25	1.75	1.04	1.60	0.98	3.68	3.26	0.28	1.08	0.09	0.18	1.04	1.12	1.06	3.50	0.12	3.28	0.32
1.80	1.25	1.75	1.04	1.60	0.98	3.92	3.47	0.28	1.08	0.09	0.18	1.04	1.12	1.06	3.50	0.12	3.28	0.32
2.00	1.25	1.75	1.04	1.60	0.98	4.17	3.68	0.28	1.08	0.09	0.18	1.04	1.12	1.06	3.50	0.12	3.28	0.33

Note: $a^* = 1.0+11^2+12^2$

$b^* = \ln(10*13)$

$c^* = \exp(16*17^{0.5})$

$\phi = 7/(8*15*18)$

The numbers (#1,2,3...) represent the column number.

Table 5.6 Calculation of resistance factor for FHWA method in mixed soil profiles

FHWA method ($\beta_T = 3.0$)

1	2	3	4	5	6	7	8	9	10	11	12	13	14	15	16	17	18	19
Q_{Dn}/Q_{Ln}	γ_D	γ_L	λ_D	λ_L	λ_R	$6*(2*1+3)$	$4*1+5$	V_R	$1.0+9^2$	V_D	V_L	a^*	$10*13$	$14^{0.5}$	β_T	b^*	c^*	ϕ
1.00	1.25	1.75	1.04	1.60	1.24	3.72	2.64	0.20	1.04	0.09	0.18	1.04	1.08	1.04	3.00	0.08	2.32	0.58
1.20	1.25	1.75	1.04	1.60	1.24	4.03	2.85	0.20	1.04	0.09	0.18	1.04	1.08	1.04	3.00	0.08	2.32	0.59
1.40	1.25	1.75	1.04	1.60	1.24	4.34	3.06	0.20	1.04	0.09	0.18	1.04	1.08	1.04	3.00	0.08	2.32	0.59
1.60	1.25	1.75	1.04	1.60	1.24	4.65	3.26	0.20	1.04	0.09	0.18	1.04	1.08	1.04	3.00	0.08	2.32	0.59
1.80	1.25	1.75	1.04	1.60	1.24	4.96	3.47	0.20	1.04	0.09	0.18	1.04	1.08	1.04	3.00	0.08	2.32	0.59
2.00	1.25	1.75	1.04	1.60	1.24	5.27	3.68	0.20	1.04	0.09	0.18	1.04	1.08	1.04	3.00	0.08	2.32	0.59

FHWA method ($\beta_T = 3.5$)

1	2	3	4	5	6	7	8	9	10	11	12	13	14	15	16	17	18	19
Q_{Dn}/Q_{Ln}	γ_D	γ_L	λ_D	λ_L	λ_R	$6*(2*1+3)$	$4*1+5$	V_R	$1.0+9^2$	V_D	V_L	a^*	$10*13$	$14^{0.5}$	β_T	b^*	c^*	ϕ
1.00	1.25	1.75	1.04	1.60	1.24	3.72	2.64	0.20	1.04	0.09	0.18	1.04	1.08	1.04	3.50	0.08	2.67	0.51
1.20	1.25	1.75	1.04	1.60	1.24	4.03	2.85	0.20	1.04	0.09	0.18	1.04	1.08	1.04	3.50	0.08	2.67	0.51
1.40	1.25	1.75	1.04	1.60	1.24	4.34	3.06	0.20	1.04	0.09	0.18	1.04	1.08	1.04	3.50	0.08	2.67	0.51
1.60	1.25	1.75	1.04	1.60	1.24	4.65	3.26	0.20	1.04	0.09	0.18	1.04	1.08	1.04	3.50	0.08	2.67	0.51
1.80	1.25	1.75	1.04	1.60	1.24	4.96	3.47	0.20	1.04	0.09	0.18	1.04	1.08	1.04	3.50	0.08	2.67	0.51
2.00	1.25	1.75	1.04	1.60	1.24	5.27	3.68	0.20	1.04	0.09	0.18	1.04	1.08	1.04	3.50	0.08	2.67	0.51

Note: $a^* = 1.0+11^2+12^2$
 $b^* = \ln(10*13)$
 $c^* = \exp(16*17^{0.5})$
 $\phi = 7/(8*15*18)$

The numbers (#1,2,3...) represent the column number.

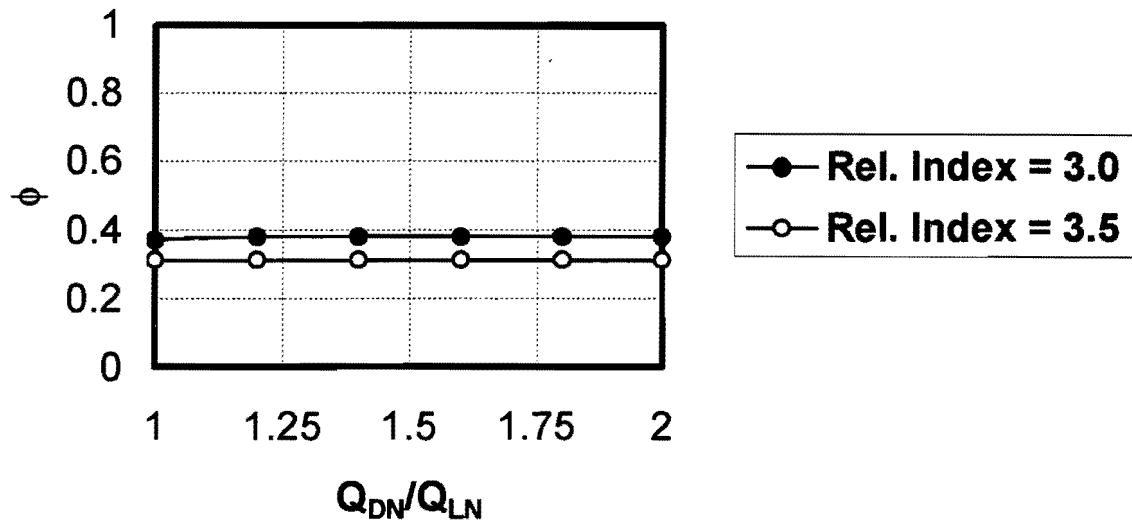


Figure 5.18. Resistance factor versus ratio of dead to live load (TxDOT method - clay)

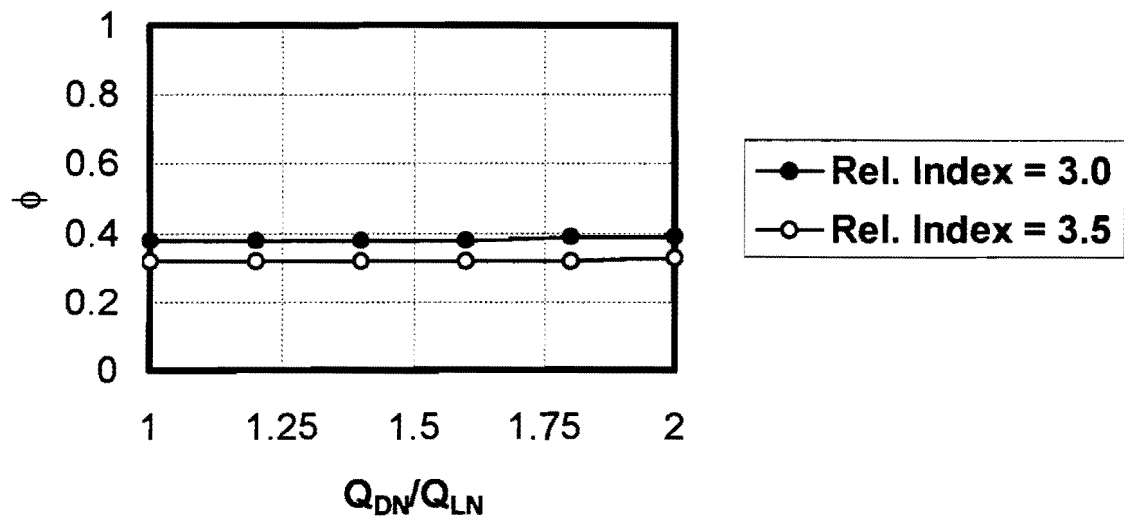


Figure 5.19. Resistance factor versus ratio of dead to live load (FHWA method - sand)

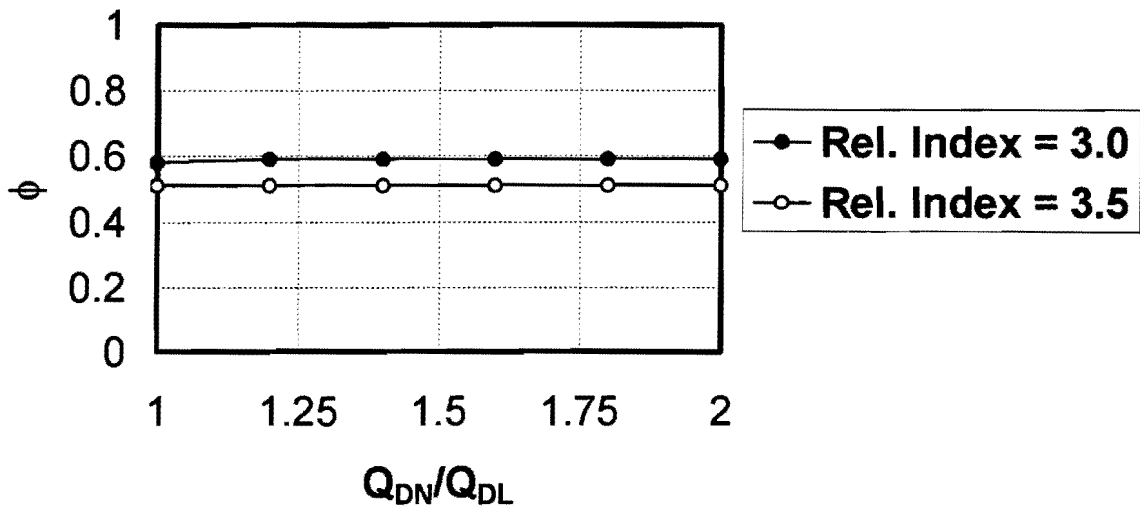


Figure 5.20. Resistance factor versus ratio of dead to live load (FHWA method - mixed soil profile)

5.2.2 ASD method

The resistance factor, based on any target degree of reliability, can be transformed into a factor of safety appropriate for use in the ASD method. In a simple bridge with two components of nominal load, dead load (Q_{DN}) and live load (Q_{LN}), the definition of the factor of safety (FS) is

$$FS = \frac{R_n}{Q_{DN} + Q_{LN}} \quad (5.7)$$

where R_n is the nominal (computed) resistance (capacity). From the LRFD formulation ($\eta = 1$),

$$\gamma_D Q_{DN} + \gamma_{LN} = \phi R_n \quad (5.8)$$

By combining Equations (5.7) and (5.8) and solving for FS,

$$FS = \frac{\gamma_D \frac{Q_{DN}}{Q_{LN}} + \gamma_L}{\phi \left(\frac{Q_{DN}}{Q_{LN}} + 1 \right)} \quad (5.9)$$

Again using $\gamma_D = 1.25$ and $\gamma_L = 1.75$ and ratios of nominal dead load to nominal live load of 1.0 to 2.0, FS was obtained from the computed values of ϕ corresponding to various design methods and target reliability indexes. The calculations for the TxDOT and FHWA methods, for clay and for sand and mixed profiles, respectively, are given in Tables 5.7 through 5.9, and the results are plotted in Figures 5.21 through 5.23.

The results suggest that the required factors of safety tend to become smaller with increasing ratio of dead load to live load (e. g., for long-span bridges). Using the FHWA method in mixed soil profiles, a value of $FS = 2.8$ appears to be appropriate for the range of parameters considered here for a degree of reliability of 0.9998. If a lower reliability can be accepted (e. g., 0.9987), then FS can be reduced to about 2.5.

The resistance factors for the TxDOT method in clay are lower than those reported here for the FHWA method in mixed soil profiles. Likewise, the factors of safety are higher for the TxDOT method. The FHWA method in sand has resistance factors and factors of safety that are near those for the TxDOT method in clay.

Table 5.7 Calculation of factor of safety for TxDOT method in clay

TxDOT method ($\beta_T = 3.0$)

1	2	3	4	5	6	7	FS
Q_{DN}/Q_{LN}	γ_L	γ_D	$2+3*1$	$1.00+1$	ϕ	$5*6$	$4/7$
1.00	1.75	1.25	3	2.00	0.37	0.74	4.05
1.20	1.75	1.25	3.25	2.20	0.38	0.84	3.87
1.40	1.75	1.25	3.5	2.40	0.38	0.91	3.85
1.60	1.75	1.25	3.75	2.60	0.38	0.99	3.79
1.80	1.75	1.25	4	2.80	0.38	1.06	3.77
2.00	1.75	1.25	4.25	3.00	0.38	1.14	3.73

TxDOT method ($\beta_T = 3.5$)

1	2	3	4	5	6	7	FS
Q_{DN}/Q_{LN}	γ_L	γ_D	$2+3*1$	$1.00+1$	ϕ	$5*6$	$4/7$
1.00	1.75	1.25	3	2.00	0.31	0.62	4.84
1.20	1.75	1.25	3.25	2.20	0.31	0.68	4.78
1.40	1.75	1.25	3.5	2.40	0.31	0.74	4.73
1.60	1.75	1.25	3.75	2.60	0.31	0.81	4.63
1.80	1.75	1.25	4	2.80	0.31	0.87	4.60
2.00	1.75	1.25	4.25	3.00	0.31	0.93	4.57

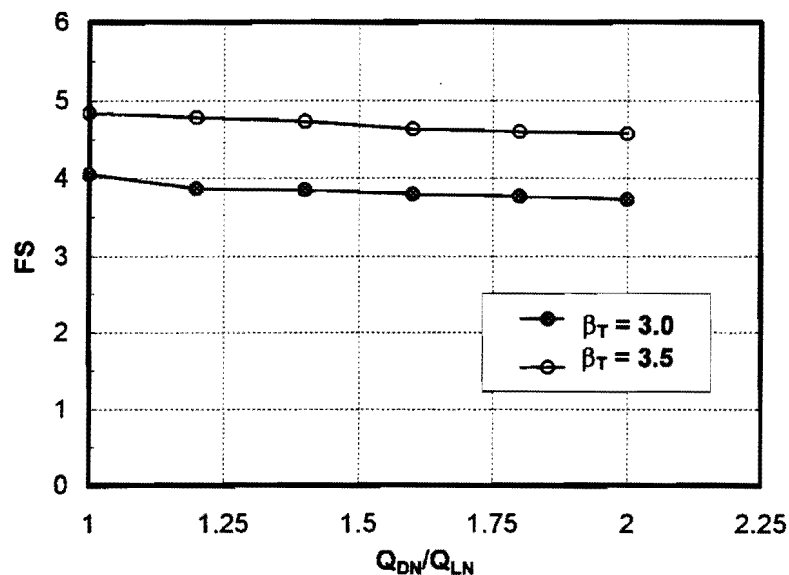


Figure 5.21. Safety factor versus ratio of dead to live load (TxDOT method - clay)

Table 5.8 Calculation of factor of safety for FHWA method in sand

FHWA method ($\beta_T = 3.0$)

1	2	3	4	5	6	7	FS
Q_{Dn}/Q_{Ln}	γ_L	γ_D	$2+3*1$	$1.00+1$	ϕ	$5*6$	$4/7$
1.00	1.75	1.25	3	2.00	0.38	0.76	3.95
1.20	1.75	1.25	3.25	2.20	0.38	0.84	3.87
1.40	1.75	1.25	3.5	2.40	0.38	0.91	3.85
1.60	1.75	1.25	3.75	2.60	0.38	0.99	3.79
1.80	1.75	1.25	4	2.80	0.39	1.09	3.67
2.00	1.75	1.25	4.25	3.00	0.39	1.17	3.63

FHWA method ($\beta_T = 3.5$)

1	2	3	4	5	6	7	FS
Q_{Dn}/Q_{Ln}	γ_L	γ_D	$2+3*1$	$1.00+1$	ϕ	$5*6$	$4/7$
1.00	1.75	1.25	3	2.00	0.32	0.64	4.69
1.20	1.75	1.25	3.25	2.20	0.32	0.70	4.64
1.40	1.75	1.25	3.5	2.40	0.32	0.77	4.55
1.60	1.75	1.25	3.75	2.60	0.32	0.83	4.51
1.80	1.75	1.25	4	2.80	0.32	0.90	4.44
2.00	1.75	1.25	4.25	3.00	0.33	0.99	4.29

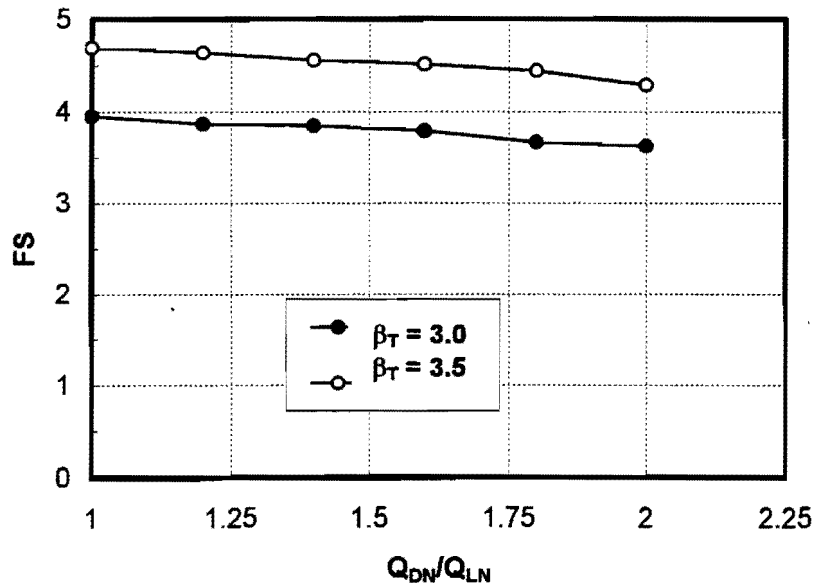


Figure 5.22. Safety factor versus ratio of dead to live load (FHWA method - sand)

Table 5.9 Calculation of factor of safety for FHWA method in mixed soil profile

FHWA method ($\beta_T = 3.0$)

1	2	3	4	5	6	7	FS
Q_{Dn}/Q_{Ln}	γ_L	γ_D	$2+3*1$	$1.00+1$	ϕ	$5*6$	$4/7$
1.00	1.75	1.25	3	2.00	0.58	1.16	2.59
1.20	1.75	1.25	3.25	2.20	0.59	1.30	2.50
1.40	1.75	1.25	3.5	2.40	0.59	1.42	2.47
1.60	1.75	1.25	3.75	2.60	0.59	1.53	2.44
1.80	1.75	1.25	4	2.80	0.59	1.65	2.42
2.00	1.75	1.25	4.25	3.00	0.59	1.77	2.40

FHWA method ($\beta_T = 3.5$)

1	2	3	4	5	6	7	FS
Q_{Dn}/Q_{Ln}	γ_L	γ_D	$2+3*1$	$1.00+1$	ϕ	$5*6$	$4/7$
1.00	1.75	1.25	3	2.00	0.51	1.02	2.94
1.20	1.75	1.25	3.25	2.20	0.51	1.12	2.90
1.40	1.75	1.25	3.5	2.40	0.51	1.22	2.86
1.60	1.75	1.25	3.75	2.60	0.51	1.33	2.83
1.80	1.75	1.25	4	2.80	0.51	1.43	2.80
2.00	1.75	1.25	4.25	3.00	0.51	1.53	2.78

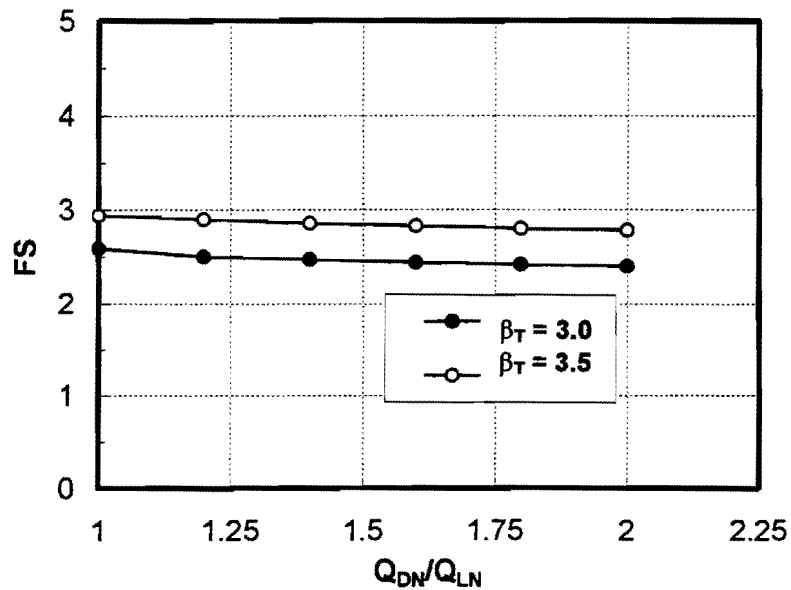


Figure 5.23. Safety factor versus ratio of dead to live load (FHWA method - mixed soil profile)

One reason that the FHWA method in mixed soil profiles has much higher resistance factors (ϕ) and lower factors of safety (FS) than the TxDOT method in clay and the FHWA method in sand is that the bias factor ($\lambda_R = 1.24$) for the former method is higher than those for the other two, making it inherently more conservative, and the scatter is low ($V_R = 0.20$). The TxDOT method in clay is also somewhat conservative ($\lambda_R = 1.16$) but has a relatively high degree of scatter, as exhibited by its coefficient of variation ($V_R = 0.35$). On the other hand the FHWA method in sand is quite accurate ($\lambda_R = 0.98$) and exhibits average scatter ($V_R = 0.28$), but the absence of conservatism in the method requires a relatively high factor of safety. This implies that resistance and safety factors need to be somewhat more conservative for CFA piles in clay and sand profiles than for CFA piles in mixed sand-clay profiles if the design methods considered here are used.

5.3. ESTIMATION OF SETTLEMENT OF AXIALLY LOADED CFA PILES

Although settlements at working loads were small in the loading tests, there may be occasions on which explicit computations of settlement must be made. The load test data shown in Figures 4.25 and 4.26 suggest that the load-settlement data can be normalized and that settlement estimates at any load can be estimated from the normalized load-settlement relations shown in Figure 5.24.

In order to derive the relationships in Figure 5.24, applied loads Q from Figure 4.26 (3-minute readings) were divided by the measured value of ultimate resistance Q_t [Equation (3.1)] for the each pile, and the corresponding measured pile-head settlements w from Figure 4.26 were divided by nominal pile diameter D . For any of the soil profiles tested, Figure 5.24 can be used for design purposes. However, if groups of CFA piles are installed and

loaded, consideration should be given to including the effects of group action, which increases settlement.

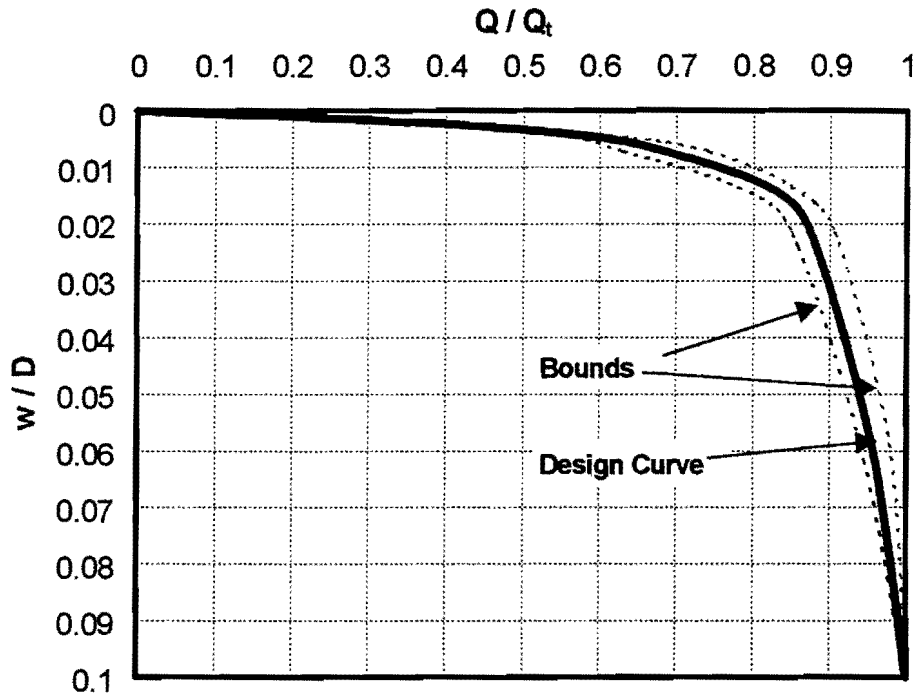


Figure 5.24. Design relationship for settlement prediction from field tests

This page is intentionally blank.

CHAPTER 6 CONSTRUCTION SPECIFICATION

6.1. INTRODUCTION

This preliminary construction specification was modified from the preliminary specification that was submitted as part of the final report for TxDOT project 7-3921 (Hassan et al., 1997). The modifications were based on further observations during the field tests reported in Chapter 4, on conversations with developers of the PIR monitoring system (Pile Dynamics, Inc.) and upon the observation of data for a large construction project involving CFA piles in Ingleside, Texas. That site, although outside of the Houston District, is located in the Beaumont formation, which is dominant in the Houston area. In that project, several hundred CFA piles were monitored for grout take (manually). Graphed in Appendix C are average grout ratio for each pile vs. the number of the constructed pile in order of construction. Typical subsurface data are also given for the Ingleside site in Appendix C. Also shown in Appendix C are compression strength data for 52 mm (2 in.) cube samples of the grout for the Ingleside project, in which the grout mix design was essentially identical to the mix design in Table 4.1. The minimum, maximum and average 28-day compression strengths were 31.7 MPa (4600 psi), 47.6 MPa (6900 psi) and 39.3 MPa (5700 psi), respectively, which all exceed the minimum value recommended in this specification. These data indicate that grout of the specified strength can be produced in the Texas Gulf Coast area. The authors are grateful to Emcon, Inc., and especially to Dr. Mauricio Ochoa, for making these data available.

Significant changes from the previous preliminary specification or commentary are shown in **boldface**.

This specification is intended to be used eventually either as-is or in a modified form for CFA pile projects in the Houston District of TxDOT, for example, as a guide to revise the current special specification in the Houston District for augercast piles ("Special Specification Item 4496, Augercast Piling"). However, it is recommended that this specification or a modified form of this specification be used on one or more implementation projects involving CFA piles, perhaps as a special provision, to discover any errors or unintended effects of the special provision before adopting this specification as a standard specification.

6.2. REVISED PRELIMINARY SPECIFICATION

Preliminary Specification for Augercast (CFA) Pile Construction in Coastal Texas Soils

with Commentary

XXXX.1. Description. An augercast pile is defined as any foundation that is made by rotating a continuous-flight, hollow-stem auger into the ground to the specified pile depth, or until the specified refusal criteria are satisfied. Grout shall then be injected through the auger shaft under continuous positive pressure, as the auger is being withdrawn, in order to exert a positive upward grout pressure on the earth-filled auger flights as well as lateral pressure on the soil surrounding the grout-filled pile hole. Reinforcing steel, if specified, is inserted into the column of fluid grout following the completion of grout placement.

XXXX.2. Applicability. This item shall govern the construction of augercast pile foundations of the size and at the locations shown on the plans.

XXXX.3. Contractor Submittals.

XXXX.3.1. Pre-Bid Submittal. The foundation contractor shall provide the Engineer documentation of a minimum of three projects performed in the two-year period preceding the bid date in which augercast piles were installed successfully under subsurface and job conditions similar to those of the current project. The foundation contractor shall also provide documentation that the designated jobsite supervisor has had a minimum of three years of experience in supervision of the installation of augercast piles. Alternatively, the foundation contractor may demonstrate his or her competence to perform the work shown on the plans by installing a demonstration pile to the depth and diameter of the largest pile on the job and removing that pile from the ground for inspection by the Engineer.

Commentary: The quality of augercast piles is highly dependent upon the skill of the contractor and the specific crew that is assigned to the job. It is essential that the contractor is competent to perform the work at hand either through providing documentation of successful completion of prior jobs of a similar nature to the job being bid or by directly demonstrating his or her competence by installing a demonstration pile that does not contain defects and that has been constructed to at least the diameter and depth shown on the plans.

Since augercast pile contractors are usually subcontractors, it may also be possible to prequalify augercast pile subcontractors who have the necessary experience and to permit only those general contractors who employ prequalified augercast pile subcontractors to submit bids.

XXXX.3.2. Pile-Installation Plan. At least 30 days prior to the start of augercast pile installation the Contractor shall submit to the Engineer an augercast pile installation plan. This installation plan shall include, but not be limited to, the following items:

- a. List and sizes of proposed equipment, including cranes, augers, grout pumps, mixing equipment, and similar equipment to be used in construction, including details of procedures for calibrating pressures and volumes of grout pumps;
- b. Step-by-step description of pile installation procedures;
- c. A plan of the sequence of pile installation;
- d. Details of methods of reinforcement placement, including support for reinforcing cages at the top of the pile and methods for centering the cages within the grout column;
- e. Mix designs for all grout to be used on the job;
- f. Procedures for monitoring grout pressures during stroking and resting of the pump and for monitoring the amount of grout placed in the excavation;
- g. Procedures for protecting adjacent structures, on or off the right-of-way, that may be adversely affected by foundation construction operations; and
- h. Other required submittals shown on the plans or requested by the Engineer.

The Contractor shall demonstrate to the satisfaction of the Engineer the dependability of the equipment, techniques and source of materials to be used on the job.

Commentary: A clearly written pile installation plan can be very effective in reducing misunderstandings between the Engineer and the Contractor and can form the basis for solving potential problems before they occur, thus keeping the job on schedule and minimizing claims.

In reviewing the Contractor's submittal, the key information regarding the equipment that should be scrutinized is (1) the rated capacity and boom lengths of the crane; (2) the torque, rotational speed and weight of the gearbox on the drilling machine; (3) the horsepower of the hydraulic power unit used to turn the gearbox and auger; and (4) the positive displacement piston-ball valve pump, pump stroke displacements, engine horsepower and pump pressures of the grout pump to be used. The stiff, highly plastic clays of the Texas Gulf Coast require special consideration in sizing equipment for large-diameter augercast piles (0.61 m or larger). The minimum torque supplied by the gearbox should be 40.8 m-kN (30,000 ft-lb), and the weight of the gearbox should be at least 22.3 kN (5,000 lb). The rotational speed should be not less than 40 rpm, which requires the horsepower of the hydraulic unit $[(\text{torque in ft-lb})(\text{RPM}) (2\pi)/33,000]$ to be approximately 250 or greater. Smaller drilling rigs are widely available but are not capable of installing large-diameter augercast piles.

The contractor's plan for sequence of installation should preclude the installation of piles that are within six diameters of each other, center to center, prior to the time that the first pile installed has attained its permanent set.

XXXX.4. Protection of Adjacent Structures. The Contractor shall be solely responsible for evaluating the need for, design of, and monitoring of measures to prevent damage to adjacent structures, on or off the right-of-way. These measures shall include, but are not limited to, selection of construction methods and procedures that will prevent overexcavation and excessive migration of grout through the ground; monitoring and controlling the vibrations from construction activities, including placement of casings, sheet piling, shoring and similar ancillary features; and protecting utilities.

Structures located within 10 pile diameters clear spacing, or the planned length of the pile, whichever is greater, shall be monitored for vertical and horizontal movement in a manner approved by the Engineer within an accuracy of 0.3 mm (0.01 inch). Monitoring of adjacent structures will be done by an independent party approved by the Engineer and shall begin prior to construction of the pile or any casings, sheet piling,

shoring or similar ancillary features. In addition to monitoring for movement, the condition of the adjacent structure, including cracks and crack widths, before and after construction of the augercast piles, shall be documented. Structures that are owned by the Texas Department of Transportation shall be monitored for movement but need not be monitored for condition unless called for on the plans.

The Contractor shall notify the Engineer of any movements detected in adjacent structures as soon as they are detected and shall take any immediate remedial measures required to prevent damage to the adjacent structure.

Commentary: The installation of augercast piles can result in large settlement of the ground surface if the rate of rotation of the auger is high relative to its rate of penetration or overrotation, especially in soft sandy soils. This action can promote settlement and damage to existing structures near the location of the pile installation. In some soils, although rarely in the stiff clays of the Texas Gulf Coast, the pumping of grout can result in the grout fracturing the ground and moving a considerable distance horizontally under pressure, which can serve to lift the ground surface and structures founded on or near the ground surface, including buried conduits. Careful monitoring of the movements of adjacent structures and changes in the condition of such structures is necessary in order for the Contractor to know when his or her procedures are producing ground movements in order for immediate corrective action to be taken. During the pile installation, if a susceptible soil to densification is met, the penetration speed shall be increased or the rate of rotation of auger be reduced. Condition surveys are needed for the evaluation of the effect of the construction process on the serviceability of adjacent structures by the Engineer. The Florida DOT specification for augercast piles contains an extensive section on vibration monitoring. Such monitoring is only applicable for cases where casing or sheet piling is driven, which is not a common practice in connection with the installation of augercast piles in Texas coastal soils. In cases in which such construction practices may be needed, a special provision on vibration monitoring should be added.

XXXX.5. Materials. All materials shall conform to the requirements of the pertinent items in *Texas Department of Transportation Standard Specifications for Construction and Maintenance of Highways, Streets, and Bridges* (1995) (metric version) or the same standard specifications in their traditional units (1993), or as otherwise noted.

- | | |
|--|--|
| a. Portland cement (Types I, IP, II, and III): | Item 524 (Hydraulic Cement) |
| b. Fly ash (Type A or B): | Departmental Materials
Specification DMS-8900 (TxDOT) |
| c. Fine aggregate | Item 421 (Portland Cement
Concrete), Table 2 |
| d. Admixtures | Item 437 (Concrete Admixtures) |
| e. Water | Item 421 (Portland Cement
Concrete - 421.2 (3)) |
| f. Fluidizer (fluidifier) | ASTM C 937 |
| g. Reinforcing steel | Item 440 (Reinforcing Steel) |

Notes:

1. Type III portland cement shall not be used when the air temperature for the 12 hours following batching will exceed 15 degrees C.
2. Type B flyash shall not be used in conjunction with Type II portland cement.
3. All admixtures must be approved by the Director of Materials Section, Construction Division, as specified in Item 437. Admixtures shall be stored in accordance with Item 437, Concrete Admixtures.
4. Reinforcing steel item includes the requirements and the assemblies of reinforcing steel.

XXXX.6. Grout.

XXXX.6.1. Mix Design. The grout shall consist of a mixture of portland cement, flyash, water, sand, fluidizer, and if necessary, retarder, proportioned and mixed so that the grout will exhibit the following properties:

- a. All solids shall remain in suspension in the grout without appreciable water gain. Grout may be pumped without difficulty and that will penetrate and fill open voids in the adjacent soil.
- b. The grout shall have a fluid consistency represented by an efflux time of 32 to 36 seconds per 950 mL (quart) when tested with a flow cone in accordance with Tex-437-A (ASTM C 939) [13-mm-diameter (1/2 inch)] outlet orifice unless otherwise specified by the Engineer.
- c. The grout shall not exhibit shrinkage in excess of 0.015 % in the vertical direction, when tested in accordance with ASTM C 1090, and when housed in a 100 % humidity room at a temperature of 20 to 23 degrees C.
- d. Samples of the field grout mix, recovered and stored in cylinders 150 mm (6 in.) in diameter by 300 mm (12 in.) long, shall exhibit a compressive strength 28 days after casting of at least 28 MPa (4,000 psi), or as otherwise specified by the Engineer. Alternatively, 50-mm (2-in.) cube samples may be recovered and tested 28 days after sampling. If such a sampling method is used, the compressive strength 28 days after sampling shall be at least 30 MPa (4,400 psi). Each compressive strength determination shall consist of a minimum of one test on three separate samples, and the compressive strength shall be taken to be the numerical average of the results of three tests.

Commentary: Ideally, grout samples for flow cone testing should be taken at the outlet orifice on the auger of the drilling machine prior to the commencement of drilling, since pumping of the grout may reduce its flowability and increase efflux time. If grout delivery to the jobsite is such that sampling cannot be made at that point, the grout may be sampled from the chute of the ready-mix truck. At the discretion of the Engineer, additional samples may be taken at various times during the grouting process to ensure that consistent fluidity is being achieved. Sampling for strength and shrinkage is covered in XXXX.6.3.

XXXX.6.2. Field Operations.

- a. Only pumping equipment approved by the Engineer shall be used in the mixing and handling of grout. All oil, rust inhibitors, residual drilling slurries and similar foreign materials shall be removed from mixing drums, stirring devices, pumps and lines, and all other equipment in contact with the grout before use.

- b. All materials used to make the grout shall be accurately measured by volume or weight before they are fed into the mixer, either in the field or at the batch plant. The order of placing materials into the mixer shall be (1) water, (2) fluidizer, (3) other solids in order of increasing particle size. The fluidizer may also be added at the jobsite. If that process is followed, the order of mixing shall be (1) water, (2) other solids in order of increasing particle size, and (3) fluidizer (at the jobsite). The time of mixing shall not be less than one minute. If agitated continuously, the grout may be held in the mixer or ready mix truck for up to 2.5 hours if the air temperature is not greater than 20 degrees C (68° F), or up to 2.0 hours if the air temperature is between 20 and 38 degrees C (68° and 100° F) if other than Type III portland cement is used. Grout shall not be placed if the air temperature exceeds 38 degrees C (100° F) or is less than 4 degrees C (39° F).

c. A screen with a mesh with openings no larger than 19 mm (3/4 in.) shall be used between the mixer and the pump, or between the delivery point from a ready mix truck and the pump, to remove large particles that can clog the grout injection system.

d. The grout pump shall be a positive displacement pump with a known volume per stroke that is capable of developing peak pressures of at least 2400 kPa (350 psi) at the pump.

e. The grout pump shall be equipped with, as a minimum, a calibrated pressure gauge that can accurately monitor both the peak and minimum pressures on each pump stroke. The pressure gauge shall be positioned on the immediate outlet site of the pump at ground level in such a manner that it can be easily viewed by the Engineer. The foundation contractor shall provide the Engineer with the results of a calibration performed on the pressure gauge at the beginning of the job that will demonstrate that the pressures indicated by the pressure gauge are within 3 % of the values indicated. The foundation contractor shall also provide the Engineer with the value of the volume of grout delivered by each stroke of the pump and shall demonstrate to the Engineer that the volume of grout delivered by each stroke of the pump is within 3 % of the value provided. The equipment shall also be recalibrated at such times as the Engineer suspects that the grout delivery performance has changed.

f. For those piles where such testing is indicated on the plans, the foundation contractor shall engage an independent consultant acceptable to the Engineer to place electronic flowmeters in the grout pressure line, electronic pressure transducers in the grout pressure line and an electronic position indicator on the crane line holding the auger to make automatic measurements of grout volume, maximum grout pressure and minimum grout pressure versus depth of the injection point. **The actual minimum value of peak grout pressure at the**

pump outlet that is shown on the plans shall be maintained for all grout placement operations throughout the project.

Commentary: For noncritical foundations (e. g., sign foundations, sound-wall foundations) the amount of grout placed into the excavation is normally measured by counting the number of pump strokes required to fill the excavation with grout and multiplying by the calibrated volume of grout delivered by each pump stroke. Because some grout will be lost at the surface and because the excavation will ordinarily be slightly larger than the diameter of the auger, the volume of grout that is placed should always exceed the theoretical volume of the excavation. Empirically, the peak grout pressures at the discharge side of the pump should be at least 1725 kPa (250 psi) throughout the entire period of grout placement if the soils are loose, cohesionless and waterbearing. Lower peak pressures, in the range of 1100 kPa (160 psi), can be tolerated if the site consists of dense sand or stiff clay. Since grout pressure depends to some extent on subsurface conditions, minimum peak values should be shown on the plans for each project.

Commentary: For critical foundations (e. g., bearing piles for bridges and retaining walls) all piles on a job should be monitored by developing and recording graphs of volume of grout placed versus depth of the grout outlet orifice on the auger and both minimum and maximum grout pressures at the outlet point on the pump versus depth of the grout outlet orifice on the auger. Commercial, automated equipment is available through private consultants for acquiring and recording such data. In cases where such monitoring is performed, the volume of grout placed should not be less than 0.95 times the theoretical neat volume for any 0.61-m (2 foot) depth increment pile below a depth of 4.0 m (13 ft) and should not be less than 1.2 times the theoretical neat volume of the entire pile below a depth of 4.0 m (13 ft) at stiff clay or dense sand sites. Return of grout to the surface should be visible to the inspector when the auger tip is no closer to the surface than 3.0 m (9.8 ft) and should continue until the auger has been completely withdrawn. At sites where significant strata of loose sand occur, particularly where the sand is below the water table, higher average grout ratios below

4.0 m (up to 1.75) may be required by the engineer. The average maximum grout pressure over the entire depth interval should be at least 1725 kPa (250 psi) if the site contains loose, waterbearing sands or silts.

Note not for specification: In Appendix C grout ratios for 713 CFA piles for an industrial project in stiff clay varied from 1.16 to 1.99 for the entire pile. The average grout ratio is 1.42 with a standard deviation of 0.12. In the three test piles for the research project reported herein, the average grout ratio was 1.15 over the entire pile at UH, 1.6 over the entire pile at Baytown and 1.5 at Rosenberg. The average grout ratio for the UH pile was 1.21 below 4.0 m (13 ft), which is within the lower limit of the overall grout ratios measured for the industrial project. The UH pile performed very well under load. When the UH pile was constructed, grout return was observed when the auger tip was at a depth of 4.6 m (15 ft), and continuous flow of grout was observed at the ground surface thereafter. Even though the grout volume ratios were generally less than 1.0 above this depth, there was no indication from CSL tests or from the load test that the pile was structurally defective. Therefore, a minimum grout ratio of 1.2 below 4 m (13 ft) appears appropriate.

XXXX.6.3. Grout Testing for Strength and Shrinkage. The Contractor shall make six 150-mm- (6-in.-) diameter by 300-mm- (12-in.-) long cylinder samples or six, 50-mm (2 in.) cube samples for each 38 m³ (50 yd³) of grout placed, but not less than six such samples per working day, nor less than six such samples for each batch of grout produced by the supplier. Grout samples shall be taken from the top of the completed grout column within the augercast piles. Samples shall be made more frequently if specified by the Engineer. The samples will be tested by the Texas Department of Transportation, 2 at seven days after sampling; 2 at 28 days after sampling; and 2 will be held in reserve. Those samples tested at 28 days after casting shall exhibit a minimum compressive strength of at least 28 MPa (4,000 psi).

Commentary: Where augercast piles are used for critical foundations (e. g., bearing piles for bridges and retaining walls), a greater frequency of sampling and testing is

indicated. No standard has been developed concerning this frequency, but it should be at least as great as the frequency of sampling concrete cylinders for drilled shafts and similar cast-in-place substructure or foundation elements. As a guide for strength development, grout meeting these specifications typically attains 30 % and 70 % of its 28-day compressive strength after 1 and 7 days of curing, respectively.

XXXX.7. Construction Procedures.

XXXX.7.1. Excavation. The Contractor shall perform the excavation required for the piling, through whatever materials are encountered, to the dimensions and elevations shown on the plans.

The center of any pile shall be within 25 mm (1 in.) of the location shown on the plans in a horizontal plane. The completed pile shall be plumb to within two percent, if vertical, or shall be installed to within four percent of its specified batter, as determined by the angle from the horizontal, if planned as a batter pile. Any pile in violation of these tolerances will be subject to review by the Engineer.

Should muck, organics, soft clay or other unsuitable materials be encountered within 1.5 m (5 ft) of the ground surface, such material shall be removed to its full depth, or to a depth of 1.5 m (5 ft), whichever is less, and laterally to a distance radially from the centerline of the pile not to exceed three pile diameters or 1/2 the distance to the closest adjacent pile, whichever is less. The excavation shall be backfilled with soil having a plasticity index of 20 or less, and such backfill shall be compacted to at least 95 % of its maximum dry unit weight as specified by Tex-114-E (AASHTO T 180) at within 2 % of optimum moisture content. Excavation of unsuitable surface material and backfilling shall be completed to the Engineer's satisfaction prior to the construction of augercast piles. Should more than 1.5 m (5 ft) of unsuitable surface material be encountered, the Contractor shall advise the Engineer immediately and proceed with work as directed by the Engineer. Should the Contractor suspect that any soils that are excavated are contaminated by hydrocarbons, refuse, or other environmentally hazardous material, he

or she shall contact the Engineer immediately and proceed with work as directed by the Engineer.

Adjacent piles within six diameters, center to center, of each other shall not be installed until it can be demonstrated by the Contractor that the grout in the first pile installed is fully set.

Commentary: The 25-mm (1-in.) position tolerance is based on current TxDOT specifications for drilled shafts, which have proved satisfactory. The industry standard for augercast piles is more relaxed, with a position tolerance of 75 mm (3 in.) for individual piles and 150 mm (6 in.) for piles within groups of five or more.

XXXX.7.2. Auger Equipment. The auger flights shall be continuous from the top of the auger to the bottom tip of the cutting face of the auger, with no gaps or other breaks. The length of any auger brought to the jobsite shall be such that the auger is capable of excavating a hole for the pile, and transporting grout to the bottom of that hole, to a depth that is 20 % greater than the depth of the pile shown on the plans. The auger flights shall be uniform in diameter throughout its length, and the outside diameter of the auger shall not be less than 3 % smaller than the specified diameter of the pile. Only single helix augers shall be used. The pitch of screws shall be approximately one-half of the outside diameter of the auger. The hollow stem of the auger shall be maintained in a clean condition throughout the construction operation.

The bottom of the auger flights and the cutting teeth attached thereto shall be constructed geometrically so that the bottom of the excavation will be flat.

In order to facilitate inspection the auger shall be clearly marked every 0.3 m (1 ft) along its length so that such marks are visible to the unaided eye from the ground.

The grout outlet orifice on the auger shall be located at an elevation lower than that of the cutting teeth on the bottom of the auger. This orifice shall remain closed by a plug

while the auger is being advanced into the ground. The plug shall be removed by pressure from the grout when the grouting begins.

The auger shall be guided at the ground surface by a suitable guide connected to the leads of the augercast piling rig. If the auger is over 12 m (40 ft) long, it shall also be guided by a guide above the ground-surface guide approximately half the length of the auger above the ground-surface guide. The leads that carry the rotary unit that powers the auger should be restrained against rotation by an appropriate mechanism.

The auger shall be advanced into the ground at a continuous rate and at a rate of rotation that prevents excess spoil from being transported to the ground surface. The rotation of the auger shall be stopped when the excavation reaches plan depth.

If refusal is encountered before plan depth is achieved, rotation of the auger shall be stopped, and the Contractor shall inform the Engineer. Refusal is defined here as a rate of auger penetration of less than 300 mm / minute (1 ft / minute) with equipment that is appropriate for the job. The Contractor shall then proceed as directed by the Engineer.

Commentary: At present, the maximum-sized pile that can be installed with auger equipment is about 0.61m (24 in.) in diameter by 24.4 m (80 ft) in depth. The auger should never be overrotated, since doing so may cause the soil to migrate laterally into the flights of the auger and be transported up the auger to the ground surface. This action, in turn, reduces the stresses in the ground and therefore the resistance of the pile. When refusal is reached in a predominantly cohesive soil, it may be possible to extract the auger while the excavation remains stable and replace the auger with a smaller auger that can penetrate the hard soil layer, forming a predrilled hole that can be redrilled with the auger of the proper size. In granular soil, it may be necessary to fill the excavation with drilling slurry to maintain a stable excavation when the auger is withdrawn before restarting the excavation with a smaller auger. Another solution is to grout the pile at the depth of refusal and to install additional piles to carry the required load.

XXXX.7.3. Grout Placement. The placement of grout shall start within five minutes of the completion of the excavation. Grout shall be pumped through the hollow-stem auger into the excavation with sufficient pressure [normally not less than 1.7 MPa (250 psi)] as the auger is withdrawn to completely fill the excavation and any soft or porous zones surrounding the excavation. A head of fluid grout of at least 1.5 m (5 ft) shall be maintained above the grout outlet orifice on the auger at all times. Simultaneously with the initial withdrawal of the auger, grout shall be placed through the grout outlet orifice into the bottom of the excavation at as high a pressure as feasible so as to drive the grout column up the flights of the auger for a distance of at least 1.5 m (5 ft), while slowly turning the auger in the same direction as was employed in excavation. This action is intended to spread the grout around the perimeter of the excavation and so aid in the removal of any loose material from the hole. Once the 1.5-m head of grout has been established within the flights of the auger, rotation of the auger should cease or be reduced to a very small rate, and extraction of the auger shall be commenced at a rate consistent with the rate at which the pump can deliver grout to the excavation.

Satisfactory operation of the coordination of auger withdrawal with grout pumping is indicated by maintaining minimum pressures in the grout at the ground surface, between pump strokes, at or above the value of total vertical pressure in the ground at the depth of the grout outlet orifice and by incrementally delivering grout to the hole in a volume equal to or greater than the theoretical incremental volume of the excavation.

Auger extraction must occur at a steady rate while continuously pumping grout under pressure into the excavation. If the foundation contractor pulls the auger at too slow a rate, the auger may become locked in the hole. If the auger is pulled at too high a rate, which will be indicated by grout pressures below the minimum systolic grout pressures that are given in the first paragraph in this section, or by insufficient grout takes, a neck may develop and the structural resistance of the pile may be compromised. If the above condition occurs, reinsert the auger to at least 1.5 m (5 ft) below the depth of the auger tip at the time low grout pressure or insufficient grout take were indicated or to the

bottom of the pile, resume pumping the grout, and decrease the rate of withdrawal to prevent further jumping or pressure decreases. Pumping of the grout under high pressure shall be continued until the cutting teeth of the auger have reached the ground surface. This will unavoidably result in some wasted grout, but it is a necessary detail in assuring that the top of the augercast pile will be structurally sound.

The volume of grout that has been placed in the excavation at the time the cutting teeth reach **4 m (13 ft) below the ground surface shall be at least 120 % of the theoretical neat volume of the excavation below that depth, and the grout shall be continuously visible at the surface thereafter.** If grout return is not visible when the tip of the auger is 4 m (13 ft) below the ground surface, the volume of the grout that has been placed below the depth of the tip of the auger when grout becomes visible shall not be less than 1.2 times the theoretical neat volume of the excavation below that depth. The cutting teeth shall be visually immersed in grout when they reach the ground surface; otherwise, the pile will be considered defective. In such a case the foundation contractor shall inform the Engineer immediately and proceed as directed by the Engineer.

Commentary: If the total volume of grout supplied is less than 120 % of the theoretical volume of the excavation at the time grout begins flowing to the surface and/or if the cutting teeth of the auger are not visibly immersed in grout at the completion of grouting, immediate corrective action will need to be taken by the foundation contractor if the pile is to be acceptable. In addition, if automated monitoring of incremental grout flow and pump pressure is performed and the grout placed is less than 95 % of the incremental theoretical volume for any 0.61-m increment of the pile or if the average maximum pump pressure is less than that shown on the plans (e.g., 1.7 MPa or 250 psi for loose sand), the pile should be considered as unreliable, which requires immediate action on the part of the foundation contractor. These considerations are not dependent upon whether the materials being excavated are able to retain the shape of the excavation without support from the soil-filled auger. They apply to all soil conditions.

An acceptable corrective measure is to reinstall the auger to a depth of at least 3 m (10 ft) into the grout column, or to the bottom of the pile, whichever is less, and regrouting as if the pile were being excavated for the first time. The same conditions for acceptance of the regouted pile as were applied to initial construction should be used.

A critical operation for the contractor is coordination between operation of the grout pump and withdrawal of the auger. Where possible, the same individual should control both operations. Where not possible, positive and continuous communication should be maintained between the pump operator and the operator of the drilling rig.

XXXX.7.4. Surface Cleaning and Protection. Immediately upon completion of placement of the fluid grout, the Contractor shall remove all excess grout and spoil from the vicinity of the top of the excavation and shall place a suitable temporary device within the top of the excavation, extending above the ground surface by at least 0.3 m (1 ft), to keep surface spoil from entering the grout column before the grout sets. It shall be removed without disturbing the natural soil surrounding the top of the pile once the grout has set. Following placement of this device the foundation contractor shall remove any and all loose soil that has fallen into the grout column with a suitable tool before the grout begins its initial set.

XXXXX.7.5. Reinforcing Steel Placement. The Contractor shall be responsible for furnishing the reinforcing steel and any anchor bolts or dowels shown on the plans. Any required reinforcing steel shall be placed as shown on the plans by lowering the cage within the grout column while the grout is in a fluid state.

The reinforcing steel shall be free of oil, soil, excessive rust or other deleterious material and shall be centered in the excavation with nonmetallic centralizers acceptable to the Engineer.

If cages of reinforcing steel are called for on the plans, the longitudinal bars and lateral reinforcement (spiral or horizontal ties) shall be completely assembled and placed as a unit. Where spiral reinforcement is used, it shall be tied to the longitudinal bars at a spacing not to exceed 0.3 m (1 ft) unless otherwise shown on the plans. Welding of lateral reinforcement to longitudinal bars will not be permitted unless otherwise shown on the plans.

The reinforcing steel shall not be spliced except at locations that are shown on the plans, and the reinforcing steel shall be free of any permanent distortion, such as bars bent by improper pickup. If a pile is required by the Engineer to be lengthened after the steel has been cut and cages have been assembled, the schedule of reinforcing steel, both longitudinal and lateral, shall be extended to the bottom of the pile by splicing. Splices should be as close to the bottom of the pile as possible. Accomplishment of splicing by welding shall not be permitted unless otherwise shown on the plans.

The reinforcing steel shall be placed in the grout column immediately after screening the grout and before the grout begins to take its initial set. The steel may be lowered into the grout by gravity or pushed gently to final position by the Contractor's personnel. The reinforcing steel shall be centered in the excavation by means of plastic or cementitious spacers placed at sufficient intervals along the pile and at sufficient intervals around the steel to keep the steel centered. Metallic spacers shall not be permitted.

Commentary: If the soil profile contains considerable dry or moist sand, it is critical that the cage be placed as soon as possible after placement of grout--in less than 10 minutes if possible, because the grout will stiffen very quickly under such conditions. If steel spacers are used, corrosion of the reinforcing steel can be greatly accelerated, particularly above the ground water table. Therefore, they should be avoided.

The reinforcing steel shall not be vibrated or driven into position without the approval of the Engineer.

The reinforcing steel shall be held in position within the fluid grout column by appropriate supports at the ground surface, which shall remain in place until the grout reaches a minimum of 50 % of its design strength, or three days, whichever occurs first.

XXXX.8. Cutting off. The Contractor shall cut off the tops of piles, square with pile axis at the elevations indicated, by removing fresh grout from the top of the pile or by cutting off hardened grout down to the final cutoff point at any time after initial set has occurred.

XXXX.9. Inspection and Records. The Contractor shall maintain accurate records for each pile constructed. Similar records will be maintained by the Engineer. These records shall show:

- a. Pile location;
- b. Ground surface elevation;
- c. Pile toe (bottom) depth;
- d. Depth of top of grout;
- e. Pile length;
- f. Auger diameter;
- g. Details of the reinforcing steel (number, size, and grade of longitudinal bars, size and spacing of transverse steel; outside diameter and length of cage);
- h. Flow cone efflux time and volume of grout placed;
- i. Theoretical volume of excavation (diameter = diameter of auger);
- j. Depth to which reinforcing steel was placed;
- k. Date/Time of beginning of drilling;
- l. Date/Time of completion of drilling;
- m. Date/Time grout was mixed;
- n. Date/Time ready-mix grout truck arrived at jobsite;
- o. Date/Time of beginning of grout pumping;
- p. Date/Time of completion of grout pumping;

- q. Date/Time of placement of reinforcing steel;
- r. Weather conditions, including air temperature, at time of grouting;
- s. Identification of grout samples taken from the pile, if any, and
- t. All other pertinent data relative to the pile installation.

Piles that support critical structures that are designated on the plans, or as otherwise required by the Engineer, are to be monitored using automated equipment. For such piles the following records shall be made and retained by the Contractor.

- a. Volume of grout placed versus depth of grout outlet orifice for every 0.61 m (2 ft) increment, or less, of pile placed.
- b. Average maximum and minimum pump stroke pressures at ground level for every 0.61 m (2 ft) increment, or less, of pile placed.
- c. Average maximum and minimum pump stroke pressure at the auger tip level for every 0.61 m (2 ft) increment, or less, of pile placed, if directed by the Engineer.

These data shall be provided to the Engineer in graphical form within 24 hours of the completion of the pile.

Post-installation, structural integrity tests of the piles may be specified. If so, those piles on which such tests are to be conducted will be designated on the plans, and the specific test(s) to be performed will be designated on the plans. Such tests include, but are not limited to, sonic echo tests, impulse-response tests, cross-hole sonic tests, backscatter gamma tests, fiberoptic television camera tests, and high-strain integrity tests. If such post-installation integrity tests are called for on the plans, the Contractor shall engage an independent consultant, acceptable to the Engineer, to perform those tests and to report the results, with interpretations, to the Contractor and the Engineer. The Contractor shall install access tubes, of a design acceptable to the consultant, to accommodate those

tests that require access to the interior of the augercast pile. These tubes shall be secured to the reinforcing steel and capped prior to placing the steel cage in the fluid grout.

Commentary: Automated monitoring of incremental grout volumes and pressures is a key element in assuring the structural integrity of augercast piles. The Pile Installation Recorder (PIR) is an effective system to monitor those parameters. Such monitoring should be carried out on all bearing piles for critical structures, such as bridge and retaining wall foundations. Such monitoring may also be carried out for selected, representative piles for noncritical structures, such as sound wall and sign foundations.

Post-installation integrity tests are valuable in establishing that a foundation contractor's procedures are producing acceptable piles on any given job. The most reliable of the post-installation integrity tests for identifying anomalies within the pile are those that use down-tube instruments, such as the cross-hole sonic (CSL) test, single-hole sonic test, the backscatter gamma test, and the fiberoptic television camera test. These tests all require that the foundation contractor attach appropriate access tubing to the reinforcing steel prior to placing the steel in the grout column. They also require intelligent interpretation, which should be performed by experts. Such experts cannot always determine whether an anomalous reading is a defect within the pile, however, and the final decision on acceptability of the pile must be made by the Engineer, based on construction records, the post-installation integrity test expert's report, and upon the Engineer's analysis of the possible effect on foundation performance of the potential defect.

In order to be effective, access tubes for sonic or backscatter gamma testing should be distributed evenly circumferentially around a reinforcing cage at a frequency of approximately one for every 0.3 meters (1 ft) of cage diameter. It is advisable that tubes used for cross-hole sonic tests be made of Schedule 40 steel, because such tubes will remain bonded to the grout. Polyvinyl chloride (PVC) tubes do not ordinarily remain bonded to the grout beyond a few days after the grout takes its initial set, and debonding will render the cross-hole sonic tests ineffective. PVC tubes should be used only for

backscatter gamma testing unless cross-hole sonic tests will be performed within 72 hours of casting the grout.

The necessary frequency of post-construction integrity testing is left to the judgement of the Engineer. However, a reasonable approach for load-bearing piles is to subject the first 10 to 15 piles to be constructed on a project to integrity tests to establish that the contractor's construction practice at the site is adequate. Thereafter, the frequency of such tests can be reduced, and further integrity tests even perhaps eliminated if the construction records for the remaining production piles are similar to those of the initial piles that were subjected to integrity tests.

XXXX.10. Unacceptable Piles. Unacceptable piles are defined as piles that will not carry their intended load with allowable deflections. The following constitute construction conditions that produce unacceptable piles:

- a. Piles out of position by more than 25 mm (1 in.) at the ground surface or not within the plumbness or batter limits defined in Item XXXX.7.1.
- b. Piles in which the top of the grout is more than 25 mm (1 in.) below or 75 mm (3 in.) above the elevation shown on the plans.
- c. Piles in which the grout strength or grout take is less than that required.
- d. Piles in which the steel was not inserted as required.
- e. Piles that exhibit any visual evidence of grout contamination, structural damage or inadequate consolidation (honeycombing).
- f. Piles that are inspected using post-installation integrity testing methods that are judged by the Engineer to be unacceptable.

Unacceptable piles shall be replaced or repaired at the Contractor's expense, as directed by the Engineer.

XXXX.11. Test Loading. Any required test loading of augercast piles, including both axial and lateral loading conditions, shall be in accordance with Item 405, "Foundation Test Load."

Commentary: Expedient load testing methods not covered under Item 405 can also be used to determine the load-carrying capacities of augercast piles if specified by the Engineer. These methods include driving of the completed pile with concurrent measurements of set, stress and velocity at the pile head and subsequent wave-equation analysis of the data to interpret pile capacity, and the Statnamic™ test, in which the pile is pushed rapidly into the soil in such a manner that the capacity can be determined by appropriate analysis of the measured load-movement curve.

XXXX.12. Measurement. Augercast pile foundations shall be measured by the meter (or foot) between the top of the grout and the bottom of the pile. If test loads are specified, they will be paid as a lump sum per test load.

XXXX.13. Payment. The work performed and materials furnished in accordance with this Item and measured as provided under XXXX.12 ("Measurement") will be paid for at the unit prices bid under the payment categories listed below.

Payment categories:

- a. Per linear meter (or foot) of augercast piling of the specified diameter placed without automated monitoring or post-installation integrity testing;

- b. Per linear meter (or foot) of augercast piling of the specified diameter placed with automated monitoring as indicated on the plans and without post-installation integrity testing
- c. Per linear meter (or foot) of augercast piling of the specified diameter placed without automated monitoring but with post-installation integrity testing as indicated on the plans.
- d. Per linear meter (or foot) of augercast piling of the specified diameter placed with automated monitoring and with post-installation integrity testing as indicated on the plans.

The quantities to be paid for will be the quantities in each category shown on the plans unless specific changes are required in writing by the Engineer. Unit prices that are bid will apply to the extension of any pile to a depth up to 120 % of the depth for that pile that is shown on the plans when such an increase in depth is required by the Engineer. If subsurface conditions dictate that any pile is to be installed to a depth less than that shown on the plans, and the decrease in length is approved in writing by the Engineer, the length of pile actually constructed will be paid for at the unit price bid. If increases in depth exceeding 120 % of the depth shown on the plans are required by the Engineer, or if diameters other than those that are shown on the plans are required by the Engineer, the unit prices shall be renegotiated for those piles involved.

Commentary: If the total length of all piling installed on the job is less than the total length shown on the plans because of field decisions by the Engineer, regardless of the shortfall, the Contractor will be paid only for the lengths actually installed at the unit prices bid.

Commentary: This Item applies to augercast piles constructed in predominantly cohesive and cohesionless soil profiles, in which research has been performed for the

Texas Department of Transportation. Its applicability to rock formations is unproved (1999). Additional drilling controls and payment items may be needed in such subsurface conditions.

CHAPTER 7 CONCLUSIONS AND RECOMMENDATIONS

7.1 CONCLUSIONS

This report focuses on the behavior of axially loaded CFA piles in clay and sand. Axial load test data for 43 CFA piles from the Houston-Gulf Coast area and Florida were collected, seven capacity prediction methods were selected, predictions were made, and measured capacities were compared with these predictions in Chapter 3. Three new field axial load tests were conducted on CFA piles at three test sites within the Houston District with different soil conditions (stiff clay, mixed stiff clay and loose sand, mixed stiff clay and medium dense sand). The results of the field load tests are shown in Chapter 4. In Chapter 5 comparisons between the predicted and measured axial load capacities were made after merging the test data for the three new test piles into the original database described in Chapter 3. A preliminary construction specification is included in Chapter 6. It is expected that this specification will be tested in an implementation project and modified, if necessary, prior to including it as a standard specification for the Houston District.

Conclusions from the database and the field test results are as follows:

- Comparison of several design methods (methods for computing axial resistance, documented in Chapter 3) with the load tests in the database and the new load test data collected for the current project indicated that the LPC method was the most accurate method among those examined for CFA piles entirely in clay profiles. However, the LPC method requires the use of a static cone penetrometer to characterize the soil for design, which is not an exploration tool that is utilized by TxDOT. The next most appropriate method was the TxDOT (Houston District)

design method for drilled shafts, and that method is recommended for use by TxDOT for CFA piles in clay soil profiles. The FHWA method for drilled shafts was the most accurate for CFA piles in sand, and the FHWA method was reasonably accurate (although conservatively biased but with a low coefficient of variation) for CFA piles in mixed soil profiles. The FHWA method, documented in Chapter 3, is therefore recommended for use in sands and mixed soil profiles. Factors of safety and resistance factors for LRFD are addressed for the TxDOT drilled shaft design method and the FHWA design method for drilled shafts in Chapter 5.

- Explicit calculation of settlement of CFA piles does not appear to be necessary for load-bearing piles unless such piles are installed in groups. Settlements of the individual CFA piles that were tested in this study were all less than 2 mm (0.1 in.) at one-half of the plunging load. Evaluation of settlement of pile groups was beyond the scope of this study.
- Monitoring of grout volume placement by means of magnetic flowmeters gave consistently different results from manual recordings obtained by counting pump strokes. For that reason, and because detailed, permanent records of grout take versus depth are obtained with flowmeters, automated monitoring of grout placement by means of flowmeters is recommended.
- Based on observations made in the field in this study and on data from a large industrial project, documented in Appendix C, a change has been made to the preliminary construction specification. This change requires that the grout ratio must be at least 1.2 for that part of the pile below the depth of the tip of the auger at the time grout return to the surface can be observed visually (about 4 m or 13 ft in

this study). In fact, this value may be too low in cases in which the site conditions are primarily sand, especially loose sand below the water table, and it may be too high in hard clays. However, it should be adequate for typical site conditions in the Houston area, as represented by the NGES-UH.

- Overall, the performance of the test piles can be considered excellent. The CFA piling system appears to be a viable foundation system, with appropriate construction controls as elucidated in Chapter 6, for load-bearing piles for TxDOT structures in the Houston District.

7.2. RECOMMENDATIONS FOR FURTHER RESEARCH

- The TxDOT design method for drilled shafts in clay was the most appropriate method of those studied for purely clay sites (except for the LPC method, which requires the use of a static cone penetrometer). However, the TxDOT design method for drilled shafts in sand did not lead to reliable predictions for the capacities of CFA piles in mixed soil profiles, which contained considerable sand (Baytown and Rosenberg). This design method in fact proved to be very conservative at the two mixed profile sites. Further studies of the use of this method for predicting CFA pile capacities in sand and sand-clay stratigraphies may lead to improved economy in design if TxDOT opts to use this design method for CFA piles.
- The LPC method, which is based on the use of cone penetrometer (CPT) data, was very accurate in clay soils. TxDOT should therefore give consideration to performing CPT tests in the Houston area as a basis for the design of CFA piles.

- The database developed for this study should be maintained and expanded to other sites throughout Texas where CFA piles are feasible alternatives to driven pile and/or drilled shafts. Where new pile load tests are conducted, both TxDOT cone and SPT tests should be performed in coarse-grained soils, and unconsolidated, undrained triaxial compression tests should be performed on tube (or core) samples of fine-grained soils in order to provide adequate subsurface data for making the requisite calculations. The design methods described here and other potential design methods should be tested against the soil types and geologic settings in the expanded database.
- The first logical step in implementing this research is to design a small bridge using the recommendations given here, to construct the CFA pile foundation at the bridge, and to monitor the performance of the foundation. The construction operations should be monitored, in the manner of this study, but should be expanded to include measurements of the settlement of the soil surface at selected locations, especially where CFA piles will be installed closely spaced. Settlement readings should continue during the first year of operation of the structure to ascertain whether any potentially adverse pile-soil-pile interaction effects are occurring. Selected piles should be instrumented to measure applied load, settlement and load along the pile while the bridge is in service. Sister bars using vibrating wire strain gauges or fiber-optic strain sensors should be used for long-term monitoring. Instrumentation should include pressure cells in pile caps (column footings) and/or abutments to determine how much of the bridge load is actually being carried by the CFA piles. For the first implementation study a geotechnically simple site should be selected.

REFERENCES

American Petroleum Institute (1993). *API Recommended Practice RP2A - LRFD*, Recommended Practice for Planning, Designing and Constructing Fixed Offshore Platforms Load and Resistance Factor Design, First Edition, API, Washington, DC.

Bustamante, M., and Gianceselli, L. (1981). "Portance Reele et Portance Calculee des Pieux Isoles, Sollicites Verticalement," *Revue Francaise de Geotechnique No. 16*.

Coyle, H. M., and Castello, R. (1981). "New Design Correlations for Piles in Sand," *Journal of the Geotechnical Engineering Division*, ASCE, Vol. 107, No. GT 7, pp. 965-986.

Cutter, W. A., and Warder, D. L. (1998). "The Use of ACIP Piles Adjacent to Existing Structures: Lessons Learned," in *Proceedings, Sixth Great Lakes Geotechnical and Geoenvironmental Conference on the Design and Construction of Drilled Deep Foundations*, Indianapolis, IN.

DFI (1994). *Augered Cast-in-Place Piles Manual*, Deep Foundations Institute, Sparta, NJ, 29 pp.

Ellison, R. D., D'Appolonia, E., and Thiers, G. R. (1971). "Load-Deformation Mechanism for Bored Piles," *Journal of the Soil Mechanics and Foundations Division*, ASCE, Vol. 97, No. SM4, April, pp. 661 - 677.

Hassan, K. M., O'Neill, M. W., and Vipulanandan, C. (1997). "Specification and Design Criteria for the Construction of Continuous Flight Auger Piles in the Houston Area," *Final Report*, Texas Department of Transportation, Project No. 7-3921, August.

Kenny, M. J., and Andrawes, K. Z. (1997). "Soil Disturbance During Continuous Flight Auger Piling in Sand," in *Proceedings*, 14th International Conference on Soil Mechanics and Foundation Engineering, Volume 2, Hamburg, pp. 1085 - 1090.

Kissenpfennig, J. F., Motherwell, J. T., and LaFountain, L. J. (1984). "Integrity Testing of Bored Piles Using Sonic Logging," *Journal of Geotechnical Engineering*, ASCE, Vol. 110, No. 8, August, pp. 1079 - 1089.

Kiousis, P. D., and Elansary, A. S. (1987). "Load-Settlement Relation for Axially Loaded Piles," *Journal of Geotechnical Engineering*, ASCE, Vol. 113, No. 6, June, pp. 665 - 661.

Lacy, H. S. (1998). "Protecting Existing Structures Using Bored Piles," in *Proceedings, Sixth Great Lakes Geotechnical and Geoenvironmental Conference on the Design and Construction of Drilled Deep Foundations*, Indianapolis, IN.

Leznicki, J. K., Esrig, M. I., and Gaibroris, R. G. (1992). "Loss of Ground During CFA Pile Installation in Inner Urban Areas," *Journal of Geotechnical Engineering*, ASCE, Vol. 118, No. 6, June, pp. 947 - 950.

Long, J. H., and Wysockey, M. (1998). "Drilled Shaft Axial Capacity - How Accurate are our Predictive Methods?," in *Proceedings, Sixth Great Lakes Geotechnical and Geoenvironmental Conference on the Design and Construction of Drilled Deep Foundations*, Indianapolis, IN.

McVay, M., Armaghani, B., and Casper, R. (1994). "Design and Construction of Auger-Cast Piles in Florida," *Transportation Research Record No. 1447*, TRB/NAS, Washington, DC, pp. 10 - 18.

Neely, W. J. (1991). "Bearing Capacity of Auger-Cast Piles in Sand," *Journal of Geotechnical Engineering*, ASCE, Vol. 117, No. 2, February, pp. 331 - 345.

O'Neill, M. W. (1994). "Review of Augered Pile Practice Outside the United States," *Transportation Research Record No. 1447*, TRB/NAS, Washington, DC, pp. 3 - 9.

O'Neill, M. W. (1998). "Project 89 Revisited," in *Proceedings, Drilled Shaft Foundation Symposium: Current Design Principles and Practices*, ADSC, Dallas, Texas, January, pp. 7 - 47.

Peck, R., Hansen, W. E., and Thornburn, T. H. (1974). "" *Foundation Engineering*. Second Edition, John Wiley and Sons, Inc., New York, NY.

Poulos, H. G. (1979). "Settlement of Single Piles in Nonhomogeneous Soil," *Journal of Geotechnical Engineering Division*, ASCE, Vol. 105, No. GT5, May, pp. 627 - 642.

Reese, L. C. (1978). "Design and Construction of Drilled Shafts," *Journal of the Geotechnical Engineering Division*, ASCE, Vol. 104, No. GT1, January, pp. 95 - 115.

Sharma, H. D., Harris, M. C., Scott, J. D., and McAllister, K. W. (1986). "Bearing Capacity of Bored Cast-in-Place Concrete Piles on Oil Sand," *Journal of Geotechnical Engineering*, ASCE, Vol. 112, No. 12, December, pp. 965 - 984.

Sharp, M. R., McVay, M. C., Townsend, F. C., and Barnett, C. R. (1988). "Evaluation of Pile Capacity from In Situ Tests," *Geotechnical Special Publication No. 17*, ASCE, pp. 134-156.

Texas Highway Department (1972). *Foundation Exploration and Design Manual*, Bridge Division, Second Edition, July.

Tomlinson, M. J. (1957). "The Adhesion of Piles Driven in Clay Soils," in *Proceedings*, Fourth International Conference on Soil Mechanics and Foundation Engineering, Butterworths Scientific Publications, Ltd., London, England, Vol. 2, 1957, pp. 66 - 71.

Touma, F. T. (1972). "The Behavior of Axially Loaded Drilled Shafts in Sand," dissertation presented to the Department of Civil Engineering, The University of Texas at Austin, December.

Van Impe, W. F. (1988). " Consideration on the Auger Pile Design," In *Proceedings*, First International Geotechnical Seminar on Deep Foundations on Bored and Auger Piles, Balkema, Rotterdam, pp. 193 - 218.

Van Weele, A. F. (1988). "Cast-in-site Piles - Installation Methods, Soil Disturbance and Resulting Pile Behavior," in *Proceedings*, First International Geotechnical Seminar on Deep Foundations on Bored and Auger Piles, Balkema, Rotterdam, pp. 219 - 228.

Whitworth, L. J. (1994). "Design and Construction of Starsol Piles," *Transportation Research Record No. 1447*, TRB/NAS, Washington, DC, pp. 63 - 69.

Wright, S. J., and Reese, L. C. (1979). "Design of Large-Diameter Bored Piles," *Ground Engineering*, London, United Kingdom, Vol. 12, No. 8, 1979, pp. 47-51.

Yoon, G. M., and O'Neill, M. W. (1997). "Resistance Factors for Driven Piles from Experiments," *Transportation Research Record No. 1569*, TRB/NAS, Washington, DC, pp. 47 - 56.

Appendix A

Examples of Calculations of CFA Pile Capacities from Database

Example 1: Calculation for clay case from database

Project ID: 2 KE/BE

$Q_t(5\%)=1424 \text{ kN}$

$L=18.3 \text{ m}$

Depth (m)	Soil Type	γ_d (kN/m ³)	s_u (kPa)	γ_{sat} (kN/m ³)
1.7 m				
3.3 m	C	16.7	62.24	19.63
5.5 m	C	15.7	31.12	19.63
7.9 m	C	14.3	10.05	18.9
11.0 m	C	14.9	55.54	19.22
14.3 m	C	14.4	79	19.01
17.4 m	C	13.7	104.4	18.5
19.5 m	C	16.5	116.3	20.0

Assumptions:

1. soil above G.W.L is saturated.
2. concrete and fill at the surface, $f_s = 0$.

NO1: Coyle and Castello - Tomlinson method (1981)

Side resistance:

(1)	(2)	(3)	(4)	(5)	(6)	(7)	(8)
Layer (m)	s_u (kPa)	α (Fig. 3.4)	f_s (kPa) (2)x(3)	ΔL (m)	πD (m)	A_s (m ²) (5)x(6)	ΔQ_s (kN) (4)x(7)
0 - 3.3	62.24	0.77	47.92	3.30	1.28	4.21	201.80
3.3 - 5.5	31.12	1.00	31.12	2.20	1.28	2.81	87.36
5.5 - 7.9	10.05	1.00	10.05	2.40	1.28	3.06	30.78
7.9 - 11.0	55.54	0.90	49.99	3.10	1.28	3.96	197.72
11. - 14.3	79.00	0.58	45.82	3.30	1.28	4.21	192.94
14.3-17.4	104.40	0.47	49.07	3.10	1.28	3.96	194.09
17.4-18.3	116.30	0.44	51.17	0.90	1.28	1.15	58.77

$$Q_s = 963.5 \text{ kN}$$

Toe resistance:

(1)	(2)	(3)	(4)	(5)
s_u (kPa)	q_p (kPa) (Eq. 3.21)	R (m)	A_p (m ²)	Q_p (kN) (2)x(4)
116.30	1046.70	0.20	0.13	136

$$Q_p = 136 \text{ kN}$$

Total resistance:

$$Q_t = 963.5 + 136 = 1099.5 \text{ kN}$$

NO2: API method (API RP2A,1994)

Side resistance:

(1)	(2)	(3)	(4)	(5)	(6)	(7)	(8)	(9)	(10)	(11)	(12)
Layer (m)	s_u (kN)	γ (kN/m ³)	h (m)	p_o' (kPa)	$\psi=s_u/p_o'$	α	ΔL (m)	πD (m)	A_s (m ²)	f_s (kN)	ΔQ_s (kN)
				(3)x(4)	(2)/(5)	(Eq. 3.24)			(8)x(9)	(2)x(7)	(10)x(11)
0 - 3.3	62.24	19.60	1.65	32.34	1.92	0.36	3.30	1.28	4.21	22.41	94.35
3.3 - 5.5	31.12	9.83	4.40	64.88	0.48	0.72	2.20	1.28	2.81	22.47	63.07
5.5 - 7.9	10.05	9.10	6.70	86.58	0.12	1.47	2.40	1.28	3.06	14.75	45.17
7.9 - 11.0	55.54	9.42	9.40	112.58	0.49	0.71	3.10	1.28	3.96	39.54	156.39
11. - 14.3	79.00	9.21	12.60	142.88	0.55	0.67	3.30	1.28	4.21	53.12	223.68
14.3-17.4	104.40	8.70	15.80	171.58	0.61	0.64	3.10	1.28	3.96	66.92	264.71
17.4-18.3	116.30	10.20	17.80	205.48	0.57	0.66	0.90	1.28	1.15	77.29	88.76

$Q_s =$	936 kN
---------	--------

Toe resistance:

(1)	(2)	(3)	(4)	(5)
s_u (kPa)	q_p (kPa)	R (m)	A_p (m ²)	Q_p (kN)
	(Eq. 3.25)			(2)x(4)
116.30	1046.70	0.20	0.13	136

$Q_p =$	136 kN
---------	--------

Total resistance:

$Q_t =$	$936+136 = 1072$ kN
---------	---------------------

NO3: LPC method (1981)

Side resistance:

(1)	(2)	(3)	(4)	(5)	(6)	(7)
Layer (m)	q_c (kPa)	f_s (kPa)	ΔL (m)	πD (m)	A_s (m ²)	ΔQ_s (kN)
		(Fig. 3.2)			(4)x(5)	(3)x(6)
0 - 3.3	1400.00	55.00	3.30	1.28	4.21	231.59
3.3 - 5.5	669.30	37.00	2.20	1.28	2.81	103.87
5.5 - 7.9	1300.00	54.00	2.40	1.28	3.06	165.37
7.9 - 11.0	1940.00	70.00	3.10	1.28	3.96	276.89
11. - 14.3	2550.00	75.00	3.30	1.28	4.21	315.81
14.3-17.4	2600.00	75.00	3.10	1.28	3.96	296.67
17.4-18.3	3000.00	78.00	0.90	1.28	1.15	89.58

$Q_s =$	1480 kN
---------	---------

Toe resistance:

(1)	(2)	(3)	(4)	(5)
q_c (kPa)	q_p (kPa)	R (m)	A_p (m ²)	Q_p (kN)
	(Eq.3.10)			(2)x(4)
3000.00	1125.00	0.20	0.13	114.00

$Q_p =$	114 kN
---------	--------

Total resistance:

$Q_t =$	1480+114 = 1594 kN
---------	--------------------

NO4: Reese and O'Neill (1988)

Side resistance:

(1)	(2)	(3)	(4)	(5)	(6)	(7)
Layer (m)	s_u (kPa)	ΔL (m)	πD (m)	A_s (m ²) (3)x(4)	f_s (kPa) (Eq. 3.17)	ΔQ_s (kN) (5)x(6)
0 - 3.3	62.24	1.80	1.28	2.30	34.23	78.63
3.3 - 5.5	31.12	2.20	1.28	2.81	17.12	48.05
5.5 - 7.9	10.05	2.40	1.28	3.06	5.53	16.93
7.9 - 11.0	55.54	3.10	1.28	3.96	30.55	120.84
11. - 14.3	79.00	3.30	1.28	4.21	43.45	182.97
14.3-17.4	104.40	3.10	1.28	3.96	57.42	227.15
17.4-18.3	116.30	0.50	1.28	0.64	63.97	40.81

$$Q_s = 715 \text{ kN}$$

Toe resistance:

(1)	(2)	(3)	(4)	(5)
s_u (kPa)	q_p (kPa) (Eq. 3.18)	R (m)	A_p (m ²)	Q_p (kN) (2)x(4)
116.30	1046.70	0.20	0.13	136

$$Q_p = 136 \text{ kN}$$

Total resistance:

$$Q_t = 715 + 136 = 851 \text{ kN}$$

NO5: TXDOT method (1972)

Side resistance:

(1)	(2)	(3)	(4)	(5)	(6)	(7)	(8)
Layer (m)	α	s_u (kPa)	f_s (kPa)	ΔL (m)	πD (m)	A_s (m ²)	ΔQ_s (kN)
			(2) x (3)			(5) x (6)	(4) x (7)
0 - 3.3	0.7	62.24	43.57	3.30	1.28	4.21	183.56
3.3 - 5.5	0.7	31.12	21.78	2.20	1.28	2.81	61.19
5.5 - 7.9	0.7	10.05	7.04	2.40	1.28	3.06	21.56
7.9 - 11.0	0.7	55.54	38.88	3.10	1.28	3.96	153.88
11.0 - 14.3	0.7	79.00	55.30	3.30	1.28	4.21	232.99
14.3 - 17.4	0.7	104.40	73.08	3.10	1.28	3.96	289.24
17.4 - 18.3	0.7	116.30	81.41	0.90	1.28	1.15	93.55

$$Q_s = 1036 \text{ KN}$$

Toe resistance:

(1)	(2)	(3)	(4)
q_p (kPa)	R (m)	A_p (m ²)	Q_p (kN)
			(1) x (3)
383.20	0.20	0.13	49.82

$$Q_p = 50 \text{ kN}$$

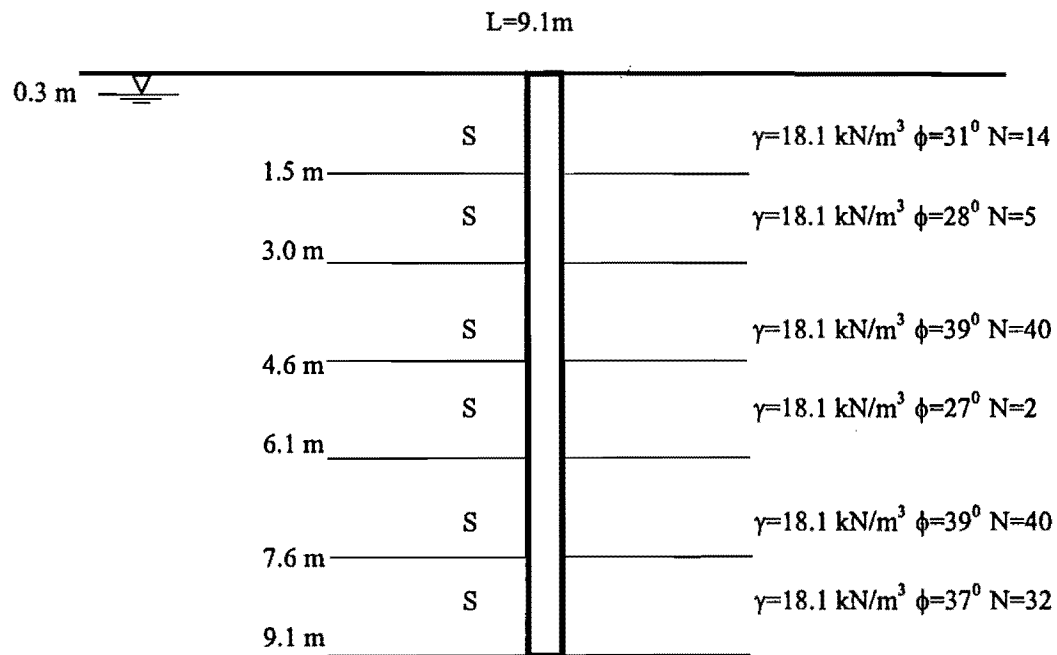
Total resistance:

$$Q_t = 1036 + 50 = 1086 \text{ kN}$$

Example 2: Calculation for sand case from database

Project ID: 25 PB/MCM

$Q_u(5\%)=294 \text{ kN}$



Assumptions:

1. γ is saturated density.
2. soil above G.W.L is saturated.

NO1: Wright and Reese method (1979)

Side resistance:

(1)	(2)	(3)	(4)	(5)	(6)	(7)	(8)	(9)	(10)	(11)	(12)	(13)
γ (kN/m ³)	h (m)	$p_0' = \gamma \cdot h$	L1 (m)	ϕ (degree)	L1* ϕ	ϕ (avg.)	$\tan\phi$	f_s (kPa)	πD (m)	ΔL (m)	A_s (m ²)	ΔQ_s (kN)
		(1)x(2)			(4)x(5)			(Eq. 3.4)			(10)x(11)	(9)x(12)
18.10	0.30		1.50	31.00	46.50	33.56	0.66	29.69	1.13	9.10	10.29	306.00
8.30	9.10	40.71	1.50	28.00	42.00							
			1.60	39.00	62.40							
			1.50	27.00	40.50							
			1.50	39.00	58.50							
			1.50	37.00	55.50							

$Q_s = 306 \text{ kN}$

Toe resistance:

(1)	(2)	(3)	(4)	(5)
N	q_p (kPa)	R (m)	A_p (m ²)	Q_p (kN)
	(Eq.3.5)			(2)x(4)
32	2042.88	0.18	0.10	208.00

$Q_p = 208 \text{ kN}$

Total resistance:

$Q_t = 306 + 208 = 514 \text{ kN}$

NO2: Neely method (1991)

Side resistance:

(1)	(2)	(3)	(4)	(5)	(6)	(7)	(8)	(9)	(10)
h (m)	γ (kN/m ³)	p_0' (kPa)	L (m)	β	f_s (kPa)	πD (m)	ΔL (m)	A_s (m ²)	ΔQ_s (kN)
		(1)x(2)		(Fig.3.1)	(3)x(5)			(7)x(8)	(6)x(9)
0.30	18.10	40.71	9.10	0.87	35.41	1.13	9.10	10.29	364
9.10	8.30								

$Q_s = 364 \text{ kN}$

Toe resistance:

(1)	(2)	(3)	(4)	(5)
N	q_p (kPa)	R (m)	A_p (m ²)	Q_p (kN)
	(Eq.3.7)			(2)x(4)
32	5822.21	0.18	0.10	593.00

$Q_p = 593 \text{ kN}$

Total resistance:

$Q_t = 364 + 593 = 957 \text{ kN}$

NO3: Coyle and Castello - Tomlinson method (1981)

Side resistance:

(1)	(2)	(3)	(4)	(5)	(6)	(7)	(8)	(9)
(degree)	L (m)	D (m)	L/D	f_s (kPa)	ΔL (m)	πD (m)	A_s (m ²)	ΔQ_s (kN)
			(2)/(3)	(Fig.3.3)			(6)x(7)	(5)x(8)
33.56	9.10	0.36	25.28	50.00	9.10	1.13	10.29	515

$$Q_s = 515 \text{ kN}$$

Toe resistance:

(1)	(2)	(3)	(4)	(5)	(6)	(7)	(8)
(degree)	L (m)	D (m)	L/D	q_p (kPa)	R (m)	A_p (m ²)	Q_p (kN)
(average)			(2)/(3)	(Fig.3.3)			(5)x(7)
37.00	9.10	0.36	25.28	4700.00	0.18	0.10	478.00

$$Q_p = 478 \text{ kN}$$

Total resistance:

$$Q_t = 515 + 478 = 993 \text{ kN}$$

NO4: LPC method (1981)

Side resistance:

(1)	(2)	(3)	(4)	(5)	(6)	(7)	(8)
ayer (m)	N	q_c (kPa)	f_s (kPa)	πD (m)	ΔL (m)	A_s (m ²)	ΔQ_s (kN)
		(Eq.3.11)	Fig. 3.2			(5)x(6)	(4)x(7)
0 - 1.5	14	4692.24	50.00	1.13	1.50	1.70	85.00
1.5 - 3.0	5	1675.80	20.00	1.13	1.50	1.70	34.00
3.0 - 4.6	40	13406	80.00	1.13	1.60	1.80	144.00
4.6 - 6.1	2	670.32	10.00	1.13	1.50	1.70	17.00
6.1 - 7.6	40	13406	80.00	1.13	1.50	1.70	136.00
7.6 - 9.1	32	10725	75.00	1.13	1.50	1.73	129.75

$$Q_s = 543 \text{ kN}$$

Toe resistance:

(1)	(2)	(3)	(4)	(5)	(6)
N	q_c (kPa)	q_p (kPa)	R (m)	A_p (m ²)	Q_p (kN)
	(Eq.3.11)	(Eq.3.9)			(3)x(5)
32	10725	1609	0.18	0.10	164.00

$$Q_p = 164 \text{ kN}$$

Total resistance:

$$Q_t = 543 + 164 = 707 \text{ kN}$$

NO5: Reese and O'Neill method (1988)

Side resistance:

(1)	(2)	(3)	(4)	(5)	(6)	(7)	(8)	(9)	(10)	(11)
Layer(m)	Z (ft)	γ (kN/m ³)	h (m)	p_o' (kPa)	β	f_s (kPa)	πD (m)	ΔL (m)	A_p (m ²)	ΔQ_s (kN)
				(3)x(4)	(Eq.3.14)	(Eq.3.13)			(8)x(10)	(7)x(10)
0 - 1.5	2.46	8.30	0.75	9.17	1.20	11.00	1.13	1.50	1.70	18.66
1.5 - 3.0	7.38	8.30	2.25	21.62	1.13	24.49	1.13	1.50	1.70	41.55
3.0 - 4.6	12.47	8.30	3.80	34.48	1.02	35.28	1.13	1.60	1.81	63.85
4.6 - 6.1	17.55	8.30	5.35	47.35	0.93	44.24	1.13	1.50	1.70	75.05
6.1 - 7.6	22.47	8.30	6.85	59.80	0.86	51.42	1.13	1.50	1.70	87.24
7.6 - 9.1	27.40	8.30	8.35	72.25	0.79	57.32	1.13	1.50	1.70	97.24

$$Q_s = 384 \text{ kN}$$

Toe resistance:

(1)	(2)	(3)	(4)	(5)
N	q_p (kPa)	R (m)	A_p (m ²)	Q_p (kN)
	(Eq. 3.15)			(2)x(4)
32	1838.59	0.18	0.10	187.00

$$Q_p = 187 \text{ kN}$$

Total resistance:

$$Q_t = 384 + 187 = 571 \text{ kN}$$

NO6: API method (API RP2A, 1994)

(1)	(2)	(3)	(4)	(5)	(6)	(7)	(8)	(9)	(10)	(11)	(12)
ayer (m)	N	δ (degree) (Table 3.1)	$\tan\delta$	γ (kN/m ³)	h (m)	p_o' (kPa) (5)x(6)	f_s (kPa) (Eq.3.26)	πD (m)	ΔL (m)	A_s (m ²) (9)x(10)	ΔQ_s (kN) (8)x(11)
0 - 1.5	14	20	0.36	8.30	0.75	9.17	3.34	1.13	1.50	1.70	5.66
1.5 - 3.0	5	15	0.27	8.30	2.25	21.62	5.79	1.13	1.50	1.70	9.83
3.0 - 4.6	40	30	0.58	8.30	3.80	34.48	19.89	1.13	1.60	1.81	36.00
4.6 - 6.1	2	15	0.27	8.30	5.35	47.35	12.69	1.13	1.50	1.70	21.53
6.1 - 7.6	40	30	0.58	8.30	6.85	59.80	34.50	1.13	1.50	1.70	58.53
7.6 - 9.1	32	30	0.58	8.30	8.35	72.25	41.69	1.13	1.50	1.70	70.72

$Q_s = 202 \text{ kN}$

Toe resistance:

(1)	(2)	(3)	(4)	(5)	(6)	(7)	(8)	(9)
γ (kN/m ³)	h (m)	p_o' (kPa) (1)x(2)	N	N_q (Table 3.1)	q_p (kPa)	R (m)	A_p (m ²)	Q_p (kN) (6)x(8)
8.30	9.10	80.96	32	40.00	3238.40	0.18	0.10	329

$Q_p = 329 \text{ kN}$

Total resistance:

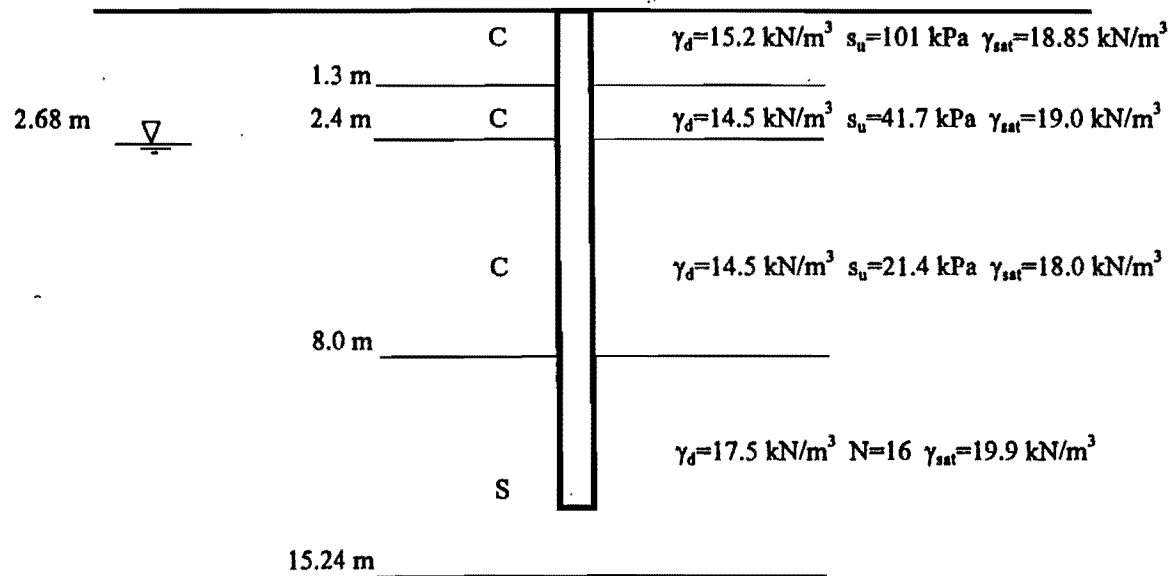
$Q_t = 202 + 329 = 531 \text{ kN}$

Example 3: Calculation for mixed soil profile case from database

Project ID: 12MI/BS

$Q_u(5\%)=1475 \text{ kN}$

$L=13.72 \text{ m}$



Assumptions:

1. soil above G.W.L is saturated.
2. concrete and fill at the surface, $f_s = 0$.

NO1: Coyle and Castello - Tomlinson method (1981)

Side resistance:

Clay

(1)	(2)	(3)	(4)	(5)	(6)	(7)	(8)
Layer (m)	s_u (kPa)	α (Fig.3.4)	f_s (kPa) (2)x(3)	ΔL (m)	πD (m)	A_s (m ²) (5)x(7)	ΔQ_{s1} (kN) (4)x(8)
0 - 1.3	101.00	0.49	49.49	1.30	1.12	1.45	71.87
1.3 - 2.4	41.70	1.00	41.70	1.10	1.12	1.23	51.24
2.4 - 8.0	21.40	1.00	21.40	5.60	1.12	6.26	133.88

$Q_{s1} = 257 \text{ kN}$

sand

(1)	(2)	(3)	(4)	(5)	(6)	(7)	(8)	(9)	(10)	(11)
Layer (m)	N	ϕ (degree)	L (m)	D (m)	L/D (4)/(5)	f_s (kPa) (Fig.3.3)	ΔL (m)	πD (m)	A_s (m ²) (8)x(9)	ΔQ_{s2} (kN) (7)x(10)
8.0 - 13.72	16	32	13.70	0.36	38.53	45.00	5.72	1.12	6.39	287.55

$Q_{s2} = 288 \text{ kN}$

$Q_s = Q_{s1} + Q_{s2} = 257 + 288 = 545 \text{ kN}$

Toe resistance:

(1)	(2)	(3)	(4)	(5)	(6)	(7)	(8)	(9)
N	ϕ (degree)	L (m)	D (m)	L/D (3)/(4)	q_p (kPa) (Fig.3.3)	R (m)	A_p (m ²)	Q_p (kN) (6)x(8)
16	32	13.70	0.36	38.53	4000.00	0.18	0.10	397.25

$Q_p = 397 \text{ kN}$

Total resistance:

$Q_t = 545 + 397 = 942 \text{ kN}$

NO2: API method (API RP2A,1994)

Side resistance: Clay layers

(1)	(2)	(3)	(4)	(5)	(6)	(7)	(8)	(9)	(10)	(11)	(12)
Layer (m)	s_u (kPa)	γ (kN/m ³)	h (m)	p_o' (kPa)	$\psi = s_u/p_o'$	α	ΔL (m)	πD (m)	A_s (m ²)	f_s (kN)	ΔQ_s (kN)
				(3)x(4)	(2)/(5)				(8)x(9)	(2)x(7)	(10)x(11)
0-1.3	101.00	18.85	0.65	12.25	8.24	0.30	1.30	1.28	1.66	29.80	49.59
1.3-2.4	47.10	18.90	1.85	34.93	1.35	0.43	1.10	1.28	1.41	20.28	28.56
2.4-8.0	21.40	9.09	5.20	70.70	0.30	0.91	5.60	1.28	7.17	19.45	139.41

$$Q_{s1} = 217.56 \text{ kN}$$

Side resistance: Sand layer

(1)	(2)	(3)	(4)	(5)	(6)	(7)	(8)	(9)	(10)	(11)	(12)
Layer (m)	N	δ (degrees)	$\tan \delta$	γ (kN/m ³)	h (m)	p_o' (kPa)	f_s (kPa)	πD (m)	ΔL (m)	A_s (m ²)	Q_{s2} (kN)
										(9)x(10)	(8)x(11)
8.0 - 13.72	16	25	0.47	9.09	10.86	122.20	45.95	1.28	5.72	7.32	336.43

$$Q_s = Q_{s1} + Q_{s2} = 217.56 + 336.43 = 554.0 \text{ kN}$$

$$Q_{s2} = 336.43 \text{ kN}$$

Toe resistance:

(1)	(2)	(3)	(4)	(5)	(6)	(7)	(8)	(9)
γ (kN/m ³)	h (m)	p_o' (kPa)	N	N_q	q_p (kPa)	R (m)	A_p (m ²)	Q_p (kN)
(avg)		(1) X (2)		(Table 3.1)	(3)*(5)			(6) * (8)
10.81	13.72	148.26	16.00	20	2966.26	0.18	0.10	296.63

$$Q_p = 296.63 \text{ kN}$$

Total resistance:

$$Q_t = 554.0 + 296.6 = 850.6 \text{ kN}$$

NO3: LPC method (1981)

Side resistance:

Clay

(1)	(2)	(3)	(4)	(5)	(6)	(7)	(8)	(9)	(10)	(11)
Layer (m)	s_u (kPa)	γ (kN/m ³)	h (m)	P_0 (kPa)	q_c (kPa)	f_s (kPa) (Fig.3.2)	ΔL (m)	πD (m)	A_s (m ²) (8)x(9)	Q_{s1} (kN) (7)x(10)
0 - 1.3	101.00	18.85	0.65	12.30	1729.30	65.00	1.30	1.12	1.45	94.40
1.3 - 2.4	41.70		1.85	34.90	743.80	40.00	1.10	1.12	1.23	49.15
2.4 - 8.0	21.40	8.20	5.20	71.20	435.00	20.00	5.60	1.12	6.26	125.12

sand

$$Q_{s1} = 269 \text{ kN}$$

(1)	(2)	(3)	(4)	(5)	(6)	(7)	(8)
Layer (m)	N	q_c (kPa) (Eq.3.11)	f_s (kPa) (Fig.3.2)	πD (m)	ΔL (m)	A_s (m ²) (5)x(6)	Q_{s2} (kN) (4)x(7)
8.0 - 13.72	16	5362.56	60.00	1.12	5.72	6.39	383.39

$$Q_{s2} = 384 \text{ kN}$$

$$Q_s = Q_{s1} + Q_{s2} = 269 + 384 = 652 \text{ kN}$$

Toe resistance:

(1)	(2)	(3)	(4)	(5)	(6)
N	q_c (kPa) (Eq.3.11)	q_p (kPa) (Eq.3.9)	R (m)	A_p (m ²)	Q_p (kN) (3)x(5)
16	5362.56	804.38	0.18	0.10	79.88

$$Q_p = 80 \text{ kN}$$

Total resistance:

$$Q_t = 652 + 80 = 732 \text{ kN}$$

NO4: Reese and O'Neill method (1988)

Side resistance:

clay

(1)	(2)	(3)	(4)	(5)	(6)	(7)
Layer (m)	s_u (kPa)	ΔL (m)	πD (m)	A_s (m ²)	f_s (kPa)	Q_{s1} (kN)
				(3)x(5)	(Eq.3.17)	(5)x(6)
0 - 1.3	101.00	1.30	1.12	1.45	55.55	80.67
1.3 - 2.4	41.70	1.10	1.12	1.23	22.94	28.18
2.4 - 8.0	21.40	5.60	1.12	6.26	11.77	73.63

$$Q_{s1} = 182 \text{ kN}$$

sand

(1)	(2)	(3)	(4)	(5)	(6)	(7)	(8)	(9)	(10)
Layer (m)	γ (kN/m ³)	Z (ft)	$p_{o'}$ (kPa)	β	f_s (kPa)	πD (m)	ΔL (m)	A_s (m ²)	Q_{s2} (kN)
				(Eq.3.14)	(Eq.3.13)			(7)x(8)	(6)x(9)
8.0 - 13.72	18.85	35.76	118.00	0.70	82.60	1.12	5.72	6.39	527.81
	8.20								

$$Q_{s2} = 528 \text{ kN}$$

$$Q_s = Q_{s1} + Q_{s2} = 182 + 528 = 710 \text{ kN}$$

Toe resistance:

(1)	(2)	(3)	(4)	(5)
N	q_p (kPa)	R (m)	A_p (m ²)	Q_p (kN)
	(Eq.3.15)			(2)x(4)
16	919.30	0.18	0.10	91.30

$$Q_p = 91 \text{ kN}$$

Total resistance:

$$Q_t = 710 + 91 = 801 \text{ kN}$$

This page is intentionally blank.

Appendix B

Cross-hole Ultrasonic Logs of Test Piles at Variable Power Settings and Measured Grout Take Ratios for Test Piles

(Cross-hole Logs Courtesy Fugro-McClelland Southwest, Inc.)

TXDOT, UNIV. HOU. TEST SITE
 HOUSTON, TEXAS
 TP1
 Tim Roberts

Label: A
 Distance: 0.00ft
 Length: 51.02ft
 Power: B40,af
 Date: 18 Mar 1998

Label: B
 Distance: 0.00ft
 Length: 51.02ft
 Power: B30,8f
 Date: 18 Mar 1998

Label: C
 Distance: 0.00ft
 Length: 51.02ft
 Power: B20,6f
 Date: 18 Mar 1998

Label: D
 Distance: 0.00ft
 Length: 51.02ft
 Power: B10,4f
 Date: 18 Mar 1998

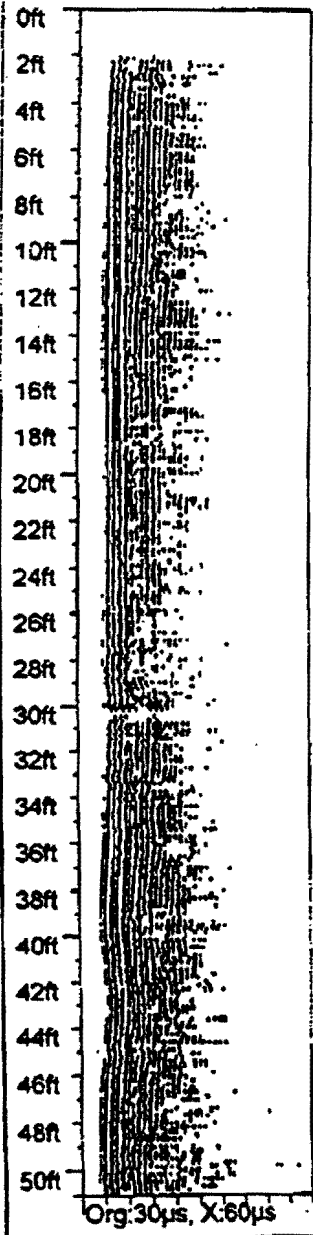
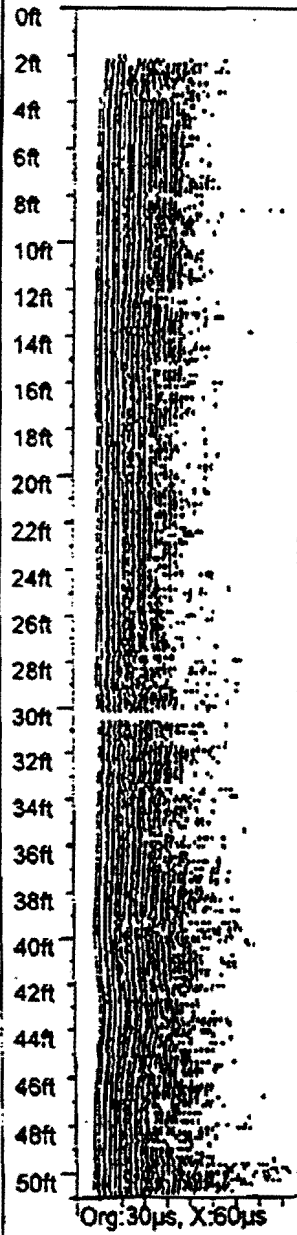
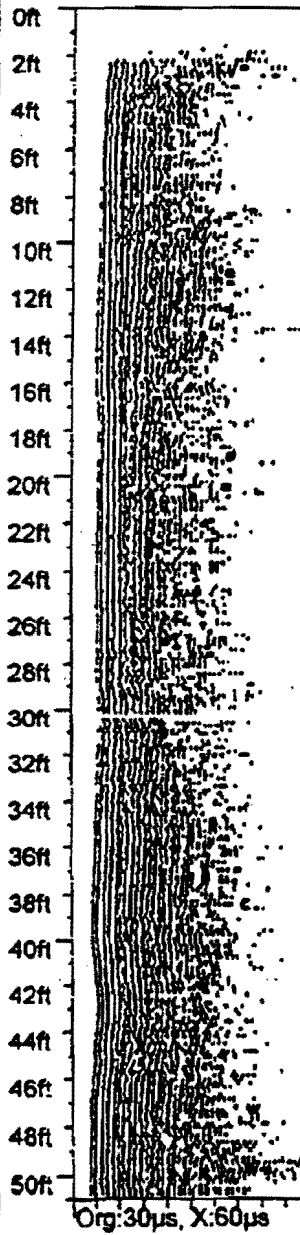
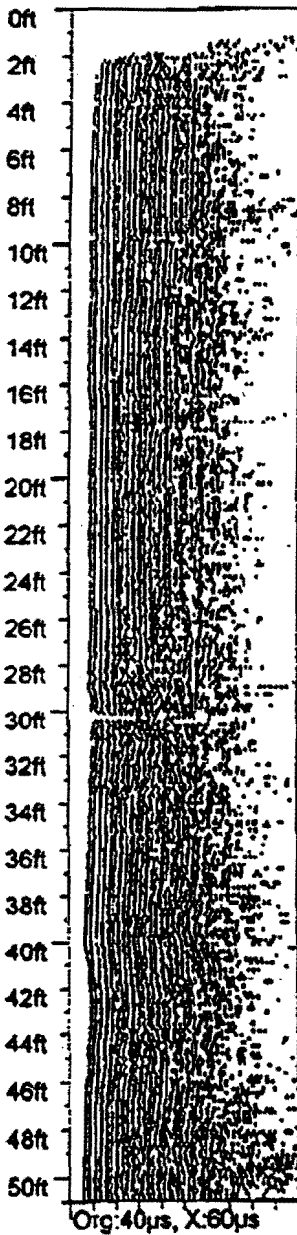


Figure B.1. Cross-hole ultrasonic log of UH test pile

TXDOT, UNIV. HOU. TEST SITE
HOUSTON, TEXAS
TP1
Tim Roberts

Label: E
Distance: 0.00ft
Length: 51.35ft
Power: B00.2f
Date: 18 Mar 1998

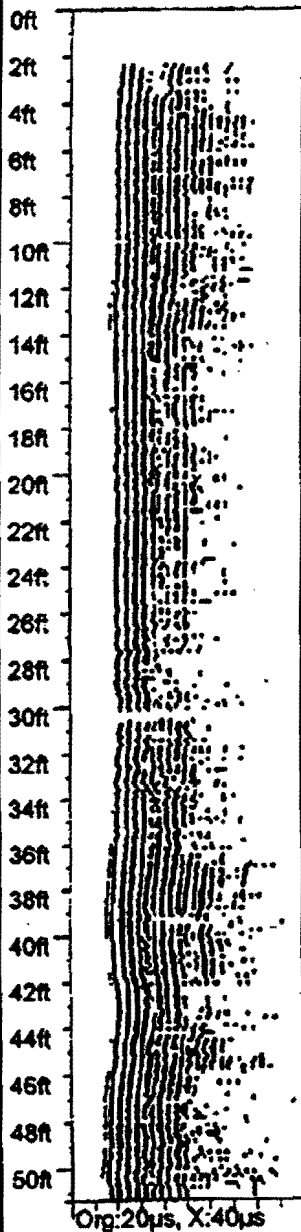


Figure B.1. Cross-hole ultrasonic log of UH test pile (Continued)

TXDOT, BAYTOWN TEST SITE
 BAYTOWN.TX.
 TEST
 Tim Roberts

Label: C
 Distance: 0.00ft
 Length: 51.02ft
 Power: D10,4f
 Date: 25 Mar 1998

Label: F
 Distance: 0.00ft
 Length: 50.69ft
 Power: C20,6f
 Date: 25 Mar 1998

Label: G
 Distance: 0.00ft
 Length: 50.52ft
 Power: B20,6f
 Date: 25 Mar 1998

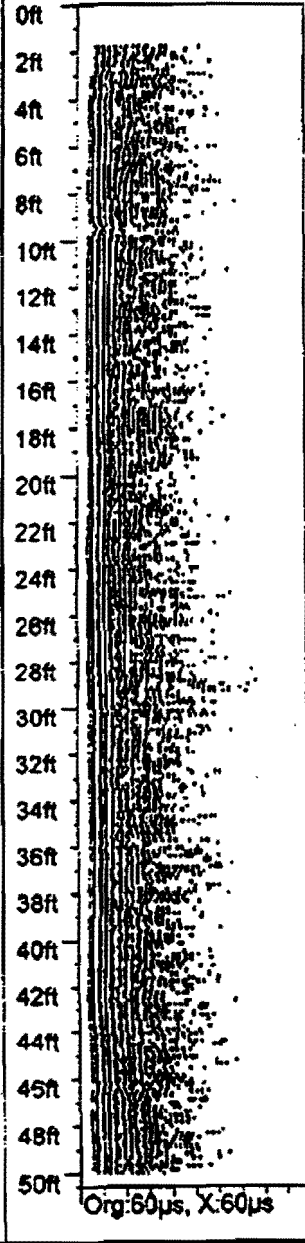
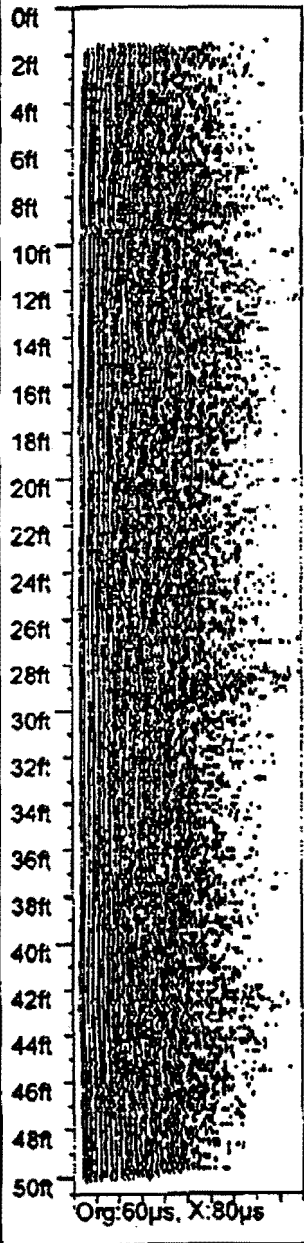
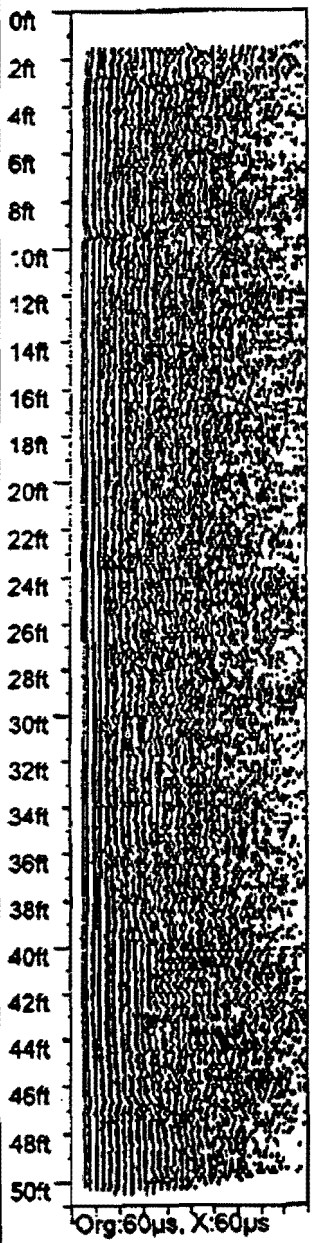


Figure B.2. Cross-hole ultrasonic log of Baytown test pile

**TXDOT-UH AUGERED CAST-IN-PLACE PILES
ROSENBURG, TX.
TEST
Tim Roberts**

Label: C
Distance: 0.00ft
Length: 30.68ft
Power: B10,4f
Date: 09 Apr 1998

Label: D
Distance: 0.00ft
Length: 30.84ft
Power: B20,6f
Date: 09 Apr 1998

Label: E
Distance: 0.00ft
Length: 30.68ft
Power: B30,8f
Date: 09 Apr 1998

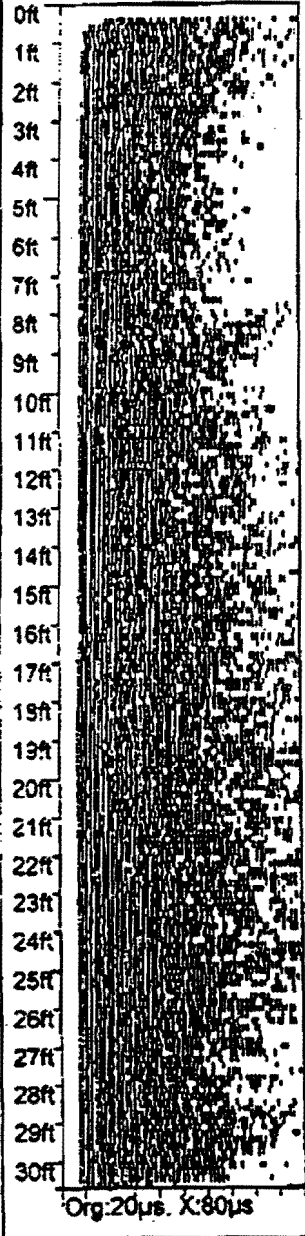
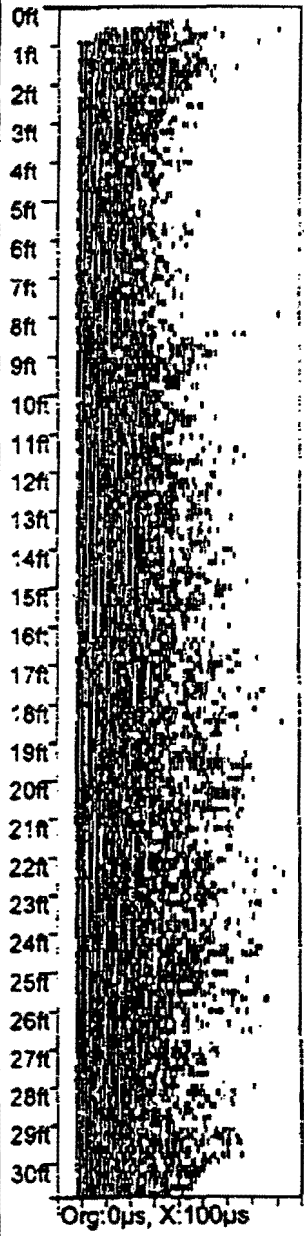
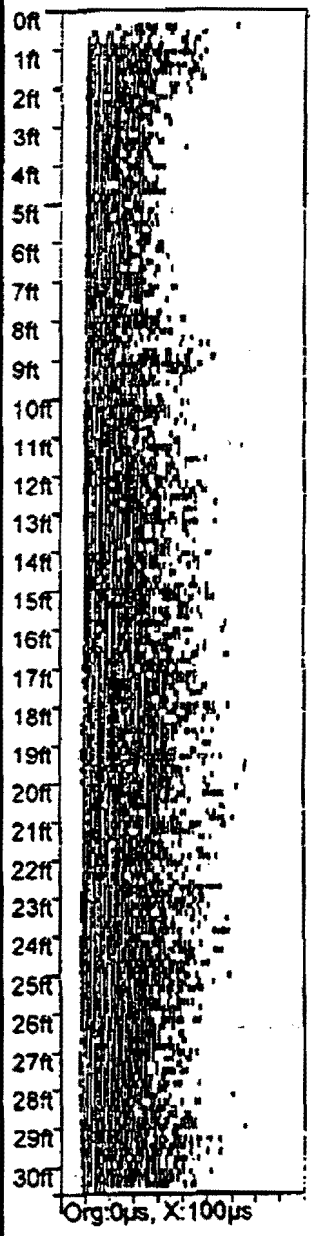


Figure B.3. Cross-hole ultrasonic log of Rosenberg test pile

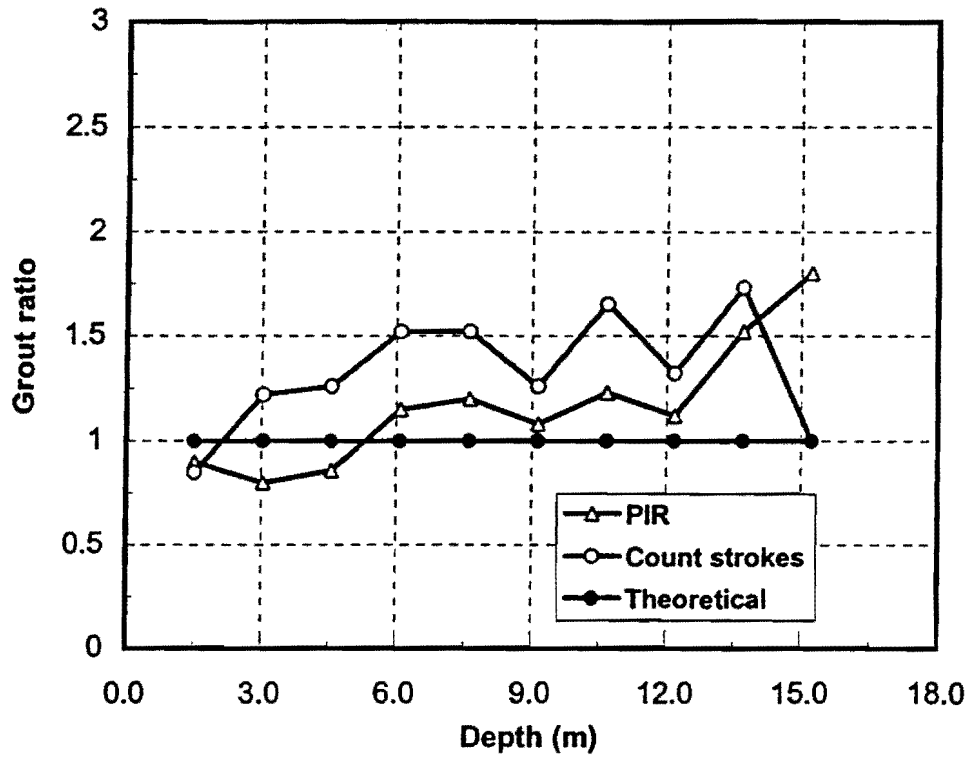


Figure B.4. Grout ratio for UH test pile

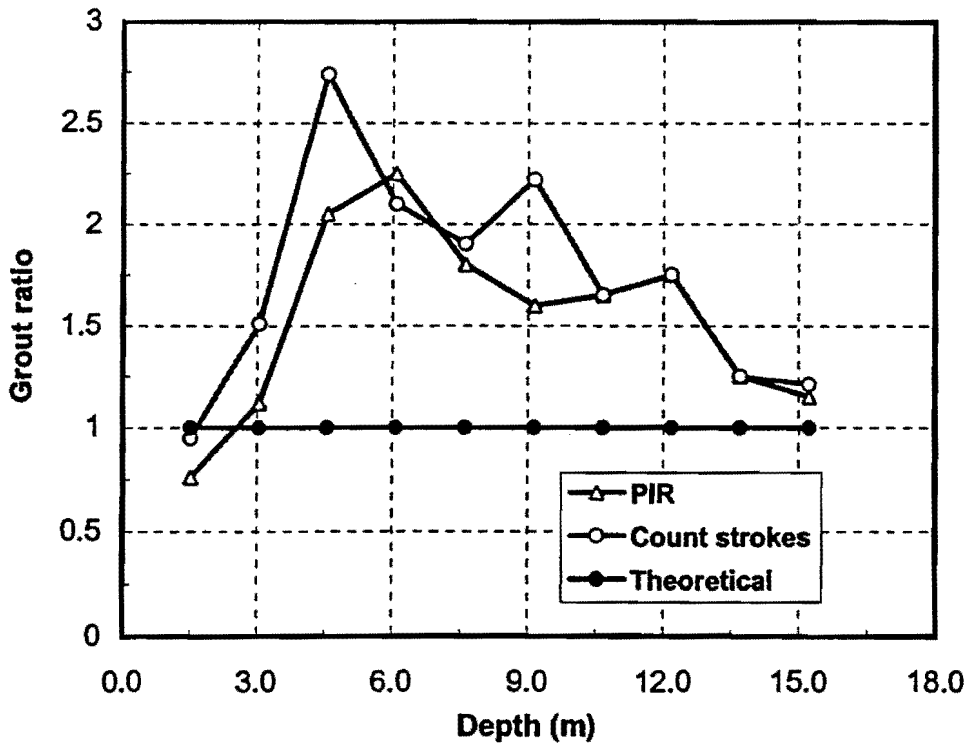


Figure B.5. Grout ratio for Baytown test pile

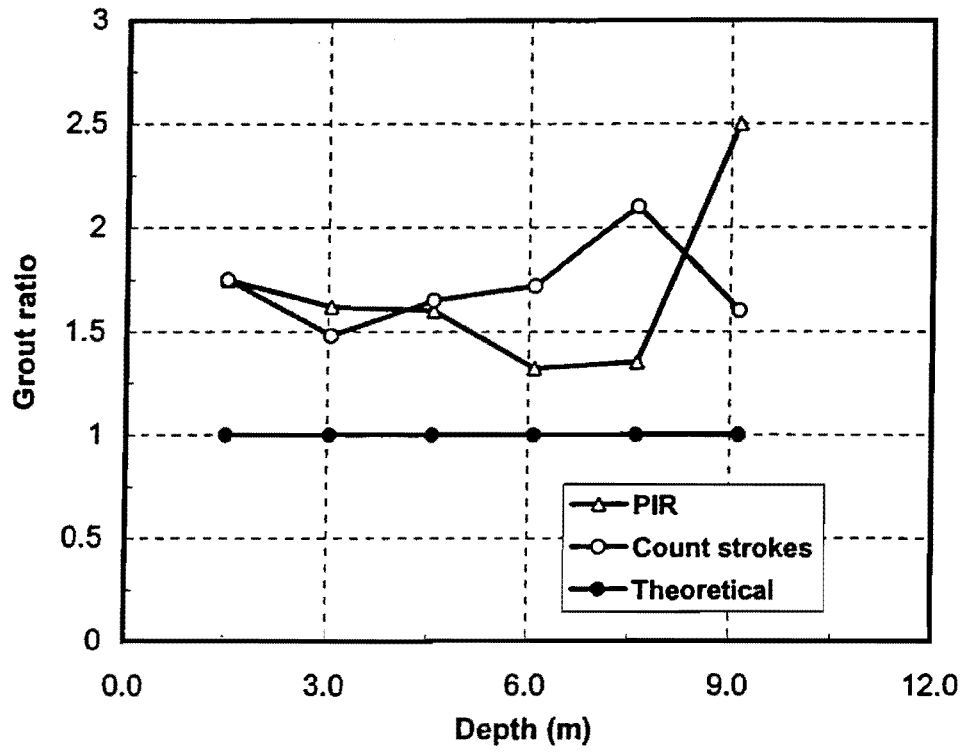


Figure B.6. Grout ratio for Rosenberg test pile

This page is intentionally blank.

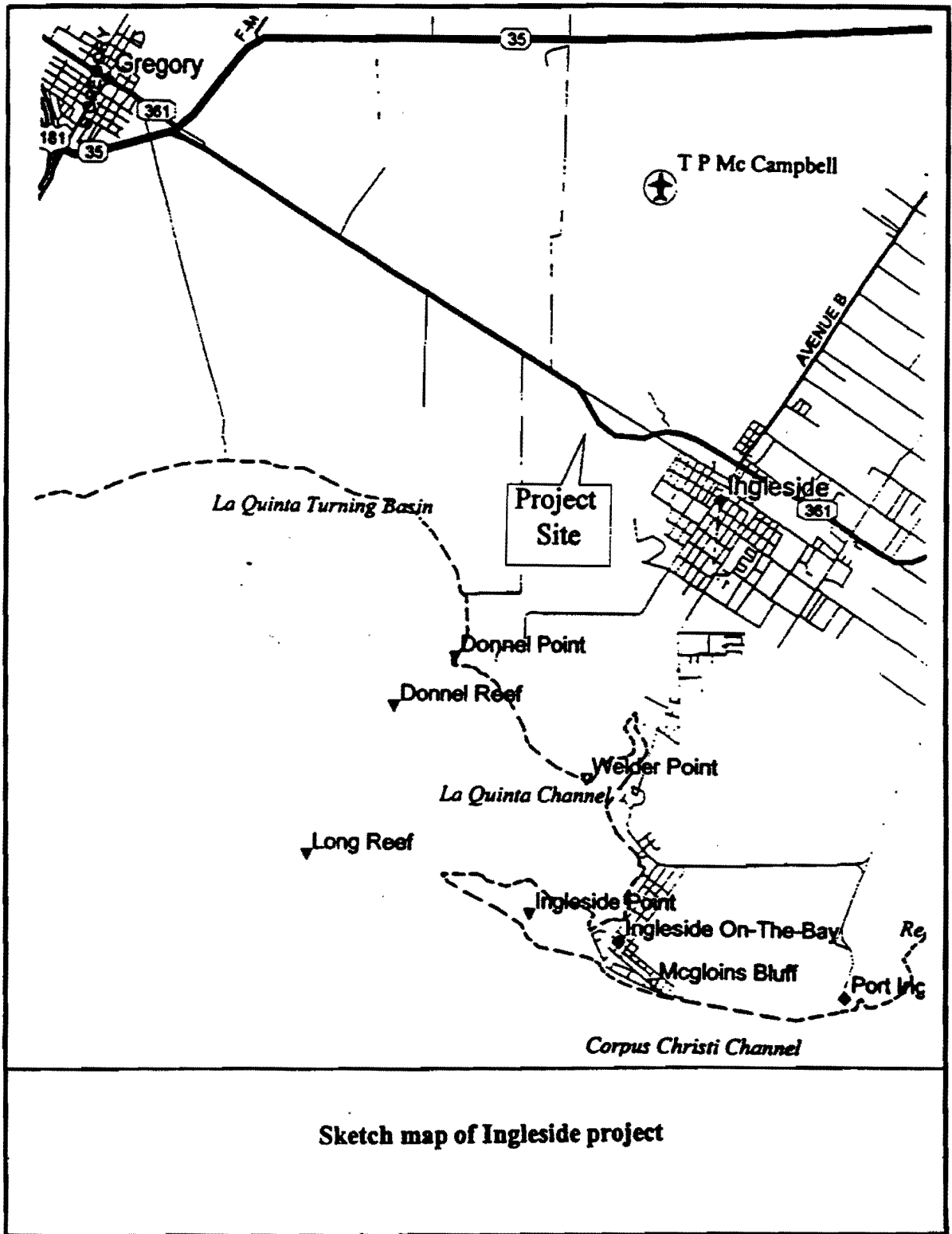
Appendix C

Ingleside Cogeneration Project

Ingleside, Texas

CFA Pile Data

(Courtesy Emcon, Inc.)



Sketch map of Ingleside project

LOG OF BORING B-1

PROJECT: Ingleside Cogeneration
Ingleside, Texas

DEPTH (ft)	SAMPLE TYPE SYMBOL / USCS	COORDINATES: 807821.2 ft; 2405300.1 ft		MOISTURE CONTENT (%)	DRY UNIT WEIGHT (pcf)	LIQUID LIMIT (%)	PLASTICITY INDEX (%)	COMPRESSION STRENGTH (tsf)	FAILURE STRAIN (%)	CONFINING PRESSURE (psf)	PASSING #200 SIEVE (%)	OTHER TESTS PERFORMED	
		SURFACE ELEVATION: 20.2 ft											
		DRILLING METHOD: Dry Augered: 0 ft to 14 ft Wash Bored: 14 ft to 100 ft		POCKET PEN (tsf) (T) TORVANE (tsf)	STD. PENETRATION TEST (blows/ft)								
MATERIAL DESCRIPTION													
36	[Hatched Pattern]												
37													
38				93.2		34	88		1.10 (%)	0.5		100	
39													
40													
41	[Hatched Pattern]												
42													
43		Medium dense tan to light gray CLAYEY SAND (SC), very fine, moist											
44													
45													
46	[Hatched Pattern]	with sandstone, 48 to 50'		92.2		18	114				33		
47													
48													
49													
50													
51	[Hatched Pattern]	Very stiff tan to light gray CLAY (CH), moist											
52													
53				93.0									
54													
55													
56	[Hatched Pattern]	Very stiff tan to light gray SANDY CLAY (CL), moist with sand seams and calcareous material, 58 to 60'											
57													
58				92.0		18	110	41	25	3.00	11.5	25	78
59													
60													
61	[Hatched Pattern]	Dense light gray to tan SILTY SAND (SM) with sandstone, 63 to 65'											
62													
63													
64													
65													
66	[Dotted Pattern]												
67													
68						24							
69													
70													

COMPLETION DEPTH: 100.0 ft.
 DATE BORING STARTED: 1/27/98
 DATE BORING COMPLETED: 1/27/98
 ENGINEER/GEOLOGIST: J. Brown
 PROJECT No.: 63645-001.001

REMARKS: Consistency of cohesionless to semi-cohesive soils without SPT N values correlated from adjacent CPT data from location C-2. CN - Consolidation sample * - Slit-sided failure

Continued Next Page

Stratification lines represent approximate strata boundaries. In situ, the transition may be gradual.

LOG OF BORING B-1

PROJECT: Ingleside Cogeneration
Ingleside, Texas

DEPTH (ft)	SAMPLE TYPE SYMBOL / USCS	COORDINATES: 807821.2 ft; 2405300.1 ft SURFACE ELEVATION: 20.2 ft DRILLING METHOD: Dry Augered: 0 ft to 14 ft Wash Bored: 14 ft to 100 ft	(F) POCKET PEN (tsf) (T) TORVANE (tsf)	STD. PENETRATION TEST (blows/ft)	MOISTURE CONTENT (%)	DRY UNIT WEIGHT (pcf)	LIQUID LIMIT (%)	PLASTICITY INDEX (%)	COMPRESSIVE STRENGTH (tsf)	FAILURE STRAIN (%)	CONFINING PRESSURE (psf)	PASSING #200 SIEVE (%)	OTHER TESTS PERFORMED
		MATERIAL DESCRIPTION											
71													
72													
73													
74				22								8	
75													
76													
77													
78													
79													
80													
81													
82													
83					18	108						4	
84													
85													
86													
87													
88													
89													
90													
91													
92													
93													
94		Very dense light gray to tan SANDY SILT (ML)		50/4 in								88	
95													
96													
97													
98													
99		water bearing, 98 to 99'		73									
100		with clay seam at 99.5'											
101		Bottom @ 100'											
102													
103													
104													
105													
COMPLETION DEPTH: 100.0 ft. DATE BORING STARTED: 1/27/88 DATE BORING COMPLETED: 1/27/88 ENGINEER/GEOLOGIST: J. Brown PROJECT No.: 63648-001.001			REMARKS: Consistency of cohesionless to semi-cohesive soils without SPT N values correlated from adjacent CPT data from location C-2. CN - Consolidation sample * - Slit-sides failure										

Stratification lines represent approximate strata boundaries. In situ, the transition may be gradual.

LOG OF BORING B-6

PROJECT: Ingleside Cogeneration
Ingleside, Texas

DEPTH (ft)	SAMPLE TYPE SYMBOL / USCS	COORDINATES: 806310.0 ft; 2405790.0 ft		(F) POCKET PEN (tsf)	(T) TORVANE (tsf)	STD. PENETRATION TEST (blows/ft)	MOISTURE CONTENT (%)	DRY UNIT WEIGHT (pcf)	LIQUID LIMIT (%)	PLASTICITY INDEX (%)	COMPRESSIVE STRENGTH (tsf)	FAILURE STRAIN (%)	CONFINING PRESSURE (pcf)	PASSING #200 SIEVE (%)	OTHER TESTS PERFORMED
		SURFACE ELEVATION: 18.0 ft													
		DRILLING METHOD:													
		Dry Augered: 0 ft to 14 ft													
		Wash Bored: 14 ft to 100 ft													
		MATERIAL DESCRIPTION													
1	[Diagonal Hatching]	Stiff dark gray SANDY CLAY (CL), moist		074.6			14		48	32					
2															
3															
4	[Diagonal Hatching]	tan below 6'		072.0											
5															
6															
7							21	83	41	23	0.80	2.0			
8															
9	[Dotted Pattern]	Dense tan SILTY SAND (SM) with sandstone @ 9'					24	88						40	
10															
11															
12		with water bearing sands below 12'					21	108							38
13															
14															
15							38								
16															
17															
18							46								
19															
20															
21															
22															
23			very dense below 23'												
24						56								42	
25															
26															
27															
28															
29						50									
30			with sandstone @ 30'												
31															
32															
33															
34	[Diagonal Hatching]	Very stiff light gray to reddish brown CLAY (CH), slickensided		074.0			28	89			2.48	3.3	14		
35															

COMPLETION DEPTH: 75.0 ft
 DATE BORING STARTED: 1/28/98
 DATE BORING COMPLETED: 1/28/98
 ENGINEER/GEOLOGIST: J. January
 PROJECT No.: 63648-001.001

REMARKS:

Continued Next Page

Stratification lines represent approximate strata boundaries.
 In situ, the transition may be gradual.

LOG OF BORING B-6

PROJECT: Ingleside Cogeneration
Ingleside, Texas

DEPTH (ft)	SAMPLE TYPE SYMBOL / USCS	COORDINATES: 806310.0 ft; 2405790.0 ft SURFACE ELEVATION: 18.0 ft DRILLING METHOD: Dry Augered: 0 ft to 14 ft Wash Bored : 14 ft to 100 ft										(F) POCKET PEN (ref) (T) TORVANE (ref)	STD. PENETRATION TEST (blow/ft)	MOISTURE CONTENT (%)	DRY UNIT WEIGHT (pcf)	LIQUID LIMIT (%)	PLASTICITY INDEX (%)	COMPRESSIVE STRENGTH (ref)	FAILURE STRAIN (%)	CONFINING PRESSURE (pcf)	PASSING #200 SIEVE (%)	OTHER TESTS PERFORMED
		MATERIAL DESCRIPTION																				
36																						
37																						
38																						
39																						
40																						
41																						
42																						
43																						
44																						
45																						
46																						
47																						
48																						
49																						
50																						
51																						
52																						
53																						
54																						
55																						
56																						
57																						
58																						
59																						
60																						
61																						
62																						
63																						
64																						
65																						
66																						
67																						
68																						
69																						
70																						

COMPLETION DEPTH: 75.0 ft.
 DATE BORING STARTED: 1/28/88
 DATE BORING COMPLETED: 1/28/88
 ENGINEER/GEOLOGIST: J. January
 PROJECT No.: 83645-001.001

REMARKS:

Continued Next Page

Stratification lines represent approximate strata boundaries
 In situ, the transition may be gradual

LOG OF BORING B-6

PROJECT: Ingleside Cogeneration
Ingleside, Texas

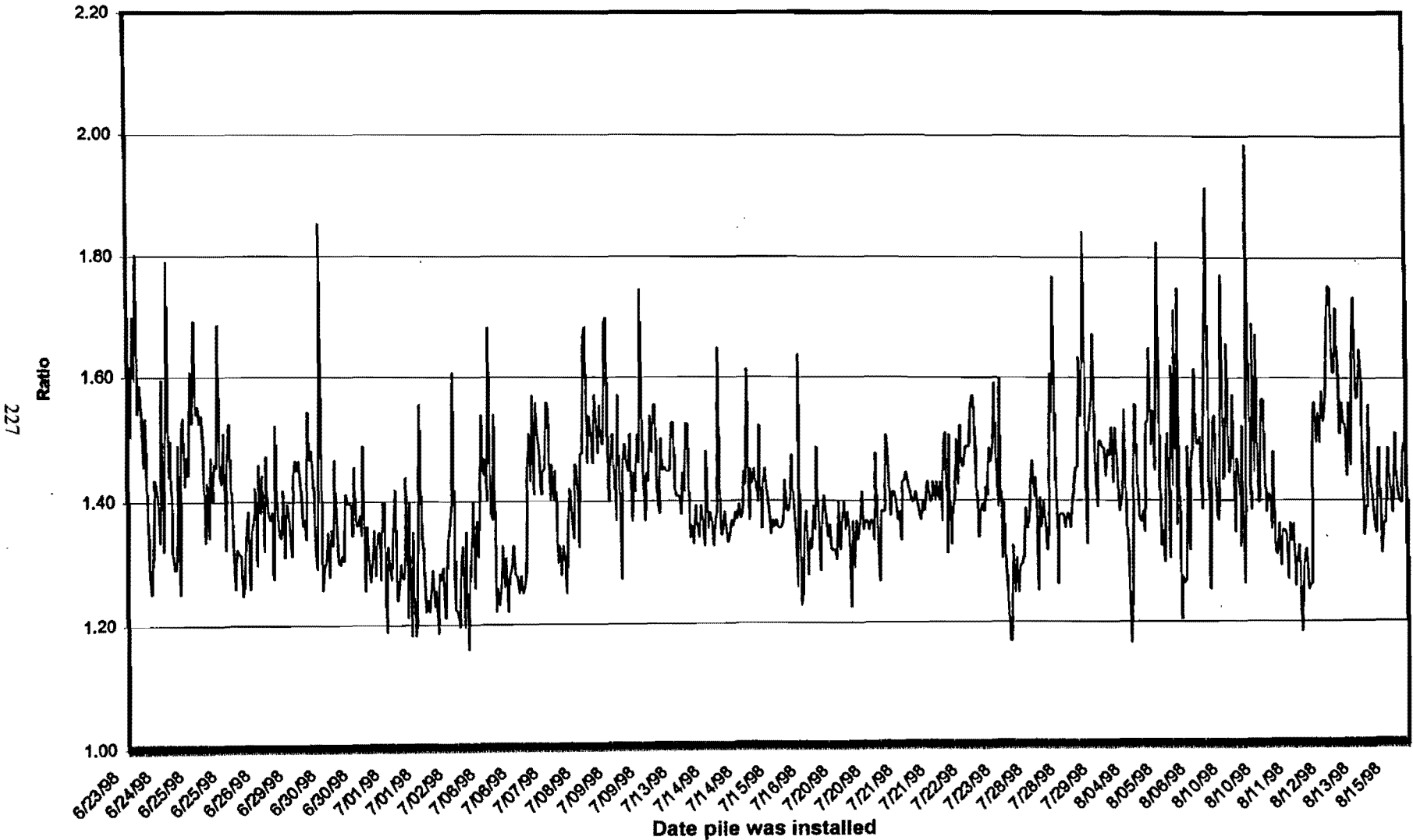
DEPTH (ft)	SAMPLE TYPE SYMBOL / USCS	COORDINATES: 806310.0 ft; 2405790.0 ft	(M) POCKET PEN (ref)	(N) TORVANE (ref)	STD. PENETRATION TEST (blows/ft)	MOISTURE CONTENT (%)	DRY UNIT WEIGHT (pcf)	LIQUID LIMIT (%)	PLASTICITY INDEX (%)	COMPRESSIVE STRENGTH (ref)	FAILURE STRAIN (%)	CONFINING PRESSURE (pcf)	PASSING #200 SIEVE (%)	OTHER TESTS PERFORMED
		SURFACE ELEVATION: 18.0 ft												
		DRILLING METHOD: Dry Augered: 0 ft to 14 ft Wash Bored: 14 ft to 100 ft												
		MATERIAL DESCRIPTION												
71														
72														
73		siltsand @ 73'												
74														
75		Bottom @ 100'												
76														
77														
78														
79														
80														
81														
82														
83														
84														
85														
86														
87														
88														
89														
90														
91														
92														
93														
94														
95														
96														
97														
98														
99														
100														
101														
102														
103														
104														
105														

COMPLETION DEPTH: 75.0 ft.
 DATE BORING STARTED: 1/28/88
 DATE BORING COMPLETED: 1/28/88
 ENGINEER/GEOLOGIST: J. January
 PROJECT No.: 63645-001.001

REMARKS:

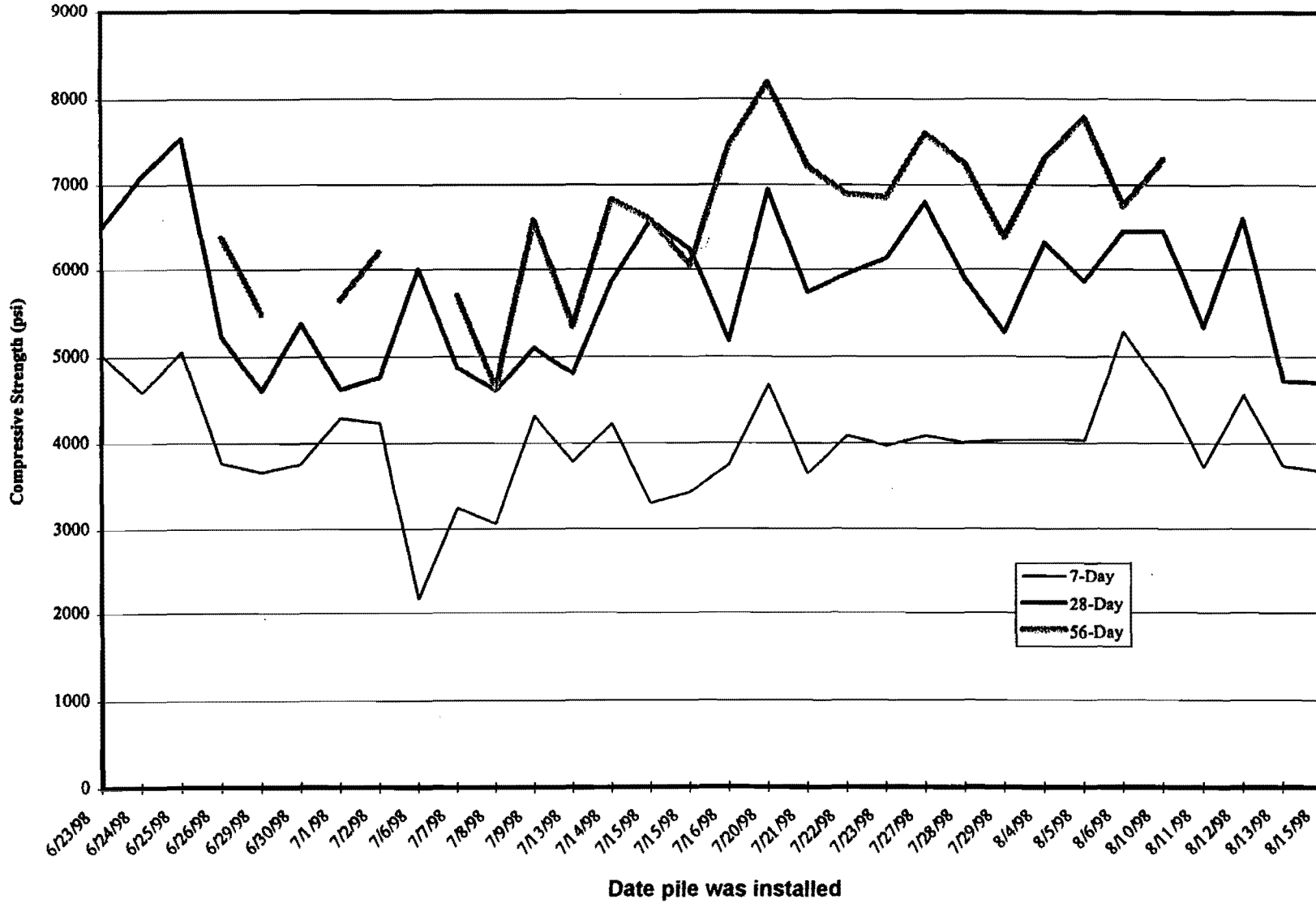
Stratification lines represent approximate strata boundaries.
 In situ, the transition may be gradual.

**Actual/Theoretical Grout Ratio Vs Date
Ingleside Cogeneration Project**



(Note: Each spike represents data for one CFA pile.)

**Grout Cube Compressive Strength Vs Date
Ingleside Cogeneration Project**



Appendix D. Chemical Resistance of Auger Grouts

This page is intentionally blank.

APPENDIX D CHEMICAL RESISTANCE OF AUGER GROUTS

D1. INTRODUCTION

A total of 49 specimens representing auger grouts and cement concrete were submerged in eight chemical solutions for up to two years (Table D.1). Changes in weight, leaching of calcium, changes in pulse velocity, and compressive strength were monitored with time to determine the durability of these materials to chemical attack.

The chemicals used in this study were (i) hydrochloric acid (HCl) at pH of 2 and 4 (relationship between weight percentage and pH is shown in Fig. D.1); (ii) sulfuric acid (H_2SO_4) at pH of 2 and 4; (iii) 0.5% and 2% sodium sulfate (Na_2SO_4); and (iv) 0.5% and 2% sodium chloride (NaCl).

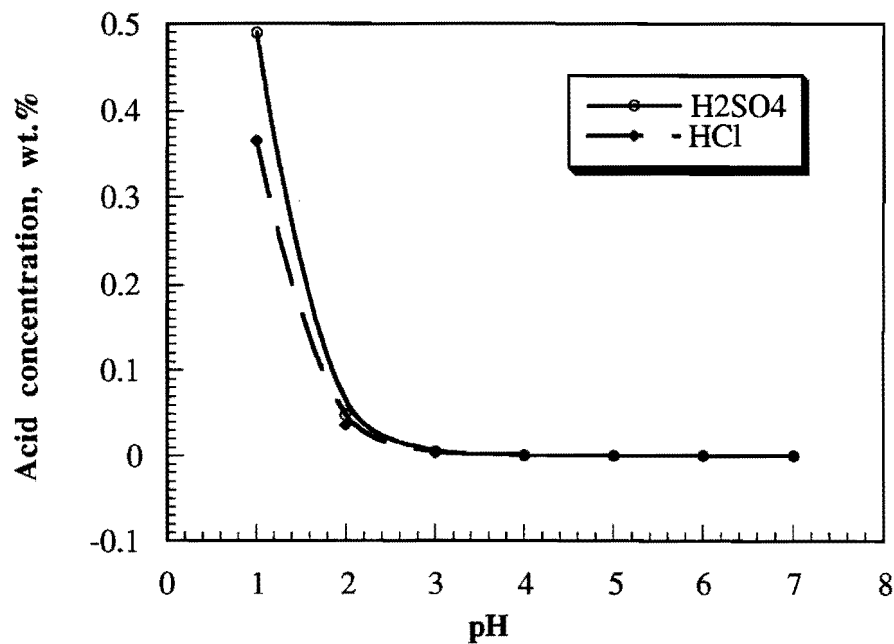


Figure D.1 pH versus concentration percentage of sulfuric and hydrochloric acid

Auger grouts for CFA piles and cement concrete specimens were collected from the field sites documented in the main report. Test specimens were fully immersed into various

chemical solutions, and at least two specimens were tested under each condition. Solutions were replaced on a regular basis since grout and concrete specimens increased the pH of the solutions. Change of appearance, weight, pulse velocity, and calcium in the leaching solutions were measured every time the solution was replaced (one cycle). The testing schedule is shown in Table D.1.

Table D.1 Number of Auger Grout and Cement Concrete Specimens Tested

Chemical solutions		Auger grouts Dry	Cement concrete Dry Wet	
HCl	pH 2	3	2	2
	pH 4	2	--	--
H ₂ SO ₄	pH 2	4	2	2
	pH 4	3	2	2
NaCl	0.5%	2	--	--
	2%	2	2	2
Na ₂ SO ₄	0.5%	3	2	2
	2%	4	2	2
Tap water		2	--	--
Subtotal			12	12
Total		25	24	

(a) Auger Grouts: Auger grout specimens were collected during the construction of the auger piles at the UH site. The specimens were cured in the humid room for 28 days before testing. A total of 25 specimens were tested in eight chemical solutions for up to two years. Tap water was used as a control fluid.

(b) Cement Concrete: Fresh concrete specimens were collected from a concrete supplier and cured in the moisture curing room for 28 days before testing. Specimens were also divided into two groups: wet and dry. Wet group specimens were immersed in deionized water until saturation for one month after they were demolded. Water absorption was measured with time. The dry group of concrete specimens were put into the chemical solution immediately after demolding.

A total of 24 specimens (12 dry and 12 wet) were tested in six solutions for up to one-and-one-half years. For concrete samples, all of the solutions, except HCl (pH 4) and NaCl (0.5%), were used.

D2. OBJECTIVES

The principal objective of this sub-study was to determine the chemical resistance of auger grouts and compare it to that of cement concrete. Specific objectives were as follows:

- (1) To evaluate the performance of auger grouts in different chemical environment (acid, sulfate and salt solutions).
- (2) To compare the chemical durability of auger grouts with cement concrete.

D3. MATERIAL COMPOSITION AND OVERALL TESTING PROGRAM

D3.1 Material Composition

The compositions of the auger grout and the concrete are given in Table D.2.

D3.2 Overall Testing Program

In these tests, 76 mm (3-inch) x 152 mm (6-inch) cylindrical specimens were used. Control tests were performed with tap water. At least two specimens were tested under the same condition, solutions were changed every month (one cycle). A schematic is shown in Figure D.2. A total of 49 specimens were tested in this study.

D3.2.1 Weight

An OHAUS GT4100 balance (accuracy of 0.1 g) was used to measure the weight of the specimens. After taking the specimens out of the jar, they were wiped with paper towels and weighted (no excess water was left on the surface).

Table D.2 Composition and Properties of Auger Grout and Concrete

Component / Property	Auger grout	Concrete
Cement (lb/cu.yd)	752 (20%)	12%
Fly ash (lb/cu.yd)	225 (6%)	3%
Coarse aggregate (lb/cu.yd)	--	45%
Fine aggregate (lb/cu.yd)	2400 (63%)	35%
Water (lb/cu.yd)	417 (11%)	5%
Additive (lb/cu.yd)	3.76 (0.5%)	--
	fluidifier	
Water /Cement	0.55	0.35
Water /Binder	0.43	--
Flowability (%)	Flow cone: 33 sec. efflux time	Slump test : 4 in.
Setting time (Hours)	5.5	--
28-day compressive strength (psi)	5000	5800
Unit weight (lb/cu.ft) (28-d)	134	145
Pulse velocity (m/s) (28-d)	4000 (13,050 ft/s)	4800 (15,650 ft/s)

D3.2.2 pH and Calcium

A pH electrode was used to measure the pH of the solution. The Ion Selective Electrode (ISE) method was used to determine the calcium concentration. Calibration for calcium was done by adding a known amount of calcium to water and measuring the voltage (mv reading) at selected pH values. The resulting calibration charts were then used to determine the calcium in the leaching solutions.

D3.2.3 Pulse Velocity

Pulse velocity measurements were made using a commercially available portable V-meter in accordance with ASTM C 597- 83. Lead zirconate titanate ceramic transducers

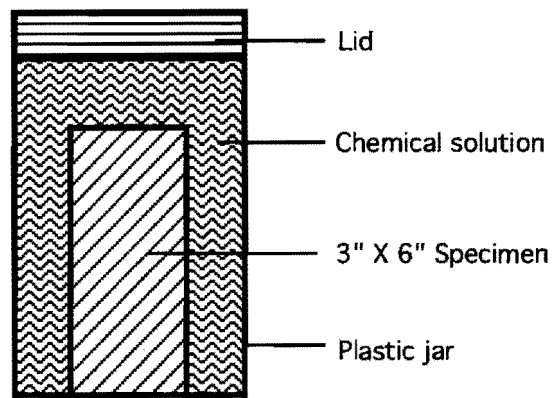


Figure D.2 Experimental setup

with natural frequencies of 150 kHz were used. Castrol water-pump grease was used to provide good coupling between the specimen and the transducers. The travel time of the ultrasonic pulse through the specimen under direct transmission, with the transducers on opposite faces along the length, was recorded to an accuracy of 0.1ms. Pulse velocity was calculated by dividing the length of the specimen by the travel time.

D4. ANALYSIS OF RESULTS

4.1 Visual Observation

The surface color changed to brown in an acidic environment and the porous surface was exposed due to etching after the cement and fly ash paste on the surface was removed by the acid.

White precipitate (CaSO_4) was observed in the H_2SO_4 and Na_2SO_4 solutions. The amount of precipitation was less in the H_2SO_4 (pH = 4) and Na_2SO_4 (0.5 %) solutions as compared to the H_2SO_4 (pH = 2) and Na_2SO_4 (2 %) solutions.

D4.1.1 Auger grouts

As described in Table D3, visible changes were observed with hydrochloric acid (HCl, pH=2), sulfuric acid (H₂SO₄, pH = 2 and 4), and in 0.5% and 2% sodium sulfate (Na₂SO₄) solutions.

Table D.3. Typical Appearance of Auger Grouts and Solutions at the end of First Test Cycle

Effect of chemical solutions		Specimens appearance	Solution
HCl	pH 2	surface color changed to brown	light brownish
	pH 4	no change	clear
H ₂ SO ₄	pH 2	surface color changed to dark brown, porous top	large amount of white precipitation
	pH 4	surface color changed to brown, porous top	small amount of white precipitation
NaCl	0.5	no change	clear
	2.0	no change	clear
Na ₂ SO ₄	0.5	crack started from ends of specimens, 1 out of 3 specimens broken from middle	small amount of white precipitation
	2.0	crack started from ends of specimens, 3 out of 4 specimens broken from middle	large amount of white precipitation
Tap Water		no change	clear

The bottoms of the auger grout specimens were partly peeled off in H₂SO₄ (pH = 2) and 0.5% and 2% Na₂SO₄ solutions. During the progress of testing, 50 per cent of the specimens in the sodium sulfate solutions failed by fracturing around the middle of the specimens. The sulfate apparently reacted with the cement-rich auger grout to form calcium sulfate, which will result in volume increase and cause cracking of the grout.

All four specimens immersed in the 2 % Na₂SO₄ (20,000 ppm) fractured in the time period of 6-8 months. Two of the three samples immersed in the 0.5% Na₂SO₄ solution fractured after 12 months. A sketch of a fractured specimen is shown in Figure D.3, where d is the diameter and h is the height.

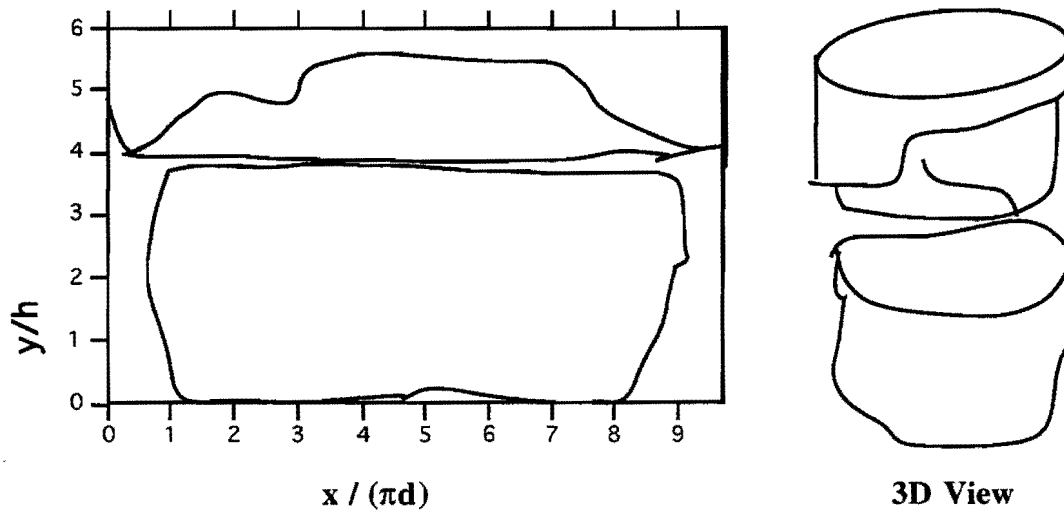


Figure D.3 Map of failed auger grout specimen in 2 % Na₂SO₄

D4.1.2 Concrete

Descriptions of the visual appearance of the concrete samples are given in Table D.4. Except for the cases of hydrochloric acid (HCl, pH = 2) and sulfuric acid (H₂SO₄, pH = 2) there were no visible changes in the solutions. The surface of the specimens changed in color to light brown in hydrochloric acid (HCl, pH = 2), and brown in sulfuric acid (H₂SO₄, pH = 2). A porous surface was observed on all of the specimens due to the reaction of acid and cement past (etching). White precipitate (CaSO₄) was observed in the

Table D.4. Typical Appearance of Concrete and Solutions at the End of First Test Cycle

Effect of chemical solutions		Specimens appearance	Solution
HCl	pH 2	surface color changed to light brown, porous top	light brownish solution
	pH 2	surface color changed to brown, porous top	brownish solution, white precipitation
H ₂ SO ₄	pH 4	clean	small amount of white precipitation
	2.0	clean	clear
Na ₂ SO ₄	0.5	clean	small amount of white precipitation
	2.0	white precipitate on surface	white precipitation

H₂SO₄ and Na₂SO₄ solutions with both high and low concentrations. The amount of precipitation was much higher in the high-concentration solutions.

D4.2 Change of pH

D4.2.1 Auger grouts

The variation of the pH of the immersion solution over the course of the test are presented in Fig. D.4. The pH of the auger grouts increased to around 12 at the end of a test cycle for all the chemical solutions, including tap water. This suggests that there may be a relatively high reaction possibility with each of the various chemical solutions for auger grouts with 20 per cent cement content. However, the increase in pH with only tap water as the leaching solution suggests that the increased pH may also simply result from the release of lime in the curing process of the portland cement in the grout.

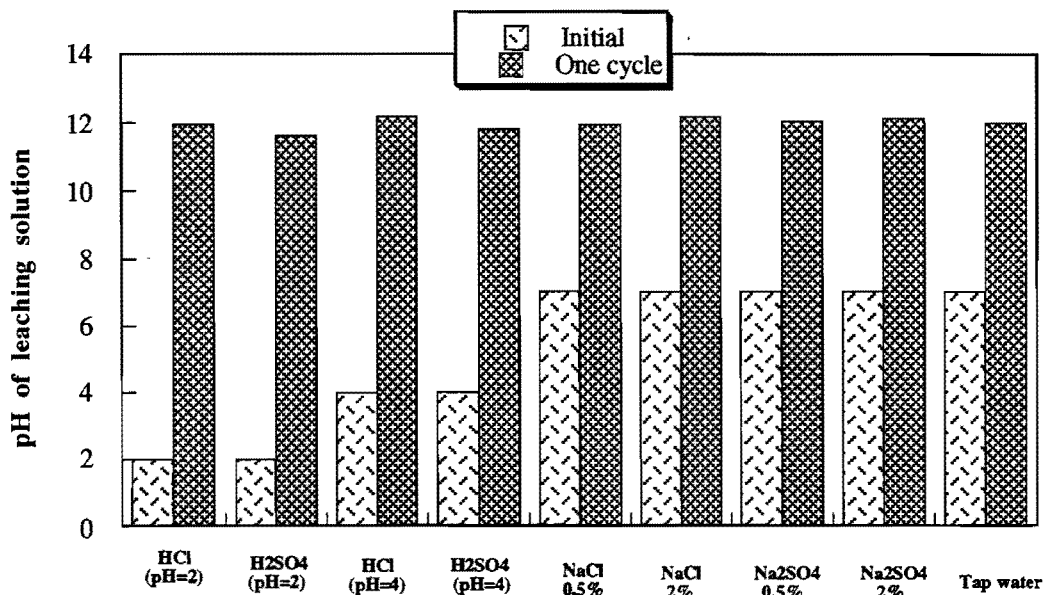


Figure D.4 Variation of pH at the end of one cycle of immersion time for auger grout specimens

D4.2.2 Concrete

The change in pH measured for the dry and wet groups of concrete and the results are presented in Fig. D.5. The cement content in the concrete was 12%, which is considerably lower than the cement content in the auger grouts (20 %). However, the results regarding change in pH of the immersing solution were similar to those for the cement grouts.

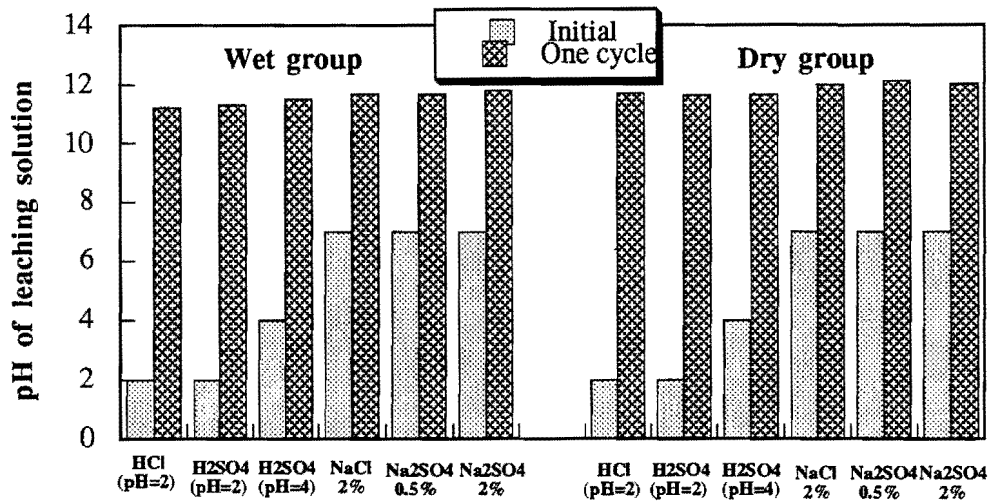


Figure D.5 Change in pH at the end of one cycle for concrete specimens (a) Wet group (b) Dry group

D4.3 Change of weight

Percentage changes in the weights of the test specimens are shown in Figs. D.6 through D.8. It should be noted that initial weight gain of the dry test specimens was followed by weight loss. The weight gain can be attributed to saturation of the specimens and constituents replaced by the reaction by-products from chemical reactions. The weight loss can be attributed to the leaching of calcium and loss of mass due to chemical attack.

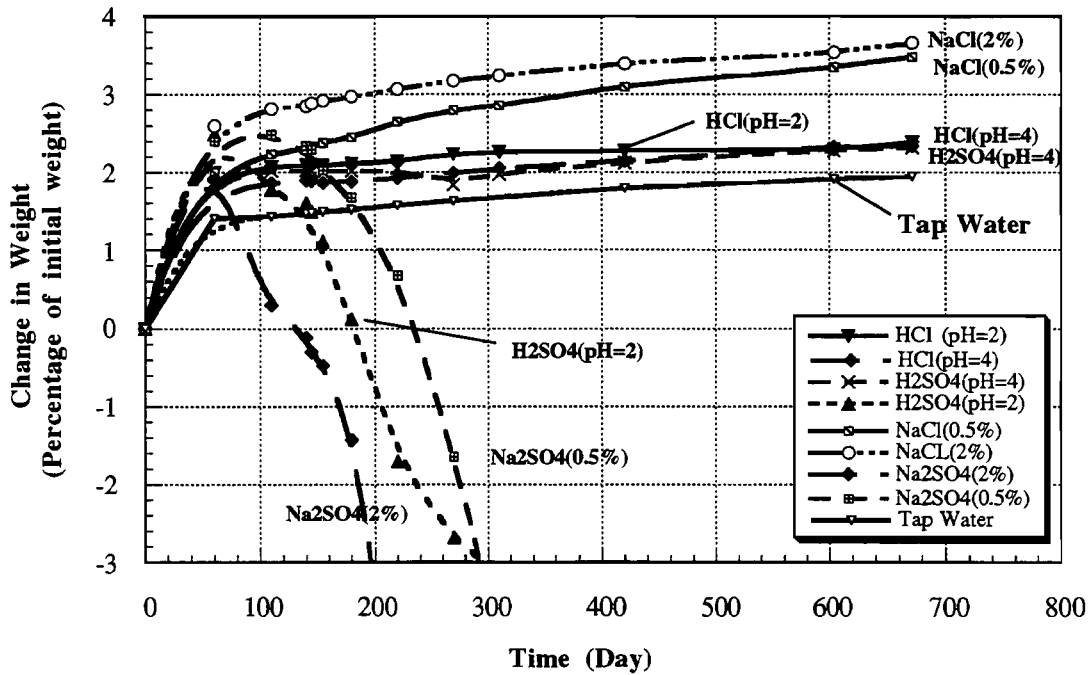


Figure D.6 Change in weight versus immersion time for auger grout specimens

For concrete, both dry and wet groups, maximum weight gains occurred in the salt solutions, and maximum weight loss occurred in the sulfuric acid at a pH of 2. There were slightly larger weight gains and losses in the dry group compared to the wet group of concrete specimens.

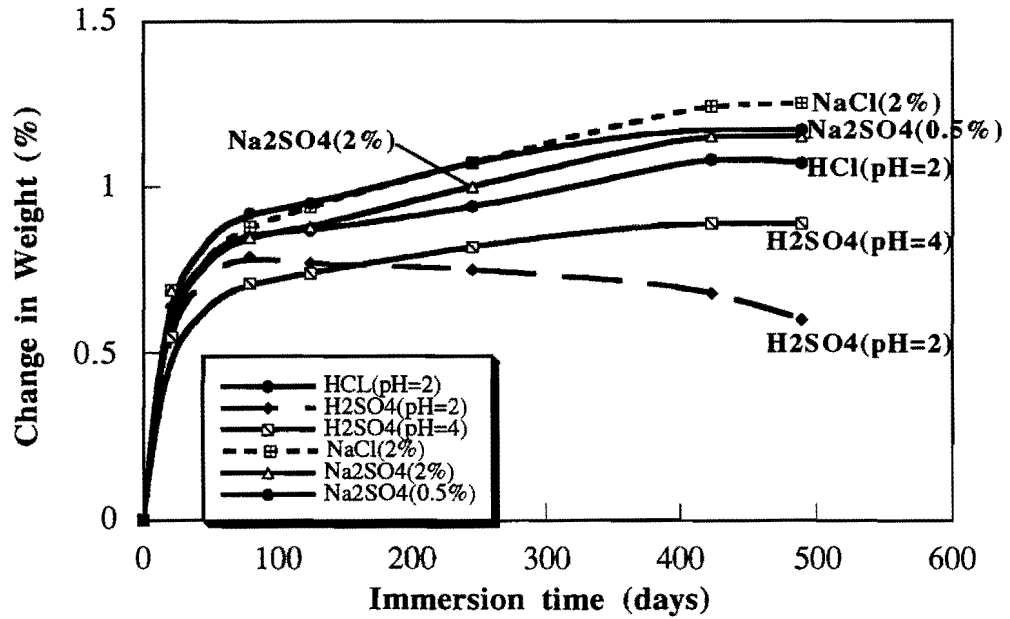


Figure D.7 Change in weight versus immersion time for the dry group concrete specimens

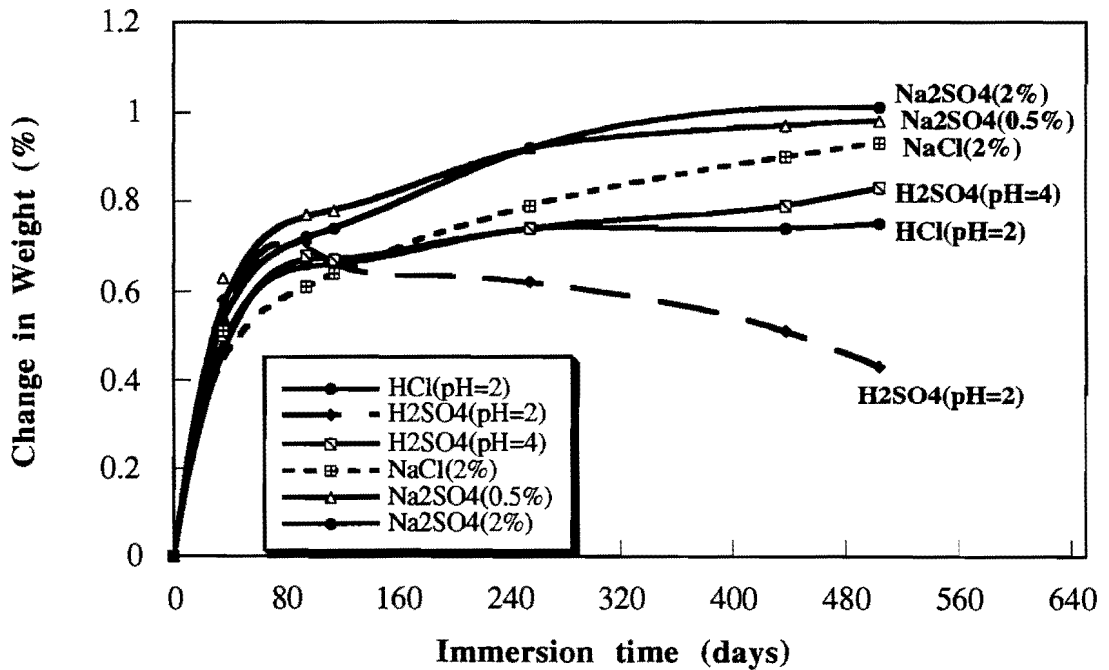


Figure D.8 Weight change versus immersion time for the wet group concrete specimens

D4.3.1 Auger grouts

Twenty-five auger grout specimens were submerged in eight chemical solutions for up to two years. The percentage changes of initial weight with immersion time is shown in Fig. D.6. The highest weight increase was observed in the first 100 days.

For auger grouts, the maximum weight gain was over 3% in the salt (NaCl) solution. The maximum weight loss was in the sodium sulfate solutions and in sulfuric acid (pH = 2).

The weight changes were clearly more significant in the auger grout specimens than in the concrete specimens.

Table D.5 Effect of Chemical Solutions for Auger Grout Specimens after Two Years of Immersion

Effect of chemical solutions		Max. weight gain		Max. weight loss		Remarks
		Time (days)	(%)	Time (days)	(%)	
HCl	pH 2	672	2.39	--	--	
	pH 4	672	2.34	--	--	
H ₂ SO ₄	pH 2	60	2.50	604	-3.42	50% of the specimens failed
	pH 4	672	2.32	--	--	
NaCl	0.5	672	3.48	--	--	
	2.0	672	3.66	--	--	
Na ₂ SO ₄	0.5	110	2.49	604	-4.02	all specimens failed, 1 out of 3 broken from middle,
	2.0	60	1.9	310	-6.51	all specimens failed, 3 out of 4 broken from middle
Tap	Water	672	1.95	--	--	

Continuous weight increase in the auger grouts was observed in the following chemical solutions: HCl (pH 2, 4); H₂SO₄ (pH 4); 0.5% NaCl, 2% NaCl and tap water. The weight gain in the reference test (tap water) was 2% after 700 days. A slightly higher weight increase was observed in the following acid solutions [HCl (pH 2, 4), and H₂SO₄ (pH 4)]. The acid solutions exhibited a weight gain in the range of 2.3 to 2.4%. The

maximum weight increase was with NaCl: 3.7 % weight gain for 2 % NaCl, and 3.5 % weight gain for 0.5 % NaCl in 670 days.

Initial weight increase followed by a decrease in weight was observed with H₂SO₄ (pH = 2) and Na₂SO₄ (0.5% and 2%). 2 % weight loss was observed after 180, 240 and 270 days in 2 % Na₂SO₄ (13, 500 ppm SO₄²⁻), H₂SO₄ (pH = 2) (480 ppm SO₄²⁻) and 0.5 % Na₂SO₄ (3380 ppm SO₄²⁻) solutions, respectively. Over 3 % weight loss was measured in the H₂SO₄ (pH = 2) solution after 600 days of testing. In 0.5 % Na₂SO₄ and 2 % Na₂SO₄ solutions the weight losses were over 4 % (after 600 days) and 6.5% (after 300 days), respectively.

The SO₄²⁻ ion apparently affected the durability of the auger grouts. This effect is further accelerated by the lower pH (pH = 2) of the sulfuric acid.

D4.3.2 Concrete

The percentage changes of weight versus immersion time are shown in Figure D.7 (dry group) and Figure D.8 (wet group). In both cases, the maximum weight gain was observed with NaCl. Weight loss was observed in the case of sulfuric acid (H₂SO₄) at a pH of 2.

Weight changes in the dry specimens were slightly higher than in the wet specimens at the beginning. A maximum weight gain of 1.25% was observed in the dry group versus 1.0% in the wet group. Maximum weight loss of 0.20% was observed in the dry group versus 0.25% in the wet group after 500 days of immersion.

Dry concrete. There was a continuous weight increase in all the cases except sulfuric acid (H₂SO₄) at a pH of 2. About 1.2% weight gain was observed in sulfate and salt solutions (1.2 % for 0.5 % and 2 % Na₂SO₄, 1.3 % for 2 % NaCl). Weight gain of 1.1% and 0.9% was observed in the case of HCl (pH 2) and H₂SO₄ (pH 4) solutions, respectively.

Weight increased during the first two cycles and then decreased in the case of H₂SO₄ (pH 2). After about 0.8% weight gain at the end of the first cycle, a weight loss of 0.2% was observed at the end of the 4th cycle for H₂SO₄ (pH 2) solution.

Weight gain and loss values are summarized for dry concrete in Table D.6.

Table D.6 Effect of Different Chemical Solutions for Dry Concrete (500 Days of Immersion)

Effect of chemical solutions		Max. weight gain		Max. weight loss	
		Time (days)	(%)	Time (days)	(%)
HCl	pH 2	490	1.07	--	--
H ₂ SO ₄	pH 2	80	0.79	490	-0.19
	pH 4	490	0.89	--	--
NaCl	2.0	490	1.25	--	--
Na ₂ SO ₄	0.5	490	1.15	--	--
	2.0	490	1.17	--	--

Wet concrete. There was continuous weight increase in all cases except for sulfuric acid (H₂SO₄) at a pH of 2. About 1.0 % weight gain was observed in all the salt solutions (1.0 % for 0.5 % and 2 % Na₂SO₄, 0.9 % for 2 % NaCl) after 500 days. Weight gains of 0.8 % and 0.9 % were observed in the cases of HCl (pH 2) and H₂SO₄ (pH 4), respectively. Weight gain and loss values are summarized for wet concrete in Table D.7.

Table D.7 Effect of Different Chemical Solutions for Wet Concrete (500 Days of Immersion)

Effect of chemical solutions		water uptake (%)	Max. weight gain		Max. weight loss	
			Time (days)	(%)	Time(days)	(%)
HCl	pH 2	0.53	500	0.75	--	--
H ₂ SO ₄	pH 2	0.58	95	0.71	500	-0.28
	pH 4	0.50	500	0.83	--	--
NaCl	2.0	0.51	500	0.93	--	--
Na ₂ SO ₄	0.5	0.63	500	0.98	--	--
	2.0	0.60	500	1.01	--	--

Weight increased within the first cycle and decreased thereafter in the case of H₂SO₄ (pH 2). After a weight gain of about 0.6% within the first 35 days being immersed into deionized water, a sharp decrease of weight of 0.2% was found at the end of the 5th cycle.

D4.4 Leaching of Calcium

The leaching of calcium from the auger grout and concrete specimens is documented in Figures D.9 - D.11 and in Table D.8 and D.9. There was approximately 145 g of calcium in each auger grouts specimen, and 98 g in each cement concrete specimen. The cumulative calcium leached out was determined by the percentage of initial weight of the specimen and of the total theoretical calcium in each specimen.

In all the cases, the amount of calcium leached increased with time.

For auger grouts, the maximum calcium leached was over 0.70 % (Fig D.9) of the initial weight of specimen. This was observed in the case of H₂SO₄ (pH 2).

For cement concrete, both dry and wet groups, calcium in the range of 0.1 to 0.2 % was released in the salt solutions, and maximum weight loss occurred in the sulfuric acid at a pH of 2. A slightly higher amount of calcium was leached in the dry group than in the wet group.

D4.4.1 Auger grouts

The lowest amount (0.13% of the initial weight, 1.3% of total calcium) of calcium leached was with the tap water (after 12 cycles). The maximum of 0.7 % of the initial weight (7.6% of total calcium) of leached calcium was observed in the case of H₂SO₄ solution at pH of 2. The amount of calcium in the immersion solutions varied from 0.28% to 0.5% of initial weight (2.8% to 5.2% of total calcium).

The percentage of calcium leached was higher in sulfuric acid compared to hydrochloric acid at the same pH. Leaching in lower pH acid solutions was greater than

than in higher pH acid solutions. More calcium leached in the lower concentration (0.5 %) of the NaCl and Na₂SO₄ solutions than at high concentration (2%). Furthermore, soluble calcium in NaCl solutions were greater than that in Na₂SO₄ solutions at comparable concentrations.

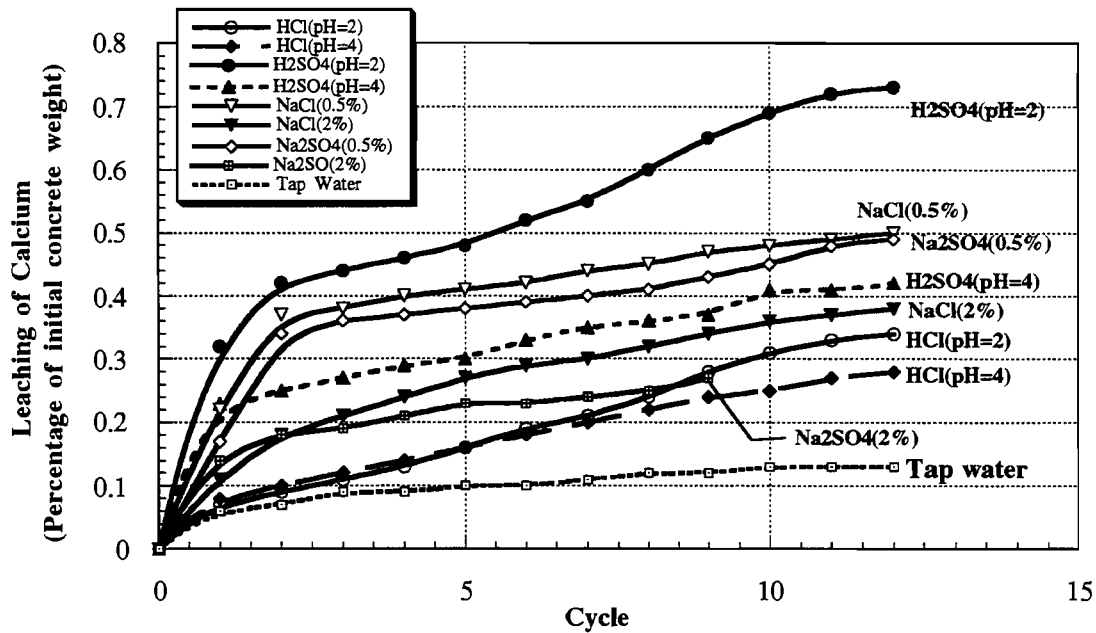


Figure D.9 Calcium versus number of cycles of leaching for auger grout specimens

Table D.8 Amount of Calcium Leached for Auger Grouts
(Two Years of Immersion)

Effect of chemical		Max. Ca ²⁺ (% of initial wt.)	Max. Ca ²⁺ (% of total calcium)
HCl	pH 2	0.34	3.52
	pH 4	0.28	2.90
H ₂ SO ₄	pH 2	0.73	7.55
	pH 4	0.42	4.35
NaCl	0.5	0.50	5.17
	2.0	0.38	3.93
Na ₂ SO ₄	0.5	0.49	5.07
	2.0	0.27	2.79
Tap	Water	0.13	1.35

4.4.2 Concrete

Maximum calcium was observed in the 2 % sulfate and salt solutions and in acids at a pH of 2. The amount of calcium leached from dry specimens was higher than from the wet specimens.

Dry group. Results from the dry group are shown on Figure D.10. A maximum of 0.18 % of the initial weight (2.9 % of total calcium) of calcium was leached in the case of the 2 % NaCl solution. A minimum of 0.07% (1.2 % of total calcium) was leached in the case of H₂SO₄ (pH 4). 0.10 % (1.6% of total calcium) was leached in the case of 0.5 % Na₂SO₄. Other cases were very close; a total of 0.15 % (2.45 % of total calcium) was observed to be leached in the case of the HCl (pH 2), H₂SO₄ (pH 2), and 2% Na₂SO₄ solutions.

**Table D.9 Effect of Different Chemical Solutions for Concrete
(500 Days of immersion)**

Effect of chemical solutions		Dry Group		Wet Group	
		Max. Ca ²⁺ (% of initial wt.)	Max. Ca ²⁺ (% of total Ca)	Max. Ca ²⁺ (% of initial wt.)	Max. Ca ²⁺ (% of total Ca)
HCl	pH 2	0.15	2.46	0.14	2.21
	pH 2	0.15	2.49	0.12	2.02
H ₂ SO ₄	pH 4	0.07	1.20	0.06	0.95
NaCl	2.0	0.18	2.87	0.14	2.30
	0.5	0.10	1.59	0.09	1.39
Na ₂ SO ₄	2.0	0.15	2.43	0.13	2.05

Wet group. The wet group results are depicted in Figure D.11 and Table D.10. The trends were similar to those for the dry specimens. The amount of calcium leached varied from 0.06 to 0.14 %. 0.14 % of the initial weight (2.2 % of total calcium) of calcium was leached out of the 2 % NaCl solution. A minimum calcium leaching of 0.06 % (1.0 % of total calcium) was observed in the case of H₂SO₄ (pH 4). 0.09% (1.4% of total calcium) leaching was observed in the case of 0.5 % Na₂SO₄ after 6 cycles.

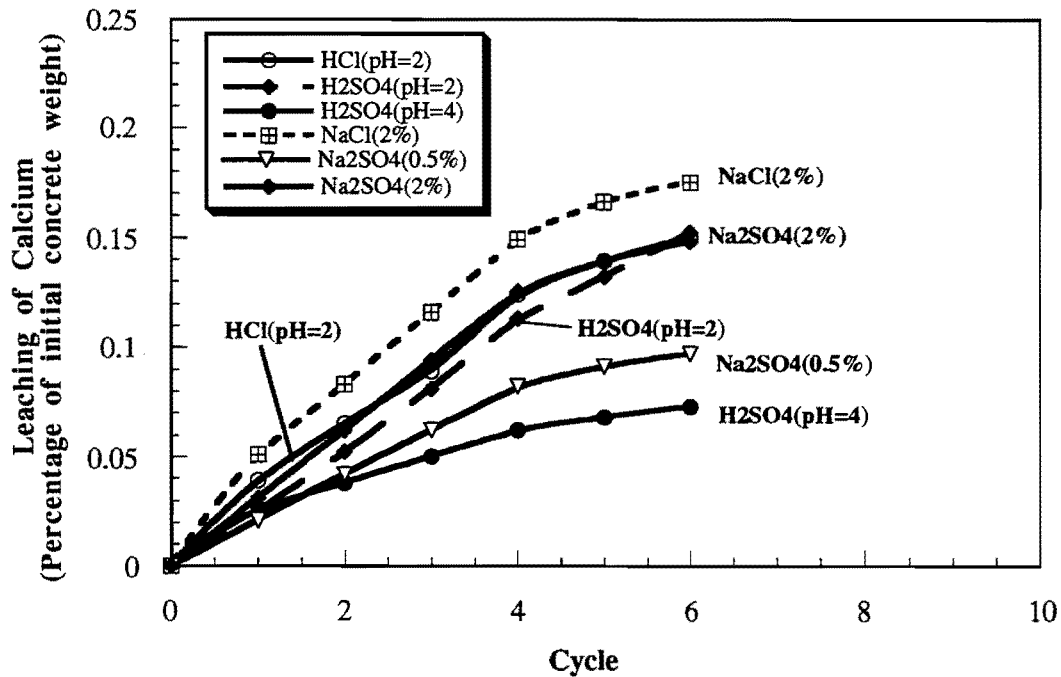


Figure D.10. Calcium leachate versus number of cycles of leaching for dry concrete

D4.5 Change in Pulse Velocity

Variations of pulse velocity for auger grouts and concrete specimens were less than 0.5% except for those specimens that failed or had severe surface deterioration due to chemical attack. The results are summarized in Figures D.12 - D.13 and in Tables D.10 - D. 12. The average initial pulse velocity of auger grouts and cement concrete, were approximately 4000 m/s (13,050 ft/s) and 4800m/s (15,650 ft/s), respectively.

D4.5.1 Auger grouts

The pulse velocity results are shown in Table D.10 and Figure D.12. Pulse velocity remained essentially constant in all cases except for H₂SO₄ (pH 2) and Na₂SO₄ (0.5% and 2%) solutions. The average pulse velocity of auger grout was 4100 m/s (13451 ft/s), with the coefficient of variance of 2% .

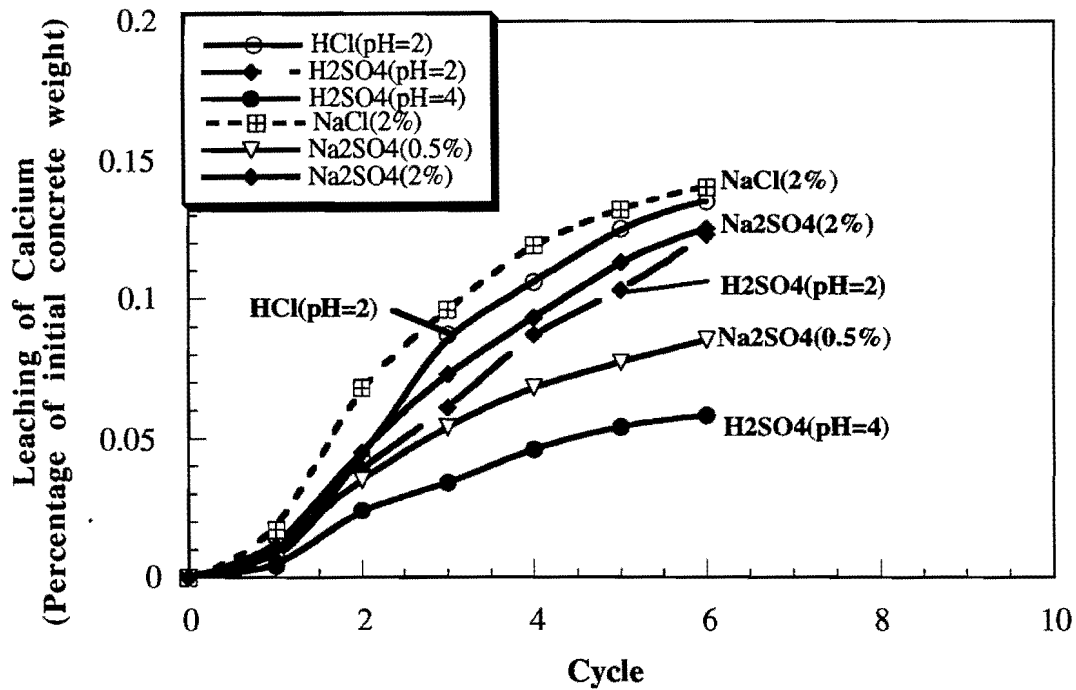


Figure D.11 Calcium leachate versus number of cycles of leaching for wet concrete

Table D.10 Effect of Different Chemical Solutions in the Pulse Velocity for Auger Grouts (Two Years of Immersion)

Effect of chemical solutions		Initial	After saturated	After 12 cycles	Remarks	
					Increase (%)	Decrease (%)
HCl	pH 2	4020	4153	4132		1
	pH 4	4020	4240	4184		1
H ₂ SO ₄	pH 2	4020	4062	3688		10
	pH 4	4020	4128	4183	1	
NaCl	0.5	4020	4258	4222		1
	2.0	4020	4098	4172	2	
Na ₂ SO ₄	0.5	4020	4075	3664		10
	2.0	4020	4187	3608		14
Tap	Water	4020	4076	4124	1	

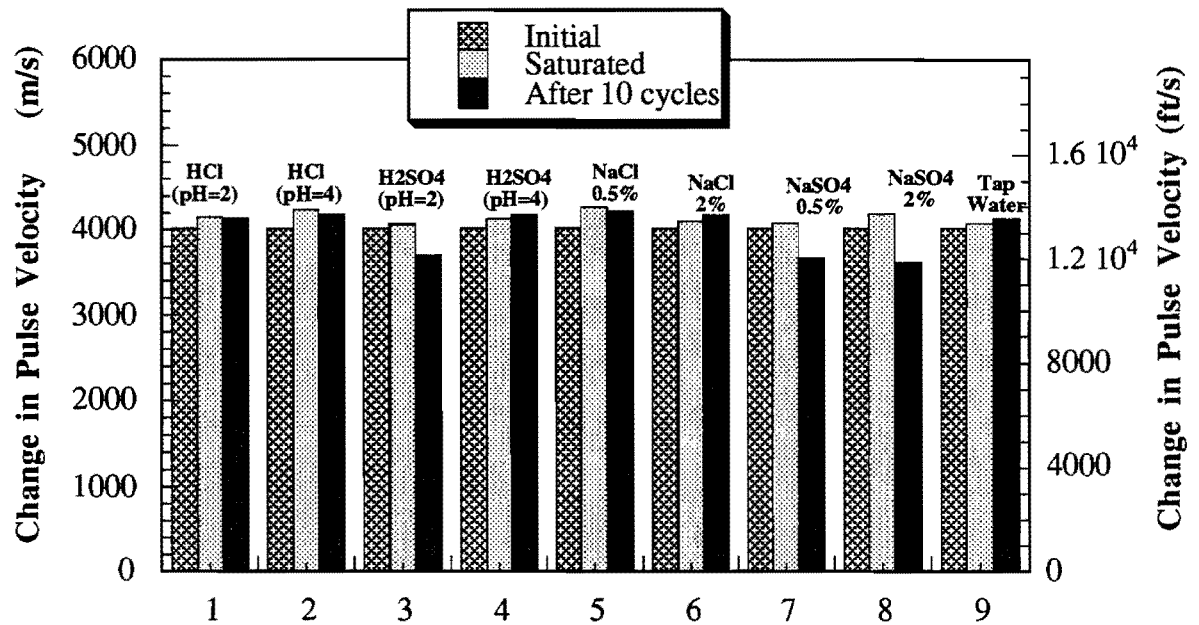


Figure D.12 Variation of pulse velocity of the auger grout specimens

After 6 to 8 cycles, the pulse velocity decreased by 14 % in the case of the 2 % Na₂SO₄ solution. After 10 cycles, pulse the velocity decreased by over 10 % in H₂SO₄ (pH 2) and 0.5% Na₂SO₄ solutions. A decrease in pulse velocity can be interpreted to be equivalent to a decrease in compressive strength, although not necessarily by the same amount.

D4.5.2 Concrete

Test details for the concretet specimens are shown in Figure D.13 and Tables D.11 adn D.12. The average initial pulse velocity of the standard concrete specimens was approximately 4800 m/s (15,750 ft/s), the coefficient of variation was 2 %. There was a slightly increase in the pulse velocity in all the cases for the dry group concrete specimens

(Fig. D.13). The pulse velocity of the wet group of concrete specimens remained within 1 % of the initial value, except in H₂SO₄ (pH 4) solution.

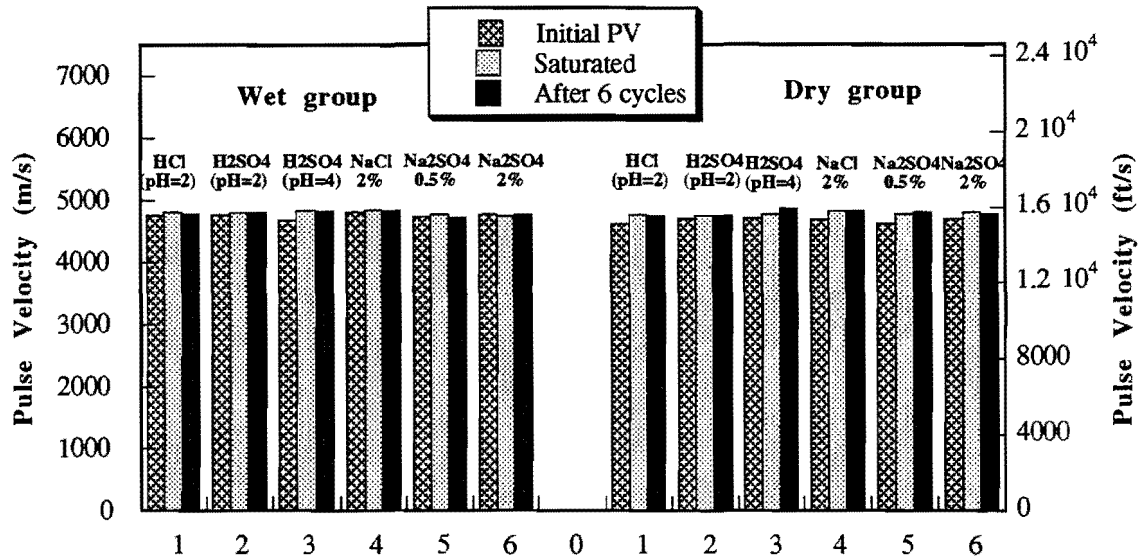


Figure D.13 Variation of pulse velocity of cement concrete specimens

Table D.11 Effect of Different Chemical Solutions on Pulse Velocity for Dry Cement Concrete (1.5 Years of Immersion)

Effect of chemical solutions		(1) Initial (dry)	After saturated by chemical solutions	(2) Changes after saturated (%)	After 6 cycles	Changes compare to (2) (%)
HCl	pH 2	4760	4810	+1	4780	-0.5
H ₂ SO ₄	pH 2	4780	4800	+0.5	4810	+0.2
	pH 4	4670	4830	+3	4830	0
NaCl	2.0%	4810	4850	+1	4830	-0.5
Na ₂ SO ₄	0.5%	4730	4770	+1	4710	-1
	2.0%	4770	4740	-1	4780	+1

Table D.12 Effect of Different Chemical Solutions on Pulse Velocity for Wet Cement Concrete (1.5 Years of Immersion)

Effect of chemical solutions		(1) Initial (dry)	(2)After saturated by water	Changes after saturated (%)	(3) After 6 cycles	Changes compare to (2) , (%)
HCl	pH 2	4620	4760	+3.0	4740	-0.5
H ₂ SO ₄	pH 2	4690	4750	+1.8	4750	0
	pH 4	4710	4770	+1.2	4870	+2.0
NaCl	2.0%	4690	4820	+2.8	4840	+0.4
Na ₂ SO ₄	0.5%	4620	4770	+3.2	4800	+0.6
	2.0%	4700	4810	+2.3	4770	-0.8

Comparison of the results for the auger grout and concrete specimens indicates that the auger grout, with its high cement factor, is more vulnerable to degradation of acoustic pulse velocity than cement concrete.

D4.6 Compression test

D4.6.1 Auger grouts

Unconfined compression strength was determined after two years for some of the auger grout specimens (Table D.13 and Figure D.14). The unconfined compressive strength of a 28-day moisture-room-cured specimen was 34.5 MPa (5000 psi), and there was a slight increase in the strength when the specimen was immersed in tap water for two years. There was a notable strength decrease in hydrochloric acid (pH 2 and 4) and larger decreases for the specimens in sulfate solutions (sulfuric acid and sodium sulfate). A 40% decrease occurred in H₂SO₄ (pH = 2) and an 80% decrease was observed in 2 % Na₂SO₄ solutions. It should be noted that the strength of air-cured specimens (up to 1 year) was about 30 % lower than for the specimen cured for 28 days in the moisture room.

Table D.13 Compression Strength of Selected Auger Grouts

Medium	Exposure age (days)	Least diameter (in.)	Compressive Strength psi (MPa)
moisture cured	28	3	5000 (34.5)
air cured	365	3	3560 (24.6)
Tap water	684	3	5200 (35.9)
HCl, pH 2	543	3	4240 (29.2)
HCl, pH 4	684	3	4850 (33.4)
H ₂ SO ₄ , pH 2	615	2.5	3040 (21.0)
NaCl, 2%	543	3	6080 (41.9)
Na ₂ SO ₄ , 0.5%	615	2.4	1190 (8.2)

5. CONCLUSIONS

Auger grouts were tested in eight chemical solutions representing acids, salts and sulfates for a period of two years. Performance of auger grouts were compared to the performance of dry and saturated cement concrete under similar environmental conditions. The following can be summarized.

1. For auger grouts, the maximum weight gain of over 3% was observed with a salt solution (2% NaCl) over two years. By contrast, the maximum weight gain for cement concrete was about 1% in 500 days.
2. For auger grouts, 2% weight loss was observed after 180, 240 and 270 days in the sulfate solutions. For cement concrete weight loss of 0.2 to 0.3% was observed with H₂SO₄ (pH = 2) solution after 500 days. This indicates a faster degradation of auger grouts in a sulfate environment.
3. For auger grouts, a maximum of 0.7% of the initial weight (7.6% of total calcium) of the calcium was observed in the leaching H₂SO₄ solution at a pH of 2 after 24 months. For wet and dry concrete specimens, only 0.12 % , and 0.15 % of the initial weight (2.3% , and 2.9% of total calcium) of the calcium was observed in H₂SO₄ solution at a pH of 2 after 17 months. Leaching of calcium in sulfates was therefore about five times higher in auger grouts compared to cement concrete.

4. The average pulse velocities of the auger grout and cement concrete were 4000 m/s (13,050 ft/s) and 4800m/s (15,650 ft/s) respectively. Slightly more degradation of pulse velocity was observed in the auger grouts over time. Sulfate solutions [except H₂SO₄ (pH = 4)] affected the pulse velocity of the grouts negatively.
5. There was a notable compressive strength decrease in auger grouts immersed in hydrochloric acid (pH 2 and 4) and a larger decrease for the auger grout specimens in sulfate solutions (sulfuric acid and sodium sulfate). It should also be noted that the strength of air-cured grout specimens (up to 1 year) was about 30% lower than that of the 28-day moisture-cured specimen. 5. Sulfuric acid (H₂SO₄) at pH = 4 with 5 ppm sulfate had minimal effect on the grouts and cement concrete.

Based on this study, it can be expected that auger grouts will not perform as well as normal cement concrete in aggressive soil environments that contain sulfates and acids. It is quite possible that the chemical degradation can be accounted for in design by providing sufficient cross-sectional area of grout or additives that can mitigate the effects of these chemicals when such aggressive soils are encountered.